Advancing Process Control using Orthonormal Basis Functions

Advancing Process Control using Orthonormal Basis Functions

ADVANCING PROCESS CONTROL USING ORTHONORMAL BASIS FUNCTIONS

PROEFSCHRIFT

ter verkrijging van de graad van doctor aan de
Technische Universiteit Eindhoven, op gezag van de
rector magnificus prof.dr.ir. F.P.T. Baaijens, voor een
commissie aangewezen door het College voor Promoties,
in het openbaar te verdedigen op

donderdag 16 februari 2023 om 13:30 uur

door

Ahmad Alrianes Bachnas

geboren te Yogyakarta, Indonesia

Dit proefschrift is goedgekeurd door de promotoren en de samenstelling van de promotiecommisie is als volgt:

Voorzitter:	prof. dr. ir. A.B. Smolders.
Promotoren:	prof. dr. S. Weiland
	dr. ir. R. Tóth
Leden:	prof. dr. ir. A.W. Heemink (Technische Universiteit Delft)
	prof. dr. ir. Y. Zhu (Zhejiang University)
	prof. dr. ir. P.M.J. Van den Hof
	prof. dr. ir. K.J. Keesman (Universiteit Wageningen)
	dr. ir. L. Ariaans (IPCOS B.V)

Het onderzoek dat in dit proefschrift wordt beschreven is uitgevoerd in overeenstemming met de TU/e Gedragscode Wetenschapsbeoefening.

This dissertation has been completed in fulfillment of the requirements of the Dutch Institute of Systems and Control (DISC) for graduate study.

This research was part of SMART project and financially supported by Eurostars Eureka

A catalogue record is available from the Eindhoven University of Technology Library.

ISBN: 978-90-386-5656-4

This thesis was prepared with the LaTeX documentation system.

Print and Cover design : Gildeprint.

Summary

Ever growing demands for both consumer and industrial products drive chemical and petrochemical industries to optimize the quantity and quality of their production. The companies that have the core business in the process industry are competing with each other to dominate the market. Development of the current process technologies provide a competitive edge for companies to ensure their leading market positions. One of the major problems for the *Advanced Process Control* (APC) element of the process industry is to sustain high performance of the control in the presence of discrepancy between prediction model and process of interest. This thesis investigates new methods to tackle this problem by taking into account model inaccuracy and variation of process dynamics. The control mechanism proposed in this thesis is based on *Orthonormal Basis Functions* (OBFs) as a novel prediction model. The detailed descriptions of research motivations, questions, and literature surveys are addressed in Chapter 1 of this thesis.

The second part of this thesis, Chapter 2-3, Addresses methods to optimally select basis poles of the OBF models from a finite set of system poles. Furthermore, we provide a method to utilize our proposed algorithms for a model of a system that is obtained via system identification procedure. Lastly, by conducting a simulation study, we showed that the proposed methods outperform the state of the art basis selection algorithm in the sense of obtaining basis poles with better performance measure. The simulation study also shows a reasonable computational load of each algorithm which can be directly implemented in industrial practice.

The third part of this thesis, Chapter 4, Addresses the case where the OBF-based prediction model is adapted per control cycle to capture the time-varying behavior of the system of interest. The adaptation is based on an iterative identification procedure of the coefficients of the OBF prediction model. Conducting system identification for OBF-based models has a strong benefit due to direct applicability of the PEM identification framework and hence the consistent estimation of the OBF model coefficients. Afterwards, the MPC scheme for OBF-based prediction model is formulated. The MPC scheme, as well as the feasibility and stability results, are then extended to the time-varying case. The proposed MPC is first tested in academic case study, where we have shown that the proposed method can capture the time-varying dynamics of a given system and manage to achieve the goal of set-point tracking.

The fourth part of this thesis, Chapter 5, Addresses the case where the OBF-

based prediction model describes variations in the dynamics of the system of interest that can be characterized by an external signal called the scheduling variable. Two LPV identification approaches are provided to identify the LPV-OBF model before the MPC is commissioned. The local LPV identification approach can be seen as an interpolation of the dynamical behavior of the system, while the global LPV identification approach is a direct identification method based on a single data set that is measured from the system. Afterwards, the LPV-OBF MPC scheme is formulated. The MPC scheme utilizes a designated steady-state target and extra penalty term for tracking purposes. The space of the steady-state pair is characterized by a vector which is used as an argument of minimization for the MPC problem. Such setting helps us in establishing feasibility and stability guarantees of the MPC scheme. The proposed MPC is first tested in academic case study, where we show that the proposed method can capture the parameter-varying dynamics of a given system and manage to achieve the goal of set-point tracking.

The last part of this thesis is where the proposed LTV-OBF MPC and LPV-OBF MPC are tested in two industrial case studies. A High purity distillation column case and a Dual distillation column case which are common in process industry, are used for the demonstration. The knowledge of the variations of system dynamics becomes the key element that differentiate the two proposed MPC schemes and their applications on the selected case studies.

Contents

1 CHAPTER

Introduction

Ever growing demands for both consumer and industrial products drive chemical and petrochemical industries to optimize the quantity and quality of their production. The companies that have the core business in the process industry are competing with each other to dominate the market. Development of the current process technologies provide a competitive edge for companies to ensure their leading market positions. This thesis investigates new methods to cope with the expectations of next generation of process technologies from the view point of control engineering so as to deal with present day challenges. This involves the design of automated systems that realize desired behavior of process operation by deciding on the actuation of the process based on sensor information. The first chapter is dedicated to describe the motivation and the reasoning behind the research of this thesis. Key issues that are considered in this thesis are highlighted and the main research problem is formulated. Finally, outline of the thesis is given to conclude this chapter.

1.1 Research motivation

The general motivation for the research presented in this thesis is to contribute to the improvement of the current generation of control methods in process industry. To specify what is considered as "improvement" and "current situation", we first elaborate on the situation in the process industry as well as the current implementation of control solutions in this domain. Afterwards, we highlight the key elements that are treated in this thesis.

1.1.1 Current situation in the process industry

The process industry includes all industries that have a core business in processing resources. These processes, which can either be continuous or batch produc-

tion, involve the chemical transformation of raw or pre-processed materials into other products. The end products of these industries can be found in our daily life. Food, beverages, pharmaceutical products, oil, gas, paper, etc., are just simple examples of the products of process industry. These products improve the quality of human life. As welfare levels, the demands on these products grow exponentially. This situation stimulates the economic position of the process industry. Companies are competing with each other to take the biggest share of the market in terms of increasing the throughput of their production while reducing the operational cost. The innovation of industrial technologies and improved production methods are some of the key enablers to have a favorable economic position in this competition. However, as a negative result, the natural resources are being overconsumed and start to deplete. People and organizations are becoming aware and concerned of environmental issues that are caused by industrial production. Hence, the industry is more and more pressured to operate in an environmental friendly manner. Indeed, this situation leads to further challenges for this sector. The operational constraints in industrial processes become stricter than ever. The industry needs to obey not only mechanical-chemical constraints of the processes, but also environmental regulations that are imposed on them. They need to ensure that their operations are safe, environmental friendly, efficient in resources, and at the same time, yield a healthy financial profit to ensure favorable economic position.

1.1.2 Control systems in the process industry

The aforementioned situations urge the process industry to optimize their processes and plant operation with respect to multiple objectives and constraints. Designing better control systems that can govern and improve plant operation based on these aspects is one of the key elements that can help achieving these goals. To illustrate the involvement of control system in the process industry, let us take an example of a binary distillation column that is depicted in Fig. 1.1.

In this distillation process, a propane-propene mixture is fed into the column with the purpose to separate the mixture into propene and propane components with a prescribed level of purity. These two components are the outputs of the process and are known as the *Controlled Variables* (CVs). The desired purity level of the CVs can be obtained by controlling variables such as reboiler temperature, cooling temperature in the condenser, feed flows, etc. The variables that are manipulated for this purpose are called the *Manipulated Variables* (MVs). One example of the possible combinations of MVs in this distillation column is the vapor flow and the reflux flow (Skogestad 1997). Controlling the CVs via the MVs requires an optimization that is carried out by the control system. At a higher level of process control, the interaction of the CVs and the MVs need to be set such that the company obtains a positive revenue via operating the distillation process. At the macro level, economic objectives are translated to set-points and operating conditions of the distillation process. At the micro scale, keeping a single MV at a desired level requires precise sensor-control-actuator interaction.

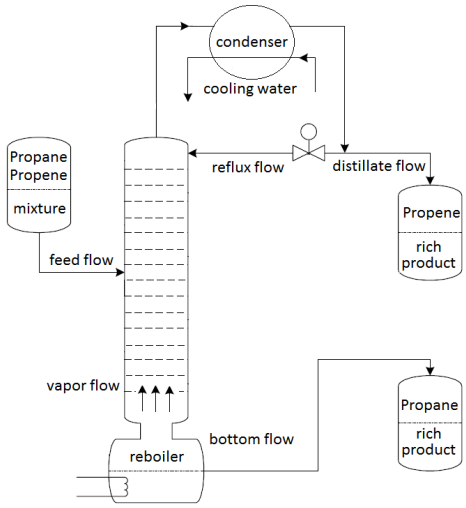

Figure 1.1: Process diagram of a distillation column.

The control mechanism in the process industry from the top to the bottom level is summarized in a hierarchical control scheme that is depicted in Fig.1.2. This hierarchical control scheme is a well established operational scheme in the process industry (Huesman 2011). The reason why a hierarchical control scheme is used instead of only a single centralized controller to steer the whole process is to cope with the different complexities and time scales of various elements and processes involved in the production facilities. It is nearly impossible in terms of both required knowledge and resources to design a single controller that is able to optimize the profit with respect to all aspects involved in the production process. Simultaneously, coping with all the economical, physical, and technical objectives would be a problem with daunting complexity needed to be solved with the fastest rate of variation in the system. Hence separation of these problems in term of time and scale becomes the only feasible mechanism applicable in the process industry. This has led to a distinguished set of layers in a control hierarchy for industrial processes which are defined as follows:

- *The scheduling and planning layer.*
  The top layer of this hierarchical scheme has the sole aim to maximize profit or the economic revenue of the process. This layer takes into consideration the demand of the market, the availability of the resources, and other economical constraints. From this information, the scheduling layer decides the target of the production: which production facilities (such as a single distillation column depicted in Fig. 1.1) should be operated, and which facilities need to undergo maintenance. The time scale of the scheduling and planning layer ranges from days to months.

- *The real-time optimization layer.*
  The role of the Real-Time Optimization (RTO) layer is to translate targets

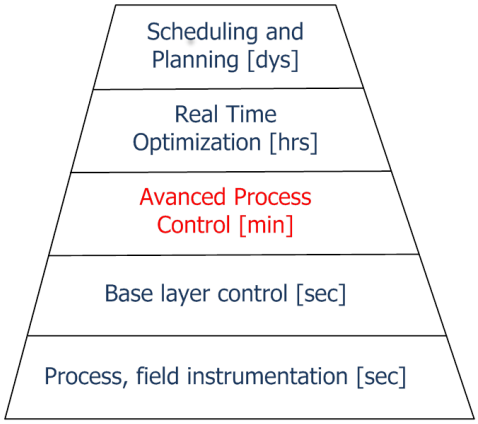

Figure 1.2: Process control hierarchy.

and criteria that are set at the scheduling layer into optimal operating points for the production units. In the distillation column example, the operating points are the desired purity level of the products or the CVs of the process. The time scale in this layer ranges from hours to days.

- *The advanced process control layer.*
  The Advanced Process Control (APC) layer, which is usually implemented in the form of a *Model Predictive Control* (MPC), tracks the operating point that is given by the RTO layer. To accomplish this task, the MPC calculates or determines the trajectories of the MVs of the process while respecting the operational constraints. The operational speed of the APC layer needs to be faster than the RTO to ensure that the targeted levels of the CVs are met before the RTO layer gives a new operating point. The time scale of the APC layer ranges from minutes to hours.

- *The base-layer control and field instrumentation layer.*
  The last layer of the hierarchy consists of two layers that are often considered as a single layer due to the interconnection between control-sensor-actuator components. This layer usually operates in a Distributed Control System (DCS) environment and has objectives such as reaching and maintaining the MVs that are requested by the APC layer. In the aforementioned distillation column example, this layer needs to control both the vapor and the reflux flows via controlling other variables in the process. The reflux flow is controlled by adjusting the cooling water in the condenser, while the vapor flow is controlled by adjusting the heat of the reboiler. Controlling this process is necessary since both variables can fluctuate easily as an effect of internal dynamics or outside disturbances. These two variables are usually controlled separately by a low-level controller that is implemented in the form of a *Proportional-Integral-Differential* (PID) controller. The time scale of the variables involved in this layer is smaller than the time scale of the APC layer and ranges from milliseconds to minutes.

For the past decades, this hierarchical process control scheme has served as the backbone of many controlled processes and production facilities in the process industry.

1.1.3 Current challenges in process control

The demand on plant-wide improvement, in terms of both quality and quantity of the products, results in the growing complexity of the chemical-mechanical processes and their corresponding production facilities. These conditions, along with the tighter economic margins, lead to various new challenges that are emerging in each layer of the process control hierarchy. The RTO layer needs to adjust the operating points of the production units depending on the market condition and the available resources. The APC layer needs to deal with tighter constraints originating from either mechanical-chemical operations and environmental regulations. The low-level controllers and the instrumentation need to operate more precisely to obtain faster and steadier responses of the process variables. The APC layer, which bridges the requirement from the upper layers to the capability of the bottom layers, is considered to be the most important layer as it eventually leads to a plant-wide improvement in the least costly manner if compared to other layers.

The APC layer can either hide or compensate the effect of the changes that are happening in other layers. Moreover, improvement of the APC layer can be achieved without conducting major changes in the design and operation of the plant. To implement changes in the base control and field instrumentation layer, one needs to either re-tune the low-level controllers or upgrade the instrumentation package of actuator-control-sensor devices since they usually come in one package. Re-tuning the PID controllers of this layer is nothing more than a regular maintenance procedure since it is almost impossible to achieve better performance than what the instrumentation is designed to accomplish. Replacing the existing instrumentation package with a more effective design in most cases is expensive. Additionally, to have a significant impact on the overall improvement of the plant operations, all field instrumentation need to undergo improvement. The condition of the base layer is relevant for the APC layer. Since the APC layer is governing all instrumentation at once, a well designed APC layer can take the current condition of the instrumentation into consideration so as to achieve the highest performance with the instruments. On the other hand, achieving improvement by adjusting the top layer of the hierarchy is not a trivial task. A cluster of production units or facilities in process industry usually already has a planned operation or a fixed design operation. Changing the way these facilities are operated will have an immediate impact on other layers. The RTO will then determine a different optimal trajectory for the CVs which might be complicated or difficult to track with the design of the lower layers. At the end, the APC layer and not the base layer that needs to find the best possible MVs on the basis of the instrumentation. So if the APC layer can not attain the operation point that is set by the RTO, the improvement of the plant operation cannot be achieved.

1.1.4 Performance variability of the APC layer

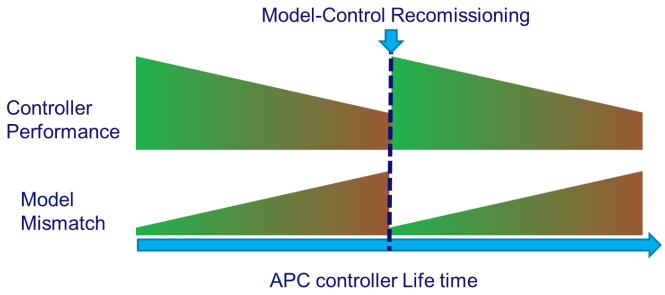

Figure 1.3: Illustration of APC performance versus time.

The importance of the APC layer has been motivated in the previous section. However, in practice, serious limitations of this layer can be observed with standard designs. To give an illustration, consider the example of the performance of a typical APC layer given in Fig. 1.3. It can be seen that the performance of the APC layer degrades over time. Such situation, which is also highlighted in Bauer and Craig (2008), is attributed to the growing discrepancy between the model used in the MPC implementation of this layer and the actual processes that need to be controlled. The model is not able to accurately describe the future behavior of the actual system anymore and has, therefore, a poor prediction capacity. Sources for the changes in the dynamics of the actual system are:

- Variability of raw materials: Wether its unintended or due to economical reasons, the materials that are used in a process may vary from time to time; e.g., variation on the feed composition of propane-propene mixture of the distillation column depicted in Fig. 1.1. Such change affects the mass-balance equation and hence the actual system dynamics.

- Inevitable aging of the plant and instrumentation: Any physical-mechanical equipment will eventually deteriorate; e.g. aging in the reboiler and the condensor of the distillation column depicted in Fig. 1.1, as well as degradation in the performance of sensors and actuators on any instrumentation.

- Change of operating point: Due to variations in the demand of the production (economical reason), the RTO might set operating points that are not considered when the model of the actual process is built. This leads to limited accuracy of the prediction.

- Effect of maintenance, process shutdown, and initialization: Due to the inherent nature of nonlinearity of the plant, each and every maintenance of production unit might slightly alter the dynamics of that plant. Accumulating effects of these changes can lead to a significant mismatch between the assumed model and the actual dynamics of the plant.

If the model of the process does not match with the actual dynamics, unwanted situations such as loss of disturbance attenuation, bad tracking performance, and eventually loss of stability of controlled the plant can occur. These situations, of course, were not intended at the time of the design of the APC. When the performance of the APC deteriorates, the operator of the process needs to shut down the APC layer and operate the process manually to avoid major damage of the equipment and to avoid further economic loss from the poor performance (Ozkan et al. 2016). Manual control is continued until the APC is recommissioned and becomes operational again with the updated condition of the process. The recommissioning procedure of the APC layer, that includes updating the model and re-tuning the controller, is an expensive and effortful procedure. The recommissioning is costly since the production facilities often need to be halted for some time to gather the necessary data for modeling and tuning the controller accordingly. The necessity of recommissioning the APC is usually avoided by re-tuning the controller parameters in a more aggressive fashion. By doing so, process operation is no longer optimal, safe, or efficient. This leads to a growing mismatch between the process behavior and its predictability. Improvement of the APC schemes, which can provide solutions for these situations, is the key topic of this thesis.

1.2 Research objective

The intricacy between the potential of plant-wide improvement that can be achieved by improving the APC layer and the inevitable performance degradation of the APC layer lead us to the formulation of the research objective of this thesis:

- Primary research objective -

Improve the performance of APC by taking into account model inaccuracy and variation of process dynamics that are causing the plant-model mismatch.

The results reported in this thesis were obtained in the European Union project named SMART. The goal of the project was to develop a set of breakthrough APC technologies aimed at drastically reducing *Total Cost of Ownership* (TCO) by means of more streamlined APC implementation and automatic maintenance. The return of capital investment in the APC technology can be made faster and its economic benefit can be sustained if periodic maintenance, which stem from the model inaccuracy, can be avoided or at most delayed. In order to pinpoint the key issues that need to be addressed to attain this goal, we provide detailed overview of the two main ingredients of the APC layer in the next section. These two fundamental elements are the MPC and the modeling approaches to obtain an accurate model of the process.

1.3 Literature survey

First, we provide an overview of the state-of-the-art and the current developments in both MPC and modeling approaches in the process industry. These observations serve as the basis to develop our proposed improvements of these technologies.

1.3.1 Model predictive control

We start with introducing the basic concept of MPC and then continue with the current development and application of MPC in the process industry. Afterwards, we investigate the current solutions and MPC schemes to deal with model inaccuracy.

Basic concept of MPC

MPC is a model based control technique that systematically deals with multivariable processes and process constraints so as to optimize a given performance criterion. The core concept of MPC is the so-called receding horizon principle (Maciejowski 2002; Rawlings and Mayne 2009). This principle is given in Figure 1.4.

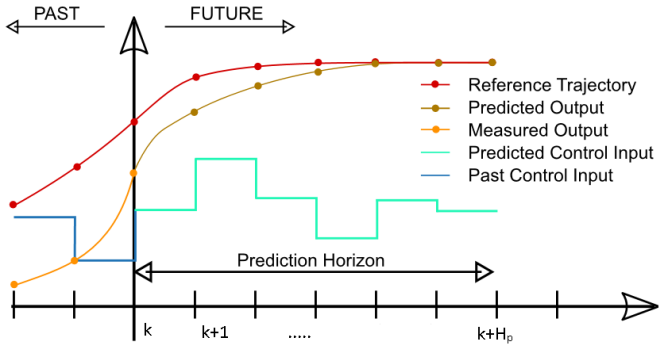

Figure 1.4: Illustration of receding horizon principle.

In general, the receding horizon principle means that at each time sample, a new control action (or the value of the MVs) is computed with respect to a prediction of future behavior and the available measurements of the plant. The control action is obtained by solving a constrained optimization problem that has the goal to regulate or to track a given set point/trajectory and to obey operational constraints. The future prediction is obtained from the model of the process. Since the parameters in the optimization problem are updated with respect to the current measurements at each time sample, the MPC is able to handle and reject disturbances in the processes. As a result of combining optimization, prediction of

future trajectories of the CVs, and current measurement, the MPC designs an optimal trajectory for the MVs to achieve the goal set by the RTO layer. An example of an MPC structure is illustrated in Figure 1.5.

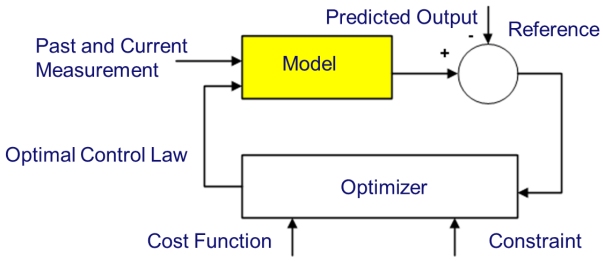

Figure 1.5: Core concept of an MPC scheme.

Theoretical development and application of MPC in the process industry

The extensive application and theoretical advancement of MPC have resulted in a vast amount of published methods. The earliest record on MPC coincides with the first application of MPC in the process industry. Over the years, various MPC schemes were developed starting from the ones using finite impulse response models (Richalet et al. 1978) to step response models (Cutler and Ramaker 1979) and afterwards transfer function models (Clarke et al. 1987). Lately, the state-space model has become the standard way of posing MPC problems. Via this representation, it is considerably easier to show and guarantee important properties such as recursive feasibility and stability (Mayne et al. 2000). Many review papers (Mayne (2014), Morari and Lee (1999)) and books (Maciejowski (2002),Rawlings and Mayne (2009),Grüne and Pannek (2011)) have been published at regular intervals. The latest review of Mayne (2014) gives an extensive overview of the latest developments, current challenges, and possible directions of research in MPC. The application of MPC is not restricted only to the process industry. Many successful applications of MPC have been reported in the area of power grids, rail networks, and the automotive industry (See Di Cairano (2012)).

In the process industry, numerous successful applications as well as recent developments are well captured in survey papers and books such as Qin and Badgwell (2003b) and Camacho and Alba (2013). Part of the success of MPC in the process industry is credited to three important aspects.

1. The first property is the systematic way to control *multivariable systems*. This property is present in most control schemes that belong to the "optimal control" category such as H_∞ control, Linear Quadratic Regulator (LQR), etc. These controllers take an explicit model of the multivariable system into account and produce optimal control actions by minimizing a control relevant cost function.

2. The second property is the *constraint handling* capability. MPC can handle inherent constraints such as physical or chemical constraints, or user defined constraints such as environmental constraints, safety constraint, etc. The explicit formulation of these constraints in the optimization typically results in tighter control action that drive the process closer to its boundary of operation.

3. The last property is related to the receding horizon principle. By re-evaluating the optimality of the control actions with respect to the current situation and updating the control sequences at every subsequent time sample, the MPC is able to reject disturbances and compensate for unwanted behavior.

Generally, one distinguishes two major types of MPC. These are Linear MPC and Nonlinear MPC. These two types are distinguished based on the type of prediction model. Although all the process and production facilities display nonlinear behavior, most of the industrial applications of MPC are Linear MPC. The reasons for this are the scale of industrial processes, fixed working point, and the limited amount of computation time until the next control action is required by the base level controller. The common optimization problem of a Linear MPC is a convex quadratic problem for which reliable algorithms are available that can solve the optimization problem in a timely manner. In addition, most applications to date have been in refineries (Qin and Badgwell 2003b), where the primary objective is to maintain the process at a desired steady-state (regulator problem), rather than moving rapidly from one operating point to another (servo problem).

The linear MPC, of course, has limitations. Problems such as regulatory control of a highly nonlinear process that is subject to large and frequent disturbances (pH control, etc.), or servo control where the operating point changes frequently and corresponds to a sufficiently wide range of nonlinear process dynamics (polymer manufacturing, ammonia synthesis, etc.) are proven to be challenging for linear MPC (Qin and Badgwell 2000). A prediction model that is based on a linear model of the process, is not sufficient to describe the actual system dynamics on the aforementioned problems. Resorting to a nonlinear MPC scheme, can sometimes be the only solution to remedy these problems. The price for using a nonlinear scheme are the considerably larger computational burden due to the non quadratic formulation of the control relevant cost function, loss convexity in the optimization, and the difficulties to obtain accurate nonlinear models.

MPC for uncertain systems

In the research objective of this thesis, it is stated that the core problem lies in dealing with the possible discrepancy between the plant and the model. The most popular way to incorporate possible discrepancy and plant-model mismatch is to consider uncertainty in the MPC design. While major aspects of nominal MPC are well understood, the performance and properties of MPC in the presence of uncertainty is still considered as a major challenge (Mayne 2014). In general, a well established way to overcome or reduce the effects of uncertainty is by applying feedback techniques. In many instances, robust control theory (Goodwin et al.

2000) provides sufficient tools for achieving robust operation. There are multiple techniques that are used to infuse robustness in an MPC scheme (Robust MPC), wether it comes from the deterministic point of view (worst case MPC in Kothare et al. (1996), tube based MPC in Mayne et al. (2011)) or the stochastic point of view (Kwon and Han 2006; Saltik et al. 2017). Important problems in RMPC schemes such as constraint satisfaction, stability, and performance are largely open and general consensus on incorporating uncertainty has still not been made. Moreover, guaranteeing robustness in MPC often leads to a considerably larger computational load when compared to the nominal schemes.

The problem of incorporating uncertainty in MPC is not only a theoretical one, but has also practical implications. Besides the computational load, inducing robustness properties often leads to a conservative control law at each time instant. For industrial applications, where the main goal is maximizing economic revenue, a conservative control method is less preferred, and robustness is mostly established in an ad-hoc manner (Mayne 2016). Another method to deal with growing plant-model mismatch is to incorporate an automated maintenance scheme for the MPC such as proposed in Tran et al. (2012). This work utilizes performance monitoring coupled by frequency domain controller matching to do online updates of the tuning variable of the MPC. However, the performance of the controlled process that can be augmented from this procedure is limited and subjected to the plant-model mismatch. If the uncertainty is not reduced, then there is a limitation on what robust model based controllers can achieve. Lastly, recent study of Rosolia and Borrelli (2018) explore possibility of using machine learning technique to handle uncertainty by iteratively constructing safety sets based on recent information of the system.

1.3.2 Modeling approaches to obtain prediction models

The prediction model is an integral part in an MPC scheme. In general, there are two approaches considered to obtain a prediction model. The first one is based on a first principle description of the process, while the second one relies on measurement data of the process. A comparison between both approaches in terms of the properties that are relevant for the understanding of plant-model mismatch is given after the description of each of these modeling approaches.

First principles based modeling approach

A first principle model is built from the combination of the mathematical, physical, and chemical relations along with the knowledge of the process. Due to diversity of physical laws and process knowledge involved in building such a model, the required amount of resources in both time and level of expertise can be enormous. If such a model is concisely built, the model can accurately describe variations of the dynamics in the process including a wide range of operating points. The resulting models from this approach tend to be very complex in terms of the total number of algebraic or differential equations in the model. In order to limit

the complexity and to some extent the required resources to build the model, the physics of the process are often chosen to be modeled only at the macro level. When linearized at a given operating condition, the complexity of the linearized model is attributed to the number of states, expansion coefficients, or polynomial terms for each particular representation. The complexity of the models can also be controlled by using model order reduction techniques (Beck et al. 1996). From the MPC point of view, the complexity of a first principle model can be disadvantageous. The computational load of the controller typically grows quadratically with respect to the complexity of the model in the linear MPC case and can grow exponentially in the nonlinear MPC case. For linear MPC schemes, a first principle model needs to be linearized in an operating point before it can be used as a prediction model. The applications of first principle models in MPC schemes can be found in Qin and Badgwell (2000). The models obtained via first principle modeling approaches are not only used for control purposes, but also for production planning, scheduling, and non-control related purposes such as training, predictive maintenance, etc.

Data driven modeling approach

Data-driven models are obtained from operational data of the process. The data can be gathered from a dedicated test or can be collected during online operation. From a data set inferred from the process, the model is constructed by using either system identification or parameter estimation techniques. A model that is derived using system identification techniques is usually compact, but its capability in terms of explaining the general dynamics of the process is limited. The first limitation comes from the model set/class that is inherently selected for the identification. The accuracy of the model depends on the model structure selection as well as the criterion used to obtain the model. The second limitation comes from the limited information that is available in the data set. At best, the model can only give an accurate description of the local behavior of the process corresponding to the operation recorded in the data set. A dedicated experiment is necessary to excite the process so as to extract the data that is also required to build an accurate model. From the MPC point of view, the inherent compactness of the model means that the complexity of the controller is implicitly bounded as well. The limited complexity of the process that can be explained by this modeling approach can lead to difficulties when doing a servo-based control task or if there are variations in the operating conditions. Applications of the MPC scheme where the prediction model uses a data-driven model can be found in Zhu (2001).

Comparison of the modeling approaches

Each of the aforementioned modeling approaches has its own merits and benefits in terms of addressing the growing plant-model mismatch problem. The properties of both modeling approaches are captured in Table 1.1. These properties are attributed to the richness or the capability of the model to describe a wide range

Table 1.1: Properties of modeling approaches.

	First Principle	**LTI Data Driven**
Validity	Global	Local
Complexity	Large	Small / controllable
Accuracy	Knowledge dependent	Data dependent
Requirement	Expertise	Experimental data

of operating conditions and the flexibility of the model to be changed when variation in the process is detected. First principle models are valid in a wider range of operating conditions when compared to data-driven based models. The data-driven modeling approach often aims to yield time-invariant models, assuming the extracted data to be sufficiently representing the future behavior of the actual system (Ljung 1999). If the process changes over time, this technique gradually yields a larger plant model mismatch. If the flexibility of the model is being compared, the structure of the first-principle model is rigid and cannot be adjusted as easily as the data-driven model. The structure of data-driven models can be changed based on the model set selection. There are many cases where an adjusted model set can better explain additional data records from the system. This situation might occur since there are changes in operation or physical structure of the system whether they are accounted for or not. Last but not least, we need to consider the effort of obtaining the model. Building accurate first principle models requires more resources, both in terms of time and knowledge, compared to a data driven model. However, in order to obtain an accurate data-driven model, one might have to give extra excitation to the system to get information about the dynamical behavior of the system. The excitation signals need to be designed are subject to many constraints on duration, incurred economic loss, safety, and richness for identifying parameters (Zhu et al. 2013; Bombois and Scorletti 2012). This can be seen as the cost of the data-driven method. In industrial practice, the resulting identified models tend to be more accurate than first principle model.

1.4 Research questions

From the survey given in Section 1.3, it is clear that solving performance deterioration of the APC layer that is caused by a growing discrepancy between the actual process and prediction model is an open problem. Available methods for handling such discrepancy, from either a deterministic (RMPC schemes) and stochastic (Scenario and Risk based MPC scheme) point of view, are not widely accepted by the industry. These methods are similar in the sense that they aim to solve the discrepancy between model and plant by assuming that the mismatch is an uncertainty whose magnitude can reliably be handled by a (robustly performing) controller. They are also similar in the sense that the discrepancy persists over time, where no adaptation to the plant model and no adaptation to the APC are implemented. This leads to sub-optimal control actions where the control performance can fall short of expectations. From these facts, we can see that reducing

plant-model discrepancy while preserving or adapting the controller is the key point of augmenting the performance of the APC layer. This statement leads us to the research question of this thesis:

- Primary research question -

How to reduce the discrepancy between the prediction model in MPC and the process of interest so as to sustain high performance of the controller? In particular, how and when should the update of the controller and model take place?

In order to provide an answer to the research question, we structure and divide the research question into several subquestions. These subquestions are given as follows:

1. What are the sources of the discrepancy between the plant and the model? What is the efficient way to handle it from a control point of view?
2. What are the resources that can be used to reduce this discrepancy? How to effectively utilize these resources for this purpose?
3. How to mitigate any possible negative effect (stability and performance degradation of the controlled system) caused by the discrepancy?

We describe the proposed answers to these sub-questions in the next section on research methodology.

1.5 Research methodology and thesis outline

In this section, we reveal our proposed methodologies to answer the subquestions that are listed in Section 1.4. Subquestion 1 is addressed in Section 1.5.1 while Subquestion 2 is addressed in Section 1.5.2 and Section 1.5.3. Section 1.5.4 addresses the problem that is posed in Subquestion 3. The proposed methodologies are referenced to their corresponding chapters of this thesis. Since the chapters interlink with each other, the exact relation between each of the chapters along with the contributions of this thesis are given at the end of this section

1.5.1 Sources of discrepancy between plant and prediction model

Uncertainty and inaccuracy in modeling are unavoidable. The first subquestion is the initial step to address the discrepancy between the plant and the model. In practice, the dynamics of the actual system are never fully understood and may vary over time. In the survey of Takatsu et al. (1998), the most cited source of the modeling inaccuracy is the continuous change in the operating conditions.

As the model inaccuracy grows, the synthesized controller encounters reduced potential to provide appropriate control actions to satisfy the control task. We can distinguish the following changes that occur in the plant:

a. Unknown and unmeasurable changes, when undetected changes or failures occur in the process.

b. Known and measurable changes, where the changes are based on known and measurable parameters whose values vary. Specifically, these include scheduled changes of operating conditions.

The MPC, particularly the prediction model, need to be equipped to handle or reduce plant-model mismatch with respect to these two types of changes. In Section 1.3.2 we mentioned and compared two modeling approaches. From the comparison, it can be seen that data-driven modeling methods have the upper hand to handle these two type of changes. A data-driven model can be easily modified for this purpose. Indeed, a data-driven model has a limiting factor of a small range of validity due to the often used linear structure of the model. However, there are existing frameworks where one enriches the linear structure in the model with possible variations in its parameters. Some successful frameworks are the *Linear Time-Varying* (LTV) systems (Zerz 2006) and *Linear Parameter Varying* (LPV) systems (Tóth 2010). These two frameworks offer powerful system representations to incorporate each of the aforementioned changes that can occur in the plant. Possible utilization of these frameworks to limit and possibly reduce the model inaccuracy is the answer to Subquestion 2 and is described in the next subsection.

1.5.2 Reducing plant-model mismatch by system identification

In the operation of a process or a production facility, the available information that can be used to handle the discrepancy are the blueprint of the facilities and offline or online data about physical-chemical quantities that are measured. From a data-driven modeling perspectives, the data can be used to model the system behavior and update the models if necessary. In order to utilize this information, we propose to use the framework of system identification. The main goals of utilizing the system identification framework are to bound, shape, and reduce model inaccuracy or uncertainty. The system identification framework consists of approaches on experiment design, data processing, model structure and criterion selection, model validation and residual analysis (Ljung 1999). The framework allows us to characterize model uncertainty with respect to measurement and process noise affecting the data set and guarantee asymptotic convergence of the model estimate to the true system dynamics under mild conditions such as persistency of excitation in the data set and that the system of interest lies in the selected model set.

In this thesis, system identification is used with two different model classes which correspond to capturing different sources of discrepancy between plant and the model that are mentioned earlier in Section 1.5.1. The first one is the *Linear Time-Varying* (LTV) case, where system identification is used in an iterative

manner to capture unknown changes happening in the plant. The applied system identification procedure is the same as in LTI system identification where the identification can be done in either a direct or a recursive fashion. The second approach is *Linear Parameter-Varying* (LPV) identification (Tóth 2010). For the LPV case, the identification is conducted in either a global or local identification of the parameter varying model. For both modelling approaches, the capability of each of the techniques to bind and shape the uncertainty of the model depends on the selection of the model structure. Moreover, the model structure itself has a direct impact on the following control synthesis step and the resulting closed-loop dynamics. In the next subsection, we describe the selected model structure and motivate our selection.

1.5.3 Capturing changes by OBF-based model structures

We need to have a model structure that is capable of describing a system on its designed operating regime with a relatively simple, low complexity parametrization. One possible way to achieve this structure is by using a *Finite Impulse Response* FIR model structure. It is known that the FIR representation can capture any stable linear system if a long enough expansion is considered (Franklin et al. 1990). However, the numerous expansion coefficients may lead to variance issues and hence a problem with model uncertainty. The candidate modeling approach needs to be able to describe a wide range of systems on the designed operating regime while only minimally affected by the bias and variance of the resulting model estimates. Fortunately, there exists a particular model structure that possesses both qualities. This model structure is based on *Orthonormal Basis Functions* (OBF) (Ninness and Gustafsson (1997),Heuberger et al. (2005)).

The capability of the OBF model structure as a general approximator of nonlinear systems is shown in Boyd and Chua (1985). The utilization of OBF to describe nonlinear systems fit both the LTV and LPV frameworks that we propose to handle changes in the plant. Moreover, an OBF-based model structure has attractive properties from the system identification point of view such as favorable tradeoff between bias and variance and linearity in its parameters. These properties are reinforced by a proper selection of the basis functions. The basis function selection also provides a mechanism for incorporating prior information (blueprint) of the system in the model. By properly selecting the basis functions we can shape the richness of the model in the sense of describing possible changes that are probable in the plant. Moreover, the basis selection also serves as a tuning knob from the perspective of controller design to adjust the complexity of the model of the plant. The basic theory of OBF is provided in Chapter 2 while the basis selection procedure is given in Chapter 3. In the next subsection, Subquestion 3 of the research question is addressed.

1.5.4 OBF-based MPC schemes

In our attempt to reduce the discrepancy between the plant and the model, the parameters of the OBF model are going to vary. The variation of the model leads

to the variation of the closed-loop system which can jeopardize the control performance. In some extreme cases, closed-loop stability may be lost. Hence, we need to ensure that the implementation of OBF models to handle plant-model mismatch leads to minimum effect on the MPC controller. Unfortunately, the literature on the implementation of OBF-based prediction models in an MPC scheme is minimal. The work of Douik et al. (2007) utilizes an OBF-based prediction model in an RMPC scheme. Another work of Patwardhan et al. (2006) and their series of papers utilize OBF for either state observers or fault diagnosis purposes. The possible advantages of using an OBF-based predictor model to handle plant-model discrepancy and to ease the MPC design are not considered in these works. Besides being used in the prediction model, the OBF framework can be used to parameterize the synthesized input for MPC (Wang (2009) and van Donkelaar (2000)). This input parameterization is used to achieve infinite horizon prediction property.

In our proposed OBF-based MPC scheme, we aim to reduce the discrepancy between the plant and the model so as to sustain high performance of the controller. It is mentioned in the previous subsections that two different frameworks of LTV and LPV systems are used to handle different type of changes which are the unknown and unmeasurable changes and the known and measurable changes. These two frameworks lead to two different MPC schemes which are the LTV-OBF MPC scheme and the LPV-OBF MPC scheme. Each of these two schemes is coupled with different system identification procedures and each of them is described in details in separate chapters of this thesis. In the LTV case, system identification is conducted iteratively to update the parameters of the OBF prediction model. Furthermore, we guarantee crucial controller properties such as closed-loop stability and performance. These are described in details in Chapter 4. In the LPV case, we consider a predetermined change in the predictor model by constructing an LPV model that explicitly captures the system dynamics in the designed operating regime. The MPC scheme needs to handle the predetermined changes in the model. A detailed description of the LPV-OBF MPC scheme can be found in Chapter 5. Although OBF models can be used to model unstable systems (Tóth 2010), we restrict ourselves to predictive control formulation for stable processes. If the process under consideration has unstable modes, it is assumed that these modes are stabilized by feedback. Lastly, we demonstrate our proposed MPC scheme in industrially relevant case study in Chapter 6.

1.5.5 Outline and contribution of the thesis

The remaining chapters of this thesis are organized in the following way: Chapter 2 provides preliminary material on notation and mathematical background. Chapter 2 also gives a brief introduction into the theory on OBFs and basis selection. The main contributions are given in Chapters 3, 4, 5, and 6 and the relation between the chapters is depicted in Figure 1.6. The arrowed line indicates how the chapters are linked with the other chapters, while the dashed line shows the theories that support parts within the chapters.

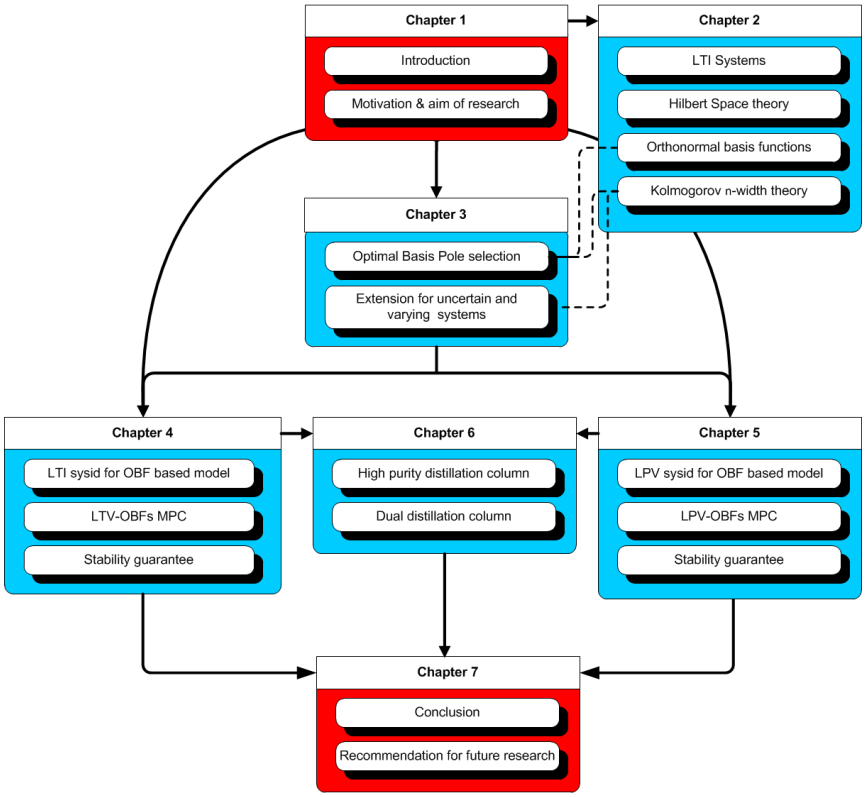

Figure 1.6: Thesis content.

2 CHAPTER

Preliminaries

This chapter is devoted to providing an overview of established theories and their respective notations that are used throughout this thesis. This chapter starts with a brief description of linear time-invariant (LTI) systems and their representations. In Section 2.3, the concepts of linear time-varying (LTV) and linear parameter-varying (LPV) systems as extensions of the class of LTI systems are introduced. In Section 2.4, fundamental concepts from Hilbert space theory are given. These basics and definitions are important as fundamental knowledge to introduce the concepts and descriptions related to orthonormal basis functions (OBF).

2.1 Linear Time-Invariant systems

In this thesis, we adopt the viewpoint where systems are considered as operators that map input signals to output signals. In the adopted framework, it is assumed that it has been decided which signals are inputs and which are outputs. This decision depends on the prior knowledge of the application regarding the cause and effect of those signals. In the process industry, the input signals are often referred to as the *Manipulated variables* (MV's), and the output signals are also known as the *Controlled variables* (CV's). The input-output signals are usually represented as continuous time signals (defined on $\mathbb{R}$ or $\mathbb{R}_{[0,\infty)}$) or discrete time signals (defined on $\mathbb{Z}$ or $\mathbb{Z}_{[0,\infty)}$) . Most signals related to real world applications are continuous time signals. However, to enable processing of such signals in the digital environment, they are usually discretized or sampled at equidistant time instants. From Shannon's sampling theorem (Åström and Wittenmark 1990), we learned that as long as the frequency content of the continuous time signal is band limited, the continuous signal can be recovered from its discrete-time samples without approximation loss provided that the sampling time is small enough.

Throughout this thesis, both the input signal $u \in \mathbb{U}^{\mathbb{Z}}$ (where the time sample $u(k)$ belongs to the input signal space $\mathbb{U} \subseteq \mathbb{R}^{n_u}$) and the output signal $y \in \mathbb{Y}^{\mathbb{Z}}$

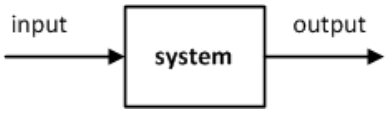

Figure 2.1: LTI System

(where the time sample $y(k)$ belongs to the output signal space $\mathbb{Y} \subseteq \mathbb{R}^{n_y}$) are considered to be infinite sequences:

$$u := \{u(k)\}_{k=-\infty}^{k=\infty}, \tag{2.1}$$

$$y := \{y(k)\}_{k=-\infty}^{k=\infty}, \tag{2.2}$$

with $k \in \mathbb{Z}$. System G governs the mapping between the input signal space to the output signal space

$$G : \mathbb{U}^{\mathbb{Z}} \to \mathbb{Y}^{\mathbb{Z}}. \tag{2.3}$$

We call system 2.3 linear if G is a linear map and time invariant if time shifted inputs produce the same outputs shifted in time, i.e. $q^\tau G = G q^\tau, \forall \tau$ with q the forward shift operator, and q^τ corresponds to $q^\tau u(k) := u(k + \tau)$. In this thesis, we only consider discrete time causal systems, i.e. the output $y(k)$ of a system measured at time k does not depend on future inputs $u(k + n)$ at $k + n$ for any $n > 0$. Depending on the dimension of the signals, the system is called a

- SISO (single-input, single-output) system: if both input and output signals are scalar: $n_u = 1; n_y = 1$.
- SIMO (single-input, multi-output) system: if the input signal is scalar while the output signal is multivariable: $n_u = 1; n_y > 1$.
- MISO (multi-input, single-output) system: if the input signal is multivariable while the output signal is scalar: $n_u > 1; n_y = 1$.
- MIMO (multi-input, multi-output) system: if both input and output signals are multivariable: $n_u > 1; n_y > 1$.

Remark 2.1 *It is worth to mention that there are other viewpoints that consider implicit system definitions. One of the examples is the behavioral approach that considers all signals involved in a given system as collections of trajectories of the respective system without an a priori distinction between inputs and outputs (Polderman and Willems 1991).*

2.2 Representations of LTI system

Three system representations of LTI systems are considered in this thesis. The representations are the series expansion representation, the transfer function representation, and the state-space representation. Although the systems of interest

in this thesis, in general, are MIMO systems, for simplicity and introductory purpose, the representations presented in this section are given in the SISO form. The MIMO formulation of a system is further treated in Section 2.5 along with the introduction of *Orthonormal Basis Functions* (OBF).

2.2.1 Series expansion representation

The series expansion representation expresses the linear and causal mapping between input and output as:

$$y(k) = \sum_{\tau=0}^{\infty} g(\tau)u(k-\tau), \quad k \in \mathbb{Z}, \tag{2.4}$$

where the output signal at time k is a convolution of the input signal with the sequence $g(\tau) \in \mathbb{R}$. Since only causal systems are considered in this thesis, we have $g(\tau) = 0$ for $\tau < 0$ and thus the convolution (2.4) is written only with respect to past input sequences. The function g is called the impulse response of the system as it is equal to the output y of the system given an input u of a unit pulse:

$$u(k) = \delta(k) := \begin{cases} 1, & \text{if } k = 0; \\ 0, & \text{if } k \neq 0; \end{cases}$$

If g has no compact support, then (2.4) is known as an *Infinite Impulse Response* (IIR) representation. When g has a compact support, then (2.4) is called a *Finite Impulse Response* (FIR) representation. For the latter, there exists an $n > 0$ such that (2.4) is equivalent with

$$y(k) = \sum_{\tau=0}^{n} g(\tau)u(k-\tau), \quad k \in \mathbb{Z}, \tag{2.5}$$

where n is the *length* of the impulse response.

2.2.2 Transfer function representation

The transfer function representation of system G expresses the relation between the input and the output signals in the frequency domain $z \in \mathbb{C}$:

$$U(z) := [\mathcal{Z}(u)](z) = \sum_{k=-\infty}^{\infty} u(k)z^{-k} \tag{2.6}$$

$$Y(z) := [\mathcal{Z}(y)](z) = \sum_{k=-\infty}^{\infty} y(k)z^{-k}, \tag{2.7}$$

where $\mathcal{Z}$ denotes the z-transform operator and $z \in \mathbb{C}$ is any complex number for which the infinite series (2.6) or (2.7) converge. The set of all $z \in \mathbb{C}$ for which

(2.6) or (2.7) are well defined as an infinite series expansion are called the *region of convergence*, i.e. $\mathcal{R}(u) \subseteq \mathbb{C}$ and $\mathcal{R}(y) \subseteq \mathbb{C}$. The z-transform leads to a frequency domain representation of the system, where $G := \mathcal{Z}(g)$ governs the relation of the frequency spectrum of the input $U(z)$ and output $Y(z)$ according to

$$Y(z) = G(z)U(z), \tag{2.8}$$

with

$$G(z) = [\mathcal{Z}(g)](z) = \sum_{\tau=-\infty}^{\infty} g(\tau)z^{-\tau}, \tag{2.9}$$

where $z \in \mathbb{C}$ and $G(z)$ is the z-transform of the impulse response (2.4).

In general, the transfer function representation of a system consists of ratios of finite order polynomials in $z \in \mathbb{C}$:

$$G(z) = \frac{\sum_{i}^{l} n_i z^i}{\sum_{j}^{m} d_j z^j}, \tag{2.10}$$

where $n_i \in \mathbb{R}, \forall i = \{1, \ldots, l\}$ and $d_j \in \mathbb{R}, \forall j = \{i, \ldots, m\}$. If the coefficients of the numerator and denominator polynomials are real, then the transfer function is called real-rational. The values of z that result in a zero numerator are known as the zero(s) of the system, while the values that lead to a zero valued denumerator are known as the pole(s) of the system. Poles of a system dictate that the output response of the system is composed from specific exponential trajectories. The zeros of a system describe the frequencies at which the input does not contribute to the output. A system is called *proper* if $\lim_{z\to\infty} G(z) < \infty$. If $\lim_{z\to\infty} G(z) = 0$, then the transfer function is called *strictly proper*.

2.2.3 State-space representation

The state-space representation of system G is defined as:

$$x(k+1) = Ax(k) + Bu(k), \tag{2.11}$$
$$y(k) = Cx(k) + Du(k), \tag{2.12}$$

with $A \in \mathbb{R}^{n_\mathrm{x}\times n_\mathrm{x}}, B \in \mathbb{R}^{n_\mathrm{x}\times n_\mathrm{u}}, C \in \mathbb{R}^{n_\mathrm{y}\times n_\mathrm{x}}, D \in \mathbb{R}^{n_\mathrm{y}\times n_\mathrm{u}}$. A state-space representation with matrices A, B, C, D is a state-space realization of the transfer function (2.9) if

$$G(z) = D + C(zI - A)^{-1}B, \tag{2.13}$$

while its impulse response coefficients satisfy

$$g(\tau) = \begin{cases} D, & \tau = 0; \\ CA^{\tau-1}B, & \tau > 0; \\ 0, & \tau < 0. \end{cases} \tag{2.14}$$

Note that a representation of a MIMO system in a state-space form has a more intuitive formulation compared to the previous two representations. A state space realization is called a minimal realization of $G(z)$ if the state dimension n_{x} is minimal among all possible realizations of $G(z)$.

2.2.4 BIBO stability

One of the most commonly used stability notions for proper finite dimensional LTI systems is the notion of *Bounded-Input-Bounded-Output* (BIBO) stability. Systems that are BIBO stable produce a uniformly bounded output when a uniformly bounded input is applied. Formally, this means that for any $u \in \ell_2$, (space of square summable sequences) we have

$$y = Gu \in \ell_2 \tag{2.15}$$

and the corresponding ℓ_2 gain of the system $G : \ell_2 \to \ell_2$, defined as

$$\|G\|_2 = \sup_{u \in \ell_2} \frac{\|Gu\|_2}{\|u\|_2}, \tag{2.16}$$

is finite. So, in particular, $\|y\|_2 \leq \|G\|_2 \|u\|_2$ for any input $u \in \ell_2$. The norm $\|.\|_2$ is also called the induced norm of the system over the ℓ_2 spaces. Fundamental descriptions of these function spaces, inner product, and induced norm can be found in Section 2.4.

2.3 Linear Time-Varying and Linear Parameter-Varying systems

An LTI system assumes the same linear relation between input and output sequences for all time instances. However, almost all chemical-mechanical processes in the process industry are by nature nonlinear and are subject to time-varying effects. This means that a rigid model description by an LTI representation can become obsolete after a period of time. A known method to tackle this variability while still preserving linearity between the input-output relation is to allow variations in the model parameters. The variation itself can, in general, be divided into two types. The first one is when the cause of the variation is unknown but the parameters are changing with respect to time. Such system classes are denoted as Linear Time-Varying (LTV) systems (Zerz 2006). The second perspective considers known sources of the time-varying changes in the parameters of the system. The parameter changes are governed by *scheduling variables*. Systems that fall in this category are called Linear Parameter-Varying (LPV) systems (Tóth 2010).

2.3.1 General description of LTV and LPV systems

The interpretation of the variation in the linear dynamics can be made from the perspective of a time-variant impulse response. The impulse response of both

LTV and LPV systems are not restricted to be invariant over time and can possibly change at different time instances. For the LTV case we have:

Definition 2.1 *The output of a linear time-varying system $\mathcal{F}$ can be written as:*

$$y(k) = \sum_{\tau=0}^{\infty} g_k(\tau)u(k-\tau), \quad k \in \mathbb{Z} \tag{2.17}$$

where the input-output mapping at time k is governed by the parameterized impulse response $g_k(\tau)$.

Note that dependence of g_k in (2.17) on the time index k expresses the variation of the impulse response. By our consideration, this variation may happen for every value of k and can be piecewise constant or triggered by conditions of the process. For the LPV case we have:

Definition 2.2 *Let $p : \mathbb{Z} \to \mathbb{R}^{n_p}$ be a mapping called scheduling variable. We consider $\mathcal{S}$ to be a linear parameter-varying system if the output can be written as:*

$$y(k) = \sum_{\tau=0}^{\infty} g(p(k), \ldots, p(k-\tau), \tau)u(k-\tau), \quad k \in \mathbb{Z}, p(k) \in \mathbb{R}^{n_p} \tag{2.18}$$

where the input-output mapping depends the whole trajectory [1] of the scheduling variable $p(k)$. The parameter-varying impulse response of the system is denoted by $g(p(k), \ldots, p(k-\tau), \tau)$.

The major difference between the LTV and LPV case is how their impulse response are characterized. This difference originates from the knowledge on what is causing the change in the dynamics of the system. In (2.17), the source of the change is unknown in most cases, and hence the relation between different impulse responses for different time indices are not given explicitly. In contrary, the relation of impulse responses of (2.18) are explicitly described as a function of the scheduling variable $p(k)$.

2.3.2 Momentary description of LTV and LPV systems

A momentary frequency domain interpretation of LTV and LPV systems can be obtained directly from the z-transformation of their momentary impulse responses. If the function $g_k(\tau)$ in (2.17) is z-transformed into the frequency domain, we obtain a transfer function for each index time k.

[1] This general form of LPV systems is also known to have *dynamic dependence*, i.e., dependence on $p(k), \ldots, p(k-\tau)$ at index τ.

Definition 2.3 *The time-varying momentary transfer function representation associated with* (2.17) *is written as:*

$$G_k(z) = [\mathcal{Z}(g_k)](z) = \sum_{\tau=-\infty}^{\infty} g_k(\tau) z^{-\tau}. \tag{2.19}$$

If the function $g(p(k), \ldots, p(k-\tau), \tau))$ in (2.18) is z-transformed into the frequency domain, we obtain a transfer function that depends on the trajectory $p(k)$, $\ldots, p(k-\tau)$.

Definition 2.4 *The parameter-varying momentary transfer function representation associated with* (2.18) *is written as:*

$$G(p, k, z) = [\mathcal{Z}(g(p, k))](z) = \sum_{\tau=-\infty}^{\infty} g(p(k), \ldots, p(k-\tau), \tau) z^{-\tau}. \tag{2.20}$$

Note that (2.19) qualifies as a frequency response of the LTV system $\mathcal{F}$ in the sense that $y(k) = [\mathcal{Z}^{-1}\{G_k U\}]_k$. Thus, if $u(k) = \sin(\omega_o k)$ with $\omega_o \in [-\phi, +\phi]$ then the response is $y(k) = G_k(e^{j\omega})\sin(\omega_o k + G_k(e^{j\omega}))$. Note as well that the use of "G_k" as a notation for the momentary transfer function of $\mathcal{F}$ is used to emphasize that it corresponds to the transfer function of an LTI system G_k that momentary describes the dynamics of $\mathcal{F}$ at time moment k. Observe that $g_k(\tau) = g(p(k), \ldots, p(k-\tau), \tau)$ provided that the whole trajectory of p is known. In that case $G_k(z) = G(p, k, z)$ for all k, z.

2.3.3 Frozen description of LTV and LPV systems

Now we introduce the concept of *frozen* description which capture the linear dynamics of either an LTV system $\mathcal{F}$ for a given time instance or an LPV system $\mathcal{S}$ for a given value of the scheduling variable.

Introduce a time-varying state-space representation:

$$\begin{array}{ll} x(k+1) & = A_k x(k) + B_k u(k), \\ y(k) & = C_k x(k) + D_k u(k), \end{array} \tag{2.21}$$

where $A_k \in \mathbb{R}^{n_{\mathrm{x}} \times n_{\mathrm{x}}}, B_k \in \mathbb{R}^{n_{\mathrm{x}} \times n_{\mathrm{u}}}, C_k \in \mathbb{R}^{n_{\mathrm{y}} \times n_{\mathrm{x}}}, D_k \in \mathbb{R}^{n_{\mathrm{y}} \times n_{\mathrm{u}}}$. Now, for a fixed k, the corresponding impulse response of (2.21) is given as follows::

$$\tilde{g}_k(\tau) = \begin{cases} D_k, & \tau = 0; \\ C_k A_k^{\tau-1} B_k, & \tau > 0; \\ 0, & \tau < 0. \end{cases} \tag{2.22}$$

Note that (2.22) represent the impulse response of the LTI system $(A_k, B_k\ , C_k, D_k)$ at time moment k if k would be frozen (not varying anymore). If the function $\tilde{g}_k(\tau)$ in (2.22) is z-transformed into the frequency domain, we obtain a frozen transfer function for each index time k.

Definition 2.5 *The time-varying frozen transfer function representation associated with* (2.17) *is written as:*

$$\tilde{G}_k(z) = [\mathcal{Z}(\tilde{g}_k)](z) = \sum_{\tau=-\infty}^{\infty} \tilde{g}_k(\tau) z^{-\tau}. \tag{2.23}$$

where impulse response of $\tilde{g}_k$ is identical for all k.

Note the subtle difference between g_k of (2.17) is and $\tilde{g}_k$ of (2.23) which is described in the following corollary.

Corollary 2.1 *In general*

$$g_k(\tau) \neq \tilde{g}_k(\tau), \tag{2.24}$$

since

$$g_k(\tau) = C_k\big(\prod_{l=1}^{\tau-1} A_{k-l}\big) B_{k-\tau} \;\; \textit{for} \;\; \tau > 0. \tag{2.25}$$

However, as soon as the variation in the system dynamic over time becomes slow, the difference between the momentary and the frozen transfer function becomes negligible.

Similarly, a *frozen* description of the dynamics can be introduced in the parameter-varying case. Consider a parameter-varying state-space representation[2]:

$$\begin{array}{ll} x(k+1) & = A(p(k))x(k) + B(p(k))u(k), \\ y(k) & = C(p(k))x(k) + D(p(k))u(k), \end{array} \tag{2.26}$$

where $A(p(k)) \in \mathbb{R}^{n_{\mathrm{x}} \times n_{\mathrm{x}}}, B(p(k)) \in \mathbb{R}^{n_{\mathrm{x}} \times n_{\mathrm{u}}}, C(p(k)) \in \mathbb{R}^{n_{\mathrm{y}} \times n_{\mathrm{x}}}, D(p(k)) \in \mathbb{R}^{n_{\mathrm{y}} \times n_{\mathrm{u}}}$. The corresponding frozen impulse response of (2.26) is given as follows:

$$\tilde{g}(p(k), \tau) = \begin{cases} D(p(k)), & \tau = 0; \\ C(p(k)) A^{\tau-1}(p(k)) B(p(k)), & \tau > 0; \\ 0, & \tau < 0. \end{cases} \tag{2.27}$$

Again, (2.27) represent the impulse response of the LTI system $(A(p(k)), B(p(k))$ $, C(p(k)), D(p(k)))$ at time moment k if $(p(k))$ would remain constant (not varying with time k). If the function $\tilde{g}(p(k), \tau)$ in (2.27) is z-transformed into the frequency domain, we obtain a transfer function for each index time k.

Definition 2.6 *The parameter-varying frozen transfer function representation associated with* (2.17) *is written as:*

$$\tilde{G}(p(k), z) = [\mathcal{Z}(\tilde{g}(p(k)))](z) = \sum_{\tau=-\infty}^{\infty} \tilde{g}(p(k), \tau) z^{-\tau}. \tag{2.28}$$

where impulse response $\tilde{g}(p(k), \tau)$ depends only on the instantaneous value of scheduling variable $p(k)$.

[2]Eq (2.22) corresponds to a wider class of systems that can be represented by (2.26). For a general form of LPV-SS representations refer to (Tóth 2010)

The difference between momentary and frozen parameter-varying description is captured in the following corollary:

Corollary 2.2 *In general*

$$g(p(k),\ldots,p(k-\tau),\tau) \neq \tilde{g}(p(k),\tau), \tag{2.29}$$

since

$$g(p(k),\ldots,p(k-\tau),\tau) = C(p(k))\big(\prod_{l=1}^{\tau-1} A(p(k-l))\big)B(p(k-l)) \;\; \textit{for} \;\; \tau > 0. \tag{2.30}$$

However, as soon as the scheduling variable p becomes slowly varying or constant[3]*, the difference between the momentary and the frozen transfer functions become negligible.*

Both transfer functions (2.28) and (2.23) give a snapshot of the linear dynamics for a given time or value of the scheduling variable. The state-space representations of the LTV and LPV systems ((2.21) and (2.26)) are further used for prediction models in our proposed MPC schemes. More detailed description of the prediction model and how they are handled in system identification, are mentioned in their corresponding chapters (Chapter 4 for LTV systems and Chapter 5 for LPV systems).

Remark 2.2 *It is worth to note that the transformation between equivalent representations in case of LTV and LPV systems is far from trivial. We refer to Zerz (2006); Tóth (2010) for more detailed descriptions on how to conduct transformations as well as their consequences for both types of systems. In this thesis, we defined the representations as the mathematical setting for our proposed solutions, and we do not explore or utilize the transformations between these representations.*

2.4 Basics of Hilbert space theory

This section contains material on Hilbert spaces that are important in the context of this thesis. This material covers a number of basic descriptions and definitions such as the inner product, orthogonality, sets, and basis functions in a Hilbert space. Afterwards, special attention is given to a particular Hilbert space which is a Hardy space of stable transfer functions.

2.4.1 Fundamental definitions of a Hilbert space

A Hilbert space $\mathcal{H}$ is a linear vector or function space that is equipped with an inner product (Kreyzig 1978). The inner product induces a norm in a Hilbert space which makes the Hilbert space also a normed space. Definitions are given as follows:

[3] A constant scheduling variable is a subclass of possible scheduling trajectories.

Definition 2.7 *An inner product on a vector space $\mathcal{X}$ is a bilinear functional $\langle . \ , . \rangle : \mathcal{X} \times \mathcal{X} \to \mathbb{R}$ with the properties*

1. *Linearity $\langle \alpha_1 f_1 + \alpha_2 f_2, g \rangle = \alpha_1 \langle f_1, g \rangle + \alpha_2 \langle f_2, g \rangle, \forall \ \alpha_1, \alpha_2 \in \mathbb{R}$.*
2. *Symmetry $\langle f, g \rangle = \langle g, f \rangle$.*
3. *Positivity $\langle f, f \rangle \geq 0$ and $\langle f, f \rangle = 0 \iff f = 0$.*

A vector space $\mathcal{X}$ that is equipped with an inner product is an inner product space denoted by $(\mathcal{X}, \langle . \ , . \rangle)$.

Definition 2.8 *An inner product space $(\mathcal{X}, \langle . \ , . \rangle)$ defines a normed space $(\mathcal{X}, \|.\|)$ with norm $\|f\| := \langle f \ , f \rangle^{\frac{1}{2}}$.*

The *Cauchy sequence* is defined as follows:

Definition 2.9 *A Cauchy sequence in $\mathcal{X}$ is a sequence $\{f_k\}_{k=1}^{\infty}, f_k \in \mathcal{X}$ with the property that $\lim_{k,l \to \infty} \|f_k - f_l\| = 0$.*

A Hilbert space is defined as follows:

Definition 2.10 *A Hilbert space $\mathcal{H}$ is an inner product space that is complete in the sense that every* Cauchy sequence *in $\mathcal{H}$ attains a limit belonging to $\mathcal{H}$ (converges to an element in $\mathcal{H}$).*

In a Hilbert space, a measure of similarity between its elements is characterized by the inner product. If the similarity measure of two elements is equal to zero, then they are called orthogonal with each other.

Definition 2.11 *An arbitrary pair of elements $f, g \in \mathcal{H}$ is called orthogonal if $\langle f, g \rangle = 0$. This is also written as $f \perp g$. For sets $\mathcal{J}_1, \mathcal{J}_2 \subset \mathcal{H}$, we call $\mathcal{J}_1$ and $\mathcal{J}_2$ orthogonal if $\langle s_1, s_2 \rangle = 0$ for all $s_1 \in \mathcal{J}_1, s_2 \in \mathcal{J}_2$. If $\mathcal{J}_1$ and $\mathcal{J}_2$ are orthogonal, we write $\mathcal{J}_1 \perp \mathcal{J}_2$.*

The orthogonality property is also used to give a definition of the completeness[4] of a given set $\mathcal{J}$ in a Hilbert space $\mathcal{H}$.

Definition 2.12 *$\mathcal{J} \subset \mathcal{H}$ is complete if there are no non-zero elements $f \in H$ for which $f \perp \mathcal{J}$.*

Another essential definition related to a Hilbert space is the notion of projection.

[4]Note that completeness of a set and completeness of a space are entirely different things which are not to be confused. Completeness of a set is also named as total, maximal, fundamental, or basic.

Definition 2.13 *An operator $\Pi_{\mathcal{J}} : \mathcal{H} \to \mathcal{J}$ is called a projection of $\mathcal{H}$ onto $\mathcal{J} \subseteq \mathcal{H}$ if it obeys $Im\Pi_{\mathcal{J}} = \mathcal{J}$ and $\Pi_{\mathcal{J}}\Pi_{\mathcal{J}} = \Pi_{\mathcal{J}}$. Moreover, the projection $\Pi_{\mathcal{J}}x$ of $x \in \mathcal{H}$ onto $\mathcal{J}$ is the unique element $s^* = \Pi_{\mathcal{J}}x \in \mathcal{J}$ with the property that $\langle x - s^*, s\rangle = 0, \forall s \in \mathcal{J}$*

A projection can easily be carried out in terms of basis expansions of subspaces. This is especially useful in conjunction with the notion of a basis of a Hilbert space, which has paramount importance in the scope of this thesis. The interaction between a projection and a basis is given in Section 2.4.2 while the definition of a basis is given as follows:

Definition 2.14 *A set $\{\phi_j\}_{j\in J}$ is a basis of $\mathcal{H}$ if for all $v \in \mathcal{H}$ there exist unique coefficients $\{c_j\}_{j\in J}$ such that $v = \sum_{j\in J} c_j\phi_j$. For countable infinite sets $J = \{1, 2, \dots, \}$, the latter expansion means that*

$$\lim_{j_o\to\infty} \|v - \sum_{j=1}^{j_o} c_j\phi_j\| = 0. \tag{2.31}$$

The coefficients c_j are called the expansion coefficients of v with respect to the basis $\{\phi_j\}_{j\in J}$. As a consequence, $v \in \mathcal{H}$ can be written as

$$v = \sum_{j\in J} c_j\phi_j. \tag{2.32}$$

The convergence of this sum should be interpreted in the sense of (2.31). The statement (2.32) holds for any $v \in \mathcal{H}$ if and only if the basis $\{\phi_j\}_{j\in J}$ span the complete Hilbert space $\mathcal{H}$.

Remark 2.3 *The formulation of* (2.31) *infers the countability of a given set of basis. Only separable Hilbert spaces have countable bases. In the non countable case,* (2.31) *and* (2.32) *do not hold. Thus, a Hilbert space H is called separable if there exists a countable subset for which the closure with respect to the inner product norm coincides with the space itself.*

2.4.2 Orthonormal basis of a Hilbert space

In order to construct a basis of a Hilbert space, each of the basis elements need to be linearly independent with respect to each other. A set consisting of mutually orthogonal elements is called orthogonal and a basis constructed of an orthogonal set is called an orthogonal basis. Orthonormal is the normalization of an orthogonal set and is an extra property that is often used to avoid computational sensitivity that occurs due to the disparity between the norms of the elements in an orthogonal set.

Definition 2.15 *(Orthogonal and orthonormal set) A set of functions $\{\phi_i\}_{i\in J}$ in a Hilbert space $\mathcal{H}$ is an* orthogonal set *if all its elements are mutually orthogonal, i.e. $\langle\phi_i, \phi_j\rangle = 0 \forall i, j \in J$ except for $i = j$. If, in addition, $\|\phi_i\| = 1$, $\forall i \in J$, then the set is called an* orthonormal set.

Definition 2.16 *(Orthogonal and orthonormal basis) An* orthogonal basis *of a Hilbert space $\mathcal{H}$ is an orthogonal set $\{\phi_i\}_{i\in J}$ that is a basis in $\mathcal{H}$. If in addition, the functions ϕ_i are normalized in the sense that $\|\phi_i\| = 1, \forall i \in J$, then it is called an* orthonormal basis *of $\mathcal{H}$.*

The utilization of orthogonal bases further simplifies the parameterization of an element in a Hilbert space. The motivation of using orthogonal and orthonormal basis can be seen in the following example:

Example 2.1 *Suppose that $v \in \mathcal{J}$ where $\mathcal{J} = span\{\phi_i\}_{i=1}^n$, how to find the coefficients c_i of an expansion $v = \sum_{i=1}^n c_i\phi_i$?*

For $j \in \{1, \ldots, n\}$ we have $\langle v, \phi_j\rangle = \sum_{i=1}^n c_i\langle\phi_i, \phi_j\rangle$, and hence:

$$\underbrace{\begin{bmatrix}\langle\phi_1,\phi_1\rangle & \cdots & \langle\phi_n,\phi_1\rangle\\ \vdots & \ddots & \vdots\\ \langle\phi_1,\phi_n\rangle & \cdots & \langle\phi_n,\phi_n\rangle\end{bmatrix}}_{G_c}\begin{bmatrix}c_1\\ \vdots\\ c_n\end{bmatrix} = \underbrace{\begin{bmatrix}\langle v,\phi_1\rangle\\ \vdots\\ \langle v,\phi_n\rangle\end{bmatrix}}_{b}. \tag{2.33}$$

The expansion coefficients $c = [c_1, \ldots, c_n]^\top$ can be obtained by inverting G_c in (2.33)*, i.e. $c = {G_c}^{-1}b$. For a set of non orthogonal basis, the invertibility of G_c is non trivial. For a set of orthogonal basis, G_c is diagonal and non singular and thus it is easy to invert it. Moreover, for a set of orthonormal basis, G_c is an identity matrix and hence we have $c_i = \langle v, \phi_i\rangle$.*

It can be seen that for an orthogonal or orthonormal basis, it is easier to decouple the contribution of each basis element (coefficient c_k in (2.32)) to describe an element in a given subspace of a Hilbert space. The importance of orthogonality of a basis is further strengthened when an element $x \in \mathcal{H}$ is projected on a given subspace $\mathcal{J} \subset \mathcal{H}$ with $\mathcal{J} = \text{span}\{\phi_i\}_{i=1}^n$.

Let $x = \sum_{j=1}^\infty d_j\tilde{\phi}_j$ and let $s^* = \sum_{i=1}^n c_i\phi_i$ be the projection of x on $\mathcal{J}$, thus $s^* = \Pi_{\mathcal{J}}x$. Then, by Definition 2.13, we have $\langle x - s^*, \phi_i\rangle = 0$ for all $i = 1, \ldots, n$. This relation is equivalent with

$$\langle\sum_{j=1}^n d_j\tilde{\phi}_j, \phi_i\rangle = \langle\sum_{i=1}^n c_i\phi_i, \phi_i\rangle,$$

and as well equivalent with

$$\sum_{j=1}^n d_i\langle\tilde{\phi}_j, \phi_j\rangle = \sum_{i=1}^n c_i\langle\phi_i, \phi_i\rangle,$$

and thus, in particular, by taking $\tilde{\phi}_j = \phi_i$, it follows that $c_i = d_i$, for $i \leq n$. Therefore $s^* = \sum_{i=1}^n d_i\phi_i$ whenever $x = \sum_{i=1}^\infty d_i\phi_i$.

2.4.3 Orthonormalization of a set in $\mathcal{H}$

Any countable set of linearly independent functions in a Hilbert space $\mathcal{H}$ can be transformed into an orthogonal set that has the same linear span. The orthogonalization of a set along with the normalization procedure is called an orthonormalization method. One of the well-known orthonormalization methods is the Gram-Schmidt orthonormalization procedure (Kreyzig 1978).

Definition 2.17 *Given the set of linearly independent functions $\{\phi_i\}_{i=1}^n \subset \mathcal{H}$, an orthonormal set $\{\tilde{\phi}_i\}_{i=1}^n$ with span$\{\phi_i\}_{i=1}^n$ = span$\{\tilde{\phi}_i\}_{i=1}^n$, is obtained through a recursive procedure:*

$$\begin{cases} \tilde{\phi}_1 = \|\phi_1\|^{-1}\phi_1, & i = 1; \\ \tilde{\phi}_i = \|v_i\|^{-1}v_i \;\; \textit{with} \;\; v_i = \phi_i - \sum_{j=1}^{i-1}\langle \phi_i, \tilde{\phi}_j\rangle \tilde{\phi}_j, & 1 < i \leq n. \end{cases} \tag{2.34}$$

Some notable examples of orthonormal bases of a Hilbert space that are frequently used in the system and control field of study are:

- The space $\mathcal{H}$ of square summable sequences $\ell_2(\mathbb{N})$. An example of a set of basis functions in this space is $\{\psi_i(\tau)\}_{i\in\mathbb{N}} = \{\delta_i(\tau)\}_{i\in\mathbb{N}}, \tau \in \mathbb{N}$ which is the unit pulse sequence where the non zero element is located at $i = \tau$:

$$\delta_i(\tau) := \begin{cases} 1 & i = \tau; \\ 0 & i \neq \tau. \end{cases}$$

- The *Hardy space* $\mathcal{H}_2(\mathbb{E})$. An example of set of basis functions in this space is the pulse basis $\{\phi_i(z)\}_{i\in\mathbb{N}}$ with $\phi_i(z) = z^{-i}, z \in \mathbb{C}, i \in \mathbb{Z}$. This particular space is used and further explained in detail in the following subsection.

2.4.4 The spaces of real-rational and stable discrete-time systems

The *Hardy space* $\mathcal{H}_2(\mathbb{E})$ is a space of complex valued functions that are analytic in the exterior $\mathbb{E} = \{z \in \mathbb{C} \mid |z| > 1\}$ of the unit disc $\mathbb{D} = \{z \in \mathbb{C} \mid |z| \leq 1\}$ and square integrable over the unit circle $\mathbb{T} = \{z \in \mathbb{C} \mid |z| = 1\}$.

Definition 2.18 *(Inner product of $\mathcal{H}_2(\mathbb{E})$) The* Hardy space *is a separable Hilbert space with inner product defined as:*

$$\langle G_1, G_2\rangle_{\mathcal{H}_2(\mathbb{E})} = \frac{1}{2\pi}\int_{-\pi}^{\pi} G_1(e^{iw})G_2^*(e^{iw})dw. \tag{2.35}$$

Further in this thesis, special attention is given to a specific subspace of the Hardy space which contains all real rational transfer functions which are analytic in $\mathbb{E}$ and strictly proper i.e., $\lim_{z\to\infty}|G(z)| = 0$. This subspace is denoted by $\mathcal{RH}_2(\mathbb{E})$.

2.4.5 Isomorphic space with the Hardy space

The Hilbert spaces of $\ell_2(\mathbb{N})$ and $\mathcal{H}_2(\mathbb{E})$ are isomorphic with respect to each other. The isomorphism is defined by the z-transform $\mathcal{Z}$. Consider $g \in \ell_2(\mathbb{N})$, then

$$G(z) = [\mathcal{Z}\{g\}](z) = \sum_{i=1}^{\infty} g(\tau) z^{-\tau}, \tag{2.36}$$

belongs to $\mathcal{H}_2(\mathbb{E})$. Conversely, if $G \in \mathcal{H}_2(\mathbb{E})$ then

$$g(\tau) = \mathcal{Z}^{-1}\{G(z)\}, \tag{2.37}$$

belongs to $\ell_2(\mathbb{N})$ and satisfies $\delta(\tau) = 0$ for $\tau < 0$. Note that $\mathcal{Z}^{-1}\{\cdot\}$ is the inverse z-transform on the appropriate region of convergence. It follows that due to the isomorphism, we have

$$\|g\|_2 = \|G\|_{H_2}. \tag{2.38}$$

If the transformation is conducted on $g_1, g_2 \in \ell_2(\mathbb{N})$ with $\delta_1(\tau) = 0, \delta_2(\tau) = 0$ for $\tau < 0$ and that result in $G_1, G_2 \in \mathcal{H}_2(\mathbb{E})$, the inner product between these two pairs are given as

$$\langle g_1, g_2 \rangle_{\ell_2(\mathbb{N})} = \langle G_1, G_2 \rangle_{\mathcal{H}_2(\mathbb{E})}. \tag{2.39}$$

The isomorphism is also presented between particular subspaces of these two aforementioned spaces. Particularly, we are interested in the relation between $\mathcal{RH}_2(\mathbb{E})$ and $\mathcal{R}\ell_2(\mathbb{N})$. This isomorphism means that any sequence $g \in \mathcal{R}\ell_2(\mathbb{N})$ in the series expansion representation (2.4) corresponds to one and only one function $G \in \mathcal{RH}_2(\mathbb{E})$ in the transfer function representation (2.9), and vice versa. The orthonormal basis of these spaces is a core ingredient of the results presented in this thesis and is further elaborated in the next section.

2.5 Orthonormal basis functions of $\mathcal{RH}_2(\mathbb{E})$

This section covers one of the core elements in this thesis which is the *Orthonormal Basis Function* (OBF) model structure. We start with reformulating the series expansion representation and the transfer function representation using OBFs. Afterwards, the description on the truncation of the model structure is given and a method to construct these OBFs is motivated. The available methods of selecting a set of OBFs based on the selected optimality measure are given to conclude this section.

2.5.1 OBF model structure

Given a complete set of orthonormal basis $\{\phi_i\}_{i=1}^{\infty}$ of $\mathcal{RH}_2(\mathbb{E})$, the transfer function $G \in \mathcal{RH}_2^{n_\mathrm{y} \times n_\mathrm{u}}(\mathbb{E})$ (space of $n_\mathrm{y} \times n_\mathrm{u}$ matrices with elements in $\mathcal{RH}_2$) of any strictly proper asymptotically stable MIMO LTI system can be written as:

$$G(z) = \sum_{i=1}^{\infty} \mathsf{w}_i \phi_i(z), \tag{2.40}$$

where $\mathsf{w}_i \in \mathbb{R}^{n_\mathrm{y} \times n_\mathrm{u}}$ is a matrix of expansion coefficients whose (m,n)-th entry $\mathsf{w}_i^{[m,n]}$ corresponds to the m-th output and n-th input channel associated with $G^{[m,n]}(z)$ of $G(z)$:

$$\mathsf{w}_i^{[m,n]} = \langle \phi_i, G^{[m,n]} \rangle_{\mathcal{H}_2}. \tag{2.41}$$

Similarly, let $\{\psi_i\}_{i=1}^{\infty}$ be an orthonormal basis of $\mathcal{R}\ell_2(\mathbb{N})$. According to (2.36), any impulse response $g \in \mathcal{R}\ell_2^{n_\mathrm{y} \times n_\mathrm{u}}(\mathbb{N})$ is associated with a $G \in \mathcal{RH}_2^{n_\mathrm{y} \times n_\mathrm{u}}(\mathbb{E})$ and can be written as

$$g(\tau) = \sum_{i=1}^{\infty} \mathsf{w}_i \psi_i(\tau). \tag{2.42}$$

Since $\{\psi_i(\tau)\}_{i=1}^{\infty}$ and $\{\phi_i(z)\}_{i=1}^{\infty}$ are related via the $\mathcal{Z}$-transform (See Section 2.4.5) in the sense that $\phi_i = \mathcal{Z}(\psi_i)$, then the expansion coefficients w_i in both (2.42) and (2.40) are equal with each other.

Remark 2.4 *Note that representations* (2.40) *and* (2.42) *are given in terms of scalar basis of their corresponding spaces. In the MIMO case, this particular selection leads to a matrix of expansion coefficients* w_i*. In order to describe a MIMO system with scalar expansion coefficients, one needs to select a MIMO formulation of OBFs such as given in Heuberger et al. (2005). A scalar type of basis is used instead of a MIMO one because this particular type of basis functions has well worked out properties that are useful in the context of modeling and control in this thesis. More on the type of the basis and the implication of such selection are explained further in this section.*

2.5.2 Truncation of the OBF model structure

In practice, it is often required to have a finite number of terms in (2.40) or (2.42) such as done in *Finite Impulse Response* (FIR) models. In contrast with FIR structures, the OBF parameterization allows a broad class of basis functions where each basis function has an infinite impulse response sequence. The truncation of (2.40) with respect to the first n_b basis functions of $\{\phi_i\}_{i=1}^{\infty}$ is given by:

$$G_{n_\mathrm{b}}(z) = \sum_{i=1}^{n_\mathrm{b}} \mathsf{w}_i \phi_i(z). \tag{2.43}$$

By the last observation in Section 2.4.2, observe that (2.43) is the orthogonal projection of $G \in \mathcal{RH}_2$ onto $\mathrm{span}\{\phi_i\}_{i=1}^{n_\mathrm{b}}$. Any such truncation incurs an error $\bar{G}_{n_\mathrm{b}}(z) := G(z) - G_{n_\mathrm{b}}(z)$, where the error norm (induced by the inner product) for each (m,n)-th entry of $G(z)$ is defined by:

$$\| G^{[m,n]} - G_{n_\mathrm{b}}^{[m,n]} \|_{\mathcal{H}_2}^2 = \sum_{i=n_\mathrm{b}+1}^{\infty} (\mathsf{w}_i^{[m,n]})^2. \tag{2.44}$$

The implication of using a set of general OBFs rather than the pulse basis is twofold. From the modeling perspective, the freedom to select the OBFs $\{\phi_i\}_{i=1}^{\infty}$ gives

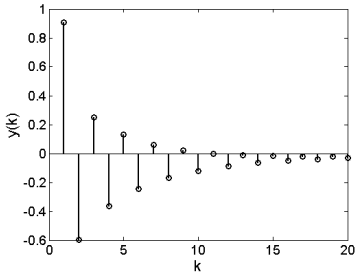

(a) Impulse response $g = \mathcal{Z}^{-1}\{G\}$

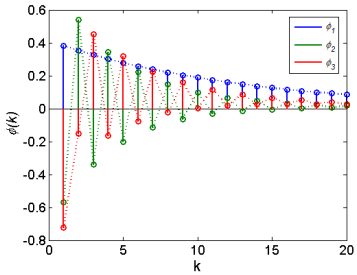

(b) Impulse response of the OBFs $\{\phi_i\}_{i=1}^{3}$

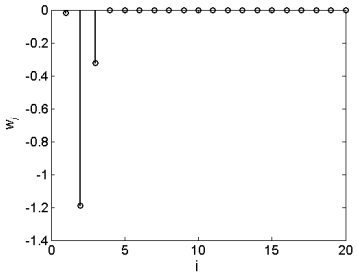

(c) Coefficients of the OBF model $G_3(z)$

Figure 2.2: Comparison between the length of truncation for FIR and OBF models.

the user a handle to select the basis functions such that arbitrary low error in (2.44) can be obtained using only a low truncation order n_b. Moreover, in terms of identification with the OBF model structure, one can obtain decreased variance of the model estimate $G_{n_\mathrm{b}}(z)$ if compared to the FIR case (Ninness et al. 1996; Heuberger et al. 2005). From the point of view of model based control synthesis, OBF structure provides an additional degree of freedom to adjust the complexity of the controller by selecting the basis functions and the truncation length. The comparison between the length of truncation of a FIR model and an OBF model is illustrated in the following example.

Example 2.2 *Given a SISO LTI system with transfer function $G(z)$ for which the impulse response is depicted in Figure 2.2(a), and an orthonormal set of OBFs $\{\phi_i(z)\}_{i=1}^{\infty}$. The impulse response of the first three OBFs is shown in Figure 2.2(b). Figure 2.2(c) shows that the OBF model only need three expansion coefficients to describe $G(z)$ by $G_3(z)$ of* (2.43) *with low error in the sense of* (2.44)*. Contrary to Figure 2.2(c), Figure 2.2(a) shows that FIR model (which is constructed by the pulse basis) need at least a truncation length of 15 to obtain low error in describing $G(z)$.*

The question that follows from the truncation of an OBF model structure is how to select or construct the set of $\{\phi_i(z)\}_{i=1}^{\infty}$. This question will be addressed further in the remaining sections in this Chapter.

2.5.3 Classes of OBFs

Orthonormal basis in $\mathcal{RH}_2(\mathbb{E})$ are often considered in terms of *Takenaka-Malmquist* (TM) functions which cover wide arrays of well-known bases such as pulse basis, *Laguerre* basis, *Kautz* basis, and *Hambo* basis (Ninness and Gustafsson 1997; Heuberger et al. 2005). TM OBFs are defined as:

$$\phi_i(z) = \frac{\sqrt{1-|\lambda_i|^2}}{z-\lambda_i} \prod_{j=1}^{i-1} \frac{1-\lambda_j^* z}{z-\lambda_j}, \quad i = 1, 2, 3, \ldots, \tag{2.45}$$

where $\lambda_i \in \mathbb{D}$ for all $i = 1, 2, 3, \ldots$, are complex numbers inside the unit disc that appear as either real numbers or pairs of complex conjugate numbers and obey the *Szász* Condition of $\sum_{i=1}^{\infty} 1 - |\lambda_i| < \infty$. The latter is a sufficient condition for completeness of the basis. In Heuberger et al. (2005), it is shown that set of OBFs generated by (2.45) is an orthonormal basis of $\mathcal{RH}_2(\mathbb{E})$ since it originates from conducting Gram-schmidt orthonormalization procedure (as explained in Section 2.4.3) to an infinite sequence of linearly independent functions:

$$\hat{\phi}_i(z) = \frac{1}{z-\lambda_i}, \quad i = 1, 2, 3, \ldots. \tag{2.46}$$

The selected values for each (or complex conjugate pairs) $\lambda_i \in \mathbb{D}$ of the sequence $\{\lambda_i\}_{i=0}^{\infty}$ satisfying the *Szász* Condition, determine the type and the properties of the set of basis functions, as well as the subspace spanned by a finite subset of them. Complex poles $\lambda_i \in \mathbb{D}$ need to appear as complex conjugate pairs to guarantee that the associated impulse responses of (2.40) are real-valued.

Some examples of notable basis functions that can be parameterized by (2.45) are given below.

Example 2.3 *Suppose $\lambda_i = 0, \forall\, i \in \mathbb{Z}_+$. Then the resulting basis is known as the pulse basis $\phi_i(z) = z^{-i}$. Given a value of $\bar{a} \in \mathbb{R}_{(-1,1)}$. Suppose $\lambda_i = \bar{a}$ for all $i \in \mathbb{Z}_+$. Then the resulting basis is known as the* Laguerre *basis:*

$$\begin{aligned} \phi_1 &= \frac{\sqrt{1-\bar{a}^2}}{z-\bar{a}}, \\ &\vdots \\ \phi_i &= \frac{\sqrt{1-\bar{a}^2}}{z-\bar{a}} \left(\frac{1-\bar{a}z}{z-\bar{a}}\right)^{i-1}. \end{aligned} \tag{2.47}$$

Given a complex conjugate pole pair $\mathfrak{c}, \mathfrak{c}^* = \mathfrak{a} \pm i\mathfrak{b} \in \mathbb{D}$, with $\mathfrak{a}, \mathfrak{b} \in \mathbb{R}_{(-1,1)}$. Suppose $\lambda_{2i-1} = \mathfrak{c}$, $\lambda_{2i} = \mathfrak{c}^*$ for all $i \in \mathbb{Z}_+$. Then the resulting OBFs is known as the Kautz basis*:*

$$\begin{aligned} \phi_{2i-1} &= \frac{\sqrt{1-\mathfrak{b}^2}(z-\mathfrak{a})}{z^2+\mathfrak{a}(\mathfrak{b}-1)z-\mathfrak{b}} \left(\frac{-\mathfrak{b}z^2+\mathfrak{a}(\mathfrak{b}-1)z+1}{z^2+\mathfrak{a}(\mathfrak{b}-1)z-\mathfrak{b}}\right)^{i-1}, \\ \phi_{2i} &= \frac{\sqrt{1-\mathfrak{b}^2}\sqrt{1-\mathfrak{a}^2}}{z^2+\mathfrak{a}(\mathfrak{b}-1)z-\mathfrak{b}} \left(\frac{-\mathfrak{b}z^2+a(\mathfrak{b}-1)z+1}{z^2+\mathfrak{a}(\mathfrak{b}-1)z-\mathfrak{b}}\right)^{i-1}. \end{aligned} \tag{2.48}$$

Example 2.3 provides particular selections or patterns of λ_i to describe $\phi_i(z)$ of (2.45). These selections lead to well-defined infinite sequences of $\{\lambda_i\}_{i=1}^{\infty}$ that produce an infinite sequence of OBFs $\{\phi_i\}_{i=1}^{\infty}$. These OBFs constitute a complete orthonormal basis for $\mathcal{RH}_2(\mathbb{E})$ (Heuberger et al. 2005).

Alternative to the OBFs that are provided in Example 2.3, a complete orthonormal basis for $\mathcal{RH}_2(\mathbb{E})$ can be constructed by repeating a priory selected $\{\lambda_i\}_{i=1}^{n_\mathrm{b}} \subset \mathbb{D}$ in the sense of:

$$\{\lambda_i\}_{i=1}^{n_\mathrm{b}} = \{\lambda_i\}_{i=n_\mathrm{b}+1}^{2n_\mathrm{b}} = \dots, \tag{2.49}$$

up to infinite repetition. Note that such a repetition, trivially satisfies the *Szász* condition. This particular repetition is the basic step in the construction of *Generalized Orthonormal Basis Functions* (GOBF), the most general subclass of TM OBFs.

2.5.4 Construction and state space formulation of GOBFs

In this subsection, the construction of GOBFs along their state-space formulation is given. The state-space formulation of OBF models is essential for this thesis since most of the control/identification methods and analysis in the following chapters are conducted in the state-space form. The construction of GOBFs is based on an all-pass filter, defined as follows:

Definition 2.19 *A function $H \in \mathcal{H}_2(\mathbb{E})$ is called an all-pass filter, if*

$$H(z)H^*(1/z^*) = 1, \quad \forall z \in \mathbb{C}. \tag{2.50}$$

Such function if rational, is completely determined, modulo the sign by its poles $\lambda_i \in \mathbb{D}, \forall i = 1, \dots, n_\mathrm{b}$.

Consider a single input single output asymptotically stable first order all-pass filter $H_i(z)$ given as:

$$\breve{H}_i(z) = \frac{z - \bar{\mathfrak{a}}_i}{1 - \bar{\mathfrak{a}}_i z}, \quad -1 < \bar{\mathfrak{a}}_i < 1, \tag{2.51}$$

where $\bar{\mathfrak{a}}_i$ denote a real valued λ_i. A state-space realization of this filter can be given as:

$$\left[\begin{array}{c|c} \breve{A}_i & \breve{B}_i \\ \hline \breve{C}_i & \breve{D}_i \end{array}\right] = \left[\begin{array}{c|c} \bar{\mathfrak{a}}_i & \sqrt{1-a_i} \\ \hline \sqrt{1-\bar{\mathfrak{a}}_i} & -\bar{\mathfrak{a}}_i \end{array}\right]. \tag{2.52}$$

Introduce a second order all-pass filter $H_j(z)$ with transfer function:

$$\breve{H}_j(z) = \frac{-\mathfrak{b}_j z^2 + \mathfrak{a}_j(\mathfrak{b}_j - 1)z + 1}{z^2 + \mathfrak{a}_j(\mathfrak{a}_j - 1)z - \mathfrak{b}_j}, \quad -1 < \mathfrak{a}_j < 1, -1 < \mathfrak{b}_j < 1 \tag{2.53}$$

where $\mathfrak{a}_j$ and $\mathfrak{b}_j$ denote the real and imaginary part of a complex conjugate pair of poles λ_j and λ_j^*. Note that (2.53) constitute two basis of ϕ_j and ϕ_{j+1}. The state-space realizations of this filter can be given as:

$$\left[\begin{array}{c|c} \breve{A}_j & \breve{B}_j \\ \hline \breve{C}_j & \breve{D}_j \end{array}\right] = \left[\begin{array}{cc|c} \mathfrak{a}_j & \mathfrak{b}_j\sqrt{1-\mathfrak{a}_j^2} & \sqrt{1-\mathfrak{a}_j^2}\sqrt{1-\mathfrak{b}_j^2} \\ \sqrt{1-\mathfrak{a}_j^2} & -\mathfrak{a}_j\mathfrak{b}_j & -\mathfrak{a}_j\sqrt{1-\mathfrak{b}_j^2} \\ \hline 0 & \sqrt{1-\mathfrak{b}_j} & -\mathfrak{b}_j \end{array}\right]. \tag{2.54}$$

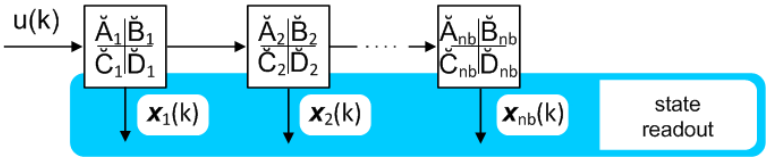

Figure 2.3: Cascaded connection of all-pass filters.

The two filters (2.51), (2.53), and any possible sequence of these filters, can be connected in a cascaded network such as depicted in Fig 2.3.

For two filters, which can be a combination of first and/or second order pass filters, this connection can be formulated as:

$$\left[\begin{array}{c|c} A_{n_\mathrm{b}} & B_{n_\mathrm{b}} \\ \hline C_{n_\mathrm{b}} & D_{n_\mathrm{b}} \end{array}\right] = \left[\begin{array}{cc|c} \breve{A}_1 & 0 & \breve{B}_1 \\ \breve{B}_2\breve{C}_1 & \breve{A}_2 & \breve{B}_2\breve{D}_1 \\ \hline \breve{D}_2\breve{C}_1 & \breve{C}_2 & \breve{D}_2\breve{D}_1 \end{array}\right]. \tag{2.55}$$

This construction can be recursively applied for cascaded connection on $n_\mathrm{b} > 2$ filters.

Suppose that we have a n_b cascaded connection of filters that follows the formulation of (2.55). Then the input to state transfer function for the cascaded network of n_b filters can be written as:

$$\varphi_{n_\mathrm{b}}(z) := (zI - A_{n_\mathrm{b}})^{-1} B_{n_\mathrm{b}} \tag{2.56}$$

which is a vector of transfer function consisting of n_b elements

$$\varphi_{n_\mathrm{b}}(z) = \begin{bmatrix} \phi_1(z) \\ \phi_2(z) \\ \vdots \\ \vdots \\ \vdots \\ \phi_{n_\mathrm{b}}(z) \end{bmatrix}. \tag{2.57}$$

Note that connection with (2.53) constitute 2 elements instead of 1 element of (2.51) and hence (2.57) is the natural partitioning of φ_{n_b} in terms of n_b numbers of real and imaginary pole components. Furthermore, we can see that the i-th element of (2.57) is the same as the i-th Takenaka Malmquist basis of (2.45) that constitute a basis in $\mathcal{RH}_2(\mathbb{E})$.

In order to span the complete $\mathcal{RH}_2(\mathbb{E})$ space, the cascaded connection of all-pass filters can be repeated infinitely. For n_e number of repetition of $\varphi_{n_\mathrm{b}}(z)$ we

have:

$$\varphi_{n_\mathrm{e},n_\mathrm{b}}(z) = \begin{bmatrix} \phi_1(z) \\ \phi_2(z) \\ \vdots \\ \phi_{n_\mathrm{b}}(z) \\ \phi_{n_\mathrm{b}+1}(z) \\ \phi_{n_\mathrm{b}+2}(z) \\ \vdots \\ \phi_{2\cdot n_\mathrm{b}}(z) \\ \vdots \\ \phi_{n_\mathrm{e}\cdot n_\mathrm{b}}(z) \end{bmatrix}, \tag{2.58}$$

which constitutes $n_\mathrm{e} \cdot n_\mathrm{b}$ number of basis functions $\{\phi_i\}_{i=1}^{n_\mathrm{e}\cdot n_\mathrm{b}}$. The formulation of the cascaded network of (2.58) is given as follows:

Definition 2.20 *Suppose that minimal and balanced (hence orthogonal) realization of cascaded network of arbitrary combination of filters* (2.51) *and* (2.53) *is given in the state space matrices* ($A_{n_\mathrm{b}} \in \mathbb{R}^{n_\mathrm{b}\times n_\mathrm{b}}, B_{n_\mathrm{b}} \in \mathbb{R}^{n_\mathrm{b}}, C_{n_\mathrm{b}} \in \mathbb{R}^{1\times n_\mathrm{b}}, D_{n_\mathrm{b}} \in \mathbb{R}$) *corresponding to* n_b *number of basis functions. For these given orthogonal realizations, the cascaded network has a minimal and orthogonal state space realization where the* $A_{n_\mathrm{e},n_\mathrm{b}}$ *and* $B_{n_\mathrm{e},n_\mathrm{b}}$ *matrices are given as:*

$$A_{n_\mathrm{e},n_\mathrm{b}} = \begin{bmatrix} A_{n_\mathrm{b}} & 0 & \dots & 0 \\ B_{n_\mathrm{b}}C_{n_\mathrm{b}} & A_{n_\mathrm{b}} & 0 & 0 \\ \vdots & \vdots & \ddots & \vdots \\ B_{n_\mathrm{b}}\prod_{j=2}^{n_\mathrm{e}-1} D_{n_\mathrm{b}}C_{n_\mathrm{b}} & B_{n_\mathrm{b}}\prod_{j=3}^{n_\mathrm{e}-1} D_{n_\mathrm{b}}C_{n_\mathrm{b}} & \dots & A_{n_\mathrm{b}} \end{bmatrix}, \quad . \tag{2.59}$$

$$B_{n_\mathrm{e},n_\mathrm{b}} = \begin{bmatrix} B_{n_\mathrm{b}} \\ B_{n_\mathrm{b}}D_{n_\mathrm{b}} \\ \vdots \\ B_{n_\mathrm{b}}\prod_{j=1}^{n_\mathrm{e}-1} D_{n_\mathrm{b}} \end{bmatrix}. \tag{2.60}$$

Under the trivially satisfied Szász *condition, the elements of the vector of transfer functions*

$$\varphi_{n_\mathrm{e},n_\mathrm{b}}(z) := (zI - A_{n_\mathrm{e},n_\mathrm{b}})^{-1} B_{n_\mathrm{e},n_\mathrm{b}}, \tag{2.61}$$

constitute $n_\mathrm{e} \cdot n_\mathrm{b}$ *number of basis for* $\mathcal{RH}_2(\mathbb{E})$. *When* $n_\mathrm{e} = \infty$, *the resulting OBFs* $\{\phi_i\}_{i=1}^{\infty}$ *of* (2.61) *span the complete* $\mathcal{RH}_2(\mathbb{E})$ *space. Such an OBF sequence is known as* Generalized Orthonormal Basis Functions *(Heuberger et al. 2005).*

By using the OBFs produced by (2.61), any element $G \in \mathcal{RH}_2(\mathbb{E})$ can be approximated as the orthogonal projection to the span of $\{\phi_i\}_{i=1}^{n_\mathrm{e}\cdot n_\mathrm{b}}$:

$$G_{n_\mathrm{e},n_\mathrm{b}}(z) = \sum_{i=1}^{n_\mathrm{e}\cdot n_\mathrm{b}} \mathsf{w}_i \phi_i(z), \tag{2.62}$$

with a state space realization of:

$$\begin{aligned} x(k+1) &= A_{n_\mathrm{e},n_\mathrm{b}} x(k) + B_{n_\mathrm{e},n_\mathrm{b}} u(k) \\ y(k) &= [\mathsf{w}_1 \ \mathsf{w}_2 \ \dots \ \mathsf{w}_{n_\mathrm{e}\cdot n_\mathrm{b}}] x(k) \end{aligned} \tag{2.63}$$

where $A_{n_\mathrm{e},n_\mathrm{b}} \in \mathbb{R}^{n_\mathrm{e}\cdot n_\mathrm{b} \times n_\mathrm{e}\cdot n_\mathrm{b}}$, $B_{n_\mathrm{e},n_\mathrm{b}} \in \mathbb{R}^{n_\mathrm{e}\cdot n_\mathrm{b}}$, and $\mathsf{w}_i \in \mathbb{R}$. The OBF model $G_{n_\mathrm{e},n_\mathrm{b}}(z)$ is depicted in Figure 2.4.

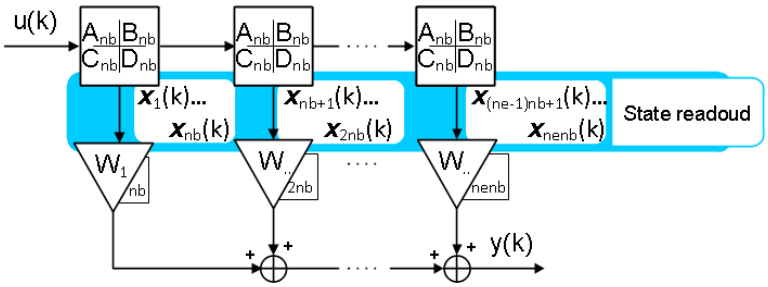

Figure 2.4: Cascaded structure of (2.62).

In the MIMO case when $G \in (\mathcal{RH}_2(\mathbb{E}))^{n_\mathrm{y}\times n_\mathrm{u}}$, the OBF model (2.62) can be written in the form:

$$\begin{aligned} x(k+1) &= \underbrace{\begin{bmatrix} A_{n_\mathrm{e},n_\mathrm{b}} & \dots & 0 \\ \vdots & \ddots & \vdots \\ 0 & \ddots & A_{n_\mathrm{e},n_\mathrm{b}} \end{bmatrix}}_{A\in\mathbb{R}^{n_\mathrm{g}\times n_\mathrm{g}}} x(k) + \underbrace{\begin{bmatrix} B_{n_\mathrm{e},n_\mathrm{b}} & \dots & 0 \\ \vdots & \ddots & \vdots \\ 0 & \ddots & B_{n_\mathrm{e},n_\mathrm{b}} \end{bmatrix}}_{B\in\mathbb{R}^{n_\mathrm{g}\times n_\mathrm{u}}} u(k) \\ y(k) &= \underbrace{\begin{bmatrix} \mathsf{w}_1^{[1,1]} & \dots & \mathsf{w}_{n_\mathrm{e}\cdot n_\mathrm{b}}^{[1,1]} & \mathsf{w}_1^{[1,2]} & \dots & \mathsf{w}_{n_\mathrm{e}\cdot n_\mathrm{b}}^{[1,n_\mathrm{u}]} \\ \vdots & \ddots & \vdots & \vdots & \ddots & \vdots \\ \mathsf{w}_1^{[n_\mathrm{y},1]} & \dots & \mathsf{w}_{n_\mathrm{e}\cdot n_\mathrm{b}}^{[n_\mathrm{y},1]} & \mathsf{w}_1^{[n_\mathrm{y},2]} & \dots & \mathsf{w}_{n_\mathrm{e}\cdot n_\mathrm{b}}^{[n_\mathrm{y},n_\mathrm{u}]} \end{bmatrix}}_{\theta^\top} x(k) \end{aligned} \tag{2.64}$$

where $n_\mathrm{g} = n_\mathrm{e}\cdot n_\mathrm{b}\cdot n_\mathrm{u}$, $x(k) \in \mathbb{R}^{n_g}$ is the number of the cascaded network of filters (2.61) that is repeated for n_u number of input channels $u(k) \in \mathbb{R}^{n_\mathrm{u}}$, and $y(k) \in \mathbb{R}^{n_\mathrm{y}}$ is the output of the system. The coefficient $\theta \in \mathbb{R}^{n_\mathrm{g}\times n_\mathrm{y}}$ consists of the stacked expansion coefficients $\mathsf{w}_i^{[n_\mathrm{y},n_\mathrm{u}]}$ for all possible input-output channel.

2.5.5 Optimality of an OBF set

The advantage of using GOBFs to describe a $G \in \mathcal{RH}_2(\mathbb{E})$ is the possibility to characterize the approximation error (convergence rate) as n_e, the length of cascaded networks increases. Suppose that a SISO system with $G \in \mathcal{RH}_2(\mathbb{E})$ is aimed to be modeled in the form of (2.62). Introduce $\Phi_{n_\mathrm{b}} \subset \mathcal{RH}_2(\mathbb{E})$ as the subspace spanned by $\{\phi_i(z)\}_{i=1}^{n_\mathrm{b}}$ and $\Phi_{n_\mathrm{e}} \subset \mathcal{RH}_2(\mathbb{E})$ as the subspace spanned by n_e number of cascaded network of $\{\phi_i(z)\}_{i=1}^{n_\mathrm{b}}$. According to Heuberger et al. (2005); Oliviera e

Silva (1996), the approximation error has exponential rate of convergence (with rate $\rho_{n_\mathrm{b}} \in \mathbb{R}_{(0,1)}$) regarding $\bar{G}_{n_\mathrm{e},n_\mathrm{b}}(z) := G(z) - G_{n_\mathrm{e},n_\mathrm{b}}(z)$:

$$\|\bar{G}_{n_\mathrm{e},n_\mathrm{b}}\|_{\mathcal{H}_2} \approx (\rho_{n_\mathrm{b}})^{n_\mathrm{e}} \|\bar{G}_{1,n_\mathrm{b}}\|_{\mathcal{H}_2}, \quad \forall\, n_\mathrm{e} = 1, 2, 3, \ldots. \tag{2.65}$$

In order to improve the convergence rate of the approximate model (2.62), the selection of the all pass filter poles $\{\lambda_i\}_{i=1}^{n_\mathrm{b}}$ becomes a crucial task. The set of n_b poles that corresponds to the fastest convergence rate is considered as the generating poles of the optimal basis functions to describe $G(z)$ at truncation order n_b. It is shown in Oliviera e Silva (1996), that the rate of convergence ρ_{n_b} in (2.65) has an upperbound of

$$\rho_{n_\mathrm{b}} \leq \max_{\xi \in \Omega} \prod_{i=1}^{n_\mathrm{b}} \left| \frac{\xi - \lambda_i}{1 - \lambda_i^* \xi} \right|, \tag{2.66}$$

where $\Omega \subset \mathbb{D}$ is the set of poles of the transfer function $G(z)$.

The procedure to select the all pass filter poles $\{\lambda_i\}_{i=1}^{n_\mathrm{b}}$ from the information of poles Ω is also known as the inverse *Kolmogorov n-width* (KnW) problem with $n = n_\mathrm{b}$. The KnW concept, originates from Pinkus (1985), and it is used as a quality measure of the capability of a set of basis functions $\{\phi_i(z)\}_{i=1}^{n_\mathrm{b}}$ to describe a subset of transfer functions $\mathcal{T} \subset \mathcal{RH}_2(\mathbb{E})$.

Definition 2.21 ***Kolmogorov n-Width.***
Let $\mathcal{T}$ be a closed set of $\mathcal{RH}_2(\mathbb{E})$, and $\mathcal{M}_n$ is the collection of all n dimensional subspaces of $\mathcal{RH}_2(\mathbb{E})$. The KnW of $G \in \mathcal{T}$ is given by:

$$\pi_n(\mathcal{T}) = \inf_{\Phi_n \in \mathcal{M}_n} \sup_{G \in \mathcal{T}} d_{\mathcal{RH}_2(\mathbb{E})}(G, \Phi_n), \tag{2.67}$$

where

$$d_{\mathcal{RH}_2(\mathbb{E})}(G, \Phi_n) = \inf_{F \in \Phi_n} \| G - F \|_{\mathcal{RH}_2(\mathbb{E})}, \tag{2.68}$$

describes the distance between $G \in \mathcal{RH}_2(\mathbb{E})$ and a subspace Φ_n of $\mathcal{RH}_2(\mathbb{E})$.

In this way $\pi_n(\mathcal{T})$ describes smallest possible $d_{\mathcal{RH}_2(\mathbb{E})}$ that can be achieved for all G in $\mathcal{T}$ that is projected to the subspace Φ_n. The smallest possible distance $d_{\mathcal{RH}_2(\mathbb{E})}$ lead to smallest possible worst case approximation (truncation) error when G is described by using n basis function. The subspace $\Phi_n \in \mathcal{M}_n$, for which π_n is minimal, is called the optimal subspace in the KnW sense. This optimal subspace describes the best possible approximation of $\mathcal{T}$ in the worst-case sense. Furthermore, in the sense of (2.65) and (2.66), this correspond to the lowest value of ρ_{n_b} that can be achieved using n_b basis function (Oliviera e Silva 1996). It is also stated in the same work, that the zeros of the transfer functions do not give a dominant contribution for the convergence rate and hence the pole location of the to be approximated transfer function is the only determining factor to select the best OBFs in the KnW sense.

Remark 2.5 *The characterization of the convergence rate* (2.65) *of the error for each input-output channel of a MIMO system can be written using same set of OBFs for all channel. In this manner, we have an upper bound for the convergence of the approximation error of all the channels. Furthermore, it is shown in Heuberger et al. (2005) that for a given set of OBFs $\{\phi_i(z)\}_{i=1}^{n}$, the convergence rate between two cases of:*

- *multiple transfer functions with single (or multiple) pole*
- *single transfer function with multiple poles*

are the same as long as the set of poles Ω for both cases are equal. We can also use this result to asses the quality of a given set of OBFs $\{\phi_i(z)\}_{i=1}^n$ to approximate system dynamics described by a set of LTI systems (i.e LTI system with parametric uncertainty, LPV system, etc.).

2.5.6 KnW distance based basis selection techniques

Based on the description given in Section 2.5.5, the optimal basis poles in the KnW distance sense can be formulated as follows:

Definition 2.22 ***Basis pole selection problem***
Given $\Omega \subset \mathbb{D}$, find n_b optimal pole locations, $\lambda_i^o \in \mathbb{D}, i = 1, 2, \ldots, n_\mathrm{b}$ by solving the following optimization problem:

$$P_{\mathrm{KnW}} := \min_{\lambda_1,\ldots,\lambda_{n_\mathrm{b}} \in \mathbb{D}} \max_{\xi \in \Omega} \prod_{i=1}^{n_\mathrm{b}} \left| \frac{\xi - \lambda_i}{1 - \xi \lambda_i^*} \right|. \tag{2.69}$$

For $\Omega = \lambda(G)$, i.e., the poles of a given $G \in \mathcal{RH}_2(\mathbb{E})$, the attained minimum of (2.69), denoted by J^o, describes the best achievable upperbound for the convergence rate ρ_{n_b} of Eq. (2.65):

$$\rho_{n_\mathrm{b}} \leq J^o. \tag{2.70}$$

The pole selection problem (2.69) is a difficult rational min-max problem over $\mathbb{D}$. Several works attempted to give a solution to this problem:

- Oliviera e Silva (1996)
  In this work, λ_i is parameterized using a technique similar to the Schur-Cohn stability test in the denominator of $G_b(z)$. Although it simplifies the real and complex conjugate pairs of the pole selection, this restricts the construction of basis function as well as the possible space spanned by the basis functions.
- Patwardhan et al. (2006)
  Direct pole and coefficient estimation in a prediction error minimization scheme. This problem is solved with a direct application Nonlinear Programming technique and hence the optimality of the resulting pole-coefficient estimation is questionable. Moreover, this technique has a computation issue even for a small number of poles.
- Tóth et al. (2009)
  The so called Fuzzy Kolmogorov c-Max algorithm is the latest result in the selection of the OBFs. This algorithm asymptotically obtains optimal OBFs as the fuzzyness parameter goes to infinity. However, in order to obtain an appropriate tuning parameter for the algorithm to be working as intended, the user needs several iterations.

2.6 Summary

In this chapter, an overview of established theories that are used in this thesis have been given. We have introduced multiple representation forms of LTI, LTV, and LPV system. These three types of system classes are of paramount importance for this thesis. Furthermore, we have described the basic theory of Hilbert spaces which is used as the foundation for the theories related to the OBF-based model structure. We have provided a procedure to construct an OBF-based model and then described the theory related to the selection of the OBFs.

3 CHAPTER

Optimal Basis Pole Selection

This chapter is devoted to solving the basis pole selection problem for the OBF-based models. Since OBF-based models are extensively used in this thesis, selecting optimal basis poles for the OBFs in terms of approximation error of the resulting model is of paramount importance. After the introduction section, the basis pole selection problem is formally stated in Section 3.2. In Section 3.3, the basis pole selection problem is reformulated and adequate parameterization of the poles is selected. In Section 3.4, novel basis pole selection algorithms are proposed as a solution to the problem. In Section 3.5, the issue of uncertainty of pole locations, caused by uncertainty in model parameters, is addressed. In Section 3.6, performance of the proposed basis selection algorithm is demonstrated on simulation examples.

3.1 Introduction

Finite Impulse Response (FIR) model structures have been widely used in the process industry as a modeling tool to approximate the dynamical behavior of a system (Qin and Badgwell 2003b; Goodwin et al. 2005). The modeling procedure for such a model structure is relatively easy to be accomplished due to its simplicity, while it has powerful approximation capabilities. However, the simplicity of the model comes with a drawback as an accurate model of the plant, or the system of interest, may require long or infinitely many parameters. If parameter estimation or system identification techniques are conducted with such a model, the variances of the estimated parameters are going to be high. This means that the obtained model tends to have low accuracy in case of moderate or high noise conditions. One possible way to avoid this problem and achieve a parsimonious model is to use richer basis functions such as Laguerre basis or Kautz basis instead of the generic pulse basis. The aforementioned basis functions are known for their ability to impose prior knowledge of the plant or the system of interest (Lee 1932;

Kautz 1954). Laguerre basis is used to describe a dominant time constant of the system while Kautz basis is used to capture resonant modes of the system. However, when a complex system with multiple distinct modes is attempted to be modeled by using these two bases, it is apparent that these basis functions are not rich enough to obtain a parsimonious model. The work of Heuberger (1990) introduces a generalization of the Laguerre and Kautz basis into the so-called Hambo basis, which can incorporate multiple modes of the system of interest. It is not until the late 1990s that the relations between those basis functions are written systematically and embodied into the notion of GOBFs (Ninness and Gustafsson 1997; Heuberger et al. 2005).

The parameterization of a system or signal in GOBFs leads to computationally attractive techniques in various field of studies. The implication of using this basis in the context of system identification has been well summarized in Ninness and Gustafsson (1999). Utilization of GOBFs as signal parameterization technique for *Model Predictive Controller* (MPC) scheme can be seen in Wang (2009). Some examples of recent developments in the utilization of GOBFs include the work of Darwish et al. (2018) that uses the basis functions as regularization in Bayesian based identification, and the work of Bachnas et al. (2015a) that utilize the model structure to induce adaptivity in an MPC scheme. However, a key point that is often less emphasized is that the advantages of using the GOBFs model structure largely depend on the selection of the basis functions. This means that regardless of the purpose or where the GOBF framework is being applied, the implementation of the framework with well selected basis functions will certainly outperform the implementation where no emphasis on the selection is being made.

The task to select a set of OBFs from an arbitrary and possibly infinite dimensional space is not a trivial exercise. This problem is also a reason why parameterization of the basis functions in terms of Hambo basis or GOBFs is advantageous. The effect of this particular choice is that instead of selecting functions, we are now selecting poles of the all-pass filter that is used to construct the basis functions Heuberger et al. (2005). For the Laguerre basis and Kautz basis, due to the simplicity of their structure, the optimal selection can be solved analytically. However, for an arbitrary number of basis poles, the pole selection problem often needs to be solved numerically. A pragmatic approach for pole selection was suggested in van Donkelaar et al. (1998). In this work, a new set of basis functions is estimated in each iteration step and then model reduction procedure is applied to reduce the number of the basis function. This method can work in practice, but without any guarantee of convergence. Another method written in Bodin et al. (1997) utilizes a heuristic approach on selecting the basis poles.

In this Chapter, we adopt a line of reasoning proposed by Oliviera e Silva (1996) to characterize optimal basis poles with respect to the (possible) poles of the system of interest. The system of interest in the context of this thesis is restricted to be stable systems only. This optimality condition arises from the *Kolmogorov n-width* (KnW) concept of Pinkus (1985) that was originally utilized to express capability of a model set to describe a certain subset of systems. The model set is characterized by the poles of the basis generating filters, while the subset of systems is distinguished by the pole locations of their transfer function represen-

tations. In this manner, the selection of the basis poles can be cast into a nonlinear optimization problem. Several basis selection techniques are already proposed using this optimality condition. The work of Oliviera e Silva (1996) combines the optimality condition with a specific parameterization method and solves it via a non linear optimization technique. The work of Patwardhan and Shah (2005) tries to solve this problem by attaching the optimality notion to the one step-ahead prediction error minimization criterion. Another work of Tóth et al. (2009) explores and extends the notion of optimal poles for not only LTI systems, but also LPV systems. What we perceive to be lacking in the aforementioned works is either the exploitation of the structure of the problem, or the complexity of the procedures that requires the user to have sufficient knowledge to optimally run the basis selection technique. The structure of the optimality condition should point towards which optimization tools are suitable to solve the basis selection problem. From observing the basis selection problem, tools like *Sequential Quadratic Programming* (SQP), *Randomized Algorithm* (RA), and *Sum of Squares Programming* (SOSP) lead to basis selection techniques with simple tuning procedures. Moreover, due to the selected optimality condition, the basis selection techniques that we propose can be used to optimize the basis for a GOBF model of an LTI system, parametric uncertain LTI system, or an LPV system. This capability is further demonstrated in the following chapters in this thesis.

This chapter is constructed as follows. First, the basis pole selection problem is given in Section 3.2. In Section 3.3, the basis selection problem is solved by selecting an adequate parametrization of the poles. The re-formulation of basis pole selection problem is needed to select the proper optimization tools to optimally select the poles. These tools are described in Section 3.4, and are followed by the proposed basis pole selection algorithms. Section 3.5 addresses the issue on how our proposed algorithms can be used for an uncertain set of system poles. In order to deal with such a case, a region of uncertain system poles is constructed on which the basis selection methods are applied. In Section 3.6, the proposed basis selection algorithm is demonstrated on a simulation example. The performance of the proposed methods are compared with each other as well as with the current state-of-the-art. Lastly, in Section 3.7, conclusions on the presented results are drawn to end this chapter.

3.2 The basis pole selection problem

The convergence rate of the approximation error of an OBF model with the inner function $G_{n_\mathrm{e},n_\mathrm{b}} \in \mathcal{RH}_2(\mathbb{E})$ to describe the system of interest $G \in \mathcal{RH}_2(\mathbb{E})$ is dictated by the selection of the poles of $G_{n_\mathrm{e},n_\mathrm{b}} \in \mathcal{RH}_2(\mathbb{E})$ (See Section 2.5.6 for details on the approximation error and the convergence rate). The set of n_b basis pole locations of the OBF model is obtained by solving the basis pole selection problem for a given set of the system poles $\{\xi_k\}_{k=1}^{n_\mathrm{z}} = \Omega \subset \mathbb{D}$ with cardinality n_z:

Definition 3.1 ***Basis pole selection problem***
Given a set of system poles $\{\xi_k\}_{k=1}^{n_\mathrm{z}} = \Omega \subset \mathbb{D}$, *find* n_b *pole locations,* $\lambda_l^o \in \mathbb{D}, l =$

$1, 2, \ldots, n_\mathrm{b}$ *by solving the following optimization problem:*

$$P_{KnW} := \min_{\lambda_1,\ldots,\lambda_{n_\mathrm{b}} \in \mathbb{D}} \max_{\xi_1,\ldots,\xi_{n_z} \in \mathbb{D}} \prod_{l=1}^{n_\mathrm{b}} \left| \frac{\xi_k - \lambda_l}{1 - \xi_k \lambda_l^*} \right|. \tag{3.1}$$

The attained minimum of (3.1)*, denoted by* J^o*, describe the upperbound of the convergence rate* ρ_{n_b} *(of Eq.* (2.65)*) :*

$$\rho_{n_\mathrm{b}} \leq J^o, \tag{3.2}$$

with a G_{n_b} *inner function generated basis using the pole locations of* $\{\lambda_1^o, \ldots, \lambda_{n_\mathrm{b}}^o\}$*.*

The cost function corresponding to (3.1) is defined as follows:

Definition 3.2 *Define the cost function of basis pole selection problem* $J : \mathbb{D}^{n_\mathrm{b}} \to \mathbb{R}$ *as*

$$J(\lambda_1, \ldots, \lambda_{n_\mathrm{b}}) := \max_{\xi_1,\ldots,\xi_{n_z} \in \mathbb{D}} \prod_{l=1}^{n_\mathrm{b}} \left| \frac{\xi_k - \lambda_l}{1 - \xi_k \lambda_l^*} \right|. \tag{3.3}$$

the component of the cost function for l*-th basis pole and* k*-th system pole* $J_{l,k} : \mathbb{D}^2 \to \mathbb{R}$ *is:*

$$J_{l,k}(\lambda_l, \xi_k) := \left| \frac{\xi_k - \lambda_l}{1 - \xi_k \lambda_l^*} \right|. \tag{3.4}$$

In order to solve the basis pole selection problem (3.1), the problem is reformulated in the following section.

3.3 Solving the basis pole selection problem

Selection of a set of n_b basis poles $\{\lambda_l\}_{l=1}^{n_\mathrm{b}}$ that is optimal in terms of (3.1) corresponds to a min-max problem over the complex domain. Since most optimization techniques are more suitable in the domain of real numbers, parameterization of the problem in $\mathbb{R}$ is practically convenient. Furthermore, the min-max optimization problem can also be reformulated to simplify the solution of basis poles selection problem.

3.3.1 Reparameterization of the basis poles

In this work, a generic representation of complex numbers is used instead of the Schur-Cohn stability based parameterization (see Oliviera e Silva (1996)). The generic representation is used to avoid restricting the degree of freedom in the basis pole selection. There are two generic representations of a complex number which are the *cartesian form* or the *polar form*. The *cartesian form* is used throughout this work since it leads to a simpler derivation and formulation of the gradient of the cost function (3.3) when compared to the *polar form*. As mentioned in Oliviera e Silva (1996) and Heuberger et al. (2005), using the *cartesian form* to solve (3.1) requires pre-specifying how many of real and complex conjugate pairs are expected among the basis poles which is called "pole configuration". The arrangement problem to determine the configuration is illustrated as follows:

Example 3.1 *For $n_b = 10$ the possible configuration of real and complex conjugate pair of poles are:*

$$\begin{aligned} P_1 &= \{real, real, real, real, real, real, real, real, real, real\} \\ P_2 &= \{\text{real}, real, real, real, real, real, real, cp\} \\ P_3 &= \{real, real, real, real, real, real, cp, cp\} \\ P_4 &= \{real, real, real, real, cp, cp, cp\} \\ P_5 &= \{real, real, cp, cp, cp, cp\} \\ P_6 &= \{cp, cp, cp, cp, cp\} \end{aligned} \tag{3.5}$$

In this example, it can be seen that for a small or medium number of basis poles ($n_b < 10$), the possible combinatorial pairing of real and complex conjugate pairs of basis poles corresponds to 6 unique configurations. Hence, the utilization of cartesian form for pole parameterization is justified. Furthermore, In Section 3.6.3, it is shown that prior information of the system can help to narrow down the possible configurations of poles to determine the optimal basis pole configuration.

Remark 3.1 *In Example 3.1, it is inferred that the order or the sequence of real poles and complex conjugate pole pairs is not important. However, the sequence of the selected basis poles $\{\lambda_l\}_{l=1}^{n_\mathrm{b}}$ indeed changes the resulting OBFs $\{\phi_l\}_{l=1}^{n_\mathrm{b}}$. What remains invariant is the span$(\{\phi_l\}_{l=1}^{n_\mathrm{b}}) \subset \mathcal{RH}_2(\mathbb{E})$ regardless the ordering of the basis poles. For a set of basis poles $\{\lambda_l\}_{l=1}^{n_\mathrm{b}}$, we follow the ordering method mentioned in Chapter 10 of Heuberger et al. (2005). This method is tailored to avoid numerical issues that might rise due to difference of the magnitudes of the expansion coefficients w_i (of the OBF model* (2.62)*).*

In the *cartesian form*, the complex numbers corresponding to the system poles and the basis poles can be written as:

$$\begin{aligned} \xi_k &= \mathfrak{x}_k + i\mathfrak{y}_k, \\ \lambda_l &= \mathfrak{a}_l + i\mathfrak{b}_l, \end{aligned} \tag{3.6}$$

where $\mathfrak{x}_k, \mathfrak{y}_k, \mathfrak{a}_l, \mathfrak{b}_l \in \mathbb{R}_{(-1,1)}$ for $k = 1, \ldots, n_\mathrm{z}$ and $l = 1, \ldots, n_\mathrm{b}$. The *cartesian form* requires the extra condition $\mathfrak{a}_l^2 + \mathfrak{b}_l^2 < 1$ for each of the complex conjugate pole pairs to ensure that $\{\lambda_l\}_{l=1}^{n_\mathrm{b}} \subset \mathbb{D}$.

In the *cartesian form*, each of the component of cost function (3.4) can be expressed as:

$$J_{l,k}(\mathfrak{a}_l, \mathfrak{b}_l, \mathfrak{x}_k, \mathfrak{y}_k) = \left(\frac{(\mathfrak{x}_k - \mathfrak{a}_l)^2 + (\mathfrak{y}_k - \mathfrak{b}_l)^2}{(1 - \mathfrak{x}_k\mathfrak{a}_l - \mathfrak{y}_k\mathfrak{b}_l)^2 + (\mathfrak{y}_k\mathfrak{a}_l - \mathfrak{x}_k\mathfrak{b}_l)^2} \right)^{1/2}. \tag{3.7}$$

The next step of the re-parameterization of (3.1) is to distinguish (3.7) in case of real poles or complex conjugate pole pairs. Introduce the set of real valued basis poles as $\bar{\mathsf{a}} = \{\bar{\mathfrak{a}}_i\}_{i=1}^{n_r}$ with $\bar{\mathfrak{a}}_i \in \mathbb{R}_{(-1,1)}$ and the set of complex conjugate pole pairs as $\mathsf{a} = \{\mathfrak{a}_j\}_{j=1}^{n_c}, \mathsf{b} = \{\mathfrak{b}_j\}_{j=1}^{n_c}$ with $\mathfrak{a}_j \in \mathbb{R}_{(-1,1)}$ and $\mathfrak{b}_j \in \mathbb{R}_{(0,1)}$. Denote n_r as the total number of real valued basis poles and n_c as the total number of complex conjugate pole pairs. Introduce

$$N_{r,i}(\bar{\mathfrak{a}}_i, \mathfrak{x}_k, \mathfrak{y}_k) = (\mathfrak{x}_k - \bar{\mathfrak{a}}_i)^2 + (\mathfrak{y}_k)^2, \tag{3.8}$$

as the contribution of a real valued basis pole to the numerator of (3.7), and

$$D_{r,i}(\bar{\mathfrak{a}}_i, \mathfrak{x}_k, \mathfrak{y}_k) = (1 - \mathfrak{x}_k\bar{\mathfrak{a}}_i)^2 + (\mathfrak{y}_k\bar{\mathfrak{a}}_i)^2, \tag{3.9}$$

as the contribution of a real valued basis pole to the denumerator of (3.7). Introduce

$$N_{c,j}(\mathfrak{a}_j, \mathfrak{b}_j, \mathfrak{x}_k, \mathfrak{y}_k) = ((\mathfrak{x}_k - \mathfrak{a}_j)^2 + (\mathfrak{y}_k - \mathfrak{b}_j)^2). \\ ((\mathfrak{x}_k - \mathfrak{a}_j)^2 + (\mathfrak{y}_k + \mathfrak{b}_j)^2), \tag{3.10}$$

as the contribution of a complex conjugate basis pole pair to the numerator of (3.7), and

$$D_{c,j}(\mathfrak{a}_j, \mathfrak{b}_j, \mathfrak{x}_k, \mathfrak{y}_k) = ((1 - \mathfrak{x}_k\mathfrak{a}_j - \mathfrak{y}_k\mathfrak{b}_j)^2 + (\mathfrak{y}_k\mathfrak{a}_j - \mathfrak{x}_k\mathfrak{b}_j)^2). \\ ((1 - \mathfrak{x}_k\mathfrak{a}_j + \mathfrak{y}_k\mathfrak{b}_j)^2 + (\mathfrak{y}_k\mathfrak{a}_j + \mathfrak{x}_k\mathfrak{b}_j)^2). \tag{3.11}$$

as the contribution of a complex conjugate basis pole pair to the denumerator of (3.7).

Furthermore, denote

$$N(\bar{\mathsf{a}}, \mathsf{a}, \mathsf{b}, \mathfrak{x}_k, \mathfrak{y}_k) = \prod_{i=0}^{n_r} N_{r,i}(\bar{\mathfrak{a}}_i, \mathfrak{x}_k, \mathfrak{y}_k) \prod_{j=0}^{n_c} N_{c,j}(\mathfrak{a}_j, \mathfrak{b}_j, \mathfrak{x}_k, \mathfrak{y}_k), \tag{3.12}$$

and

$$D(\bar{\mathsf{a}}, \mathsf{a}, \mathsf{b}, \mathfrak{x}_k, \mathfrak{y}_k) = \prod_{i=0}^{n_r} D_{r,i}(\bar{\mathfrak{a}}_i, \mathfrak{x}_k, \mathfrak{y}_k) \prod_{j=0}^{n_c} D_{c,j}(\mathfrak{a}_j, \mathfrak{b}_j, \mathfrak{x}_k, \mathfrak{y}_k), \tag{3.13}$$

which combine the contribution of the n_r numbers of real valued basis poles and n_c numbers of complex conjugate basis pole pairs. For $i, j = 0$, we define $N_{r,0}, D_{r,0}, N_{c,0}, D_{c,0} := 1$. With the newly introduced notation, we have:

$$\prod_{l=1}^{n_b} J_{l,k}^2(\mathfrak{a}_l, \mathfrak{b}_l, \mathfrak{x}_k, \mathfrak{y}_k) = \frac{N(\bar{\mathsf{a}}, \mathsf{a}, \mathsf{b}, \mathfrak{x}_k, \mathfrak{y}_k)}{D(\bar{\mathsf{a}}, \mathsf{a}, \mathsf{b}, \mathfrak{x}_k, \mathfrak{y}_k)}. \tag{3.14}$$

Within the domain of the system poles $\{\xi_k\}_{k=1}^{n_z} \subset \mathbb{D}$, and basis poles $\{\lambda_l\}_{l=1}^{n_b} \subset \mathbb{D}$ solving the optimization problem (3.1) as

$$\tilde{P}_{\mathrm{KnW}} := \min_{\mathfrak{a}_1, \mathfrak{b}_1, \ldots, \mathfrak{a}_{n_b}, \mathfrak{b}_{n_b} \in \mathbb{R}_{[-1,1]}} \max_{\mathfrak{x}_1, \mathfrak{y}_1, \ldots, \mathfrak{x}_{n_z}, \mathfrak{y}_{n_z} \in \mathbb{R}_{[-1,1]}} \prod_{l=1}^{n_b} J_{l,k}^2. \tag{3.15}$$

can be beneficial if compared to solving the original problem (3.1). Within the domain of the optimization variables, the minimizer of (3.15) corresponds to the minimizer $(\{\lambda_i^o\}_{i=1}^{n_b})$ of (3.1). However, the gradient of the quadratic cost function $J_{l,k}^2$ has a simpler form than the gradient of $J_{l,k}$. Since most optimization techniques rely on the gradient of the cost function, a simpler gradient form might ease the implementation of such techniques. After the cost function have been reparameterized, the next step is to reformulate (3.15) into a simpler problem for which general optimization techniques can be applied.

3.3.2 Reformulation of the basis poles selection problem

On top of having a min-max problem (3.15), the cost function of this problem is a non-continuous function in its domain and hence its gradient is not always computable. This problem hinders the application of powerful gradient-based optimization methods and forces to resort to gradient free or gradient approximation based approaches, such as finite difference. For the min-max problem, it is stated in Boyd and Vandenberghe (2004) that a min-max problem can be re-casted into a constrained minimization problem. After the min-max problem is reformulated, we need to find a continuous approximation of the new cost function. This approximation needs to have the same characteristics as the cost function, especially with respect to the minimizer $\{\lambda_i^o\}_{i=1}^{n_\mathrm{b}}$.

In order to reformulate the min-max problem, introduce $\gamma \in \mathbb{R}_{(0,1]}$ as the upperbound of (3.14).

$$\frac{N(\bar{\mathsf{a}}, \mathsf{a}, \mathsf{b}, \mathfrak{x}_k, \mathfrak{y}_k)}{D(\bar{\mathsf{a}}, \mathsf{a}, \mathsf{b}, \mathfrak{x}_k, \mathfrak{y}_k)} \leq \gamma \quad , \forall k = 1, \ldots, n_\mathrm{z}. \tag{3.16}$$

For arbitrary values of $\mathfrak{x}_k, \mathfrak{y}_k, \mathfrak{a}_l, \mathfrak{b}_l \in \mathbb{R}_{(-1,1)}$ that belong to the domain of the system poles $\{\xi_k\}_{k=1}^{n_\mathrm{z}} \subset \mathbb{D}$ and the domain of the basis poles $\{\lambda_l\}_{l=1}^{n_\mathrm{b}} \subset \mathbb{D}$, the variable γ describes the upperbound of the attained minimum of (3.15):

$$(J^o)^2 \leq \gamma. \tag{3.17}$$

By utilizing this upperbound, given a set of reparameterized system poles $\{\mathfrak{x}_k, \mathfrak{y}_k\}_{k=1}^{n_\mathrm{z}}$, the optimization problem of (3.15) can be re-casted as:

$$\begin{aligned} P_{\mathrm{ref}}: \quad & \min_{\gamma, \bar{\mathsf{a}}, \mathsf{a}, \mathsf{b}} \quad \gamma \\ & \text{s.t} \quad \frac{N(\bar{\mathsf{a}}, \mathsf{a}, \mathsf{b}, \mathfrak{x}_1, \mathfrak{y}_1)}{D(\bar{\mathsf{a}}, \mathsf{a}, \mathsf{b}, x_1, y_1)} \leq \gamma, \\ & \qquad\quad \vdots \\ & \qquad\quad \frac{N(\bar{\mathsf{a}}, \mathsf{a}, \mathsf{b}, \mathfrak{x}_{n_z}, \mathfrak{y}_{n_z})}{D(\bar{\mathsf{a}}, \mathsf{a}, \mathsf{b}, \mathfrak{x}_{n_z}, \mathfrak{y}_{n_z})} \leq \gamma. \end{aligned} \tag{3.18}$$

If the minimum of (3.18) is attained, then $(J^o)^2 = \gamma$. The optimization problem (3.18) has a linear cost function in the decision variables $(\gamma, \bar{\mathsf{a}}, \mathsf{a}, \mathsf{b})$ and a set of n_z rational function inequalities. The basis pole selection problem (3.18) amounts to minimizing the upper bound value γ. However, the constraint (3.18) still consists of non-continuous functions. The next step is to reformulate the constraints of (3.18). Provided that $D(\bar{\mathsf{a}}, \mathsf{a}, \mathsf{b}, \mathfrak{x}_k, \mathfrak{y}_k) > 0$, each inequality is equivalent to:

$$\tilde{J}_k(\gamma, \bar{\mathsf{a}}, \mathsf{a}, \mathsf{b}) = N(\bar{\mathsf{a}}, \mathsf{a}, \mathsf{b}, \mathfrak{x}_k, \mathfrak{y}_k) - \gamma D(\bar{\mathsf{a}}, \mathsf{a}, \mathsf{b}, \mathfrak{x}_k, \mathfrak{y}_k) \leq 0, \tag{3.19}$$

This condition holds anywhere in the domain of the decision variables $(\gamma, \bar{\mathsf{a}}, \mathsf{a}, \mathsf{b})$ that satisfy $\{\xi_k\}_{k=1}^{n_\mathrm{z}} \subset \mathbb{D}$ and $\{\lambda_l\}_{l=1}^{n_\mathrm{b}} \subset \mathbb{D}$. It can be seen that the polynomial function (3.19) is continuous and hence the gradient of this function is computable

everywhere in the domain of the decision variable. By using relation (3.19), we reach the final reformulation of the basis pole selection problem which is now defined as:

Definition 3.3 ***Reformulated basis pole selection problem:***
Given a set of reparameterized system poles $\{\mathfrak{x}_k, \mathfrak{y}_k\}_{k=1}^{n_z}$*, and prior selection of the number of real valued basis poles* n_r *and complex conjugate pairs of basis poles* n_c*. Find the set of reparameterized optimal pole locations* $\{\bar{\mathsf{a}}, \mathsf{a}, \mathsf{b}\}$ *by solving the following optimization problem:*

$$P_{\text{sel}} := \begin{array}{ll} \min\limits_{\gamma, \bar{\mathsf{a}}, \mathsf{a}, \mathsf{b}} & \gamma \\ s.t & \tilde{J}_k(\gamma, \bar{\mathsf{a}}, \mathsf{a}, \mathsf{b}) \leq 0; \quad k = 1, \ldots, n_{\text{z}}. \end{array} \tag{3.20}$$

The minimizer $\bar{\mathsf{a}}^o = \{\bar{\mathfrak{a}}_i^o\}_{i=1}^{n_r}$ *corresponds to the real valued optimal basis poles:*

$$\lambda_l = \bar{\mathfrak{a}}_l^o, \;\; l = 1, \ldots, n_r \tag{3.21}$$

while $\mathsf{a}^o = \{\mathfrak{a}_j\}_{j=1}^{n_c}, \mathsf{b}^o = \{\mathfrak{b}_j\}_{j=1}^{n_c}$ *correspond to the complex conjugate basis pole pairs:*

$$\lambda_{n_r+2l-1} = \mathfrak{a}_l^o + i\mathfrak{b}_l^o, \lambda_{n_r+2l} = \mathfrak{a}_l^o - i\mathfrak{b}_l^o, \;\; l = 1, \ldots, n_c. \tag{3.22}$$

The attained minimum of (3.20) *is denoted by* γ^o *and obeys the relation of*

$$\gamma^o = (J^o)^2, \tag{3.23}$$

where J^o *is the minimum of the original problem* (3.1)*. The gradient of* $\tilde{J}_k$ *in* (3.20) *is given by:*

$$\nabla \tilde{J}_k = \left[-D(\bar{\mathsf{a}}, \mathsf{a}, \mathsf{b}) \;\; \frac{\partial \tilde{J}_k}{\partial \bar{\mathfrak{a}}_1} \;\; \ldots \;\; \frac{\partial \tilde{J}_k}{d\bar{\mathfrak{a}}_i} \;\; \frac{\partial \tilde{J}_k}{\partial \mathfrak{a}_1} \;\; \frac{\partial \tilde{J}_k}{\partial \mathfrak{b}_1} \;\; \ldots \;\; \frac{\partial \tilde{J}_k}{\partial \mathfrak{a}_j} \;\; \frac{\partial \tilde{J}_k}{\partial \mathfrak{b}_j} \right]^\top. \tag{3.24}$$

The derivation of the gradient (3.24) *can be found in the Appendix A.1.*

These constraints can be brought into the cost function by multipliers. An analytical solution to problem (3.20) for the configuration of a single real valued basis pole (i.e. $n_{\text{b}} = n_r = 1, n_c = 0$) can be given. This is illustrated as follows:

Example 3.2 *For* $n_r = 1$*, we can write* (3.19) *as*

$$(-1 - \gamma\mathfrak{x}_k^2 - \gamma\mathfrak{y}_k^2)\bar{\mathfrak{a}}_1^2 + (2\gamma\mathfrak{x}_k - 2\mathfrak{x}_k)\bar{\mathfrak{a}}_1 + \mathfrak{x}_k^2 + \mathfrak{y}_k^2 - \gamma \leq 0, \;\; k = 1, \ldots, n_{\text{z}}. \tag{3.25}$$

By substituting the set of reparameterized system poles $\{\mathfrak{x}_k, \mathfrak{y}_k\}_{k=1}^{n_z}$ *into* (3.25) *and replacing "*$\leq$*" with "*$=$*", we have* n_z *set of 2nd order polynomials equations in* γ *and* $\bar{\mathfrak{a}}_1$ *which is simple enough to be solved to find the values for both variables.*

However, for general configuration of basis poles, the number of multivariate polynomials in $\tilde{J}_k$ complicates the analytical solution of (3.20). Hence, we have to rely on using numerical optimization tools. We need to select numerical optimization tools that can be used to solve the optimization problem of (3.20) in an efficient manner.

3.4 Optimization tools for basis poles selection

The basis pole selection problem of (3.20) has a linear cost function with polynomial (non-linear) inequality constraints. We propose three methods to solve this problem. The methods are *Sequential Quadratic Programming* (SQP), *Randomized Algorithm* (RA), and *Sum of Squares Programming* (SOSP). We first describe the basic concept and theory of each of these optimization tools to give a better understanding of their utilization for solving the basis pole selection problem. The equations related to each of these methods are tailored towards the basis pole selection problem.

3.4.1 Sequential quadratic programming

Sequential Quadratic Programming (SQP) is an iterative *Non-Linear Programming* (NLP) algorithm that allows us to mimic Newton's method for constrained optimization just as it is done for the unconstrained case. This method utilizes the Hessian of the Lagrangian function of the original problem to construct a QP subproblem. This subproblem is then used to formulate a line search procedure to reach the numerical solution for the original problem (Nocedal and Wright 2006).

Core concept of the SQP Algorithm

A generic description of SQP algorithm for the basis pole selection problem (Definition 3.3) is given to understand the concept of the algorithm. Introduce

$$v = \text{col}(\{\gamma, \bar{\mathsf{a}}, \mathsf{a}, \mathsf{b}\}) \in \mathbb{R}^{n_{\text{obj}}},$$

with $n_{\text{obj}} = 1 + n_r + 2n_c$, as the vectorized form of the optimization variables. Introduce v_k as the value of v at the k-th iteration of the SQP algorithm. Without index k, v is seen as the search direction of the SQP algorithm. Introduce the Lagrangian function for (3.20):

$$L(v) = \gamma - \sum_{j=1}^{n_z} \mu_j \tilde{J}_j(v). \tag{3.26}$$

where $0 \leq \mu_j \leq 1$ are the Lagrangian multipliers, $\tilde{J}_j$ is given in (3.19), and $j = 1, \ldots, n_z$. The SQP algorithm constructs the QP subproblem (quadratic cost with linear constraints) for (3.20) in each k-th iteration of the algorithm. The QP subproblem is given as follows:

$$\begin{aligned} P_{\text{sqp}} := \quad & \min_{v \in \mathbb{R}^{n_{\text{obj}}}} \quad \tfrac{1}{2} v^\top H_k v + v \\ & \text{s.t} \quad \nabla \tilde{J}_j(v_k)^\top v + \tilde{J}_j(v_k) \leq 0, \qquad j = 1, \ldots, n_z, \end{aligned} \tag{3.27}$$

where $\nabla \tilde{J}_j(v_k)$ is Equation (3.24) evaluated at v_k, $\tilde{J}_j(v_k)$ is Equation (3.19) evaluated at v_k, and H_k is (a positive definite approximation of) the Hessian matrix of

the Lagrangian function

$$H_k = \frac{\partial^2}{\partial v^2} L(v)\bigg|_{v=v_k}. \tag{3.28}$$

In general, the implementation of an SQP algorithm utilizes an approximation of the Hessian where the value of H_0 is initialized with a positive definite matrix. The value of v_{k+1} for the next iteration of the SQP algorithm is obtained by:

$$v_{k+1} = v_k + \alpha_k v, \tag{3.29}$$

where α_k is the step length and v is the solution of the QP subproblem (3.27). The value of α_k can be obtained via evaluating (3.19) in the search direction (3.29). Alternatively, one can determine the optimal step length by using a merit function such as given in (Nocedal and Wright 2006). The Hessian update for the $k+1$-th iteration of (3.27) is based on the Broyden-Fletcher-Goldfarb-Shanno (BFGS) method:

$$H_{k+1} = H_k + \frac{q_k q_k^\top}{q_k^\top s_k} - \frac{H_k s_k s_k^\top H_k^\top}{s_k^\top H_k s_k}, \tag{3.30}$$

where

$$s_k = v_{k+1} - v_k, \tag{3.31}$$

$$q_k = \sum_{i=1}^{m} \mu_i \tilde{J}_j(v_{k+1}) - \sum_{i=1}^{m} \mu_i \tilde{J}_j(v_k). \tag{3.32}$$

The SQP iteration is continued until $q_k^\top s_k$ being greater than or equal to a pre-specified tolerance value. Further details on the SQP algorithm can be found in Chapter 18 of Nocedal and Wright (2006).

Remark 3.2 *The generic implementation of SQP can be conducted via available non/commercial solvers such as* `fmincon`*, etc (Matlab 2022). These solvers provide the approximation of the Lagrangian multiplier for each iteration, the initial value for the hessian H_o, and the optimal step length α_k. In most solvers, analytic form of the gradient* (3.24) *is optional. If manual implementation of SQP is needed, the Hessian needs to be computed and the Lagrangian multiplier can be obtained via solving a set of equations related to the* Karush-Kuhn-Tucker *(KKT) condition of the optimization problem. We select the* `fmincon` *solver for implementing the SQP algorithm. Next to SQP, we have studied several NLP algorithms such as Barrier function, Active Sets, etc. Among these methods, the SQP has given the shortest computation time with a result that is less sensitive for moderate number of basis poles ($n_\mathrm{b} > 5$).*

Implementation of SQP

The implementation of the SQP in the `fmincon` environment is straightforward. The required elements for solving the basis pole selection problem (3.20) are:

- Number of real valued basis poles n_r and complex conjugate basis pole pairs n_c.

- The cost function (3.20).
- The inequality constraint (3.19) and its gradient (3.24) for each of the given system poles $\{\xi_k = \mathfrak{x}_k + i\mathfrak{y}_k\}_{k=1}^{n_z}$.
- Domain of the optimization variables:

$$\begin{array}{l} \gamma \in \mathbb{R}_{[0,1)}, \\ \bar{\mathfrak{a}} = \{\bar{\mathfrak{a}}_i\}_{i=1}^{n_r} \quad \text{with} \quad \bar{\mathfrak{a}}_i \in \mathbb{R}_{(-1,1)}, \\ \mathfrak{a} = \{\mathfrak{a}_j\}_{j=1}^{n_c} \quad \text{with} \quad \mathfrak{a}_j \in \mathbb{R}_{(-1,1)}, \\ \mathfrak{b} = \{\mathfrak{b}_j\}_{j=1}^{n_c} \quad \text{with} \quad \mathfrak{b}_j \in \mathbb{R}_{(0,1)}. \end{array} \tag{3.33}$$

- The constraint for complex conjugate basis pole pairs: $\mathfrak{a}_j^2 + \mathfrak{b}_j^2 < 1$ for $j = 1, \ldots, n_c$.

However, due to the nonlinear characteristic of the problem, the solution of the algorithm is sensitive with respect to the initial value of v_0. The algorithm becomes more sensitive as the dimension of decision variables increases. One way to avoid finding unsatisfactory local optima is by running the algorithm multiple times with different initial points. The initial points can be picked randomly around the possible set of system poles Ω. The result with the lowest γ is then picked as the solution of the algorithm. The implementation of multiple SQPs with random initialization is described in Algorithm 1.

Algorithm 1 SQP basis pole selection using multiple `fmincon`)

Require :

- Required elements for the `fmincon` environment
- Total number of algorithm runs: n_{run}

Ensure: $n = 1$
  while $n \leq n_{\text{run}}$ **do**
    Select a random initial value for the n-th run $v_0^{[n]}$
    Run `fmincon` with the cost function, gradients, and $v_0^{[n]}$
    Collect the final value $v_{k_{\text{end}}}^{[n]} = v_{k_{\text{end}}}$
    $n \leftarrow n + 1$
  end while
  Select the final value $v_{k_{\text{end}}}^{[n]}$ with the smallest γ for all algorithm runs $n = 1, \ldots, n_{\text{run}}$

3.4.2 Randomized algorithm

The reformulated problem (3.20) is still a difficult non-linear optimization problem that is also subject to the curse of dimensionality. Hence, the *Randomized Algorithms* (RA) which do not suffer from such a curse of dimensionality (Tempo

et al. 2013), represent an attractive alternative to solve the basis selection problem. The search space (domain) for the basis poles that is limited to the unit disc is also a favorable condition for the RA. Moreover, since the basis selection problem is almost always solved in an offline manner, we can adjust the accuracy of the solution depending on the number of iterations (time) and the resources (computational power) that we have.

Core concept of the randomized algorithm

The RA is based on the theorem of *The Law of Large Numbers for Empirical Probability* and *The Law of Large Numbers for Empirical Minimum* (Tempo et al. 2013). In this framework, we assume that the parameterized set of basis poles $\{\bar{\mathsf{a}}, \mathsf{a}, \mathsf{b}\}$ consists of random variables with a particular probability distribution. In this probabilistic sense, for a deterministic set of system poles $\{\xi_k = \mathfrak{x}_k + i\mathfrak{y}_k\}_{k=1}^{n_z} = \Omega$, we can describe the maximum value of:

$$\max_{\mathfrak{x}_k, \mathfrak{y}_k \in \Omega} \frac{N(\bar{\mathsf{a}}, \mathsf{a}, \mathsf{b}, \mathfrak{x}_k, \mathfrak{y}_k)}{D(\bar{\mathsf{a}}, \mathsf{a}, \mathsf{b}, \mathfrak{x}_k, \mathfrak{y}_k)} := f_\gamma(\bar{\mathsf{a}}, \mathsf{a}, \mathsf{b}), \tag{3.34}$$

by using a probability density function denoted by f_γ.

However, due to nonlinearity of (3.34), the probability density function f_γ is difficult to compute even with a priori knowledge on the probability distribution of the parameterized set of basis poles. The approximation of f_γ can be obtained by computing the empirical estimate of the density function based on finite number of *multisamples*[1] of the basis poles. The set of N number of *multisamples* of the basis poles is denoted by

$$\{[\bar{\mathsf{a}}, \mathsf{a}, \mathsf{b}]^{(i)}\}_{i=1}^{N}, \tag{3.35}$$

where the index in $[\bar{\mathsf{a}}, \mathsf{a}, \mathsf{b}]^{(i)}$ corresponds to the i-th sample.

Introduce a performance level $\gamma \in \mathbb{R}_{[0,1)}$ as the possible value of (3.34). Assuming that f_γ is known, the probability of having a set of basis poles that result in a value of (3.34) that is less than γ is written as:

$$R(\gamma) = \Pr\{f_\gamma(\bar{\mathsf{a}}, \mathsf{a}, \mathsf{b}) \leq \gamma\}. \tag{3.36}$$

The computation of empirical estimate of (3.36) is defined as follows:

Definition 3.4 *Given a performance level γ and a set of N multisamples $\{[\bar{\mathsf{a}}, \mathsf{a}, \mathsf{b}]^{(i)}\}_{i=1}^{N}$, the empirical estimate of* (3.36) *can be computed by:*

$$\hat{R}_N(\gamma) = \frac{1}{N} \sum_{i=1}^{N} \mathbb{I}_{RA}([\bar{\mathsf{a}}, \mathsf{a}, \mathsf{b}]^{(i)}), \tag{3.37}$$

where $\mathbb{I}_{RA}$ is an indicator function that is given by:

$$\mathbb{I}_{RA}([\bar{\mathsf{a}}, \mathsf{a}, \mathsf{b}]^{(i)}) = \begin{cases} 1 & \textit{if } f_\gamma([\bar{\mathsf{a}}, \mathsf{a}, \mathsf{b}]^{(i)}) \leq \gamma, \\ 0 & \textit{otherwise}. \end{cases} \tag{3.38}$$

[1] randomly taken samples of the parameters of interest from their respective domain.

The asymptotic convergence of the empirical estimate (3.37) to (3.36) as $N \to \infty$ is guaranteed (Tempo et al. 2013). For a finite set of *multisamples*, a certification of the empirical estimate (3.37) in the probabilistic sense can be made. The certification of the validity of an empirical estimate is described by a variable called the confidence level $\delta \in \mathbb{R}_{(0,1)}$. Furthermore, it is stated in Tempo et al. (2013); Bai et al. (1997) that the minimum number of *multisamples* needed to reach a predetermined confidence level δ varies depending on the implementation of the RA and the methods used to obtain the set of *multisamples*. The minimum number of the required *multisamples* is attained by assuming a uniform distribution of the samples over the domain of the parameters. We propose two types of RA's to obtain a sample of the parameterized basis poles $[\bar{\mathsf{a}}, \mathsf{a}, \mathsf{b}]^{(\mathsf{i})}$ that is approximately equal to:

$$f_\gamma([\bar{\mathsf{a}}, \mathsf{a}, \mathsf{b}]^{(\mathsf{i})}) \approx \gamma^*, \tag{3.39}$$

where

$$\gamma^* = \inf_{\bar{\mathsf{a}},\mathsf{a},\mathsf{b}} f_\gamma(\bar{\mathsf{a}}, \mathsf{a}, \mathsf{b}). \tag{3.40}$$

Remark 3.3 *In computing the solution of the RA, time is mostly spent on drawing a sample* (3.35) *and computing* (3.34) *for that particular sample. Hence, application of parallel computing can speed up the computation time to complete N number of iterations.*

Implementation of RA based on direct worst case approximation

In this algorithm, the empirical estimate of γ^* is analyzed with respect to the total volume of the domain of the random variable $[\bar{\mathsf{a}}, \mathsf{a}, \mathsf{b}]$. The portion of the domain that is not represented by the set of *multisamples* is characterized by $\beta \in \mathbb{R}_{(0,1)}$. More specifically, the probability to obtain the empirical estimate with respect to almost all possible samples of $[\bar{\mathsf{a}}, \mathsf{a}, \mathsf{b}]$ is given by:

$$\Pr\left\{ \hat{R}_N(\gamma^*) \geq \beta \right\} \geq 1 - \delta. \tag{3.41}$$

For this type of RA, the minimum number of the required *multisamples* to achieve such result is given by:

$$N_{wc} = \frac{\log 1/\delta}{\log 1/\beta}. \tag{3.42}$$

The approximate value of (3.39) is obtained via

$$\gamma_N^* = \min_{i \in \{1,\ldots,N_{wc}\}} f_\gamma([\bar{\mathsf{a}}, \mathsf{a}, \mathsf{b}]^{(\mathsf{i})}). \tag{3.43}$$

For this particular implementation, there is no guarantee that γ_N^* is actually close to γ^*. The bound only guarantees (in the probabilistic sense) that almost all possible values of $f_\gamma(\bar{\mathsf{a}}, \mathsf{a}, \mathsf{b})$ will be bigger than $\hat{\gamma}_N^*$ with high probability of at least $1 - \delta$. In other words, the possible values of $\bar{\mathsf{a}}, \mathsf{a}, \mathsf{b}$ that correspond to $f_\gamma(\bar{\mathsf{a}}, \mathsf{a}, \mathsf{b})$ being smaller than the obtained $\hat{\gamma}_N^*$, has a volume measure that is smaller than $\beta \cdot 100\%$ of the domain of $\bar{\mathsf{a}}, \mathsf{a}, \mathsf{b}$. If the density function is sufficiently smooth, the estimated and actual minimum may be close. The implementation of direct worst case RA is described in Algorithm 2.

Algorithm 2 RA basis pole selection using direct worst case approximation

Require :

- Number of real valued basis poles n_r and complex conjugate basis pole pairs n_c.
- Set of system poles $\{\xi_k = \mathfrak{x}_k + i\mathfrak{y}_k\}_{k=1}^{n_z}$.
- Confidence level $0 < \delta < 1$.
- Volume density $0 < \beta < 1$.
- Number of iteration N_{wc} from (3.42)

Ensure: $i = 1$
  while $i \leq N_{wc}$ **do**
    Draw the i-th sample $[\bar{\mathsf{a}}, \mathsf{a}, \mathsf{b}]^{(i)}$
    Compute $f_\gamma([\bar{\mathsf{a}}, \mathsf{a}, \mathsf{b}]^{(i)})$ using (3.34)
    $i \leftarrow i + 1$
  end while
  Obtain γ_N^* from the *multisamples* using (3.43)
  Select the i-th sample $[\bar{\mathsf{a}}, \mathsf{a}, \mathsf{b}]^{(i)}$ that results in $f_\gamma([\bar{\mathsf{a}}, \mathsf{a}, \mathsf{b}]^{(i)}) = \gamma_N^*$

Implementation of RA based on probabilistic performance verification

For this type of RA, the algorithm consists of two parts which are the minimization of the performance level γ and finding a sample that corresponds to $f_\gamma([\bar{\mathsf{a}}, \mathsf{a}, \mathsf{b}]^{(i)}) < \gamma$. The performance level is minimized in an iterative manner (e.g. by a *bisection based search* strategy) up until we cannot find feasible sample from the *multisample* that satisfies $f_\gamma([\bar{\mathsf{a}}, \mathsf{a}, \mathsf{b}]^{(i)}) < \gamma$. Such confidence level is then denoted by γ_N^* and the relation between $R(\gamma_N^*)$ of (3.36) and its empirical estimate is given by:

$$\Pr\{R(\gamma_N^*) - \hat{R}_N(\gamma_N^*) < \epsilon\} \geq 1 - \delta, \tag{3.44}$$

where $\epsilon \in \mathbb{R}_{(0,1)}$ is the probabilistic error value. The minimum number of *multisamples* that need to be drawn for each iteration in order to achieve (3.44) follow the *one sided Chernoff bound* (Tempo et al. 2013):

$$N_v = \frac{1}{2\epsilon^2} \log \frac{1}{\delta}. \tag{3.45}$$

The one-sided bound is used because its not possible to have $\hat{\gamma}_N^* < \gamma^*$. We can interpret the result of this algorithm as follows. If we can not find any samples that obey $f_\gamma([\bar{\mathsf{a}}, \mathsf{a}, \mathsf{b}]^{(i)}) < \hat{\gamma}_N^*$ after N_v *multisamples* have been taken from the last iteration to minimize γ, then that particular $\hat{\gamma}_N^*$ is approximately close to the γ^* of (3.39) with confidence level of $1 - \delta$. The implementation of a probabilistic performance verification RA is described in Algorithm 3.

Algorithm 3 RA basis pole selection using probabilistic performance verification (a bisection based search strategy

Require :

- Number of real valued basis poles n_r and complex conjugate basis pole pairs n_c
- Set of system poles $\{\xi_k = \mathfrak{x}_k + i\mathfrak{y}_k\}_{k=1}^{n_z}$
- Confidence level $0 < \delta < 1$
- Accuracy level $0 < \epsilon < 1$
- Number of iteration N_v from (3.45)

Ensure: $i = 1$, $\gamma_{\max} = 1$, and $\gamma_{\min} = 0$
  Calculate the actual search point $\gamma = \frac{\gamma_{\max} - \gamma_{\min}}{2} + \gamma_{\min}$
  while $\gamma - \gamma_{\min} < \epsilon$ **do**
    Draw the i-th sample $[\bar{\mathsf{a}}, \mathsf{a}, \mathsf{b}]^{(i)}$
    Compute $f_\gamma([\bar{\mathsf{a}}, \mathsf{a}, \mathsf{b}]^{(i)})$ by (3.34)
    if $f_\gamma([\bar{\mathsf{a}}, \mathsf{a}, \mathsf{b}]^{(i)}) < \gamma$ **then**
      Save the candidate sample $[\bar{\mathsf{a}}, \mathsf{a}, \mathsf{b}]^{(i)}$
      Set $\gamma_{\max} \leftarrow \gamma$
      Set $\gamma \leftarrow \frac{\gamma_{\max} - \gamma_{\min}}{2} + \gamma_{\min}$
    else if $f_\gamma([\bar{\mathsf{a}}, \mathsf{a}, \mathsf{b}]^{(i)}) > \gamma$ and $i < N_v$ **then**
      $i \leftarrow i + 1$
    else if $f_\gamma([\bar{\mathsf{a}}, \mathsf{a}, \mathsf{b}]^{(i)}) > \gamma$ and $i = N_v$ **then**
      Set $\gamma_{\min} \leftarrow \gamma$
      Set $\gamma \leftarrow \frac{\gamma_{\max} - \gamma_{\min}}{2} + \gamma_{\min}$
    end if
  end while
  Set $\gamma_N^* \leftarrow \gamma$
  Use the candidate sample $[\bar{\mathsf{a}}, \mathsf{a}, \mathsf{b}]^{(i)}$

3.4.3 Sum of squares programming

When the value of γ in (3.20) is fixed, the optimization problem becomes a feasibility problem. A feasibility problem for a set of polynomial inequalities are equivalent with finding the *Sum Of Squares* (SOS) of the polynomials (Parrilo 2000). In contrary with the previous two algorithms, the solution of an SOSP is always the global optimum due to its convexity. However, by casting the basis selection problem as an SOS problem, we are solving the proxy of the true problem. Hence, only the resulting value of γ can be used and not the minimizer (basis poles). The minimal value of γ for a given set of system poles is obtained via *bisection based search* strategy.

Core idea of SOSP

The SOSP algorithm is based on the SOS decomposition of multivariate polynomials which can be efficiently computed using *semi definite programming* (SDP) (Parrilo 2000). A multivariate polynomial $f(x_1, \ldots, x_2) := f(x)$ is an SOS if there exist polynomials $f_1(x), \ldots, f_m(x)$ such that

$$f(x) = \sum_{i=1}^{m} f_i^2(x). \tag{3.46}$$

Clearly, if $f(x)$ is SOS then $f(x) \geq 0$. Verification wether $f(x)$ is SOS or not is a more tractable problem than verifying wether $f(x) \geq 0$. Introduce $X(\mathfrak{x}_k, \mathfrak{y}_k)$ as a column matrix containing multivariate polynomials in terms of $\mathfrak{x}_k, \mathfrak{y}_k \in \Omega$. Introduce $A(\gamma, \bar{\mathsf{a}}, \mathsf{a}, \mathsf{b})$ as a positive semi definite matrix with a structure that follows (3.19). The inequality constraints of (3.20) can be written as an SOS of:

$$X(\mathfrak{x}_k, \mathfrak{y}_k)^\top A(\gamma, \bar{\mathsf{a}}, \mathsf{a}, \mathsf{b}) X(\mathfrak{x}_k, \mathfrak{y}_k) \geq 0, \quad k = 1, \ldots, n_{\mathrm{z}}. \tag{3.47}$$

In order to illustrate the structure of (3.47), we provide an example as follows:

Example 3.3 *For $n_r = 1$ we can write* (3.19) *as*

$$(\gamma\bar{\mathsf{a}}_1^2 - 1)\mathfrak{x}_k^2 + (\gamma\bar{\mathsf{a}}_1^2 - 1)\mathfrak{y}_k^2 + 2(\bar{\mathsf{a}}_1 - \gamma\bar{\mathsf{a}}_1)\mathfrak{x}_k + \gamma + \bar{\mathsf{a}}_1^2 \geq 0. \tag{3.48}$$

Afterwards, the structure (3.47) *is obtained by collecting the polynomials of $\mathfrak{x}_k, \mathfrak{y}_k$:*

$$\begin{pmatrix} \mathfrak{x}_k \\ \mathfrak{y}_k \\ 1 \end{pmatrix}^\top \begin{pmatrix} \gamma\bar{\mathsf{a}}_1^2 - 1 & 0 & \bar{\mathsf{a}}_1 - \gamma\bar{\mathsf{a}}_1 \\ 0 & \gamma\bar{\mathsf{a}}_1^2 - 1 & 0 \\ \bar{\mathsf{a}}_1 - \gamma\bar{\mathsf{a}}_1 & 0 & +\gamma + \bar{\mathsf{a}}_1^2 \end{pmatrix} \begin{pmatrix} \mathfrak{x}_k \\ \mathfrak{y}_k \\ 1 \end{pmatrix} \geq 0 \tag{3.49}$$

By specifying a value of γ, finding a positive semi definite matrix $A(\gamma, \bar{\mathsf{a}}, \mathsf{a}, \mathsf{b})$ that satisfies (3.47) is a convex feasibility problem in the domain of the parameterized basis poles $\{\bar{\mathsf{a}}_\mathsf{i}, \mathsf{a}_\mathsf{i}, \mathsf{b}_\mathsf{i}\}_{i=1}^{n_r+2n_c}$. The smallest possible value of γ that still satisfies the feasibility problem can be obtained iteratively via a *bisection based search strategy*. After obtaining the minimum of γ, (3.19) can be re-casted as equalities and the optimum can be calculated by finding the roots of the resulting multi-argument polynomial. However, this final step is a complicated mathematical problem in itself.

Implementation of SOSP

The feasibility problem (3.47) solved by reformulating it as an SDP that can be solved efficiently using SDP solvers such as `SDPT3`. Since, SOSP always leads to a relaxation of the original polynomial optimization problem, the obtained minimizer is often not a good approximation of the minimizer of the un-relaxed problem. Due to this reason, this algorithm is more suited to validate or falsify the solution from the previously proposed solutions of the SQP and the RA. The implementation of SOSP is described in Algorithm 4.

Algorithm 4 SOSP basis pole selection using SDPT3

Require :

- Number of real valued basis poles n_r and complex conjugate basis pole pairs n_c.
- Set of system poles $\{\xi_k = \mathfrak{x}_k + i\mathfrak{y}_k\}_{k=1}^{n_z}$
- Stopping condition of the bisection search ϵ

Ensure: $\gamma_{\max} = 1$, and $\gamma_{\min} = 0$
  Construct $X(\mathfrak{x}_k, \mathfrak{y}_k)$ and $A(\gamma, \bar{\mathsf{a}}, \mathsf{a}, \mathsf{b})$
  Compute polynomials $\mathfrak{x}_k, \mathfrak{y}_k$ in $X(\mathfrak{x}_k, \mathfrak{y}_k)$ for all $k = 1, \ldots, n_z$
  Calculate the actual search point $\gamma = \frac{\gamma_{\max} - \gamma_{\min}}{2} + \gamma_{\min}$
  while $\gamma - \gamma_{\min} < \epsilon$ **do**
    if If there exist $\{\bar{\mathsf{a}}_i, \mathsf{a}_i, \mathsf{b}_i\}_{i=1}^{n_r+2n_c}$ that satisfy (3.47) **then**
      Set $\gamma_{\max} \leftarrow \gamma$
      Set $\gamma \leftarrow \frac{\gamma_{\max} - \gamma_{\min}}{2} + \gamma_{\min}$
    else if If there is no $\{\bar{\mathsf{a}}_i, \mathsf{a}_i, \mathsf{b}_i\}_{i=1}^{n_r+2n_c}$ that satisfy (3.47) **then**
      Set $\gamma_{\min} \leftarrow \gamma$
      Set $\gamma \leftarrow \frac{\gamma_{\max} - \gamma_{\min}}{2} + \gamma_{\min}$
    end if
  end while
  The optimum γ^* is ϵ close to the value γ

3.4.4 Basis pole selection using other methods

We have investigated several alternative methods to solve problem (3.20). One of them is based on finding the null-space of the polynomial (3.19). For a selection of a single real pole, analytical solution can be obtained (See Example 3.2). However, for selection of more than a single pole, this becomes a problem of finding null-space of a multivariate polynomial. This leads to a computational problem where the computational time grows substantially with the number of basis poles. We have also tried to convexify the original cost function of (3.3) by casting the expression in the hyperbolic geometry framework (Bachnas et al. 2015b). However, the multiplication of the decision variable in (3.1) destroys the zero metricity and complicate this line of reasoning.

3.5 Basis pole selection for systems with uncertain pole locations

The basis pole selection problem (Definition 3.3) is formulated with the assumption of a finite and countable set of system poles. In this section, we provide a method to use the proposed basis pole selection algorithms for systems with uncertain pole locations. The uncertainty of pole locations is a result of system parameters (coefficients) that are uncertain. Such a system is usually the result of a system identification procedure used to obtain a model of a system of interest with a given confidence bound on the estimated parameters. The system identification framework and possible procedures are further described in Chapter 4 of this thesis. In order to deal with such a condition, a region of uncertain system poles needs to be constructed. The related theory for this purpose is provided in this section. Afterwards, we translate the theory into a method to construct a finite and countable set of system poles.

3.5.1 Theory of pole confidence bounds

The theory, which is described in details in Vuerinckx et al. (2001) and Tóth (2010), gives a mapping between uncertain parameters and possible corresponding pole locations. The theory provides a hypothesis test to check wether a candidate pole location is a valid pole location for a system with uncertainty in its parameter.

System with uncertain parameters

For the sake of simplicity, only the SISO case is considered. Let $\mathcal{G}$ denote an unknown discrete time system and denote $\mathcal{F}_{\theta_n}$ as a parameterized proper discrete time[2] SISO LTI model estimate with order n (Ljung 1999):

$$F\left(q,\theta_n\right)=\frac{\sum_{k=0}^{n_b} b_k q^{-k}}{1+\sum_{k=1}^{n_a} a_k q^{-k}}, \tag{3.50}$$

with q is the unit time shift operator, $\theta_n=\mathrm{col}([b_0\dots b_{n_b}a_1\dots a_{n_a}])$ is the parameter estimate vector and $n_a,n_b\in\mathbb{N}$ are the order of the nominator and denominator polynomials fulfilling $n=n_a+n_b$. The properness of $\mathcal{F}_{\theta_n}$ is guaranteed by (3.50).

Let $\hat{\theta}_n$ be the estimate of $\mathcal{G}$ using $\mathcal{F}_{\theta_n}$. Introduce θ_o as the true parameter vector corresponding to the system and $\mathbf{Q}_{\hat{\theta}_n}$ as the covariance matrix of the parameter estimate. From (Pintelon and Schoukens 2001) it follows that

$$(\hat{\theta}_n-\theta_o)^\top\mathbf{Q}_{\hat{\theta}_n}^{-1}(\hat{\theta}_n-\theta_o)\in\chi^2\left(n\right), \tag{3.51}$$

where $\chi^2\left(n\right)$ is a χ^2-distribution with n degrees of freedom. Denote $\Delta\theta_n=\theta_n-\hat{\theta}_n$ for every $\theta_n\in\Theta\subset\mathbb{R}^n$. Then for a given confidence level $\alpha\in\mathbb{R}_{[0,1]}$, the parameter

[2]Note that this theory is also applicable for continuous time systems. In the continuous case, q is substituted with the Laplace variable s and the same formulas apply.

uncertainty of $\mathcal{F}_{\hat{\theta}_n}$ can be defined as a α-percentage uncertainty ellipsoid[3] given by

$$\mathcal{E}_{\hat{\theta}_n}(\mathbf{Q}_{\hat{\theta}_n}, \alpha) = \left\{ \theta_n \in \Theta \mid \Delta\theta_n^\top \mathbf{Q}_{\hat{\theta}_n}^{-1} \Delta\theta_n \leq \chi_\alpha^2(n) \right\}, \tag{3.52}$$

where $\chi_\alpha^2(n)$ denotes the α-percentile of $\chi^2(n)$ implying the probability

$$P(\theta_o \in \mathcal{E}_{\hat{\theta}_n}(\mathbf{Q}_{\hat{\theta}_n}, \alpha)) = \frac{\alpha}{100} \in [0, 1].$$

Denote $\hat{\Omega} \subset \mathbb{C}$ as the region of poles of the model (3.50) with parameter $\theta_n \in \mathcal{E}_{\hat{\theta}_n}(\mathbf{Q}_{\hat{\theta}_n}, \alpha)$. In order to establish an uncertainty region of poles associated with each configuration of the parameters inside the ellipsoidal bound (3.52), a nonlinear transformation of the parameter confidence region is needed. This transformation can be accomplished through the method of Vuerinckx et al. (2001), which gives a hypothesis test to decide wether a candidate pole $\hat{\xi}_k \in \hat{\Omega}$ can be a pole location of a model (3.50). First, we distinquish transformation for real valued poles and complex conjugate pole pairs.

Transformation for real valued pole

Let $\xi_1 \in \hat{\Omega}$ be a real valued pole that is associated with $F(q, \hat{\theta}_n)$ (model with estimated parameter $\hat{\theta}_n$) with $n_a > 1$. Define the perturbation $\tilde{\xi}_1 = \hat{\xi}_1 + \Delta\xi_1$ such that there is a corresponding parameter vector $\tilde{\theta}_n \in \Theta$. Note that $\tilde{\theta}_n$ is not unique because ξ_1 only determines the denominator parameters. If $\tilde{\theta}_n \in \Theta$ exists, then it can be chosen such that the numerator parameters $[\tilde{b}_0, \ldots, \tilde{b}_{n_b}]$ of $\tilde{\theta}_n$ are equal to the numerator parameters of $\hat{\theta}_n$. Introduce model parameter $\check{\theta}_{n-1} = \mathrm{col}([b_0, \ldots, b_{n_b} \check{a}_1, \ldots, \check{a}_{n_a-1}])$ with free parameters $[\check{a}_1, \ldots, \check{a}_{n_a-1}]$ and reparameterize $F(q, \tilde{\theta}_n)$ as

$$F(q, \tilde{\theta}_n) = F_1(q, \tilde{a}) F_2(q, \check{\theta}_{n-1})$$

with

$$F_1(q, \tilde{a}) = \frac{1}{1 + \tilde{a} q^{-1}} = \frac{1}{1 - \tilde{\xi} q^{-1}} \quad \text{and} \quad F_2(q, \check{\theta}_{n-1}) = \frac{\sum_{k=0}^{n_b} b_k q^{-k}}{1 + \sum_{k=1}^{n_a-1} \check{a}_k q^{-k}}$$

where $\check{\theta}_{n-1}$ contains the parameters of F_2. This factorization implies the existence of the transformation $\mathbf{T}_1(\tilde{\xi})$ and a vector $\mathbf{T}_2(\tilde{\xi})$ such that

$$\tilde{\theta}_n = \mathbf{T}_1(\tilde{\xi}) \check{\theta}_{n-1} + \mathbf{T}_2(\tilde{\xi}), \tag{3.53}$$

with

[3] Note that $\mathcal{E}_{\hat{\theta}_n}(\mathbf{Q}_{\hat{\theta}_n}, \alpha) \subset \Theta_n$ is not guaranteed. In the sequel, it will be shown how this condition can be enforced.

$$\mathbf{T}_1(\tilde{\xi}) = \left[\begin{array}{cccc|c} 1 & 0 & \dots & 0 & \\ \tilde{a} & 1 & \ddots & 0 & \\ 0 & \ddots & \ddots & \vdots & \mathbf{0}_{(n_a)\times(n-n_a)} \\ \vdots & \ddots & \ddots & 1 & \\ 0 & \dots & 0 & \tilde{a} & \\ \hline \multicolumn{4}{c|}{\mathbf{0}_{(n-n_a)\times(n_a-1)}} & \mathbf{I}_{(n-n_a)\times(n-n_a)} \end{array}\right]_{n\times(n-1)}$$

$$\mathbf{T}_2(\tilde{\xi}) = \left[\begin{array}{ccccc} \tilde{a} & 0 & 0 & \dots & 0 \end{array}\right]^\top_{1\times n}$$

Transformation for complex conjugate pole pairs

In case of $n_a > 2$ and a complex conjugate pole pairs $\xi_1, \xi_2 \in \hat{\Omega}$, $\xi_1 = \text{conj}(\xi_2)$ denote the perturbation of the pole pairs as $\tilde{\xi}_1 = \hat{\xi}_1 + \Delta\xi$, $\tilde{\xi}_2 = \hat{\xi}_2 + \text{conj}(\Delta\xi)$. Using the same mechanism as before, introduce the model parameter $\check{\theta}_{n-2} = \text{col}([b_0, \dots, b_{n_b}\check{a}_1, \dots, \check{a}_{n_a-2}])$ with free parameters $[\check{a}_1, \dots, \check{a}_{n_a-2}]$ and reparametrize $F(q, \tilde{\theta}_n)$ as

$$F(q, \tilde{\theta}_n) = F_1(q, \tilde{a}_1, \tilde{a}_2) F_2(q, \check{\theta}_{n-2})$$

where

$$\begin{aligned} F_1(q, \tilde{a}_1, \tilde{a}_2) &= \frac{1}{1 + \tilde{a}_1 q^{-1} + \tilde{a}_2 q^{-2}} \\ &= \frac{1}{1 - 2\text{Re}(\tilde{\xi}_1) q^{-1} + |\tilde{\xi}_1|^2 q^{-2}}, \\ F_2(q, \check{\theta}_{n-2}) &= \frac{\sum_{k=0}^{n_b} b_k q^{-k}}{1 + \sum_{k=1}^{n_a-2} \check{a}_k q^{-k}}. \end{aligned}$$

This factorization implies the existence of the transformation (3.53) with

$$\mathbf{T}_1(\tilde{\xi}) = \left[\begin{array}{cccc|c} 1 & 0 & \dots & 0 & \\ \tilde{a}_1 & 1 & \ddots & 0 & \\ \tilde{a}_2 & \tilde{a}_1 & \ddots & 0 & \\ 0 & \ddots & \ddots & \vdots & \mathbf{0}_{(n_a)\times(n-n_a)} \\ \vdots & \ddots & \ddots & 1 & \\ 0 & \dots & \ddots & \tilde{a}_1 & \\ 0 & \dots & 0 & \tilde{a}_2 & \\ \hline \multicolumn{4}{c|}{\mathbf{0}_{(n-n_a)\times(n_a-2)}} & \mathbf{I}_{(n-n_a)\times(n-n_a)} \end{array}\right]_{n\times(n-2)}$$

$$\mathbf{T}_2(\tilde{\xi}) = \left[\begin{array}{ccccc} \tilde{a}_1 & \tilde{a}_2 & 0 & \dots & 0 \end{array}\right]^\top_{1\times n}$$

where $\tilde{a_1} = -2\text{Re}(\xi_1)$ and $\tilde{a}_2 = |\xi_1|$.

Construction of the pole region

The derived transformations qualify as a projection of a single pole or complex pole pairs perturbation to the parameter domain Θ through the free parameter $\breve{\theta}_{n-1}$ or $\breve{\theta}_{n-2}$. In order to test that the $\Delta\xi$ induced parameter variation is inside $\mathcal{E}_{\hat{\theta}_n}(\mathbf{Q}_{\hat{\theta}_n}, \alpha)$, it is sufficient to show that there exist a $\breve{\theta}_{n-1}$ or $\breve{\theta}_{n-2}$ which minimizes

$$(\mathbf{T}_1(\tilde{\xi})\breve{\theta}_{n-1} + \mathbf{T}_2(\tilde{\xi}))^\top \mathbf{Q}^{-1}_{\hat{\theta}_n}(\mathbf{T}_1(\tilde{\xi})\breve{\theta}_{n-1} + \mathbf{T}_2(\tilde{\xi})), \tag{3.54}$$

and the minimum is smaller or equal than $\chi^2_\alpha(n)$. If this condition is not satisfied, then this proves the hypothesis that the pole perturbation cannot be associated with a parameter $\tilde{\theta}_n$ in $\mathcal{E}_{\hat{\theta}_n}(\mathbf{Q}_{\hat{\theta}_n}, \alpha)$. The minimization of (3.54) has an analytic solution of:

$$\breve{\theta} = \frac{\mathbf{T}_1(\tilde{\xi})^T\mathbf{Q}^{-1}_{\hat{\theta}_n}\breve{\theta}_n - \mathbf{T}_1(\tilde{\xi})^T\mathbf{Q}^{-1}_{\breve{\theta}_n}\mathbf{T}_2(\tilde{\xi})}{\mathbf{T}_1(\tilde{\xi})^T\mathbf{Q}^{-1}_{\breve{\theta}_n}\mathbf{T}_1(\tilde{\xi})}. \tag{3.55}$$

Thus for a given pole perturbation $\Delta\xi$, if $\breve{\theta}$ resulting from (3.55) satisfies that (3.54) smaller or equal to $\chi^2_\alpha(n)$, then $\tilde{\xi}$ can be the pole of the model estimate with probability α.

Based on the derived hypothesis test, it is possible to calculate the pole region $\hat{\Omega}$. Precisely, the pole region can now be described as:

$$\hat{\Omega} := \{\tilde{\xi} \in \mathbb{C}\} \mid \exists\tilde{\theta}_n \in \mathcal{E}_{\hat{\theta}_n}(\mathbf{Q}_{\hat{\theta}_n}, \alpha) \text{ s.t. } \tilde{\xi} \text{ is a pole of } F(q, \tilde{\theta}_n)\}. \tag{3.56}$$

Note that the pole region $\hat{\Omega}$ is a projection of $\mathcal{E}_{\hat{\theta}_n}(\mathbf{Q}_{\hat{\theta}_n}, \alpha)$ to a lower dimensional space. The complex region $\hat{\Omega}$ characterizes the set of pole locations that can occur with the given probability level of the model estimates. With the given hypothesis test (3.55), $\hat{\Omega}$ can be efficiently computed and visualized. This way, the perimeter bound of $\hat{\Omega}$ describes the uncertain pole locations in a worst-case sense (Tóth 2010).

3.5.2 Discretization of the uncertain pole region

With the hypothesis test at hand, we can describe a pole region $\hat{\Omega}$ with a finite and countable set of poles. This can be done by checking a set of candidate pole locations that is obtained via a simple discretization inside the unit disc. One of the simplest discretization methods is an equidistant 2-Dimensional grid with an adjustable resolution of real and imaginary coordinates axis on the cartesian form. Such a discretization gives the griding $\{\mathfrak{x}_k + i\mathfrak{y}_k\}_{k=1}^N \subset \mathbb{D}$.

Afterwards, we can check if the candidate pole locations are inside of $\hat{\Omega}$ associated with $\mathcal{E}_{\hat{\theta}_n}(\mathbf{Q}_{\hat{\theta}_n}, \alpha)$. This results in $\{\mathfrak{x}_k + i\mathfrak{y}_k\}_{k=1}^{n_z} \in \hat{\Omega}$ as illustrated in Fig.3.1. These pole location can then be used for the aforementioned basis pole selection algorithm (i.e. SQP, RA, and SOSP). Furthermore, by using the maximum modulus principle, we know that the maximum of (3.15) lies on the boundary of the set. Hence we can neglect the pole locations inside the perimeter of the region

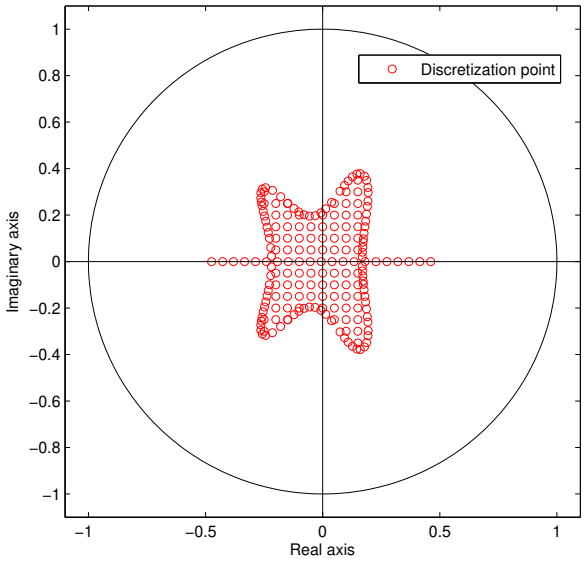

Figure 3.1: Pole locations of an uncertain model obtained via discretization of the unit disc.

of system poles $\hat{\Omega}$. This result in lower computation burden due to the reduced number of constraints in (3.20). The effect on the number of constraints (system poles) on the computation time of the algorithms is further examined in Section 3.6.5.

3.6 Simulation Study

In this section, we demonstrate the performance of the proposed basis selection algorithms on a simulation study. In this academic example, we show how to select the tuning parameters of the proposed methods. Afterward, we demonstrate a basis pole selection procedure for a system that is obtained by system identification. Due to the degree of freedom in the discretization of the unit disc, we connect this study with the investigation of the computational complexity of the basis selection algorithm.

3.6.1 Normalized upperbound

In order to measure the performance of a basis selection algorithm, we introduce the normalized upperbound of (3.20):

$$\tilde{\gamma}_{n_\mathrm{b}} = (\gamma_{n_\mathrm{b}})^{\frac{1}{n_b}} , \tag{3.57}$$

Table 3.1: Parameters corresponding to the true system (3.58).

k	1	2	3	4	5
a_k	1.65	1	0.29	$6.20 \cdot 10^{-2}$	$3.48 \cdot 10^{-2}$
b_k	1.68	2.73	2.13	0.99	0.17
k	6	7	8	9	10
a_k	$2.78 \cdot 10^{-2}$	$1.30 \cdot 10^{-2}$	$3.05 \cdot 10^{-3}$	$3.27 \cdot 10^{-4}$	$1.28 \cdot 10^{-5}$
b_k	$-4.23 \cdot 10^{-2}$	$-1.39 \cdot 10^{-2}$	$-9.97 \cdot 10^{-5}$	$6.27 \cdot 10^{-5}$	$-1.66 \cdot 10^{-6}$

where n_b is the total number of basis poles. This normalized upperbound holds since $\gamma_{n_\mathrm{b}} < 1$. Increasing the number of basis poles will certainly reduce the attained minimum J^o of (3.2) and lead to possible reduction of the convergence rate γ_{n_b}. With this normalization, we penalize the increase in the number of basis poles that does not significantly reduce the convergence rate. The main reasoning for this measure is to decide whether increasing the number of basis poles with the expense of growing complexity of the OBF model is a necessary decision or not.

3.6.2 System of interest and the settings of each algorithm

Consider a discrete 10^{th} order stable LTI system (generated by the `drss` command from Matlab) with a sampling time of 1s. The transfer function of the system is given as follows:

$$G_o(z) = \frac{\sum_{k=1}^{10} b_k z^{-k}}{1 + \sum_{k=1}^{10} a_k z^{-k}}, \tag{3.58}$$

with parameters given in Table 3.1.

This system provides a challenging basis pole selection problem due to the number and the configuration of real-complex conjugate pairs of poles (See Figure 3.2). The proposed algorithms have a number of parameters that need to be set before running the algorithm. The details on the settings for each of the proposed algorithms are as follows:

- SQP
  We conduct ten separate runs of the algorithm with randomly selected initial conditions around the vicinity of the system poles. Multiple runs with different initial conditions are done to avoid settling in local minima with a high $\tilde{\gamma}_{n_\mathrm{b}}$. By using the `fmincon` solver, we have the option to select the number of maximum iterations and tolerance level of the algorithm.

- RA
  We set the confidence level of the results to be $1 - \delta = 0.995$ for both algorithms. This confidence level means that we are 99.5% sure that the result is going to be valid. The probabilistic parameter for the worst case algorithm is set to be $\beta = 1 \cdot 10^{-6}$ while for the performance verification algorithm is

Table 3.2: Comparison of the normalized upperbound $\tilde{\gamma}_{n_\mathrm{b}}$ for each algorithm with respect to various pole configurations.

	2 real and 1 complex pairs	2 real and 2 complex pairs	4 real and 2 complex pairs
SQP	0.452	0.385	0.407
RAW	0.456	0.387	0.410
RAPF	0.454	0.386	0.412
FKcM	0.460	0.402	0.421
SOSP	0.452	0.384	0.407

set to be $\epsilon = 0.005$. These selected probability values result in the number of iterations of $N_{\mathrm{wc}} = 5298315$ for the worst case approximation RA and $N_v = 105967$ for the performance verification RA. Notice that the numbers of iterations can vary if we select different confidence levels $1 - \delta$. Due to the bisection nature of the performance verification RA, the total number of iterations for this algorithm is around $20 - 50$ times the number N_v.

- SOSP
  The SOSP does not have any tuning parameters besides the general pole configuration that is also used in the other two proposed algorithms and the stopping condition of the bisection search. We select a value of $\epsilon = 0.005$ as the stopping condition. We use the result from SOSP to verify whether the value of $\tilde{\gamma}$ that is obtained from both the SQP and RA are close to the global optima.

Each of the algorithms requires a pre-defined configuration of the numbers of real and complex conjugate pairs of basis poles. This configuration is made depending on the location of system poles. Proper selection of the basis pole configuration is described in the next subsection along with the comparison of the performance of each algorithm with respect to various pole configurations.

3.6.3 Selection and comparison of basis pole configurations

The system (3.58) has two complex pole pairs and six real poles. Both of the complex pole pairs have relatively similar distance from the center of the unit disc while the real poles are spread almost evenly at the negative real axis. Based on this information, we start with basis poles configuration of one complex pair and two real poles to represent each of the pole clusters of the system. Afterward, we gradually increase the number of real and/or conjugate pole pairs until $\tilde{\gamma}_{n_\mathrm{b}}$ of (3.57) stops decreasing. The performance of the proposed algorithms is compared with the state-of-the-art FKcM basis selection algorithm (Tóth et al. 2009). The comparison of the results for different pole configurations (number of real and complex pole pairs) can be seen in Table. 3.2 while the best configuration for each of the algorithms is shown in Figure 3.2. For the FKcM algorithm, we only need

to specify the total number of optimized pole locations. This is in fact the advantage of the FKcM algorithm over the proposed method. Due to this condition, the FKcM result in Table. 3.2 corresponds to 4, 6, and 8 basis poles.

From the table, we can see that the SQP outperforms both the randomized and the FKcM algorithm in each of the basis pole configurations. The obtained results are also close to the lower bound obtained from the SOSP algorithm. From the basis pole configuration perspective, the second configuration (2 real and 2 complex pairs) achieves the lowest $\tilde{\gamma} = 0.385$, resulting in the best basis pole configuration in terms of convergence rate. This result is well visualized with tighter perimeter line[4]. This means that for this selected case, the basis poles of the SQP method is the most optimal to describe the dynamics of the system of interest in the KnW distance sense (See Section 2.5.5 for details).

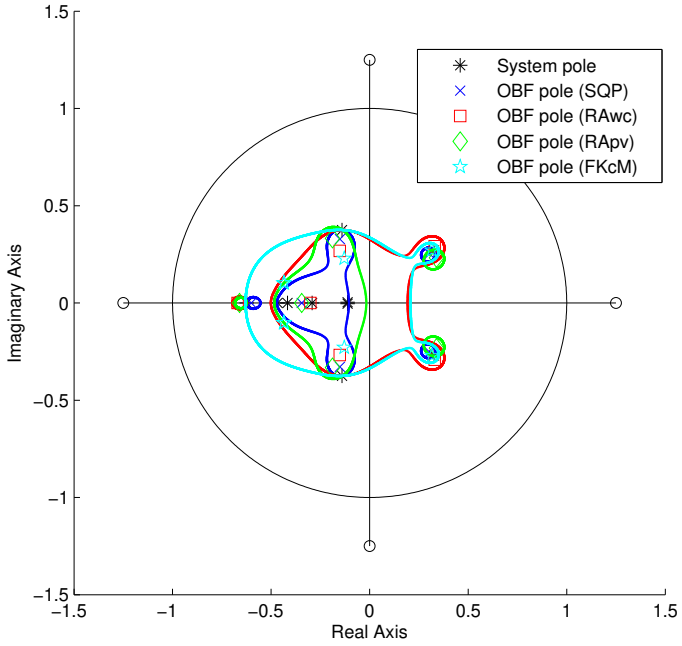

Figure 3.2: Comparison of basis pole selection results using 2 real poles and 2 complex pole pairs (marker) along with their corresponding perimeter line.

3.6.4 Pole selection for an uncertain system

In practice, the system of interest of (3.58) is not exactly known. The uncertainty of the system can either come from dynamical changes (nonlinear behavior) of

[4]Elements on the unit disc with equal value of γ based on a given set of basis poles.

Table 3.3: Parameters of the identified model (3.59).

k	1	2	3	4	5	6
a_k	$9.08 \cdot 10^{-2}$	$9.87 \cdot 10^{-3}$	$-5.21 \cdot 10^{-2}$	$-1.78 \cdot 10^{-2}$	$4.71 \cdot 10^{-2}$	$1.03 \cdot 10^{-2}$
b_k	$2.19 \cdot 10^{-2}$	1.68	$-2.22 \cdot 10^{-1}$	$5.34 \cdot 10^{-1}$	$-4.12 \cdot 10^{-1}$	$1.43 \cdot 10^{-2}$

the system or the covariance of the parameter estimate of the identified LTI system. In this simulation study, we consider the later scenario, in which we use the methodology proposed in Section 3.5 to construct pole uncertainty region of the 10th order system (3.58). In order to obtain the data set for the LTI system, we first excite the system using white noise input signal $u(k) \in \mathcal{N}(0,1)$ and obtain $N_d = 250$ samples of the output response with additive measurement noise of $v(k) \in \mathcal{N}(0, 0.1)$. Based on this measured I/O signal, we use the `OE` routine of the Matlab identification toolbox (Ljung 2006) and we obtain the model:

$$F\left(q, \hat{\theta}_{12}\right) = \frac{\sum_{k=1}^{6} \hat{b}_k q^{-k}}{1 + \sum_{k=1}^{6} \hat{a}_k q^{-k}}, \tag{3.59}$$

with the parameters given in Table 3.3.

From this model and its associated parameter covariance, we generate two different pole uncertainty regions for two confidence levels of 95% and 70%. The regions are depicted in Figure 3.3.

For confidence level of 95%, we can see four separate regions of possible conjugate pairs of system poles along with a single long line of uncertain real poles. We can see that the uncertainty region covering the real poles on the left side of the disc consist not only of a line of possible real poles, but also a complex region that has a shape similar to a half moon. This extended region can be seen as the effect of nearby complex conjugate pairs of system poles that are more dominant than the real pole. On the right side of the unit disc, we see a larger region which is a result of merging of a real and a complex conjugate pole pair region.

For a lower confidence level of 70%, we can see that each of the mentioned regions at the confidence level of 95% grow and they merge with each other. This larger region means that the system dynamics become even more uncertain if compared to the confidence level of 95%. Suddenly a system with only a single dominant resonance mode can turn out to have two dominant resonance modes in this particular case. Note that the number of discretization points directly influences the number of poles in the set $\{\mathfrak{x}_k + i\mathfrak{y}_k\}_{k=1}^{n_z} \in \hat{\Omega}$. Hence, the computational complexity can be influenced by selecting the discretization grid. In the next section, we compare the computational complexity of each of the algorithms with respect to various configuration of basis poles and numbers of system poles sampled from the pole uncertainty region that corresponds to the confidence level of 95%.

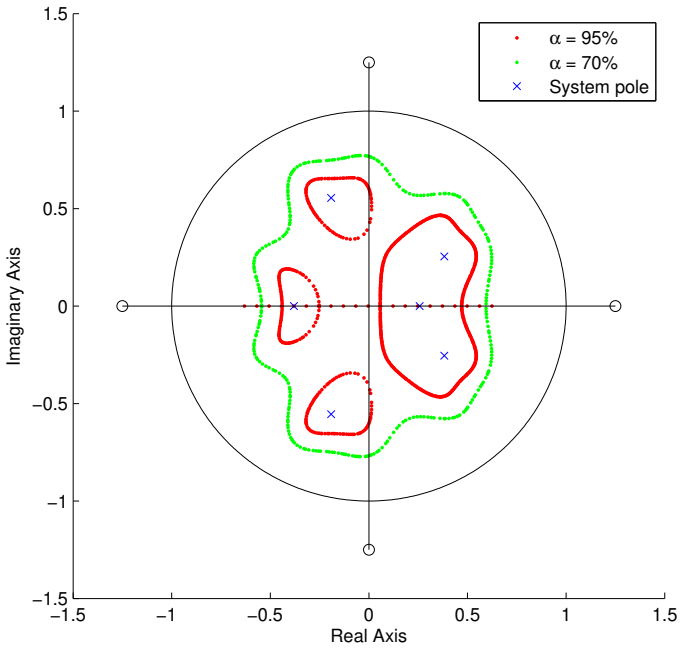

Figure 3.3: Pole regions with different confidence level

3.6.5 Computational complexity

In this section we are focusing only on the comparison of computational complexity of the proposed algorithms. There are two terms that affect the computational complexity, the first one is the configuration (number of real and complex conjugate pairs) of the basis poles, while the second one is the number of system poles. We analyze the effect of the latter by using different number of grid points in the uncertain pole region to vary the number of resulting system poles. The computational time comparison with respect to different number of grid points are given in Table 3.4. For the basis poles, we investigate different configurations of poles such as given in the earlier study in Section 3.6.3. The computational time comparison with respect to different (configurations) number of basis poles are given in Table 3.5. In these two tables, both randomized algorithms are treated as the same algorithm since basically they have similar computational times. We do not compare the FKcM algorithm for this experiment since the time needed to obtain proper tuning of the parameters of this algorithm is significantly longer than the time required to solve the problem itself. The accuracy of the pole selection of FKcM algorithm is very sensitive to the selected parameters of the algorithm. Moreover, we have shown in Section 3.6.3 that the FKcM algorithm is outperformed by our proposed algorithms. As an additional information, these experiments are conducted on a computer that is equipped with an Intel i7-3770 CPU and 16GB of

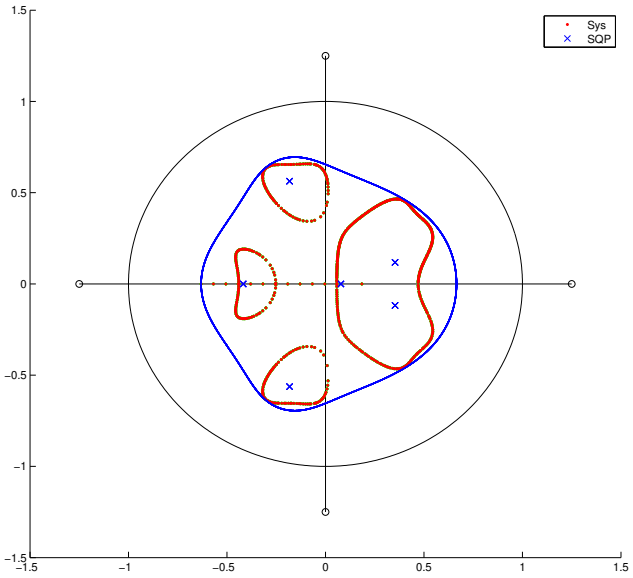

Figure 3.4: Illustration of pole selection for uncertain system poles with the corresponding perimeter line.

memory. The illustration of basis poles selection for these uncertain sets is depicted in Figure 3.4.

From Table 3.4, we can see that the computational load of the SQP and the RA is largely linear with respect to the number of system poles, while the SOSP algorithm has computation time that scales quadratically with n_{b}. Note that the number of iteration is the dominant factor on the computation time. This table only used to show a single iteration of the algorithms, where the RA methods are at least 1000 times quicker than the other algorithms since they only need to compute the value of a given function per iteration. However, the number of iterations required to attain the probability level (δ, β, and ϵ of (3.41) and (3.44)), are significantly higher (around 5 million iterations) compared to the convergences of SQP and the SOSP algorithms (around 10-20 iterations). This large amount of iteration results in at least 25-50 times longer total computational time for the RA when compared to the other two algorithms.

In Table 3.5, we can see an insignificant increase in the computation time for the RA, while the SQP algorithm increases linearly with increasing number of basis poles. It can also be seen that the computational time of the SOSP algorithm increases exponentially. The exponential increase results in an intractable problem when the SOSP is required to select 12 (or more) basis poles. Hence, we can say that the SQP algorithm is preferable for a small-medium number of basis poles,

Table 3.4: Comparison of average computation time (in seconds) per iteration with respect to different number of poles (n_z) belonging to $\hat{\Omega}$ and fixed configuration of basis poles.

n_z	SQP	RA	SOSP
20	$1.35 \cdot 10^{-1}$	$1.84 \cdot 10^{-4}$	$3.35 \cdot 10^{-1}$
30	$1.25 \cdot 10^{-1}$	$2.70 \cdot 10^{-4}$	$9.47 \cdot 10^{-1}$
50	$1.87 \cdot 10^{-1}$	$4.38 \cdot 10^{-4}$	1.47
100	$2.16 \cdot 10^{-1}$	$9.45 \cdot 10^{-4}$	2.88

Table 3.5: Comparison of average computation time (in seconds) per iteration with respect to different number of basis poles with fixed number of system poles.

	SQP	RA	SOSP
2	$1.96 \cdot 10^{-2}$	$6.67 \cdot 10^{-5}$	$9.47 \cdot 10^{-3}$
4	$5.27 \cdot 10^{-2}$	$1.48 \cdot 10^{-4}$	$3.36 \cdot 10^{-2}$
6	$4.91 \cdot 10^{-2}$	$1.03 \cdot 10^{-4}$	$9.71 \cdot 10^{-2}$
8	$9.16 \cdot 10^{-2}$	$1.23 \cdot 10^{-4}$	4.47
10	$1.22 \cdot 10^{-1}$	$1.07 \cdot 10^{-4}$	$7.47 \cdot 10^{1}$
12	$1.47 \cdot 10^{-1}$	$1.46 \cdot 10^{-4}$	$*$

while the RA is computationally more efficient for a large number of basis poles. Note that the shape of pole distribution of the system of interest determines the amount of basis poles needed for OBF model. The user of the algorithms have to determine the basis poles configuration before using the proposed algorithms (See Section 3.6.4 for example of configuration selection).

3.7 Summary

Three different basis selection algorithms for a finite set of system poles are presented in this chapter. These algorithms are based on a reformulated basis pole selection problem. These algorithms have a small number of tuning parameters and hence should be intuitive for the user. The *Sequential Quadratic Programming* (SQP) algorithm performs well by direct computation of the gradient. The *Randomized Algorithm* (RA) provides an alternative selection technique for a large number of basis poles. The *Sum of Squares* (SOSP) algorithm provides a convex global solution to the problem. However, due to the relaxation of the cost function, this algorithm can only be used as a tool to assess the result of the other two algorithms. Furthermore, we provide a method to utilize our proposed algorithms for a model of a system that is obtained via system identification procedure. Lastly, by conducting a simulation study, we showed that the proposed methods outperform the state of the art basis selection algorithm in the sense of obtaining basis poles with better performance measure. The simulation study also shows the computational load of each algorithm where the SQP algorithm excels for a small-medium number of basis poles and the RA is computationally more efficient for a large number of basis poles.

4 CHAPTER

Adaptive Predictive Control based on OBF models

This chapter is devoted to solving the plant-model mismatch problem of predictive control in case the cause of the changes in the plant dynamics is not known. In order to tackle this problem, we allow adaptation of the prediction model by employing iterative updates using an *orthonormal basis functions* (OBF) based model. After the introduction to the chapter, the problem setting is described in Section 4.2. In Section 4.3, an iterative identification mechanism for adaptation of the OBF prediction model is introduced. In Section 4.4, an MPC scheme based on OBF models is described with stability and performance guarantees for the controlled system. In Section 4.5, the MPC scheme is extended to incorporate the adaptation of OBF-based prediction model. It is proven that under the introduced adaptation scheme, the predictive control method can guarantee stability and performance of the closed-loop system even under variations of the underlying plan dynamics. In Section 4.8, a simulation study is provided to demonstrate the stability and performance properties of the proposed MPC scheme.

4.1 Introduction

Model predictive control (MPC) is widely applied in the process control field (Qin and Badgwell 2003a). This control scheme allows safe operation of the controlled plant subject to boundary and operational constraints. However, due to wear in the process and possible changes in the operational conditions, the desired performance of the controller can only be sustained for a limited time period after its commissioning. Process conditions, influencing the operation of the controller, gradually degrade due to circumstances that have not been accounted for in the control design process. These circumstances include changes in the disturbances,

operating point changes, wear, maintenance, etc. Such problems are either solved by enforcing the MPC to be robust for all possible changes in the operational conditions and disturbances, or by equipping the MPC with adaptation capabilities.

The robust solution of MPC has received enormous attention in both academia and industry. Numerous research works such as Kothare et al. (1996), Bemporad et al. (2003), Mayne et al. (2011) offer various formulations for robust MPC schemes. In the industry, earliest application for robust solutions date back to 1993. Since then, various robust MPC tools such as RMPC, DMC+, etc., have been developed for commercial purposes. Despite the popularity of robust solutions, there are several drawbacks and technical challenges affecting their practical use. The requirement on computational resources and below average initial performance for the resulting control solutions, remains two of the most challenging problems of robust MPC schemes. An alternative to the robust MPC solution is the introduction of adaptivity into the MPC scheme. This type of solution is generically known as Adaptive MPC. The purpose of introducing adaptive capability is to keep the performance of the MPC scheme at a high level from the start of commissioning and automatically adjust the controller when necessary. In a recent survey of Mayne (2014), it is mentioned that there are only few Adaptive MPC techniques (such as Marafioti et al. (2014); Genceli and Nikolaou (1996); Tanaskovic et al. (2014); Heirung et al. (2015)). The unpopularity of the adaptive type of solution stems from the difficulty of formulating and implementing it. There are two main practical restrictions of Adaptive MPC. The first one amounts to guaranteeing that the adaptation of the prediction model will converge to the dynamics of the plant or the system of interest. The second one amounts to guaranteeing that the MPC scheme remains feasible regardless of the adaptation rule of the prediction model. If the second point is not being carefully addressed, then even a slight change in the prediction model can alter the properties and the performance of MPC controlled systems.

In this chapter, we follow the adaptive MPC type of solution by addressing the above mentioned important issues: capturing the dynamics of the system of interest and guaranteeing essential closed-loop properties under model adaptation. We propose a novel data-driven MPC which is based on a finite set of *orthonormal basis functions* (OBF) as its prediction model. Online model adaptation is conducted to mitigate the discrepancy between the system of interest and the prediction model. The adaptation of the prediction model is achieved by iterative re-identification of the model coefficients. The end goal of conducting such adaptation is to maintain the control performance after the MPC has been commissioned. Moreover, the utilization of an OBF model structure as a prediction model is attractive from both modeling and control synthesis perspectives. The advantages of using OBF-based models are as follows:

1. The prior knowledge of possible changes that can happen in the system of interest can be imposed on the prediction model.

2. The nature of the OBF-based model structure allows us to augment the prediction model to be as rich as possible to capture changes in the system that are not accounted for a priori.

3. The complexity of the OBF models can be adjusted to ease the computational burden of the optimization in MPC.

4. Conducting a system identification procedure with an OBF model has attractive properties.

The prior knowledge of the system of interest can be imposed on the prediction model by selecting the OBFs. Methods to select the OBFs and the reasoning behind the selection are explained in Chapter 3. Furthermore, the construction of the OBF model follows the construction procedure that is described in Section 2.5.3. Based on this construction procedure, the preselected set of OBFs can be extended to span the complete $\mathcal{RH}_2(\mathbb{E})$ space. Hence, any possible dynamics from a system belonging to that space can be captured by the OBF model. The model complexity increases as the set of OBFs is extended. With the choice of the expansion length, the OBF model represents a tradeoff between model complexity and the ability of the model to describe the system of interest. The latter property can be well expressed in terms of minimal achievable approximation error. From a system identification perspective, the OBF model is accompanied with a well-defined stochastic framework, has a favorable bias-variance tradeoff, and it has the linear-in-the-parameter property (Heuberger et al. 2005; Ninness and Gustafsson 1997). These properties are described later in this chapter. It has been mentioned before that the adaptation of the model is conducted via iterative re-identification of the model. The model, therefore, becomes time-variant and is called a *Linear Time-Varying* (LTV) OBF model. The proposed MPC scheme takes into account the time-varying nature to ensure stability and performance of the controlled system.

This chapter is constructed as follows. First, the setting of the LTV-OBF MPC scheme is described in Section 4.2. In Section 4.3, identification techniques that can be used to obtain the LTV model are described. In Section 4.4, an MPC scheme for OBF models is introduced with stability and performance guarantees of the controlled system. In Section 4.5, the MPC scheme is extended to incorporate the adaptation of the OBF model. It is proven that under the introduced adaptation scheme, the predictive control method can guarantee stability and performance of the closed-loop system even under variations of the underlying plant dynamics. In Section 4.8, we validate the proposed scheme on an academic example.

4.2 Problem Setting of the LTV-OBF MPC scheme

In this section, the general problem setting for the proposed LTV-OBF MPC scheme is described. This section starts with the description of the LTV-OBF model and then continues with the description of the concept of adaptation, the data acquisition setting, and realization of model adaptation.

4.2.1 LTV-OBF model

Denote the momentary linear dynamics of the system of interest at an arbitrary time k with $\mathcal{F}$ (See Section 2.3 for detailed description). This description can be represented by using an OBF transfer function structure $G_{n_\mathrm{b}}(z)$ that is constructed by using a cascaded network of fixed n_b basis functions (See Section 2.5.3 for details on the OBFs construction). For different time instances k, the linear dynamics of the system might vary. The variation of the linear dynamics can be captured by allowing the OBF model parameters, denoted by θ_k, to be varying for each time instance. The variation of the OBF model parameters leads to a time-varying OBF model which is called in the sequel as an LTV-OBF model. The state-space representation of a MIMO LTV-OBF model is described as follows:

$$\begin{aligned} x(k+1) &= \underbrace{\begin{bmatrix} A_{n_\mathrm{e},n_\mathrm{b}} & \dots & 0 \\ \vdots & \ddots & \vdots \\ 0 & \ddots & A_{n_\mathrm{e},n_\mathrm{b}} \end{bmatrix}}_{A\in\mathbb{R}^{n_\mathrm{g}\times n_\mathrm{g}}} x(k) + \underbrace{\begin{bmatrix} B_{n_\mathrm{e},n_\mathrm{b}} & \dots & 0 \\ \vdots & \ddots & \vdots \\ 0 & \ddots & B_{n_\mathrm{e},n_\mathrm{b}} \end{bmatrix}}_{B\in\mathbb{R}^{n_\mathrm{g}\times n_\mathrm{u}}} u(k) \\ &= f(x(k),u(k)), \\ y(k) &= \theta_k^\top x(k), \end{aligned} \tag{4.1}$$

where $x(k) \in \mathbb{X} \subseteq \mathbb{R}^{n_g}$ is the state variable of the LTV-OBF model, $u(k) \in \mathbb{U} \subseteq \mathbb{R}^{n_\mathrm{u}}$ is the input variable of the model, and $y(k) \in \mathbb{Y} \subseteq \mathbb{R}^{n_\mathrm{y}}$ is the output variable of the model. The state dimension $n_\mathrm{x} = n_\mathrm{g} = n_\mathrm{b} n_\mathrm{e} n_\mathrm{u}$ of (4.1) depends on the number of OBF (n_b), the length of expansion (n_e), and the dimension of the input signal (n_u). The state space matrices A and B are time-invariant and their values depend on the selected OBFs. Since the OBFs are time-invariant, the OBFs selection needs to consider possible dynamical variations of the process. This task can be accomplished by the algorithms that are given in Section 3.4. With a proper selection of OBFs, the resulting LTV-OBF model with a suitable model parameter variation θ_k is guaranteed to approximate the variation of the linear dynamics of the system $\mathcal{F}$ with the smallest error in the l_2-norm sense as explained in Section 2.5.2.

The LTV-OBF model (4.1) is used as a deterministic prediction model for the proposed LTV-OBF MPC scheme. The parameter θ_k in the model is adjusted by system identification at the beginning of each control cycle. The idea behind of the proposed adaptation of the MPC scheme is explained in the next section.

4.2.2 Concept of prediction with adaptation

Conceptually, the proposed time line of operation is depicted in Figure 4.1.

The symbols that are used in Figure 4.1 are listed as follows:

- Present time k_0,

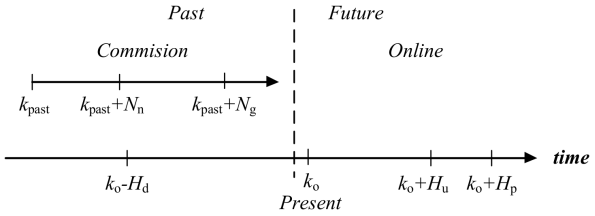

Figure 4.1: Timeline of operation.

- Arbitrary past time $k_{\text{past}} < k_0$
- Length of the global identification data $N_g \in \mathbb{N}$.
- Length of n-th local identification data $N_n \in \mathbb{N}$,
- Data horizon $H_d \in \mathbb{N}$,
- Prediction horizon $H_p \in \mathbb{N}$,
- Control horizon $H_u \in \mathbb{N}$ where $H_u \leq H_p$.

The time line can be divided into two parts which are the control commissioning part and the online part. For the control commissioning part, past input-output data of the system starting from arbitrary past time k_{past} up to $k_{\text{past}} + N_g$ are collected. This past data are used to determine the OBFs as well as the initial estimate of model parameter $\hat{\theta}_{k_0}$. The initial estimate is used as the model parameter during the first control cycle. When the controller is online, collection of past data is continued with the purpose of recursively updating the model parameter $\hat{\theta}_k$ for all $k \in \mathbb{Z}$. The length of the collected past data is called the data horizon H_d. One of the essential parts of any MPC scheme is the prediction phase where we utilize the model of the system to predict its future behavior. The length of the prediction is called prediction horizon H_p while the future prediction is defined as follows:

Definition 4.1 *The future predictions of the system of interest $\mathcal{F}$ are based on the present LTV-OBF model G_{k_0} which is associated with the estimated model parameter $\hat{\theta}_{k_0}$. For prediction purposes, the model parameter is assumed to remain static, i.e. $\hat{\theta}_{k_0} = \hat{\theta}_{k_0+i}, i = 1, \ldots, H_p$.*

The time horizon of which the MPC computes candidate control actions $u(i|k), i \in \mathbb{Z}_{[0,\infty]}$ is called the control horizon H_u. The notation $u(i|k)$ is used to describe the future or predicted input $u(k+i)$ that is calculated at time k. In most cases we consider the control horizon to be equal to the prediction horizon $H_u = H_p$. For the case of $H_u < H_p$, the control action is set to be constant after the first H_u control samples, i.e. $u(H_u|k) = u(H_u + i|k), i = 1, \ldots, H_p - H_u$.

4.2.3 Data acquisition

The identification procedure to obtain an LTV-OBF model of the system utilizes the measured input-output data of the actual process. The assumption on the input and output data is as follows:

Assumption 4.1 *The output data $y_v(k)$ is assumed to satisfy:*

$$y_v(k) := y(k) + v(k), \tag{4.2}$$

where the data of the actual process $y(k)$ is corrupted by a noise process $v(k)$. The noise can be a cumulative effect of measurement and process noise. The input data $u(k)$ is assumed to be fully known and noise free. In case $v(k)$ is assumed to be a white noise process, independent of $u(k)$, then Eq.(4.2) *is called an Output Error (OE) noise setting.*

The collection of input and output data of the system can be divided into two distinct sets of data depending on the timing of the data acquisition and its purpose. The two data sets are described as follows:

Commissioning data set

The commissioning data set is used for OBF selection as well as initial identification purposes. The data set is collected before the proposed LTV-OBF MPC scheme is commissioned to the system. In general, the past input-output data of the system is captured in one single "global" identification data set:

$$\mathcal{D}_{N_g} := \{u(k_{\text{past}} + \tau), y_v(k_{\text{past}} + \tau)\}_{\tau=0}^{N_g}, \tag{4.3}$$

where N_g is the length of data set. Note that, it is not required to obtain the data set $\mathcal{D}_{N_g}$ in a single experiment. We can divide or construct (4.3) from "local" data which contain information on the snapshots of the linear dynamics of the system. We consider these snapshots as n operating points of the system. The corresponding data sets associated with the n-th operating point is denoted by

$$\mathcal{D}_{N_n}^{(n)} := \{u(k_{\text{past}} + \tau), y_v(k_{\text{past}} + \tau)\}_{\tau=0}^{N_n}, \tag{4.4}$$

where $N_n > 0$ is the length of the n-th data set. For each $\mathcal{D}_{N_n}^{(n)}$, *Prediction Error Methods* (PEM) identification is applied to obtain an LTI-OBF model estimate.

In order to gather measurement data for identification, the actual process needs to be brought to a steady-state condition at each of the designated operating points, and then excited around the vicinity by an input signal such as small amplitude white noise, PRBS, or multisine (Bombois and Scorletti 2012). This can also be done by including prior info on the operational change to infer linear dynamics at varying operating points.

Online data set

After the MPC is commissioned, input-output data from the actual process is continued to be measured and collected in a data set. Given a present (collection) at time k, the collected data set is written as:

$$\mathcal{D}_k = \{u(k-\tau), y_v(k-\tau)\}_{\tau=1}^{H_d}, \tag{4.5}$$

where H_d is the length of stored past data. The main utilization of this data is to update the present estimate of the model parameters in terms of $\hat{\theta}_k$.

4.3 LTV-OBF identification in the PEM setting

The estimation of expansion coefficients of the OBF model structure is solved as a system identification problem in the *prediction error minimization* (PEM) setting Ljung (1999); Heuberger et al. (2005). Solving the estimation in the PEM setting is preferred since the estimation result is obtained in a well-defined stochastic framework and can benefit from the properties of PEM based identification.

4.3.1 The LTI PEM identification setting

In the PEM setting detailed in Ljung (1999), it is assumed that the data-sequences of input and output signals $\mathcal{D}_{N_n}$, as given in (4.4), describe the LTI behavior of the system of interest $G_o(z) \in \mathcal{RH}_2^{n_\mathrm{y} \times n_\mathrm{u}}(\mathbb{E})$in the sense of:

$$y_v = G_o(q)u + v, \tag{4.6}$$

where q is the time shift operator, u is a quasi-stationary signal, and v is a stationary stochastic process (see Ljung (1999) for a definition of these signal properties). Furthermore, v satisfies

$$v = H_o(q)e, \tag{4.7}$$

with a monic transfer function $H_o(z) \in \mathcal{RH}_2(\mathbb{E})$ and e is a zero-mean white noise process with variance σ_e^2. In the PEM setting, a parameterized model $G(q,\hat{\theta}), H(q,\hat{\theta})$ is hypothesized with the model parameter $\hat{\theta} \in \Theta \subset \mathbb{R}^{n_\theta}$. This model structure leads to the *one-step-ahead prediction* of (4.6):

$$\hat{y} = (1 - H(q,\hat{\theta}))^{-1} y_v + H(q,\hat{\theta})^{-1} G(q,\hat{\theta}) u. \tag{4.8}$$

The basic idea of PEM is to select $\hat{\theta}$ such that the error between the one-step-ahead prediction (4.8) and the measured output of the system $y_v(k)$

$$\varepsilon(k,\hat{\theta}) := y_v(k) - \hat{y}(k), \tag{4.9}$$

is minimized. The error (4.9) is often called the prediction error. There are a number of methods to select the model parameter $\hat{\theta}$ with respect to the prediction error. These methods are:

- Minimization of scalar-valued function of $\varepsilon(k, \hat{\theta})$ over $\hat{\theta}$ which is often called the identification criterion.
- Constructing the probability density function of $\varepsilon(k, \hat{\theta})$ to maximize the posterior probability of the model output. This method is called *Maximum likelihood method*.
- Modifying the PEM estimation, by multiplying $\varepsilon(k, \hat{\theta})$ with an auxiliary or so called instrumental signal. This is often conducted to avoid biased estimates due to inappropriate choice of noise structure or correlation of the input data with the noise due to a closed-loop setting. This method is called the instrumental variable method (Young 2008).

In this chapter, we utilize a quadratic identification (least squared prediction error) criterion :

$$W_N(\hat{\theta}, \mathcal{D}_{N_n}) = \frac{1}{N} \sum_{k=1}^{N} \varepsilon^2(k, \hat{\theta}). \tag{4.10}$$

which depends on the data set $\mathcal{D}_{N_n}$ and the estimated parameter $\hat{\theta}$. This particular identification criterion is often used in the PEM setting and is also known as the least squares criterion. Interpretation of this criterion can be given as the minimization of the power of the prediction error.

4.3.2 Advantages of identification with the OBF model

Utilization of the least square criterion (4.10) with the OBF model structure (4.1) leads to additional benefits. The first one is based on the independent parameterization of $G(q, \hat{\theta})$ and $H(q, \hat{\theta})$. By using (4.1) to describe the process model, we can assume that $H(q, \hat{\theta}) = I$. Then, the one-step-ahead prediction (4.8) associated with the resulting OBF model can be written as

$$\hat{y}(k) = \theta_k^\top x(k). \tag{4.11}$$

First we consider $\theta_k = \hat{\theta}$ for all k and later we carry the formulation to the general setting for varying θ_k.

As the OBF model has an assumed OE noise model, hence $H(q, \hat{\theta}) = I$ and (4.9) reduces to

$$\hat{y} = G(q, \hat{\theta})u. \tag{4.12}$$

Consequently, the noise is assumed to affect the estimation of $\hat{\theta}$ only in an additive manner in the prediction error (4.9). In the system identification framework, such a noise assumption is similar to the *Finite Impulse Response* and the *Output Error* settings. As an important result, in (Ljung 1999), it is shown that independent parameterization of $G(q, \hat{\theta})$ and $H(q, \hat{\theta})$, along with assuming the input to be *persistently exciting*, leads to a *consistent* estimation

$$\lim_{N \to \infty} \hat{\theta} = \theta_o \tag{4.13}$$

where θ_o gives a model $G(q,\theta_o)$ that is equal to the process dynamics $G_o(q)$ of the underlying system . This means that *consistent* estimation of the deterministic part of the system is guaranteed even when $H(q,\hat{\theta})$ is misspecified. The price to be paid is the potential variance increase due to the lack of noise modeling capability. The second important property is the linearity in the parameters. Since we have a finite data set, minimization of a quadratic criterion function leads to a quadratic optimization problem. Under linearity of ε in θ, the estimation:

$$\hat{\theta}^* = \arg\min_{\hat{\theta}} W_N(\hat{\theta}, \mathcal{D}_{N_n}) \tag{4.14}$$

has a unique solution that can be calculated analytically. Based on the previous property, under PE data, *convergence*[1] of the parameter estimate (4.14) is guaranteed with probability one (Ljung 1999).

4.3.3 Calculation of the current state of the filters

The data set only includes the measured output and input of the system. However, knowing the current state of the model $x(k)$ is also important for both modeling and control purposes. From (4.1), it can be seen that the state trajectory of the model is determined by the inputs $u(k)$ that are passed through the filter banks $\{\phi_i(q)\}_{i=1}^{n_\mathrm{b}}$. Hence, $x(k)$ can be obtained by selecting a past time instant $k_0 \ll k$ and then computing the current state $x(k)$ recursively by:

$$x(k) = A^{k-k_0}x(k_0) + \sum_{l=0}^{k-k_0-1} A^l B u(k_0+l). \tag{4.15}$$

Since the filter is stable, the effect of the initial state $x(k_0)$ gradually dies out. Hence, considering $x(k_0) = 0$ will not result in a cumulative error in the value of $x(k)$. The next state $x(k+1) = Ax(k) + Bu(k)$ can be computed directly from the current input $u(k)$. Alternatively, the state $x(k_0)$ can also be estimated with respect to the input-output data.

Remark 4.1 *Joint estimation of the current state $x(k)$ together with the variation of coefficient θ_k can be made by designing an* Extended Kalman Filter *or solving a co-estimation problem requiring nonlinear optimization. This method is not explored in this chapter since the design (stability) of the filter is a nonlinear optimization problem and it is computationally heavier compared to a direct calculation of* (4.15)*.*

4.3.4 Covariance of parameter estimates

An important aspect of estimation (4.14) is the variability of the parameter estimates with respect to data $\mathcal{D}_{N_n}$. In the most general form, and with the assumption of consistent estimation of $G_o(q)$ and $H_o(q)$, the characterization follows the

[1] Asymptotic parameter estimate is independent from the particular noise realization in the data sequence.

central limit theorem, proving that

$$\sqrt{N_n}(\hat{\theta}^* - \theta_o) \rightarrow \mathcal{N}(0, \mathbf{Q}_{\hat{\theta}_n}) \text{ as } N_n \rightarrow \infty, \tag{4.16}$$

i.e. the random variable $\sqrt{N_n}(\hat{\theta}^* - \theta_o)$ converges in distribution to a Gaussian probability density function with zero mean and covariance matrix $\mathbf{Q}_{\hat{\theta}_n}$. Note that $\mathbf{Q}_{\hat{\theta}_n}$ can only be calculated in a limited number of situations. One of these is when we have *consistent* estimation of (4.13) which is the case for identification using OBF-based model structure under the assumption that v is white (i.e. the noise model $H(q, \hat{\theta}) = I$). Introduce the matrix $\mathrm{x}_{N_n}^k \in \mathbb{R}^{N_n \times n_x}$ for a matrix of N_n past signal samples of the state evolution of the OBF model (4.1) $\{x(i)\}_{i=k-N_n+1}^k$ given the input sequence $\{u(i)\}_{i=k-N_n+1}^k$ of a data set $\mathcal{D}_{N_n}$. The matrix $\mathrm{x}_N^k \in \mathbb{R}^{N \times n_x}$ is described as:

$$\mathrm{x}_N^k = \begin{bmatrix} x(k-N_n+1) & x(k-N_n+2) & \dots & x(k) \end{bmatrix}^\top. \tag{4.17}$$

The covariance matrix in (4.16) can be written as:

$$\mathbf{Q}_{\hat{\theta}_n} = \sigma_e^2((\mathrm{x}_N^k)^\top \mathrm{x}_N^k)^{-1}, \tag{4.18}$$

where σ_e^2 is the variance of the noise v. Furthermore, the covariance matrix characterizes the uncertainty of the parameter estimate $\hat{\theta} \in \Theta \subset \mathbb{R}^{n_\theta}$:

$$\Theta = \left\{ (\hat{\theta}^* - \theta_o)\mathbf{Q}_{\hat{\theta}_n}(\hat{\theta}^* - \theta_o)^\top \right\}. \tag{4.19}$$

The parameter set Θ is an ellipsoid that is characterized by the covariance matrix. It is often beneficial to describe such an ellipsoid by a polytope. Outer or inner approximation method such as described in Bronstein (2008) can be used for this purpose.

4.3.5 Interpretation of LTI identification for LTV system

Earlier in this chapter, we mentioned that the linear dynamics of the system of interest $\mathcal{F}$ can vary for each time k. We aim to capture the LTI behavior of such system at each time k. To achieve this objective, the coefficient $\hat{\theta}$ must be estimated at each time instant k, which will be denoted by $\hat{\theta}_k$. However, due to possible changes of the LTI behavior, the older data that we have from the system may not be consistent with the system anymore. It is logical to weight the data set according to their acquisition time. This weighting is incorporated by updating the criterion function (4.10) to the weighted criterion

$$W_N(\hat{\theta}, \mathcal{D}_k) = \frac{1}{N}\sum_{k=1}^{N} \varepsilon^\top(k, \theta) W(k) \varepsilon(k, \hat{\theta}) \tag{4.20}$$

where $W(k) \in \mathbb{R}^{n_y \times n_y}$ is a predefined symmetric, positive semi-definite matrix and its value differs depending on the time k. The analytical solution of problem (4.20) is given in the next section.

Remark 4.2 *The weighting in* (4.20) *can be interpreted as having the objective to capture the* frozen *transfer function (localized dynamics of the system) instead of the* momentary *transfer function when no weighting is being used (See Section 2.3 for detailed differences between two types of transfer functions)*

4.3.6 Iterative estimation of the model coefficients

Two methods which are based on the analytic solution of (4.20), namely the weighted and recursive LS estimation, are presented for this purpose.

Weighted LS estimation

Introduce the matrix:

$$\mathsf{y}_N^k = \begin{bmatrix} y(k-N+1) & y(k-N+2) & \dots & y(k) \end{bmatrix}^\top, \tag{4.21}$$

which contains the output data for a given data set $\mathcal{D}_k$. Here we set the length of the data set $H_d = N$. The estimation problem (4.20) is solved by:

$$\hat{\theta}_k^{\mathrm{LS}*} = ((\mathsf{x}_N^k)^\top W_{\mathrm{LS}} \mathsf{x}_N^k)^{-1} (W_{\mathrm{LS}} \mathsf{x}_N^k)^\top \mathsf{y}_N^k, \tag{4.22}$$

where the tuning (hyper) parameter for this method is the number of the considered past data N and the exponential weighting $W_{\mathrm{LS}} = \mathrm{diag}\big(\{\frac{\beta^k}{\beta^N}\}_{k=1}^N\big)$ with $\beta \in \mathbb{R}_{(0,\infty)}$. The parameter N should be chosen to be larger than the settling time of the slowest step response of the system dynamics. A high value of N can reduce the estimation variance which is caused by the noise, but can also result in slow adaptation speed of the model. This situation can be remedied by the weighting W_{LS} that penalizes the effect of old data as proposed in Ljung (1999). In many practical applications, it was found that a sensible value of β is in the range of $(0, 20]$.

Recursive LS estimation

In this method, the estimation of coefficient $\hat{\theta}_k$ is based on variables that can be considered as the memory of the estimate (see Ljung (1999)). The update strategy requires computation of:

$$\hat{\theta}_k^{\mathrm{RLS}*} = \hat{\theta}_{k-1}^{\mathrm{RLS}} + L(k)\varepsilon^\top(k), \tag{4.23a}$$

$$L(k) = \frac{P(k-1)x(k)}{W_{\mathrm{RLS}} + x^\top(k)P(k-1)x(k)}, \tag{4.23b}$$

$$P(k) = \frac{1}{W_{\mathrm{RLS}}}\Big(P(k-1) - \frac{P(k-1)x(k)x^\top(k)P(k-1)}{W_{\mathrm{RLS}} + x^\top(k)P(k-1)x(k)}\Big), \tag{4.23c}$$

where $L(k) \in \mathbb{R}^{n_{\mathrm{g}}}$ is the gain matrix, and $P(k) \in \mathbb{R}^{n_{\mathrm{g}} \times n_{\mathrm{g}}}$ is the conditional covariance matrix of the estimation error. The gain matrix $L(k)$ governs the rate

of change of the estimated coefficient and can be seen as the gradient of the parameter estimate. The hyper parameter of this estimation method is the weight $W_{\mathrm{RLS}} \in \mathbb{R}_{(0,1)}$ which also known as the forgetting factor. The value of $W_{\mathrm{RLS}} \approx 1$ is a reasonable choice to allow continuous update of model coefficients. The recursive algorithm requires initial values of P and $\hat{\theta}$. Typically, the initial values are obtained by starting the recursion at a time instant k_0 with

$$P(k_0-1) = \Big[\sum_{\tau=0}^{k_0-1} x(\tau)x^\top(\tau)\Big]^{-1}, \tag{4.24a}$$

$$\hat{\theta}^{\mathrm{RLS}}_{k_0-1} = P(k_0-1)\sum_{\tau=0}^{k_0-1} x(\tau)y^\top(\tau). \tag{4.24b}$$

4.3.7 Identification in a closed-loop setting

The identification of an OBF model can be accomplished by both methodologies in a closed-loop setting. Unfortunately, this implies that $v(k)$ and $u(k)$ are correlated. Without any additional modification of (4.10), such as an *instrumental-variables* (IV) scheme Young et al. (2009), this means that there will be an estimation bias on the coefficient $\hat{\theta}_k$. If such a bias is significant, a simple IV scheme can be easily implemented provided that the excitation signal is *persistently exciting*.

4.4 Non-adaptive OBF MPC

With the OBF model at hand, an MPC scheme can be formulated. However, before going through the complete MPC control problem that includes iterative adaptation of the OBF model, the basic concept of OBF MPC is given in this section. The OBF MPC formulation is based on the well established classical MPC theory and our formulation is related to the approach of Rawlings and Mayne (2009). The definition of the MPC problem alongside the ingredients to establish recursive feasibility, convergence, and stability of the controlled system are given in this section. The notations and definitions that are written in this section are tailored towards the OBF model structure and the application of MPC in the process industry.

4.4.1 LTI MPC problem under OBF process models

In general, an MPC synthesis problem can be described by minimizing a cost function subject to operational and stability constraints with respect to a prediction of the future behavior of the system of interest. In our case, the prediction model is based on the OBF model structure of (4.1). For a non-varying OBF model, the

prediction model is written as:

$$\Sigma \begin{cases} \begin{bmatrix} x(1|k) \\ x(2|k) \\ \vdots \\ x(i+1|k) \end{bmatrix} = \begin{bmatrix} A \\ A^2 \\ \vdots \\ A^i \end{bmatrix} x(k) + \begin{bmatrix} B & 0 & \dots & 0 \\ BA & B & \dots & 0 \\ \vdots & \vdots & \ddots & \vdots \\ BA^{i-1} & BA^{i-2} & \dots & B \end{bmatrix} \begin{bmatrix} u(0|k) \\ u(1|k) \\ \vdots \\ u(i-1|k) \end{bmatrix} \\ y(i|k) = Cx(i|k). \end{cases} \tag{4.25}$$

At the time instant k, the prediction model (4.25) predicts future values of the state $x(i+1|k)$ and output $y(i+1|k)$ based on the current state value $x(k)$ and the possible future input sequence $u(i|k)$ for $i = 0, 1, \dots, N$. The future input sequence $\{u(i|k)\}_{i=0}^{N-1}$ is also denoted by $\mathbf{u}$. The time horizon N, is set equal to the prediction horizon, i.e. $N = H_p$. Additionally, we introduce $x_r \in \mathcal{X}_r \subset \mathbb{X}$ and the set $\mathcal{X}_r$ as a set of states that corresponds to a reference vector r

$$r = Cx_r. \tag{4.26}$$

In majority of process industry usecases, the reference is set to be constant and only changing in step wise manner when the system need to change its operating condition.

The MPC cost function $V_N : (\mathbb{R}^{n_\mathrm{u}})^{N+1} \times \mathbb{R}^{n_\mathrm{x}} \to \mathbb{R}$ is constructed based on the prediction model (4.25) and is formulated as follows:

$$V_N(\mathbf{u}, x(k)) := \sum_{i=0}^{N} l_i(x(i|k), u(i|k)) + V_f(x(N|k)), \tag{4.27}$$

with the stage cost $l_i : \mathbb{R}^{n_\mathrm{x}} \times \mathbb{R}^{n_\mathrm{u}} \to \mathbb{R}, i = 0, 1, \dots, N$ that is chosen as:

$$l_i(x, u) := \big(x - x_r\big)^\top C^\top Q(i) C \big(x - x_r\big) + u^\top R(i) u, \tag{4.28}$$

where $Q(i) \succ 0, R(i) \succ 0$. The exact choice of the terminal cost $V_f : \mathbb{R}^{n_\mathrm{x}} \to \mathbb{R}$ in (4.27) is explained in detail in Section 4.4.2 since its formulation requires additional definitions and reasoning related to the MPC problem. The weighting matrices $Q(i)$ and $R(i)$ are symmetric, positive definite matrices that define the performance specification. We call the cost function homogeneous if $Q(i)$ and $R(i)$ are constant for $i = 0, 1, \dots, N$. In that case we can drop the index (i) and denote these matrices as Q and R. The matrix Q is used to put emphasis on a particular output according to its importance. The tuning matrix R is utilized to mitigate the aggressiveness of the control action, i.e. the input energy.

The minimization of V_N with respect to the future input sequence $\mathbf{u}$ is solved while obeying operational and stability constraints. This minimization problem is called the MPC problem, and is formulated as follows:

Definition 4.2 ***Non-adaptive OBF MPC Problem***
Given the prediction model Σ of (4.25)*, the current state $x(k)$, and the reference r. The*

MPC problem is the optimization problem to determine:

$$\begin{aligned} P_{\mathrm{MPC}} := \quad & \inf_{\mathbf{u}} \quad V_N(\mathbf{u}, x(k)) \\ & \textit{s.t.} \quad \Sigma, && \forall \ i = 1, \ldots, N \\ & \qquad x(i|k) \in \mathbb{X}, && \forall \ i = 1, \ldots, N \\ & \qquad u_{\min} \leq u(i|k) \leq u_{\max}, && \forall \ i = 0, 1, \ldots, N-1 \\ & \qquad x(N|k) \in \mathcal{X}_f \subseteq \mathbb{X}, \end{aligned} \tag{4.29}$$

where $u_{\min}$ is the minimum value of the possible input, $u_{\max}$ is the maximum value of the possible input, and $\mathcal{X}_f$ is a stability constraint which is also known as the terminal set. Set $P_{\mathrm{MPC}} = +\infty$ when (4.29) *is infeasible (i.e. the MPC problem is ill posed).*

The goal of this MPC problem is to find the minimizer of (4.29) for each control cycle $k \in \mathbb{Z}$. The attained minimum of (4.29) is called the *primal optimum* and denoted by $V_N^*(k)$. The minimizer with respect to the *primal optimum* is called the *optimal input sequence* and is denoted by $\{u^*(i|k)\}_{i=0}^{N-1}$ or $\mathbf{u}^*$.

Only the first value of the *optimal input sequence* is applied as the control action at time k. Such control action is known as an MPC control law and is defined as follows:

Definition 4.3 *For every $k \in \mathbb{Z}$, the MPC control law is given as:*

$$u_{\mathrm{MPC}}(k) = u^*(0|k), \tag{4.30}$$

where $u^*(0|k)$ is the first element of the optimal input sequence $\mathbf{u}^*$.

The main purpose of the MPC control law is to steer the output $y(k)$ of the controlled system:

$$G_{\mathrm{CL}} \begin{cases} x(k+1) = Ax(k) + Bu_{\mathrm{MPC}}(k), & x(0) = x_0 \\ y(k) \qquad\quad = Cx(k), \end{cases} \tag{4.31}$$

towards a given reference r. If this goal is accomplished, then the MPC controller is stated to be convergent. Precisely:

Definition 4.4 *The MPC controller is* convergent *if for all $x_o \in \mathbb{X}$ and for all $r \in \mathbb{R}^{n_y}$, the MPC control law $\{u_{\mathrm{MPC}}(k)\}_{k=0}^{\infty}$ drives the output of system* (4.31) *to a given constant reference r in the sense that*

$$\lim_{k \to \infty} \parallel y(k) - r \parallel = 0. \tag{4.32}$$

The convergence described in (4.32) is defined in the asymptotic sense. An additional property, namely the stability of the MPC controller, is required to further strengthen and regulate the possible behavior of the output of the controlled system. Further definitions and results that are related to the stability of (4.31) are described in Section 4.4.2.

Before we can show that an MPC controller is both convergent and stabilizing, one of the first steps is to show the existence of the MPC control law. The existence of the MPC control law is guaranteed with the notion of feasibility of the MPC problem (4.29).

Definition 4.5 *The MPC problem* (4.29) *is called feasible at time k if the optimization problem has a solution.*

Additionally, the notion of Infeasibility of MPC problem is defined as follow:

Definition 4.6 *The MPC problem* (4.29) *is called infeasible at time k if* $\inf_{\mathbf{u}} V_N(\mathbf{u}, x(k)) = +\infty$.

From the definition of feasibility of the MPC problem, the notion of recursive feasibility follows:

Definition 4.7 *The MPC problem* (4.29) *is called recursively feasible if feasibility at time k with reference r and initial condition $x(k)$ implies feasibility of the MPC problem at time $k+1$ with the same reference r, and initial condition $x(k+1) = Ax(k) + Bu_{\mathrm{MPC}}(k)$.*

Recursive feasibility of MPC is a strong property that is used as the basic building block for showing both convergence and stability of an MPC controller. However, in order to guarantee this property, we need additional definitions that are related to the extension of the input for the prediction model (4.25) after the prediction horizon.

Definition 4.8 *At a given $k > 0$, the extended input sequence for a $K^{(k)} \in \mathbb{R}^{n_{\mathrm{u}} \times n_{\mathrm{x}}}$ is given as:*

$$u_{\mathrm{ext}}(i|k) := \begin{cases} u^*(i|k) & i = 0, \dots, N \\ K^{(k)}(x(i|k) - x_r) + u_r & i > N \end{cases} \tag{4.33}$$

where $x(i|k)$ is the state of (4.25) *with $u(i|k) = u^*(i|k)$ for $i \leq N$, while x_r and u_r are the input and the state that correspond to the reference r (See Definition 4.11).*

Definition 4.9 *Call $K^{(k)}$ in* (4.33) *a* stabilizing linear state-feedback controller *at time k if*

$$\lim_{i \to \infty} \|x(i|k) - x_r\| = 0 \tag{4.34}$$

for all initial conditions $x(k) \in \mathbb{X}$. If $K^{(k)} = K, \ \forall k$, then K is called a uniformly stabilizing linear controller.

Definition 4.10 *We call the terminal set $\mathcal{X}_f \subseteq \mathbb{X}$* closed-loop invariant *at time k if*

$$(A + BK^{(k)})(\mathcal{X}_f \ominus x_r) \subset (\mathcal{X}_f \ominus x_r), \tag{4.35}$$

where the operator $\ominus$ express element wise substraction of the set which is also called Minkowski difference. *Additionally, if $K^{(k)} = K, \ \forall k$ and $(A + BK)(\mathcal{X}_f \ominus x_r) \subset (\mathcal{X}_f \ominus x_r)$ then $\mathcal{X}_f$ is said to be* uniformly closed-loop invariant.

Definition 4.11 *Given reference vector r, define (x_r, u_r) as the unique solution to:*

$$\begin{bmatrix} A-I & B \\ C & 0 \end{bmatrix} \begin{bmatrix} x_r \\ u_r \end{bmatrix} = \begin{bmatrix} 0 \\ r \end{bmatrix} \tag{4.36}$$

where A, B, C are the associated matrices with the OBF prediction model (4.25)*.*

The consequences of these definitions is that the state evolution of the prediction model at time k:

$$x(i+1|k) = Ax(i|k) + Bu_{\text{ext}}(i|k), \tag{4.37}$$

satisfies $x(i|k) \in \mathcal{X}_f$ for all $i > N$ with an invariant $K^{(k)}$.

This result completes the necessary ingredients that are needed to set up the recursive feasibility theorem. The theorem is given as follows:

Theorem 4.1 ***Recursive feasibility guarantee***
If for any $x_k \in \mathbb{X}$, a stabilizing linear controller in the form of a varying $K^{(k)}$ (or in the form of non-varying K) exists such that:

1. *The MPC problem* (4.29) *at time k is feasible,*
2. *The terminal set $\mathcal{X}_f$ is closed-loop invariant (or uniformly closed-loop invariant),*
3. *The operational constraint u_{min} and u_{max} are constants and either the condition $u_{min} - u_r \leq K^{(k)}(\mathcal{X}_f \ominus x_r) \leq u_{max} - u_r$, or $u_{min} - u_r \leq K(\mathcal{X}_f \ominus x_r) \leq u_{max} - u_r$ is satisfied,*

are satisfied, then recursive feasibility of MPC problem (4.29) *is guaranteed.*

Proof of the theorem can be found in Appendix A.2. With the feasibility of the MPC controller at hand, we can continue to set up required definitions and formulations toward a convergent and stable MPC controller.

4.4.2 Stability guarantee

In this section, the further steps that are needed to show the convergence and stability of the controlled system (4.31) are established. More precisely, the combination of these two terms result in the notion of an asymptotically stable controlled system.

Definition 4.12 *The controlled system* (4.31) *is called asymptotically stable if it is both convergent (Definition 4.4) and the controlled state evolution is bounded in a* closed-loop invariant *set $x(k) \in \mathcal{X}, \forall k \in \mathbb{Z}$.*

In Definition 4.8-4.11, we use the local controller $K^{(k)}$ and closed-loop invariant $\mathcal{X}_f$ to guarantee recursive feasibility of the MPC controller. We further extend this result towards guaranteeing the asymptotically stable property of the controlled system G_{CL} under the MPC control law u_{MPC}. To do this, we follow the *Control Lyapunov* stability argument mentioned in Sontag (1998). The *Control Lyapunov* stability argument is relevant for a controlled system such as G_{CL} where the successor state $x(k+1)$ depend on the current state $x(k)$ and the driving control law u or u_{MPC} in the MPC case. In order to define a *Control Lyapunov* function, the definition of class $\mathcal{K}$ functions (Khalil 2002) is required:

Definition 4.13 *A function $\alpha : \mathbb{R}_+ \to \mathbb{R}_+$ belongs to class $\mathcal{K}$ if it is continuous, zero at zero, and strictly increasing; $\alpha : \mathbb{R}_+ \to \mathbb{R}_+$ belongs to class $\mathcal{K}_\infty$ if it is class $\mathcal{K}$ and unbounded $(\alpha(k) \to \infty, k \to \infty)$. A function $\gamma : \mathbb{R} \to \mathbb{R}_+$ belongs to the class of $\mathcal{PD}$ functions if it is continuous and positive everywhere except at the origin.*

The definition of a *Control Lyapunov* is given as follows:

Definition 4.14 *A function $V : \mathbb{R}^n \to \mathbb{R}$ is called a* Control Lyapunov *function if there exist $\mathcal{K}_\infty$ functions α_1, α_2, and a $\mathcal{PD}$ function α_3 defined on $\mathcal{X}_f$ such that*

$$\alpha_1(\|x - x_r\|) \leq V(x) \leq \alpha_2(\|x - x_r\|), \tag{4.38}$$

and

$$\inf_{u \in \mathcal{U}} V(Ax + Bu) - V(x) \leq -\alpha_3(\|Ax + Bu - x_r\|). \tag{4.39}$$

The existence of a control Lyapunov function for the controlled system G_{cl} of (4.31) is a sufficient condition for asymptotic stability.

The last item that is needed to be formulated to set up stability guarantee is the terminal cost $V_f(x(N|k))$ of the aforementioned MPC cost function (4.27). The terminal cost is chosen as:

$$V_f(x) = (x - x_r)^\top P(x - x_r), \tag{4.40}$$

with $P \succ 0$. This particular selection of terminal cost is interesting since it also provides a method to select a stabilizing linear controller K as a solution for LQR control synthesis. Following this line of reasoning, the following stability theorem is established:

Theorem 4.2 ***Stability guarantee.***
Suppose that there exist either a stabilizing linear control $K^{(k)}$ *or uniformly* stabilizing linear control K, *and a closed-loop invariant set $(A + BK)\mathcal{X}_f \subset \mathcal{X}_f$ such that:*

1. *The MPC problem* (4.29) *is recursively feasible,*
2. *The terminal cost $V_f(\cdot)$ is a control Lyapunov function with control law $K^{(k)}$ and invariant set $\mathcal{X}_f$,*

then MPC cost function $V_N(\cdot)$ admits a control Lyapunov function for the controlled system G_{cl} and hence the controlled system is asymptotically stable.

Proof of the theorem can be found in Appendix A.3 while the LQR control synthesis is further elaborated in Section 4.6. Theorem 4.2 completes the formulation of OBF MPC for the non-adaptive setting. In the next section, we continue with the Adaptive LTV-OBF MPC formulation.

4.5 Adaptive OBF MPC formulation

The main difference between the non-adaptive and the adaptive formulation is the OBF prediction model. In the adaptive formulation we let the prediction model to be time-varying for the calculation of the MPC control law for each time instance k. In this section, we provide the updated MPC problem for the adaptive case and highlight the difference with the classical formulation and the requirements that are needed to show feasibility as well as stability of the controlled system.

4.5.1 The LTV-OBF MPC problem

The prediction model in the adaptive setting is given as follows:

$$\Sigma_k \begin{cases} x(i+1|k) = Ax(i|k) + Bu(i|k), \quad x(0|k) = x(k), \\ y(i|k) = C_k x(i|k) = \theta_k^\top x(i|k), \end{cases} \tag{4.41}$$

where C_k, corresponds to the OBF model coefficient θ_k defined in (4.1). The matrix C_k can be varying for each time instance k. It can be seen that the prediction for $i = 0, \ldots, N$ depend on the instantaneous value of C_k at time k. For each time sample k, the value of C_k is obtained via either the LS identification (4.22) or the RLS identification (4.23).

In this section, we focus only on the adaptive LTV-OBF MPC formulation and hence we assume[2] that the matrix C_k is available for each time instance $k \in \mathbb{Z}$.

Assumption 4.2 *The coefficient θ_k is identifiable per each time instance (PE condition on the I-O data $\mathcal{D}_k$ is satisfied).*

With this assumption, we define the state and input reference for prediction case

Definition 4.15 *Given reference vector r, define (x_{rk}, u_r) as the unique solution to:*

$$\begin{bmatrix} A - I & B \\ C_k & 0 \end{bmatrix} \begin{bmatrix} x_{rk} \\ u_r \end{bmatrix} = \begin{bmatrix} 0 \\ r \end{bmatrix} \tag{4.42}$$

where A, B, C_k are the associated matrices with the OBF prediction model (4.41).

[2]In the implementation of LTV-OBF MPC (i.e. Algorithm 7), we add a method to ensure that PE condition hold

Introduce the adaptive LTV-OBF MPC cost function $V_{N|k} : (\mathbb{R}^{n_u})^{N+1} \times \mathbb{R}^{n_x} \to \mathbb{R}$ which is constructed based on the prediction model (4.25) and is formulated as follows:

$$V_{N|k}(\mathbf{u}, x(k)) := \sum_{i=0}^{N} l_{i|k}(x(i|k), u(i|k)) + V_f(x(N|k)), \tag{4.43}$$

with the stage cost $l_{i|k} : \mathbb{R}^{n_x} \times \mathbb{R}^{n_u} \to \mathbb{R}, i = 0, 1, \ldots, N$ that is written as:

$$l_{i|k}(x, u) := \big(x - x_{rk}\big)^\top C_k^\top Q_k(i) C_k \big(x - x_{rk}\big) + u^\top R(i) u, \tag{4.44}$$

where $Q(i) \succ 0, R(i) \succ 0$. Similar to the non-adaptive case, the terminal cost $V_f(x(N|k)) : \mathbb{R}^{n_x} \to \mathbb{R}$ is used to establish the stability properties of the MPC controller. The formulation and selection of the terminal cost is going to be explained in detail in Section 4.5.2. The weighting matrices $Q_k(i)$ and $R(i)$ are symmetric, positive definite matrices that define the control specification. In most cases, we set $Q_k(i) = Q_k$ and $R(i) = R$ for $i = 0, 1, \ldots, N$. Note that the weighting matrix $Q_k(i)$ have index k which is related to the time index k in a similar fashion as C_k. This means that its possible to have different value of Q_k for different k. The reasoning behind this formulation is related to the stability guarantee for the controlled system which is described further in Section 4.5.2. Following Definition 4.11, observe that x_{rk} can also vary depending on value C_k. However, due to the nature of PEM identification as explained in Section 4.3, the variation of model parameter are bounded and convergence of parameter estimate is guaranteed.

The MPC problem for the adaptive case is written similar to Definition 4.2.

Definition 4.16 ***LTV-OBF MPC Problem***
Given the prediction model Σ_k of (4.41)*, current state $x(k)$, and constant reference r, the MPC problem is written as:*

$$\begin{aligned} P_{\mathrm{TV-MPC}} := \quad & \inf_{\mathbf{u}} \quad V_{N|k}(\mathbf{u}, x(k)) \\ & \textit{s.t.} \quad \Sigma_k, && \forall \;\; i = 0, 1, \ldots, N \\ & \qquad x(i|k) \in \mathbb{X}, && \forall \;\; i = 0, 1, \ldots, N \\ & \qquad u_{\min} \le u(i|k) \le u_{\max}, && \forall \;\; i = 0, 1, \ldots, N \\ & \qquad x(N|k) \in \mathcal{X}_f \subseteq \mathbb{X} \end{aligned} \tag{4.45}$$

where $u_{\min}$ is the minimum value while $u_{\max}$ is the maximum value of the possible input signal, and $\mathcal{X}_f$ is stability constraint which also known as the terminal set. Set $P_{\mathrm{TV-MPC}} = +\infty$ when the feasible set of (4.29) *is empty (the MPC problem is ill posed). The goal of this MPC problem is to find the minimizer of* (4.29) *for each control cycle k. The attained minimum of* (4.29) *is called the* primal optimum *and is denoted by $V^*_{N|K}(k)$. The minimizer with respect to the* primal optimum *is called the* optimal input sequence *and is denoted by $\{u^*(i|k)\}_{i=1}^N$ or $\mathbf{u}^*$.*

In the adaptive case, the controlled system now exhibits a time-varying behavior:

$$G_{\mathrm{CL}_k} \begin{cases} x(k+1) = Ax(k) + Bu_{\mathrm{MPC}}(k), & x(0) = x_0 \\ y(k) \qquad\quad = C_k x(k). \end{cases} \tag{4.46}$$

Other supporting definitions for the MPC problem such as MPC control law (Definition 4.3), convergence (Definition 4.4), feasibility (Definition 4.5), recursive feasibility (Definition 4.7), the input extension (Definition 4.8), stabilizing linear controller (Definition 4.9), as well as the terminal set (Definition 4.10) remains the same for the adaptive case. The similarity on the aforementioned definitions lead to direct utilization of the recursive feasibility Theorem 4.1 for the adaptive case:

Theorem 4.3 ***Recursive feasibility guarantee for adaptive OBF MPC formulation*** *If either one of stabilizing linear controller $K^{(k)}$ or K exists such that:*

1. *The MPC problem* (4.45) *at time k is feasible,*
2. *The terminal set $\mathcal{X}_f$ is closed-loop invariant or uniformly closed-loop invariant,*
3. *The operational constraint u_{min} and u_{max} do not change for all k and either the condition $u_{min} - u_r \leq K^{(k)}(\mathcal{X}_f \ominus x_{rk}) \leq u_{max} - u_r$, or $u_{min} - u_r \leq K(\mathcal{X}_f \ominus x_{rk}) \leq u_{max} - u_r$ is satisfied,*

is satisfied, then the recursive feasibility of MPC problem (4.45) *for all k is guaranteed.*

Proof of the theorem can be found in Appendix A.4. In the other hand, the stability guarantee for adaptive case is slightly different due to the time-varying behavior of the controlled system 4.46.

4.5.2 Stability guarantee in the adaptive setting

In this section, we examine how the variation on C_k affects the stability guarantee of the LTV-OBF MPCs controller in the adaptive setting. The stability argument in the adaptive case is still based on the control Lyapunov function (Definition 4.14). We start with the observation wether the classical stability guarantee (Theorem 4.2) hold for the adaptive case. Within this theorem there are two items that are affected by the time-varying behavior:

- The construction of linear stabilizing controller K (Eq. (A.28)),
- The optimality principle (Eq. A.31).

In the adaptive case, the existence of a stabilizing linear controller K is needed such that

$$(x(N|k)-x_{rk})^\top \big((A+BK)^\top P(A+BK)-P+C_k^\top Q_k C_k+K^\top RK\big)(x(N|k)-x_{rk}) \leq 0. \tag{4.47}$$

Unlike the non adaptive case, the solution for the LQR synthesis problem needs to be valid for all possible value of C_k

$$(A+BK)^\top P(A+BK) - P \preceq -(C_k^\top Q_k C_k + K^\top RK). \tag{4.48}$$

Fortunately we know that the possible value of C_k is inside of the parameter space $\Theta \subset \mathbb{R}^{n_g \times n_y}$ which is bounded and depend on the covariance matrix of parameter estimates (See Section 4.3.4). Finding K as the solution of 4.48 can be done by solving multiple LMIs in the vertices of a polytopic approximation of Θ. The LMIs and the details of the synthesis is given in Section 4.6.

The second item which is affected by the variation of C_k is the optimality principle

$$V^*_{N|k}(x(k+1)) \leq \tilde{V}_{N|k}(x(k+1)). \tag{4.49}$$

In the adaptive cases this relation is not valid since $\tilde{l}_{i|k}$ in

$$\tilde{V}_{N|k}(x(k+1)) = \sum_{i=0}^{N} \tilde{l}_{i|k}(x(i|k+1), u_{\text{ext}}(i|k)) + V_f(x(N|k)), \tag{4.50}$$

is based on the previous value of C_k. There is a possibility that the variation on C_k lead to the relation of

$$\begin{array}{rcl} l_{i|k}(x(i|k+1), u_{\text{ext}}(i|k)) & < & \tilde{l}_{i|k}(x(i|k+1), u_{\text{ext}}(i|k)), \\ \|C_{k+1}(x(i|k+1) - x_{rk})\|_{Q_{k+1}} & < & \|C_k(x(i|k+1) - x_{rk})\|_{Q_k}, \end{array} \tag{4.51}$$

for arbitrary i which invalidates the optimality principle:

$$V_N(x(k+1)) \not\leq \tilde{V}_N(x(k+1)). \tag{4.52}$$

It is clear that in order to guarantee the decreasing property of the value function, an additional condition is required. The stability Theorem for the adaptive case then becomes:

Theorem 4.4 ***Stability guarantee in the adaptive setting.***
Suppose that there exist either a stabilizing linear control $K^{(k)}$ *or a uniformly* stabilizing linear control K*, and a closed-loop invariant set $\mathcal{X}_f$ such that:*

1. *The MPC problem* (4.45) *is recursively feasible,*
2. *The terminal cost $V_f(\cdot)$ is a control Lyapunov function with control law $K^{(k)}$ and invariant set $\mathcal{X}_f$,*
3. *The condition*

$$C_{k+1}{}^{\top} Q_{k+1}(i) C_{k+1} \preceq C_k^{\top} Q_k(i) C_k \quad \forall k \in \mathbb{Z}, i \in \mathbb{N} \tag{4.53}$$

holds.

then the MPC cost function $V_{N|k}(\cdot)$ admits a control Lyapunov function for the closed-loop system G_{clA} and hence the controlled system is asymptotically stable.

Proof of the theorem can be found in Appendix A.5. The last condition on Theorem 4.4 leads to two interpretations:

- Control synthesis: This condition determines how we need to adjust $Q_{k+1}(i)$ to counter balance the change in C_k.
- Iterative identification: This condition regulates the input-output condition of the data set $\mathcal{D}_k$ which leads to governing the experimental condition and/or adjusting the weighting of the identification method.

It is mentioned at the end of the proof of Theorem 4.4 that the stability of (4.46) can be enforced by either adjusting the sequence $Q_{k+1}(i)$ for all $i \in \mathbb{N}$ or assuming Q_k is independent of i and adjusting the matrix Q_k. The sequence of weighting matrices $Q_k(i)$ act similarly to the weighting on the identification W_{LS} in (4.22). Provided that the length of the prediction horizon H_p and the data horizon H_d are the same, it is natural to select of $Q_k(i)$ and W_{LS} to be equivalent with each other. This way, the stability of the controlled system, and in particular the condition (4.53), is being satisfied from both the view points of identification and the control.

Alternatively, for Q_k that is selected to be independent of i, one can adjust the the next value of Q_{k+1} in similar fashion as how the weighting of W_{RLS} in (4.23c) affect the value of $P(k-1)$. In summary, we can guarantee stability, no matter how often the model is updated.

Another possibility is to consider the condition of (A.35) from the interpretation of limit value of C_k and Q_k.

$$C_* := \lim_{k\to\infty} C_k, \quad Q_* := \lim_{k\to\infty} Q_k \tag{4.54}$$

Then (4.53) implies that

$$C_*{}^\top Q_*(i) C_* \preceq C_k^\top Q_k(i) C_k \quad \forall k \in \mathbb{Z}, i \in \mathbb{N}. \tag{4.55}$$

4.6 LQR control synthesis

The existence of a stabilizing LQR controller K that satisfy (4.47) is needed to show both recursive feasibility and stability of the LTV-OBF MPCs controller. The value of P and K of the corresponding robust LQR problem needs to satisfy:

$$(A+BK)^\top P(A+BK) - P \preceq -(C_k^\top Q_k C_k + K^\top R K), \tag{4.56}$$

for all $C_k \in \Theta$ (ellipsoidal parameter set (4.3.4)) and variations of Q_k. It is often beneficial to describe such an ellipsoid by a polytope. Outer or inner approximation method such as described in Bronstein (2008) can be used for this purpose. By defining vertices $\{\tilde{\theta}_i\}_{i=1}^n$ of the polytopes such that

$$\Theta \subseteq \mathrm{Co}\{\tilde{\theta}_1, \ldots, \tilde{\theta}_n\} \tag{4.57}$$

the value of P and K can be simultaneously computed by defining $S := P^{-1}$, $T := KP^{-1}$, and solving the LMI problem:

$$\begin{pmatrix} S & (AS+BT)^\top & S\tilde{\theta}_i^\top & T^\top \\ AS+BT & S & 0 & 0 \\ \tilde{\theta}_i S & 0 & Q_k^{-1} & 0 \\ T & 0 & 0 & R^{-1} \end{pmatrix} \succeq 0, \tag{4.58}$$

for all vertices $\{\tilde{\theta}_i\}_{i=1}^{n}$.

With the stabilizing LQR controller at hand, the invariant set $\mathcal{X}_f$ can be selected as a level set of

$$V_f(x) = (x - x_{rk})^\top P(x - x_{rk}).$$

The invariant set definition follow

$$\mathcal{X}_f = \{x | V_f(x) \leq \eta\} \tag{4.59}$$

with $0 < \eta \leq 1$.

The LQR control synthesis as well as invariant set definition give us the complete description of LTV-OBF MPC scheme.

4.7 LTV-OBF MPC algorithm

This section summarizes the finding of previous sections and presents the LTV-OBF MPC scheme as an algorithm. In principle the algorithm is divided into three parts:

- Preparation step of the LTV-OBF model
- Finding stabilizing linear controller
- Online LTV-OBF MPC control

Each step is presented in algorithm flow as follows:

Splitting global data set $\mathcal{D}_{N_g}$ into identification and validation data sets can be done in any ratio. The intuitive division is half and half, but having more data sets for better identification is also beneficial. For the OBF model, the input signal has a direct effect on the covariance matrix of model estimate. This defines the allowable parameter space Θ of the LTV-OBF model which we need to consider for LQR control synthesis.

Since we are going to adapt the model coefficient of the LTV-OBF model for the MPC scheme, extra input excitation needs to be injected into the closed-loop setting to maintain PE excitation. Similar excitation that leads to the covariance matrix that we used in LQR synthesis should be used. The excitation help steer the variation of the model coefficient of the LTV-OBF model. Note that this extra excitation and iterative identification can be turned off to apply LTI-OBF MPC instead of LTV-OBF MPC.

For this LTV-OBF MPC implementation, the stability of the closed-loop system can be monitored from the evolution of Eq. (4.53). Since this condition scale depends on the state-space of the LTV-OBF model, alternative formulation of Eq.(4.53) by pre and post multiplication with the current state $x(k)$ can be made.

Algorithm 5 Setting up LTV-OBF model

Require :

- Basis pole for the system of interest ($\{\lambda_i\}_{i=1}^{n_\mathrm{b}}$) (see Chapter 3 for basis selection methodology)
- Global data set $\mathcal{D}_{N_g}$
- Selected number of basis expansion n_e
- Number of input channels of the system of interest n_u
- Success Criteria for identification $0\% < \mathrm{SC} < 100\%$

Ensure: $\mathrm{BFR} = 0\%$

Select the WLS/RLS tuning parameter (See Section 4.3.6 for rule of thumb)

while $\mathrm{BFR} \leq \mathrm{SC}$ **do**

Construct a state-space OBF representation w.r.t. basis poles ($\{\lambda_i\}_{i=1}^{n_\mathrm{b}}$), number of basis expansion (n_e), and input channel n_u (i.e. Eq (2.64))

Run the WLS/RLS identification method on a part of global data set $\mathcal{D}_{N_g}$ (identification step)

Collect the initial coefficient of the LTV-OBF model θ_o for each output channel

Simulate the LTV-OBF model with coefficient from step w.r.t. the other part of the global data set $\mathcal{D}_{N_g}$ (validation step)

Compute

$$\mathrm{BFR} = 100\% \cdot \max\left(1 - \frac{\|y(k) - \hat{y}(k)\|_2}{\|y(k) - \bar{y}\|_2}, 0\right), \tag{4.60}$$

if $\mathrm{BFR} < \mathrm{SC}$ **then**

Fine-tune the WLS/RLS tuning parameters $W_\mathrm{LS}/W_\mathrm{RLS}$ in a grid like environment

else if $\mathrm{BFR} < \mathrm{SC}$ and tuning parameter space has been explored **then**

Set $n_\mathrm{e} \leftarrow n_\mathrm{e} + 1$

end if

end while

Collect the final initial coefficient θ_o of the LTV-OBF model and the compute covariance matrix of parameter estimates using Eq.(4.18).

Algorithm 6 Finding Stabilizing LQR control for LTV-OBF MPC

Require :

- Covariance matrix of parameter estimate $\mathbf{Q}_{\hat{\theta}_o}$
- Initial LTV-OBF model of the system of interest (Result from Algorithm 5)
- Control matrices Q and R.
- Polytope approximation algorithm (e.g. algorithm of Bronstein (2008))

Ensure: $i = 0$

Construct n-dimensional polytope approximation of model set Θ from the information of the covariance matrix of parameter estimate $\mathbf{Q}_{\hat{\theta}_o}$ with the center of initial coefficient θ_o

while $i = 0$ **do**

Collect all vertices of the polytope $\{\tilde{\theta}_i\}_{i=1}^{n}$ (i.e. Eq (4.57))

Construct an LMI for each vertices

Solve LMIs

if LMIs are not solvable **then**

Shrink the polytope

else if LMIs are solvable **then**

Set $i \leftarrow 1$

end if

end while

Compute matrices P and K.

Algorithm 7 LTV-OBF MPC online control

Require :

- Initial LTV OBF model of the system of interest (Result from Algorithm 5)
- Stabilizing LQR controller matrices P and K
- Control matrices Q and R (that are used for LQR control synthesis)
- Prediction-Control horizon N (value needs to be larger than the settling time of the system dynamics)
- WLS/RLS tuning matrix $W_{\mathrm{LS}}/W_{\mathrm{RLS}}$
- Vertices of n-dimensional polytope $\{\tilde{\theta}_i\}_{i=1}^{n}$ (that are used for LQR control synthesis)
- commissioned data set $\mathcal{D}_k$ consisting of the current value of input $u(k)$, output $y(k)$ (for WLS adaptation, up to n past data set depending on the length of W_{LS})

Initialize state of LTV-OBF model $x(k)$ w.r.t. the Commissioned data set $\mathcal{D}_k$ (See Section 4.3.3)
while MPC control is online **do**
Construct the MPC problem of Eq. (4.45)
Solve the MPC problem (Always solvable due to recursive feasibility Theorem 4.3)
Apply control action $u_{\mathrm{MPC}}(k)$ with added excitation for persistence excitation condition
Update commissioned data set $\mathcal{D}_k$ with the output $y(k)$
Update the current state $x(k)$ of LTV OBF model with the updated commissioned data set $\mathcal{D}_k$
Run LTV RLS/WLS model identification w.r.t. the latest data $\mathcal{D}_k$
Estimate LTV RLS/WLS model coefficient θ_{k+1}
if The model coefficient θ_{k+1} is inside the n-dimensional polytope **then**
Re-run LQR control synthesis (i.e. Algorithm 6)
Update P and K matrices
end if
if Control Performance is not satisfying (e.g MSE of tracking performance, etc) **then**
Tune Q and R matrices
Re-run LQR control synthesis (i.e. Algorithm 6)
Update P and K matrices
end if
end while

This product is similar to the stage cost $l_0\big(x(0|k), u_{\mathrm{MPC}}(k)\big)$ of the MPC without the reference state x_{rk} term:

$$x^\top(k+1)\theta_{k+1}Q\theta_{k+1}^\top x(k+1) \leq x(k)\theta_k Q\theta_k^\top x(k) \quad \forall k \in \mathbb{Z}, i \in \mathbb{N}. \tag{4.61}$$

Referring to the proof of stability Theorem 4.4 in Appendix A.5, this stage cost formulation can be a replacement condition in which we guarantee the optimality principle. This means that if the value of Eq. (4.61) converges to the reference state x_{rk}, the closed-loop stability is guaranteed.

Remark 4.3 *The evolution of model coefficient θ_k of the LTV-OBF model as well as the control matrix Q are part of the stability condition as described in Theorem 4.4 (i.e. condition of Eq.* (4.53)*). For simplification reasons, Algorithm 7 only restricts the variation of the model coefficient and does not specifically mention the condition of an iterative update on Q for each time step. This means that the stabilizing LQR control will remain valid as long as the evolution of the model coefficient is bounded by the n-dimensional polytope. In case it is desired to implement an iterative update on Q, additional rules for the Algorithm 7 and possible redefinition of the LMI for LQR synthesis in Algorithm 6 is needed to be made.*

4.8 Simulation study

The proposed control scheme in Section 4.7 is tested on a binary distillation column benchmark model that is based on a liquid-vapor flow configuration. The model is detailed in Skogestad (1997). A linearization of the model is established for the operating condition of 0.05 and 0.95 (mole fraction) of the bottom and top composition levels respectively, with corresponding liquid and vapor flows of 521 kmol/min (kilo-mole per minute) and 664 kmol/min. The sampling time of the system is chosen to be 5 minutes while the settling time of the system is 170 minutes (34 time steps). The MIMO LTI model in deviation variables is given as follows:

$$G(z) = \begin{bmatrix} \frac{0.001357z-0.0009633}{z^2-1.528z+0.5679} & \frac{-0.0009023z+0.000597}{z^2-1.528z+0.5679} \\ \frac{0.001174z-0.0009952}{z^2-1.528z+0.5679} & \frac{-0.0003762z+0.0002929}{z^2-1.528z+0.5679} \end{bmatrix}. \tag{4.62}$$

This represents a 2x2 LTI system with liquid and vapor flow as the inputs (manipulated variables) and bottom and top composition as the output (controlled variables) respectively. The generated measurements from this system are corrupted by a discrete-time output additive white noise with *signal-to-noise ratio*[3] (SNR) of 15 dB. The LTV-OBF MPC scheme will be designed and commissioned on this system with $n_{\mathrm{g}} = 4$ (i.e. $n_{\mathrm{b}} = 2$ basis poles and $n_{\mathrm{u}} = 2$ input) basis functions that are generated from the poles of the system. This pole generating mechanism also means zero approximation error i.e. $\| G^{[m,n]} - G_{n_{\mathrm{b}}}^{[m,n]} \|_{\mathcal{H}_2}^2 = 0$ (See Section 2.5.2 for

[3]The signal-to-noise ratio is defined as $\mathrm{SNR} := 10 \cdot \log_{10}\left(\frac{\|y-v\|_2^2}{\|v\|_2^2}\right)$.

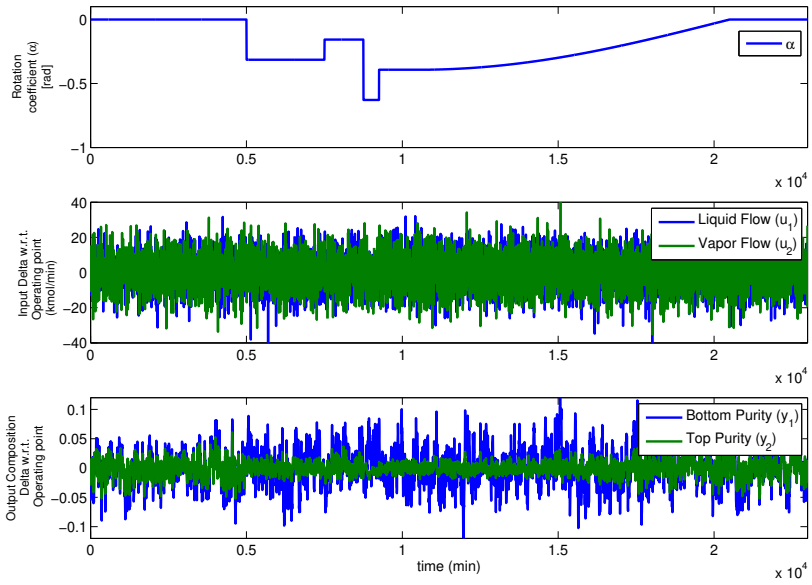

Figure 4.2: Rotation coefficient and validation data set in the open-loop setting.

Table 4.1: Open-loop validation result for the WLS and RLS approaches.

	Bottom product composition (y_1)	Top product composition (y_2)
	BFR	BFR
WLS-approach	94.88 %	87.18 %
RLS-approach	89.81 %	84.26 %

details). After the commissioning of the MPC, the plant-model mismatch will be induced as an effect of a rotation matrix:

$$G_{\text{new}}(z) = \begin{bmatrix} \cos(\alpha(k)) & -\sin(\alpha(k)) \\ \sin(\alpha(k)) & \cos(\alpha(k)) \end{bmatrix} G(z), \tag{4.63}$$

where $-\pi/5 < \alpha(k) < 0$ is the rotation coefficient at time instant k. Different rates of change of $\alpha(k)$ such as abrupt and slow changes are considered in the experiment. The considered trajectory of $\alpha(k)$ is depicted in Fig 4.2. The goal of this study is to test the ability of the LTV-OBF MPC scheme to track the change in the system while maintaining a low deviation from the given reference point.

4.8.1 Initial observation and open-loop validation

An off-line experiment (study) has been conducted which corresponds to the commissioning stage of the MPC where the hyper parameters of the estimation and

Table 4.2: Closed-loop performance of the investigated MPC approaches with respect to the given reference ($r_1 = 0.02, r_2 = 0.98$)

	Bottom product composition (y_1) MSE	Top product composition (y_2) MSE
Fixed-MPC	$7.57 \cdot 10^{-5}$	$3.54 \cdot 10^{-5}$
Oracle-MPC	$3.01 \cdot 10^{-7}$	$1.41 \cdot 10^{-6}$
LTV-OBF MPC WLS	$1.22 \cdot 10^{-5}$	$5.98 \cdot 10^{-6}$
LTV-OBF MPC RLS	$1.09 \cdot 10^{-5}$	$5.17 \cdot 10^{-6}$

the control parameters are selected. In this experiment, the system is excited with Gaussian white noise input with standard deviation of 10 kmol/min. The length of the simulation study is 23000 minutes (383 hours). It is important to note that this experimental length is not the required time to obtain the model. Instead, the length is chosen such that the estimation capabilities of the model can be assessed with respect to various rotation scenarios. The result of this experiment can be seen in Table 4.1 in terms of the average *best fit ratio* (BFR). These results correspond to the selected hyper parameters of $N = 239$, $W_{\mathrm{LS}} = \mathrm{diag}\big(\{\frac{4.5^k}{4.5^N}\}_{k=1}^{N}\big)$, and $W_{\mathrm{RLS}} = 0.97$ which are obtained via the gridding of the parameter space.

4.8.2 Closed-loop experiment

With the parameters available from Section 4.8.1, the LTV-OBF MPC is commissioned on the system. The control task is to follow a set point of $r_1 = 0.02$ and $r_2 = 0.98$ for each of the output channels under the effect of the rotation factor that is depicted in Fig. 4.2. LTV-OBF MPC synthesis follows the algorithm described in Section 4.7. Four different cases are considered for the closed-loop experiment:

- Oracle-MPC: The predictive model is equal to the true system dynamics.
- Fixed-MPC: The predictive model is fixed (i.e. single LTI-OBF model).
- LTV-OBF MPC with WLS estimation: Model coefficient is updated using Eq. (4.22)
- LTV-OBF MPC with RLS estimation: Model coefficient is updated using Eq. (4.23)

The result of the Oracle-MPC will also serve as a benchmark for the best achievable result on the selected control parameter. The LQR synthesis for the Oracle-MPC is conducted with the available model coefficient as given in Eq.(4.62) and Eq.(4.63). The Fixed-MPC case only uses a single model (initial model of the open-loop experiment) for the LQR synthesis, while both LTV-OBF MPC cases use the vertices of the polytope approximated covariance matrices of the parameter estimate to construct the LMI (See Section 4.6 for details). For the controller of all the cases, we select the control-prediction horizon value to be $N = 34$ which is based

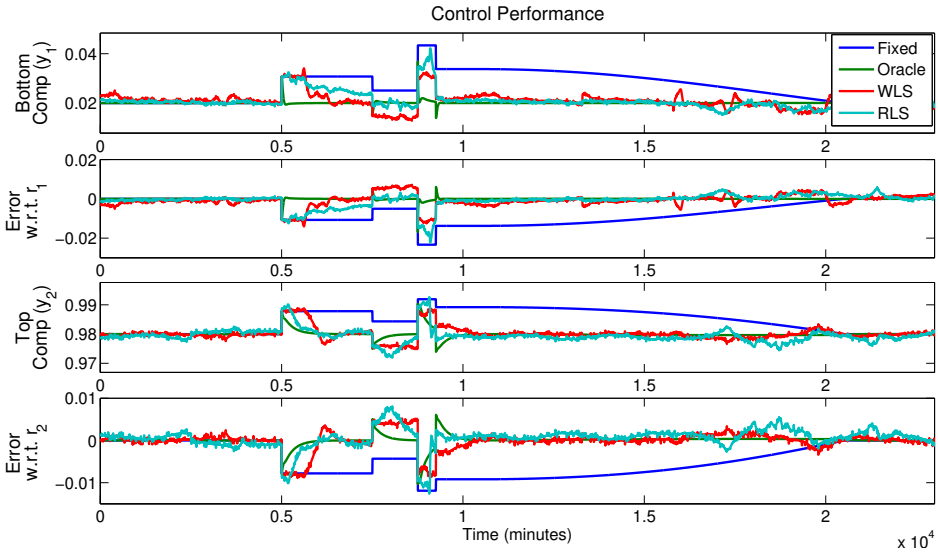

Figure 4.3: Tracking performance of four different cases of the predictive controller under rotation scenario.

on the slowest step response of the system, while the control matrices are selected to be

$$Q = \begin{bmatrix} 1/0.05 & 0 \\ 0 & 1/0.95 \end{bmatrix} \quad R = \begin{bmatrix} 1/521 & 0 \\ 0 & 1/664 \end{bmatrix} \tag{4.64}$$

The value in (4.64) correspond to the normalization of the magnitude of the inputs and outputs of the system. This is a typical initial choice of Q and R that is often used in MPC applications. The normalization is also meant to give equal importance to both output and input channels.

The related parameters of the LQR control synthesis for all four cases can be found in the Appendix A.8 and the result of the closed-loop experiment can be seen in Fig. 4.3 and Table 4.2.

From these results, it can be seen that the Fixed-MPC cannot give a proper reaction to the change in the system since the changing dynamics of the system is unknown to the predictive model. On the other hand, the LTV-OBF MPC which is based on an adaptive model, can still follow the reference in both abrupt or slow rotation scenarios. From Table 4.2, it can be seen that the recursive least-squares approach slightly outperforms the weighted least-squares approach. This result is the opposite of the open-loop simulation result (Table 4.1) where the adaptations of the system dynamics were performed better by the least-squares approach. The explanation of this behavior lays in the informativeness of the identification data set / regression matrix. In the open-loop setting (Fig. 4.2), the excitation signals in the form of white noise input contain rich information and hence the model estimation based on a long data set will produce better results. In contrary, in the closed-loop setting, the input excitation is limited. This limited excitation leads to less information in the regression matrix which penalize performance of weighted

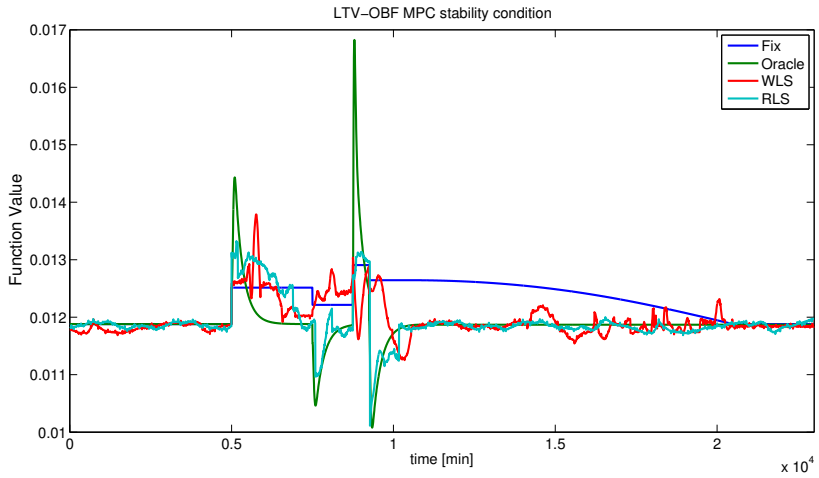

Figure 4.4: Stability condition for LTV-OBF MPC under rotation scenario.

least-squares approach more than it affect the recursive least-squares approach.

Lastly, as indicated in Section 4.7 we visualize the stability condition 4.61 in Fig 4.4. The Fixed MPC case does not have any variation in the model coefficient and hence this condition is purely driven by the state of the LTI-OBF model. Hence, the condition does not have any meaning for this Fixed MPC case. For Oracle, WLS, and RLS cases, we can see that for each jump in the rotation coefficient, the stability condition is also jumping for an instantaneous moment and then converge to the equilibrium related to the reference state x_{rk}. Note that the non-smoothness of the LTV-OBF stability parameter is due to the measurement noise and the induced excitation to maintain persistent excitation for system identification. As indicated in Section 4.7 the update on the parameter can be turned off and both WLS and RLS cases will behave more like the LTI case.

4.9 Summary

An adaptive MPC scheme that is based on an OBF prediction model is presented in this chapter. The OBF-based prediction model is adapted per control cycle to capture the time-varying behavior of the system of interest. The adaptation is based on an iterative identification procedure of the coefficients of the OBF prediction model. Conducting system identification for OBF-based model has a strong benefit due to direct applicability of the PEM identification framework and hence the consistent estimation of the OBF model coefficients. Two procedures for conducting iterative identification based on *Weighted Least Square* and *Recursive Least Square* are given. WLS estimation has the advantage of using past data while RLS estimation has the ease of tuning parameter selection for iterative identification. Afterwards, the MPC scheme for OBF-based prediction model is formulated. A classical feasibility and stability theorem is established for this MPC scheme. The MPC scheme, as well as the feasibility and stability results, are then extended to

the time-varying case. An extra stability condition is required to guarantee the stability of the controlled system. The additional condition shows that the stability of the controlled system can be established from both the control synthesis and the identification side. Lastly, by conducting a simulation study, we have shown that the proposed method can capture the time-varying dynamics of a given system and manage to achieve the goal of set-point tracking.

5 CHAPTER

Parameter-Varying Predictive Control based on OBF models

This chapter is devoted to solving the plant-model mismatch problem in case the cause of the changes in the plant dynamics is known and measurable. We utilize the *Linear Parameter-Varying* (LPV) system framework to describe the variation in the plant dynamics as variation in the parameters of the prediction model. The utilized LPV model to represent these variations is based on *Orthonormal Basis Functions* (OBF) that is identified prior to the commissioning of the MPC controller. After the introduction to the chapter, the considered problem setting is described in Section 5.2. In Section 5.3, LPV identification approaches for the considered OBF model representation are described. In Section 5.4, the LPV-OBF MPC scheme for reference tracking is proposed. It is shown that recursive feasibility and stability is guaranteed for the proposed scheme. In Section 5.5, an *Extended Kalman Filter* (EKF) is introduced. The goal of using EKF is to assist the proposed MPC method when only output measurements are available. In Section 5.7, a simulation study is conducted to demonstrate the capabilities of the proposed MPC scheme.

5.1 Introduction

Model-based control strategies are widely used for optimal operation of chemical processes. Obtaining accurate models to describe the inherently nonlinear, time-varying dynamics of chemical processes remains a challenge in most model-based control applications. One possible method to embed nonlinear dynamics while keeping the linear structure of the model is via the LPV system framework. The class of LPV systems can be seen as an extension of LTI systems as the input-output signals relation is considered to be linear in the LPV case, but this dynamic relation changes depending on an external signal called the scheduling variable

(Tóth 2010). In Bachnas (2012), the capability of data-driven LPV models to capture nonlinear behavior of a chemical process is demonstrated. Moreover, in the context of this thesis, this work shows that OBF-based LPV identification procedures are competitive with other LPV identification method. In this chapter we utilize the OBF model obtained by LPV-OBF identification in our proposed MPC scheme. The aim is to sustain high performance of control under variations of the operating conditions by ensuring minimum discrepancy between the plant and the model.

It is mentioned in Chapter 1, that the available literature on the utilization of OBFs in MPC schemes is underdeveloped for the LTI setting. In Chapter 4, we proposed an adaptive MPC scheme based on OBFs with a goal to capture unknown changes happening in the system of interest. In this scheme, OBFs played an important part in the efficiency of the resulting methodology. However, if the changes in the dynamics of the system at hand are known and measurable, for instance like a change in the operating conditions, a parameter-varying MPC scheme is more suitable compared to the adaptive scheme. This extra knowledge allows us to tackle the control problem in two different fashions. The first one is like controlling ensembles of localized system dynamics which is similar to a gain scheduling control (see in Shamma and Athans (1991), Apkarian and Gahinet (1995)). The second one is more in the global sense where continuous variation of linear dynamics are embedded in the control scheme (see (Tóth 2010)). This provides potential performance improvements over a fixed robust controller. The performance improvements inspired modification of the robust MPC solutions such as in Kothare et al. (1996), Mayne et al. (2011), Bemporad et al. (2003). It is shown in the work of Lu and Arkun (2000), Suzuki and Sugie (2006), Jurre et al. (2017) that exploiting extra information on the process variation improves feedback properties and control performance.

In this chapter, we propose a parameter-varying MPC scheme that is based on an LPV-OBF prediction model. We adopt the MPC scheme based on Limón et al. (2008) and Ferramosca et al. (2009), and extending it for the parameter-varying case. This MPC scheme is selected since it achieves set point tracking, and the modification of the MPC cost function in this scheme is advantageous for the LPV-OBF prediction model. The tracking for piece wise affine set point for a linear system can be seen as an equivalent problem of reference tracking for a parameter-varying system that varies in a piece wise affine manner. This type of variations is commonly seen in process industries. The proposed LPV-OBF MPC scheme given in this chapter consists of three parts:

- Obtaining an LPV model of the plant before recommissioning.
- Synthesizing an MPC control law for the prediction model.
- Designing an EKF for tracking problem with only output measurements.

This chapter is constructed as follows. First, the problem setting is described in Section 5.2. The problem setting specifies the LPV-OBF model, control implementation timeline, and data acquisition setting. In Section 5.3, two LPV identification methods in terms of the local and global approaches are described for

the LPV-OBF model. These two approaches provide two distinct ways of identifying an LPV-OBF model. In Section 5.4, the LPV-OBF MPC scheme for reference tracking is proposed. The MPC scheme utilizes designated steady-state target and extra penalty term for achieving output tracking. Recursive feasibility and stability guarantees are provided for the MPC scheme. In Section 5.5, an *Extended Kalman Filter* (EKF) is introduced. The EKF is used to infer the state from output measurements. In Section 5.7, a simulation study is conducted to demonstrate the performance of the proposed MPC scheme.

5.2 Problem Setting of the LPV-OBF MPC scheme

In this section, a general problem setting for the implementation of the proposed LPV-OBF MPC scheme is described. This section starts with the description of the LTV-OBF model and then continued with the considerations of the predictive control problem in terms of implementation, commissioning, and continuous operation.

5.2.1 LPV-OBF model

Denote the collection of frozen linear dynamics of the system of interest with $\mathcal{S}$ (see Section 2.3 for detailed description). By considering a frozen description of the system, the variation of the linear dynamics between the inputs and outputs of $\mathcal{S}$ can be distinguished by the instantaneous value of the scheduling variable $p(k), k \in \mathbb{Z}$. Furthermore, the linear dynamics can be represented by using an LTI-OBF transfer function $G_{n_\mathrm{b}}(z)$ that is constructed using a cascaded network of fixed n_b basis functions (See Section 2.5.3 for details on the OBFs construction). The variation of the linear dynamics of $\mathcal{S}$ can be described by allowing the expansion coefficients of the OBF model, denoted by θ, to be varying depending on scheduling variable $p(k)$. Such a variation leads to a parameter-varying OBF model which will be called as the LPV-OBF model in the sequel. The state-space representation of the resulting (*Wiener* type) LPV-OBF model is described as follows:

$$
\begin{aligned}
x(k+1) &= \underbrace{\begin{bmatrix} A_{n_\mathrm{e},n_\mathrm{b}} & \dots & 0 \\ \vdots & \ddots & \vdots \\ 0 & \ddots & A_{n_\mathrm{e},n_\mathrm{b}} \end{bmatrix}}_{A \in \mathbb{R}^{n_\mathrm{g} \times n_\mathrm{g}}} x(k) + \underbrace{\begin{bmatrix} B_{n_\mathrm{e},n_\mathrm{b}} & \dots & 0 \\ \vdots & \ddots & \vdots \\ 0 & \ddots & B_{n_\mathrm{e},n_\mathrm{b}} \end{bmatrix}}_{B \in \mathbb{R}^{n_\mathrm{g} \times n_\mathrm{u}}} u(k) \\
&= f(x(k), u(k)), \\
y(k) &= \theta^\top(p(k)) x(k),
\end{aligned} \tag{5.1}
$$

where $x(k) \in \mathbb{X} \subseteq \mathbb{R}^{n_g}$ is the state variable of the LPV-OBF model, $u(k) \in \mathbb{U} \subseteq \mathbb{R}^{n_\mathrm{u}}$ is the input variable of the model, and $y(k) \in \mathbb{Y} \subseteq \mathbb{R}^{n_\mathrm{y}}$ is the output variable

of the model. The state dimension $n_{\mathrm{x}} = n_{\mathrm{g}} = n_{\mathrm{b}} n_{\mathrm{e}} n_{\mathrm{u}}$ of (5.1) depends on the number of OBFs (n_{b}), the length of expansion (n_{e}), and the dimension of the input signal (n_{u}). The state space matrices A and B are time-invariant and their values depend on the selected OBFs. Since the OBFs are time-invariant, the OBF selection needs to consider possible dynamical variation of the process. This task can be accomplished by algorithms that are given in Section 3.4. With a proper selection of OBFs, the resulting LPV-OBF model with a suitable model coefficient function θ is guaranteed to approximate all frozen transfer functions $\mathcal{S}_k$ with the smallest error in the l_2-norm sense such as explained in Section 2.5.2. Note that the error will asymptotically go to zero as the number of OBFs goes to infinity.

The model coefficient $\theta(p(k))$ of (5.1) is a function of the *scheduling variable* $p : \mathbb{Z} \to \mathbb{P}$ with a *scheduling regime* $\mathbb{P} \subseteq \mathbb{R}^{n_{\mathbb{P}}}$. This function depends on the instantaneous value of the scheduling variable and hence the model coefficient is called to have *static*[1] dependency on the scheduling variable. There are two main sets of LPV identification approaches available to derive LPV-OBF models from data measured from the actual process:

- Local approach: Where the function $\theta(p(k))$ is identified by interpolating LTI models of $\mathcal{S}$ identified at distinct operating points inside the operating regime (collection of operating points) of the process.
- Global approach: Where direct estimation of the function $\theta(p(k))$ is conducted based on a single data set that captures the variation of the linear dynamical behavior of $\mathcal{S}$ with respect to a given trajectory of the scheduling variable.

The LPV-OBF model (5.1) is used as the prediction model for the proposed LPV-OBF MPC scheme. The time line of the MPC scheme is explained in the next section.

5.2.2 Implementation concept of the LPV-OBF MPC scheme

The implementation can be divided into two parts which are the control commissioning part and the online part. Before control is commissioned, past measurement data is used to obtain the LPV model and while the control is active, online-data is used to estimate the state of the model. The length of n-th local and global identification data ($N_n \in \mathbb{N}, N_g \in \mathbb{N}$) are associated with an arbitrary past time. The data, prediction, and control horizon (H_d, H_p, H_u) are associated with the present time k. The details on data acquisition setting is given in Section 5.3.4.

The length of which MPC is allowed to compute candidate control actions $u(i|k), i \in \mathbb{Z}_{[0,\infty]}$ is called control horizon H_u. The notation $u(i|k)$ is used to describe the future or predicted input $u(k+i)$ that is calculated at time k. In most cases we consider the control horizon to be equal to the prediction horizon $H_u = H_p$. For the case of $H_u < H_p$, the control action is set to be constant, i.e. $u(H_u|k) = u(H_u + i|k), i = 1, \ldots, H_p - H_u$.

[1] The opposite of *static* dependency is *dynamic* dependency where the function depends on the past trajectory of the scheduling variable (Tóth 2008).

5.3 LPV-OBF identification methods in the PEM setting

In this section, details of *Prediction Error Minimization* (PEM) identification for LPV-OBF models are given. We start by describing the parameterization of the scheduling dependent model coefficients. This parameterization is then used to identify the model via a local and a global LPV identification approach.

5.3.1 Parameterization of the OBF model coefficient

The expansion coefficient $\theta(p(k))$ of an LPV-OBF model is considered to be a function of the instantaneous value of the scheduling variable $p(k)$. This function embeds nonlinear and time-varying behavior of the actual process, while keeping the linear relation of the input-output signal in the model. One method to describe the function $\theta(p(k))$ is by a linear parametrization using a priori chosen set of basis functions $\{\psi_s\}_{s=1}^{n_\psi}$, $\psi_s : \mathbb{P} \to \mathbb{R}$ (Tóth 2010). In this manner, the model coefficients can be written as:

$$\theta(p(k)) = \sum_{s=1}^{n_\psi} \vartheta_s \psi_s(p(k)), \tag{5.2}$$

where $\vartheta_s \in \mathbb{R}^{n_\mathrm{y} \times n_\mathrm{u}}, s = 1, \ldots, n_\psi$ are the unknown parameters to be estimated. It is stated in Boyd and Chua (1985) that by using parameterization (5.2), the OBF model can act as a general approximator of a nonlinear system with fading memory. Here we take the same OE assumption on the noise structure as given in Section 4.2.3. Based on the PEM framework, estimation of ϑ_s can be conducted via a least square formulation. Efficient selection of $\{\psi_s\}_{s=1}^{n_\psi}$ is required such that (5.2) can adequately capture the underlying nonlinearities of the process. Prior information on how the nonlinearities affect the change in the dynamics of the process is of paramount importance for such a parameterization. One possible choice of this set of basis functions is the set of monomial basis such as given in the example below:

Example 5.1 *For a two dimensional scheduling variable* $p(k) = \begin{bmatrix} p_1(k) & p_2(k) \end{bmatrix}^\top$ *the set of monomial basis of order* 3 *are:*

$$\begin{bmatrix} \psi_1(p(k)) & \psi_2(p(k)) & \ldots & \psi_9(p(k)) & \psi_{10}(p(k)) \end{bmatrix} = \\ \begin{bmatrix} 1 & p_1(k) & p_2(k) & p_1^2(k) & p_1 p_2 & p_2^2(k) & p_1^3(k) & p_1^2 p_2 & p_1 p_2^2 & p_2^3(k) \end{bmatrix}. \tag{5.3}$$

After the set of basis functions have been selected, there are two possible ways of estimating ϑ_s. The first one is called the local approach where ϑ_s is estimated with respect to a fixed set of operating points $\{\bar{p}^{(n)}\}_{n=1}^{n_\mathrm{op}}$. The second method is referred to the global approach where the estimation of ϑ_s is based on a trajectory $\tilde{\mathbf{p}} = \{p(k+\tau)\}_{\tau=1}^{N_g}$ that contains varying values of the scheduling variable.

Remark 5.1 *In order to perform the selection of the basis functions* $\{\psi_s\}_{s=1}^{n_\psi}$*, an analysis of a first-principle model is often required. Unaccounted nonlinear behavior may appear in the measurement of the actual process due to non-ideal operation of actuators or actual morphology of the installation. Alternative to parametrization of* $\{\psi_s\}_{s=1}^{n_\psi}$*,* nonparametric *methods are available to directly estimate a functional form of the coefficients* $\theta(p(k))$ *(e.g. Laurain et al. (2012); Hsu et al. (2008)).*

5.3.2 Local approach

In the local approach, estimation of $\{\vartheta_s\}_{s=1}^{n_\psi}$ can be interpreted as an interpolation of the model coefficients of a set of models $\mathcal{M}_{\text{local}}$ which are locally identified at each operating point ($\{\theta(\bar{p}^{(n)})\}_{n=1}^{n_{\text{op}}}$). These model coefficients are interpolated by the selected basis $\{\psi_s\}_{s=1}^{n_\psi}$. Suppose that each of the operating points $\bar{p}^{(n)}, n = 1, \ldots, n_{\text{op}}$ is associated with an LTI-OBF model $G_{n_{\text{b}}}^{(n)}(z)$ with expansion coefficient $\theta(\bar{p}^{(n)})$. By assuming that the model coefficient in the operating regime is linearly parameterized according to (5.2), the estimation procedure of ϑ_s is defined as follows:

Definition 5.1 *Define the cost function of local estimation as*

$$V_{\text{local}} := \left\| \begin{bmatrix} \theta(\bar{p}^{(1)}) \\ \vdots \\ \theta(\bar{p}^{(n_{\text{op}})}) \end{bmatrix} - \underbrace{\begin{bmatrix} \psi_1(\bar{p}^{(1)}) & \ldots & \psi_{n_\psi}(\bar{p}^{(1)}) \\ \vdots & \vdots & \vdots \\ \psi_1(\bar{p}^{(n_{\text{op}})}) & \ldots & \psi_{n_\psi}(\bar{p}^{(n_{\text{op}})}) \end{bmatrix}}_{\Psi} \begin{bmatrix} \vartheta_1 \\ \vdots \\ \vartheta_{n_\psi} \end{bmatrix} \right\|_2^2 . \tag{5.4}$$

The coefficients $\{\vartheta_s\}_{s=1}^{n_\psi}$ *are obtained by the minimization of* (5.4)*:*

$$\{\vartheta_s\}_{s=1}^{n_\psi} = \underset{\{\vartheta_s\}_{s=1}^{n_\psi} \in \mathbb{R}^{n_\psi}}{\arg\min} \; V_{\text{local}}. \tag{5.5}$$

The requirements for a unique solution of (5.5) are $n_{\text{op}} > n_\psi$ and Ψ being full rank. The formulation of the model coefficient interpolation as a least square problem lead to an interesting property of the resulting LPV-OBF model. It is shown in Tóth (2010) that the interpolation of model coefficients of LTI-OBF models is equivalent to the interpolation of the dynamics of the LTI-OBF model itself. By selecting $\{\vartheta_s\}_{s=1}^{n_\psi}$ as the solution of (5.5), we minimize the dynamical error of the identified LPV-OBF model $G_{n_{\text{b}}}(z)$ (at an arbitrary value of the scheduling variable $p(k)$). This property is a strong point of conducting local LPV identification approach by using OBF models which does not hold true for local LPV identification with other model structures. Furthermore, if the noise affecting the data generating systems is not OE, $\theta(\bar{p}^{(n_{\text{op}})})$ can be identified with parametrization of the noise model $H(q, \theta)$ or via IV in the PEM framework to reduce the variance of the estimates. Then, interpolation can be conducted on the resulting parameters.

Remark 5.2 *A local LPV identification approach is often characterized by the combination of the selected interpolation scheme (input, output, coefficient) and interpolation*

methods (linear, polynomial, RBF). Interpolation of the coefficients of LTI-OBF models can be considered as a coefficient interpolation scheme. Thorough comparison between the combinations of interpolation schemes and methods can be found in Bachnas (2012).

5.3.3 Global approach

A commonly applied method for direct estimation of $\{\vartheta_s\}_{s=1}^{n_\psi}$ is the use of the LPV extension of the PEM framework ((Tóth 2010; Giarré et al. 2006)). The LPV-PEM framework utilizes one-step ahead prediction of the presumed model of the system similar to LTI-PEM (See Section 4.3 for identification in the PEM setting). In particular, by having a linear parametrization of (5.2), our goal is to estimate the parameters $\{\vartheta_s\}_{s=1}^{n_\psi}$ given a data set of the actual process $\mathcal{D}_{N_g}$. Since the noise structure of our OBF model is assumed to be OE, and under the commonly taken assumption of noise-free measurement of the scheduling variable p, the one-step-ahead prediction of the LPV-OBF model (5.1) is equivalent to the simulated response:

$$\hat{y}(k) = \theta(p(k))x(k), \tag{5.6}$$

where $x(k)$ is the instantaneous state value of the LPV-OBF model. The LPV-PEM identification criterion for the data set $\mathcal{D}_{N_g}$, along with the optimization problem to obtain $\{\vartheta_s\}_{s=1}^{n_\psi}$ are defined as follows:

Definition 5.2 *The LPV-PEM identification criterion is formulated as*

$$V_{\text{Global}}(\{\vartheta_s, \psi\}_{s=1}^{n_\psi}) := \frac{1}{N_g}\sum_{k=1}^{N} \|y(k) - \hat{y}(k)\|_2^2. \tag{5.7}$$

which is the ℓ_2-loss of the prediction error of (5.6)*. The coefficient $\{\vartheta_s\}_{s=1}^{n_\psi}$ is obtained by the minimization of* (5.7)*:*

$$\{\vartheta_s\}_{s=1}^{n_\psi} = \underset{\{\vartheta_s\}_{s=1}^{n_\psi} \in \mathbb{R}^{n_\psi}}{\arg\min}\ V_{\text{Global}}(\{\vartheta_s, \psi\}_{s=1}^{n_\psi}). \tag{5.8}$$

Due to combination of the linearity in the coefficient property of the LPV-OBF model as well as the linear parametrization (5.2), minimization of (5.7) corresponds to a least squares solution. Moreover, the unbiasedness of the estimation is guaranteed just like in the LTI setting even if v in the data set is a colored noise process. These two properties are the advantages of conducting global LPV identification of LPV-OBF models.

Remark 5.3 *If the noise in the data set is a stationary colored noise, we can use a* Box-Jenkins *noise model to decrease the asymptotic variance of the model estimate at the expense of a non-linear optimization (Tóth 2010).*

5.3.4 Data acquisition

The LPV-OBF model is derived using measured data of the actual process. The output data $y_v(k)$ is considered to be obtained according to:

$$y_v(k) := y(k) + v(k), \tag{5.9}$$

where the response of the actual process $y(k)$ is corrupted with the cumulative effect of measurement and process noise $v(k)$ which is assumed to be a stationary noise. Each of the local and global approaches have distinct characteristics and hence different requirements for data acquisition.

Local approach

In the local approach, the interpolation of LTI models is based on snapshots of linear dynamics of the actual process taken at distinct operating points. These snapshots represent multiple local linear dynamics in the designated operating regime and are characterized by the scheduling variable. To have an adequate coverage of the possible dynamics, the operating regime is gridded (often equidistantly) with respect to the domain of the scheduling variable $\mathbb{P}$. This results in grid points $\{\bar{p}^{(n)}\}_{n=1}^{n_{\text{op}}} \subset \mathbb{P}$. These points are associated with particular steady-state values of the inputs and outputs of the process that are denoted by $(\bar{u}^{(n)}, \bar{y}^{(n)})$. Selection of these operating points not only defines the achievable accuracy of the resulting model, but also sets the number of experiments needed around these operating points to derive local estimates of the behavior.

In order to gather measurement data for the purpose of identification, the actual process needs to be brought to a steady-state condition at the operating points, and then excited around the vicinity by an input signal such as a small amplitude white noise, PRBS, or multisine (Bombois and Scorletti 2012). This excitation is designed such that the system remains around the specified operating condition and the corresponding output $\breve{y}(k)$ describes the linear dynamics of the system. The corresponding data sets associated with the n-th operating point are denoted by

$$\mathcal{D}_{N_n}^{(n)} := \{u(k+\tau) - \bar{u}^{(n)}, y_v(k+\tau) - \bar{y}^{(n)}, \bar{p}^{(n)}\}_{\tau=0}^{N_n}, \tag{5.10}$$

where $N_n > 0$ is the length of the data set. For each $\mathcal{D}_{N_n}^{(n)}$, PEM identification (see Section 4.3) is applied to obtain LTI-OBF models using the same set of OBFs. The collection of these models for each operating point is denoted by $\mathcal{M}_{\text{local}}$. Note that, it is not required to obtain the data set for all n_{op} grid points in a single experiment. In fact, a separate procedure on interpolation and identification allows online update of the LTI-OBF model if necessary. The only requirement is a new data set for the selected operating points.

Remark 5.4 *Note that optimized allocation of $\{\bar{p}^{(n)}\}_{n=1}^{N_{\text{op}}}$ can seriously lower the number of required LTI experiments (Khalate et al. 2009), and hence the cost of the experimental campaign. Typically in the process domain, adequate choice of grid points is recommended to be 3-6 for each dimension of the scheduling variable.*

Global approach

Unlike in the local approach, in the global approach, the LPV-OBF model is estimated directly from a single data set

$$\mathcal{D}_{N_g} := \{u(k+\tau), y_v(k+\tau), p(k+\tau)\}_{\tau=0}^{N_g}. \tag{5.11}$$

This data set is obtained by exciting the actual process with a predesigned sequence of input $\tilde{\mathbf{u}} = \{u(k+\tau)\}_{\tau=1}^{N_g}$ that result in a scheduling trajectory $\tilde{\mathbf{p}} = \{p(k+\tau)\}_{\tau=1}^{N_g}$ inside the operating regime of the process. The necessity of single estimation data set $\mathcal{D}_{N_g}$ means that a dedicated experiment is required to obtain such a data set. This experiment also needs to be designed such that the system visits the operating domain with an adequate transient between the operating points. (Bachnas 2012; Tóth 2010).

5.4 LPV-OBF MPC scheme

In this section, we formulate an LPV-OBF MPC scheme that is based on LPV-OBF models (5.1). We incorporate and extend the MPC scheme proposed by Limón et al. (2008), Ferramosca et al. (2009) for the parameter-varying case. First, we introduce the prediction model and its corresponding parameterization of the steady-state pairs. The steady-state pairs describe the input-state pairs which can achieve steady-state condition. This steady-state pairs are then used to formulate the LPV-OBF MPC scheme. Afterwards, we describe the important properties of the control scheme such as feasibility and stability guarantee.

5.4.1 LPV-OBF prediction model

The main idea behind the MPC scheme proposed in Limón et al. (2008) and Ferramosca et al. (2009) is to have an MPC controller that drive the state x to a designated steady-state value x_s. The space of the steady-state pairs $u_s \in \mathcal{U}_s, x_s \in \mathcal{X}_s$ depend on the prediction model, and their value is selected by a parametrization variable ξ. In the context of this chapter, the prediction model is based on the LPV-OBF model (5.1):

$$\Sigma_{\text{PV}} \begin{cases} x(i+1|k) = Ax(i|k) + Bu(i|k), \quad x(0|k) = x(k) \\ y(i|k) = C(p(k+i))x(i|k). \end{cases} \tag{5.12}$$

At time instant k, the prediction model (5.12) predicts future values of the state $x(i+1|k), i = 0, 1, \ldots, N$ based on the current state value $x(k)$ and the possible future input sequence $u(i|k), i = 0, 1, \ldots, N$. The relation between the prediction of the output $y(i|k)$ and the state $x(i+1|k)$, for $i = 0, 1, \ldots, N$, is governed by the parameter-varying matrix $C(p(k+i))$ which is obtained via the identification procedure given in Section 5.3. This matrix varies according to the future value of

the scheduling variable $p(k+i), i = 0, 1, \ldots, N$. The end value of the time horizon N, is set equal to the prediction horizon, i.e. $N = H_p$.

Based on prediction model (5.12), it can be seen that any steady-state of pair x_s, u_s of such a model must satisfy the following equation

$$\begin{bmatrix} A - I_{n_x} & B \end{bmatrix} \begin{bmatrix} x_s \\ u_s \end{bmatrix} = 0_{n_x} \tag{5.13}$$

If the pair (A, B) is stabilizable, Equation (5.13) has a non-trivial solution. This solution can be parameterized as:

$$\begin{bmatrix} x_s \\ u_s \end{bmatrix} = \begin{bmatrix} M_x \\ M_u \end{bmatrix} = M_\xi \xi, \tag{5.14}$$

where $M_\xi \in \mathbb{R}^{n_\mathrm{x}+n_\mathrm{u} \times n_\xi}$ is the nullspace of (5.13) that characterizes the space of steady-state pairs $\mathcal{X}_s$ and $\mathcal{U}_s$, and $\xi \in \mathbb{R}^{n_\xi}$ is a vector that selects a particular element of x_s, u_s in this space. Further in this thesis, we also use notation of M_x and M_u which are the corresponding rows of M_ξ associated with x_s and u_s. The associated designated target output space $y_s \in \mathcal{Y}_s$ with respect to x_s is a linear mapping from the space $\mathcal{X}_s$ to $\mathcal{Y}_s$ that is governed by matrix $C(p(k))$. Precisely, the relation is defined as follows:

Definition 5.3 *The designated target output y_s is written as:*

$$y_s = C(p(k+N))x_s, \tag{5.15}$$

where $C(p(k+N))$ depend on the the value $p(k+N)$ at the end of prediction horizon.

We only consider the value at the end of prediction horizon since the reference r is considered to be constant or at most piece wise affine. This type of reference is a common set up for process industry applications. In the next section we describe the cost function of the LPV-OBF MPC.

Remark 5.5 *From* (5.13)*, we can see that the space of designated steady-state pairs (x_s, u_s) is independent of the scheduling variable p. A particular value of ξ is associated with a unique pair of (x_s, u_s) regardless on the value of $p(k)$. This is one advantage of using LPV-OBF model instead of an other LPV model that has scheduling dependent state and input matrices $A(p)$ and $B(p)$.*

5.4.2 The LPV-OBF MPC problem

The LPV-OBF MPC cost function $V_N : (\mathbb{R}^{n_\mathrm{u}})^{N+1} \times \mathbb{R}^{n_\mathrm{x}} \times \mathbb{R}^{n_\xi} \to \mathbb{R}$ is formulated as follow:

$$V_N(x(k), \mathbf{u}, \xi) = \sum_{i=0}^{N} (\|x(i|k) - x_s\|_Q^2 + \|u(i|k) - u_s\|_R^2) + \|x(N|k) - x_s\|_P^2 + V_o(y_s - r), \tag{5.16}$$

where $x(k)$ is the (initial) state at time k, r is the target reference, $\mathbf{u}$ denotes the future input sequence $\{u(i|k)\}_{i=0}^{N-1}$, the MPC weighting matrices are denoted by positive definite matrices $Q \succ 0$, $R \succ 0$, and $P \succ 0$, while u_s, x_s are the designated steady-state input and state pair associated with the parameterization variable ξ. In (5.16), we consider the prediction horizon $N = H_p$. In the case when $N > H_u$, we set $u(k+i|k) = u(k+H_u|k)$ for $i = H_u + 1, \ldots, N$. The cost function (5.16) is based on the work of Limón et al. (2008), which is slightly different than a common MPC cost function by the addition of a designated steady-state pair u_s, x_s, which are generated by the prediction model, and the additional target penalty function V_o which penalizes the difference between the reference and the designated target output y_s associated with the steady-state pair u_s, x_s. These two unique additions are further used to guarantee recursive feasibility and stability properties. The function $V_o : \mathbb{R}^{n_y} \to \mathbb{R}$ is assumed to be convex, positive definite, subdifferentiable and zero when the entry is zero. Simple example of a target penalty function that can be used is

$$V_o(y_s - r) = \|y_s - r\|_T^2 \tag{5.17}$$

where $T \succ 0$ is a positive definite matrix. Such a function contributes to the selection of ξ for tracking purpose.

The minimization of (5.16) with respect to the future input sequence $\mathbf{u}$ is solved while obeying operational and stability constraints. This minimization problem corresponds to an MPC problem which is formulated as follows:

Definition 5.4 ***LPV-OBF MPC Problem***
Given the prediction model Σ_{PV}, current state $x(k)$, reference r, and future values of the scheduling variable $p(k+i), i = 0, 1, \ldots, N$. The MPC problem is written as:

$$\begin{aligned} P_{\mathrm{PV-MPC}} := \quad & \min_{\mathbf{u},\xi} \quad V_N(x(k), \mathbf{u}, \xi) \\ & \textit{s.t.} \quad \Sigma_{\mathrm{PV}}, && \forall\ i = 0, 1, \ldots, N \\ & \quad (x(i|k), u(i|k)) \in \mathcal{Z}, && \forall\ i = 0, 1, \ldots, N \\ & \quad [x_s, u_s]^\top = M_\xi \xi, \\ & \quad (x(N|k), \xi) \in \mathcal{X}_f^w \end{aligned} \tag{5.18}$$

where the set $\mathcal{Z}$ is a polyhedron that describe the admissible set of inputs and states[2]*, and $\mathcal{X}_f^w$ are polyhedrons that describe the stability constraint regarding the end state $x(N|k)$ and vector ξ. Set $P_{\mathrm{PV-MPC}} = +\infty$ when the feasible set of* (5.18) *is empty (the MPC problem is ill posed). The goal of this MPC problem is to find the minimizer of* (5.18) *for each control cycle $k \in \mathbb{Z}$. The attained minimum of* (5.18) *is called the* primal optimum *and it is denoted by $V_N^*(k)$. The minimizer with respect to the* primal optimum *is the* optimal input sequence *which is denoted by $\{u^*(i|k)\}_{i=1}^N$ or $\mathbf{u}^*$ and the* optimal steady-state vector *ξ^*.*

Only the first value of the *optimal input sequence* $\mathbf{u}^*$ that is applied as the control action. Such control action is known as an MPC control law and is defined as follows:

[2]Notice that different definition of set of admissible input and state are used compared to LTV-OBF problem of (4.29). This is the result of using steady state characterization of (5.13) and how we incorporate nullspace M_ξ and selector variable ξ into the MPC problem

Definition 5.5 *For every $k \in \mathbb{Z}$, the MPC control law is given as:*

$$u_{\mathrm{MPC}}(k) = u^*(0|k) \tag{5.19}$$

where $u^*(0|k)$ is the first element of the optimal input sequence $\mathbf{u}^*$.

The main purpose of the MPC control law is to steer the output $y(k)$ of the closed loop system:

$$G_{\mathrm{CL-PV}} \begin{cases} x(k+1) = Ax(k) + Bu_{\mathrm{MPC}}(k), & x(0) = x_0 \\ y(k) \quad\quad = C(p(k))x(k), \end{cases} \tag{5.20}$$

towards a given reference r. If this goal is accomplished, then the MPC controller is stated to be convergent. Precisely:

Definition 5.6 *The MPC controller is* convergent *if for all $x_o \in \mathbb{X}$, for all $r \in \mathbb{R}^{n_y}$, and $p(k) \in \mathbb{P}, k \in \mathbb{Z}$, the MPC control law $\{u_{\mathrm{MPC}}(k)\}_{k=0}^{\infty}$ drives the output of system* (5.20) *to a given constant reference r in the sense that*

$$\lim_{k\to\infty} \parallel y(k) - y_s \parallel = 0. \tag{5.21}$$

where

$$\begin{aligned} &y_s = \operatorname{argmin} \parallel y(k) - y_s \parallel, \\ &\textit{s.t.} \quad x_s \in \mathcal{X}_f^w. \end{aligned} \tag{5.22}$$

The convergence described in (5.21) is defined in the asymptotic sense and an assumption need to be taken for the proposed MPC problem:

Assumption 5.1 *Future trajectory of the scheduling variable satisfies that $p(k+i) = p(k+N)$ for all $i \geq N$. Furthermore, there exist ξ such that $(x_s, u_s) \in \mathcal{Z}$,$(x_s, \xi) \in \mathcal{X}_f^w$, and $r = C(p(k+N))x_s$.*

The assumption that $p(k)$ is constant make sense for process industry applications where operating conditions are usually kept constant for longer period of time. Another condition that comply to the assumption is where the operating point is state dependent and the process is required to converge to the steady state in given period of time.

An additional property, namely the stability of the MPC controller, is required to further strengthen and regulate the possible behavior of the output of the closed loop system. Further definitions and results that are related to the stability of (5.20) is described in Section 5.4.4.

Before we can show that an MPC controller is both convergent and/or stable, one of the first steps is to show wether the MPC control law actually exists. The existence of the MPC control law is guaranteed with the concept of feasibility of the MPC problem (5.18).

Definition 5.7 *The MPC problem* (5.18) *is called feasible at time k if the optimal input sequence and optimal steady-state vector exist.*

Additionally, the notion of infeasibility of the MPC problem (5.18) is defined as follow:

Definition 5.8 *The MPC problem is called infeasible at time k if* $\inf V_N = +\infty$.

From the definition of a feasible MPC problem, the notion of recursive feasibility of an MPC problem (5.18) is then defined.

Definition 5.9 *The MPC problem is called recursively feasible if feasibility at time k with reference r, future value of the scheduling variable $p(k+i), i = 0, 1, \ldots, N$ and initial condition $x(k)$, implies feasibility of the MPC problem at time $k+1$ with the same reference r, future value of the scheduling variable $p(k+i), i = 1, \ldots, N+1$, and initial condition $x(k+1) = Ax(k) + Bu_{\mathrm{MPC}}(k)$.*

The recursive feasibility of an MPC controller is an essential property that is used as the fundamental building block to guarantee stability of an MPC controller. However, in order to guarantee this property, we need additional definitions that are related to the extension of the input for the prediction model (5.12) after the prediction horizon. This is described in the next subsection.

5.4.3 Local controller for LPV-OBF MPC

In this subsection, we introduce an extended input signal and a local controller for the LPV-OBF model (5.1) with the purpose to drive the state x to the designated steady-state x_s after the end of the prediction horizon.

Definition 5.10 *For any matrix $K \in \mathbb{R}^{n_{\mathrm{u}} \times n_{\mathrm{x}}}$, the extended input sequence is given as:*

$$u_{\mathrm{ext}}(i|k) := \begin{cases} u^*(i|k) & i = 0, \ldots, N, \\ K(x(i|k) - x_s) + u_s = Kx(i|k) + L\xi & i > N, \end{cases} \tag{5.23}$$

where $x(i|k)$ is the state of (5.12) *with $u(i|k) = u^*(i|k)$ for $i \leq N$ and $L = [-K \quad I^{n_\xi}]M_\xi$ is the matrix that parameterizes x_s and u_s.*

Definition 5.11 *Call K in* (5.23) *a* stabilizing linear controller *at time k if*

$$\lim_{i \to \infty} \|x(i|k) - x_s\| = 0 \tag{5.24}$$

for all initial condition $x(k) \in \mathbb{X}, \forall \xi \in \mathbb{R}^{n_\xi}$.

If there exist a stabilizing linear controller K, then (5.24) implies convergent MPC controller (Definition 5.6) provided that $y_s = r$ and p fulfills Assumption 5.1. This term is characterized by the target penalty function V_o.

Furthermore, we characterize the evolution of the state of the prediction model (5.12):

$$x(i+1|k) = Ax(i|k) + Bu_{\mathrm{ext}}(i|k) \quad , i > N, \tag{5.25}$$

is bounded by in an invariant set $\mathcal{X}_f$. The set $\mathcal{X}_f$ can be characterized by introducing the extended state $w(i|k) = [x(i|k), \xi]^\top$ and a closed loop augmented system:

$$w(i+1|k) = \underbrace{\begin{bmatrix} A+BK & BL \\ 0 & I^{n_\xi} \end{bmatrix}}_{A_w} w(i|k), \quad i > N \tag{5.26}$$

where I^{n_ξ} is identity matrix of dimension $n_\xi \times n_\xi$.

For a given value of ξ, the state $x(i|k)$ in (5.26) evolves to the designated designated state x_s (depending on the value of ξ) only when the matrix $A + BK$ is *Hurwitz*. Introduce the admissible invariant set $\Omega^{K,w}$ of (5.26) as a set of all possible value of $w \in \Omega^w$ that can be admissibly stabilized by the control law (5.23). Introduce W_η as a convex polyhedron

$$W_\eta = \{w = (x, \xi) : (x, Kx + L\xi) \in \mathcal{Z}, M_\xi \xi \in \eta\mathcal{Z}\} \tag{5.27}$$

where $\eta = (0, 1]$ is the so called contraction parameter and $\mathcal{Z}$ is the set of admissible set of state and input. A set $\Omega^{K,w}$ is denoted as the admissible invariant set for tracking if for all $w \in \Omega^{K,w}$, it holds that $A_w w \in \Omega^{K,w}$ and $\Omega^{K,w} \subseteq W_{\eta=1}$.

Denote $\mathcal{O}_\infty^w = \{w : A_w^k \in W_{\eta=1}, \forall k \geq 0\}$ as the maximal admissible invariant set of system (5.26). Due to the unitary eigenvalues of A_w, O_∞^w can not be finitely determined, i.e. described by a finite set of constraints (Gilbert and Tan 1991). Alternatively, as stated in Gilbert and Tan (1991), we can introduce the following convex polyhedron set

$$\mathcal{O}_{\infty,\eta}^{K,w} = \{w : A_w^k w \in W_\eta, \forall k \geq 0\}, \tag{5.28}$$

which is finitely determined for any $\eta \in (0, 1)$. Given that $\eta\mathcal{O}_\infty^{K,w} \subset \mathcal{O}_{\infty,\eta}^{K,w} \subset \mathcal{O}_\infty^w$ and since η can be chosen arbitrarily close to 1, the set $\mathcal{O}_{\infty,\eta}^{K,w}$ can be used as a polyhedral approximation of the maximal invariant set $\mathcal{O}_\infty^{K,w}$. This also means that

$$A_w \mathcal{O}_{\infty,\eta}^{K,w} \subset \mathcal{O}_\infty^{K,w}. \tag{5.29}$$

By using (5.28), the invariant set $\mathcal{X}_f$ can be selected as the projection of $O_{\infty,\eta}^{K,w}$ to the admissible state $\mathbb{X}$:

$$\mathcal{X}_f = \Pi_{\mathbb{X}}(\mathcal{O}_{\infty,\eta}^{K,w}). \tag{5.30}$$

thus achieving

$$(A + BK)x(i|k) \subset X_f \text{ for } , i > N. \tag{5.31}$$

In the next section we establish the recursive feasibility theorem

5.4.4 Recursive feasibility and stability of LPV-OBF MPC

By using Definition 5.5-5.10 as well as the set $O_{\infty,\eta}^{K,w}$ of (5.28), the feasibility of the MPC problem (5.18) can be established.

Theorem 5.1 ***Recursive feasibility of LPV-OBF MPC***
If there exist stabilizing controller K such that

1. *The MPC problem* (5.18) *at time k is feasible,*
2. *Matrix $A + BK$ is Hurwitz,*

are satisfied, then by selecting $\mathcal{X}_f^w = \Pi_{\mathbb{X}}(\mathcal{O}_{\infty,\eta}^{K,w})$ the recursive feasibility of MPC problem (5.18) *is guaranteed*

Proof of the theorem can be found in Appendix A.6.By guaranteeing recursive feasibility of the LPV-OBF MPC scheme we can establish the stability guarantee of the scheme. First, we define the notion of an asymptotically stable closed loop system.

Definition 5.12 *Closed loop system* (5.20) *is called asymptotically stable if it is both convergent (Definition 5.6) and the controlled state evolution is bounded in a* closed-loop invariant *set $x(k) \in \mathcal{X}_f, \forall k \in \mathbb{Z}$.*

We follow the *Control Lyapunov* stability argument mentioned in Sontag (1998). *Control Lyapunov* stability argument is relevant for a controlled system (5.20) where the successor state $x(k+1)$ depends on the current state $x(k)$ and the driving control law u or u_{MPC} in the MPC case. In order to define a *Control Lyapunov* function, the definition of class $\mathcal{K}$ functions (Khalil 2002) are required:

Definition 5.13 *A functions $\alpha : \mathbb{R}_+ \to \mathbb{R}_+$ belongs to class $\mathcal{K}$ if it is continuous, zero at zero, and strictly increasing; $\alpha : \mathbb{R}_+ \to \mathbb{R}_+$ belongs to class $\mathcal{K}_\infty$ if it is a class $\mathcal{K}$ and unbounded $(\alpha(k) \to \infty, k \to \infty)$. A function $\gamma : \mathbb{R} \to \mathbb{R}_+$ belongs to a class $\mathcal{PD}$ functions if it is continuous and positive everywhere except at the origin.*

The definition of a *Control Lyapunov* function is given as follows:

Definition 5.14 *A function $V : \mathbb{R}^n \to \mathbb{R}$ is called a* Control Lyapunov *function if there exists $\mathcal{K}_\infty$ functions α_1, α_2, and $\mathcal{PD}$ function α_3 defined on $\mathcal{X}_f$ such that*

$$\alpha_1(\|x - x_s\|) \leq V(x) \leq \alpha_2(\|x - x_s\|), \tag{5.32}$$

and

$$\inf_{u \in \mathcal{U}} V(Ax + Bu) - V(x) \leq -\alpha_3(\|Ax + Bu - x_s\|). \tag{5.33}$$

The existence of a control Lyapunov function for the closed loop system (5.20) is a sufficient condition for the asymptotic stability property. The stability theorem is given as follows:

Theorem 5.2 ***Stability guarantee of LPV-OBF MPC.***
Introduce $\tilde{V}_o(y_s - r)$ as the penalty term of (5.16) *computed at time $k+1$. Suppose that there exist a* stabilizing linear control *K and a closed loop invariant set $(A+BK)\mathcal{X}_f \subset \mathcal{X}_f$ such that:*

1. *The MPC problem* (5.18) *is recursively feasible,*
2. *Let* $P \in R^{n_x \times n_x}$ *be a positive definite matrix such that*

$$(A+BK)^\top P(A+BK) - P \succeq Q + K^\top RK \tag{5.34}$$

3. $\tilde{V}_o(y_s - r)$-$V_o(y_s - r) \leq 0$.

Under Assumption 5.1, the MPC cost function $V_N(\cdot)$ *admits a control Lyapunov function for the closed loop system* (5.20) *and hence the closed loop system is asymptotically stable.*

Proof of the theorem can be found in Appendix A.7. The Theorem 5.2 completes the formulation of LPV-OBF MPC scheme.

5.5 Formulation of the *Extended Kalman Filter*

For the implementation of LPV-OBF MPC, the model coefficient variations are identified before the commissioning of the MPC and not updated while the controller is online. Unaccounted change in the actual process or disturbances might lead to the growing plant-model mismatch, thus unwanted behavior such as inability to track reference or in extreme case loss of stability might incur. Hence, an EKF is utilized to correct the state of the prediction model for the tracking problem with only output measurements. Similar to the original Kalman filter, there are basically two steps in the EKF, which are the prediction step and the update step (Gelb 1974). The only notable differences is the actual computation of the Jacobian F_{k-1} and H_k which are based on the parameter-varying OBF model (5.1). The model considered in the EKF formulation is as follows:

$$\begin{aligned} x(k+1) &= Ax(k) + Bu(k) + w(k), \\ y(k) &= C(p(k))x(k) + v(k) = \theta(p(k)) + v(k), \end{aligned} \tag{5.35}$$

where $w(k)$ and $v(k)$ are gaussian white noise processes with variance R_E, and Q_E respectively. The formulation of EKF is then given as follows:

$$\begin{array}{lll} \text{Prediction Step} & & \\ \text{Predicted state estimate} & \hat{x}(k) & = Ax(k-1) + Bu(k-1), \\ \text{Predicted covariance estimate} & \hat{P}_k & = AP_{k-1}A + Q_E, \\ & & \\ \text{Update Step} & & \\ \text{Measurement residual} & \tilde{y}(k) & = y_v(k) - C(p(k))\hat{x}(k), \\ \text{Residual covariance} & S_k & = H_k\hat{P}_kH_k^\top + R_E, \\ \text{Kalman gain} & K_k & = \hat{P}_kH_k^\top S_k^{-1}, \\ \text{Update state estimate} & x(k) & = \hat{x}(k) + K_k\tilde{y}(k), \\ \text{Update covariance estimate} & P_k & = (I - K_kH_k)\hat{P}_k, \end{array} \tag{5.36}$$

with the Jacobian

$$F_{k-1} = \frac{\partial f}{\partial x} = A,$$

and

$$H_k = \frac{\partial h}{\partial x} = \theta(p(k)).$$

The EKF estimates the state $x(k)$ which minimizes the difference between the measured output $y_v(k)$ and the output of the prediction model (5.12). By using an OBF model structure, the Jacobian calculation of F_{k-1} leads to a static matrix, and H_k is the parameter dependent $\theta(p(k))$. This simplifies the usage of EKF compared to using a nonlinear model. Since the A and B matrices of the OBF model are selected properly by the method discussed in Chapter 3, the effect of un-modeled dynamics or truncation error will be minimal.

The typical value for EKF matrices is to use the information of variance of the measurement data as the entries of R_E, while the Q_k matrix needs to have a small value to maintain a relative ratio between Q_E and R_E. The smallest entry of the R_E matrix can be used for this purpose.

5.6 LPV-OBF MPC algorithm

This section summarizes the finding of previous sections and presents the LPV-OBF MPC scheme as an algorithm. In principle the algorithm is divided into three parts:

- Preparation step of the LPV-OBF model
- Finding a stabilizing linear controller
- Online LPV-OBF MPC control

The preparation step for the LPV-OBF model can be split depending on the LPV modeling approach that is selected. However, irrespective of the selected approach, efficient selection of $\{\psi_s\}_{s=1}^{n_\psi}$ is required such that the LPV-OBF model can adequately capture the underlying nonlinearities of the process. Prior information on how the nonlinearities affect the change in the dynamics of the process is of paramount importance for such a parameterization. For the local approach, the parameterization explains the evolution of identified model parameter $\{\theta(\bar{p}^{(n)})\}_{n=1}^{n_{\text{OP}}}$ in the operating regime. An example of such algorithm is as follows:

For the global approach, the evolution of $\{\vartheta_s\}_{s=1}^{n_\psi}$ through the parameter space is identified in one step w.r.t. a global data set. An example of such algorithm is as follows:

The LPV-OBF global approach will have a longer parameterization in terms of $\{\psi_s\}_{s=1}^{n_\psi}$ compared to the LPV-OBF local approach. The reason is the construction of the cost function of LPV-PEM identification criterion in least-square form requires separate parameterization of the model coefficients $\{\vartheta_s\}_{s=1}^{n_\psi}$ for each state of the OBFs.

Algorithm 8 LPV-OBF model identification using the local approach

Require :

- Basis pole for the system of interest ($\{\lambda_i\}_{i=1}^{n_\mathrm{b}}$) (see Chapter 3)
- Local identification data sets $\mathcal{D}_{N_n}^{(n)}$ for each $\{\bar{p}^{(n)}\}_{n=1}^{n_\mathrm{op}}$
- Coefficient parameterization $\{\psi_s\}_{s=1}^{n_\psi}$ (e.g. monomial basis of Eq.(5.3))
- Selected number of basis expansion n_e
- Number of input channels of the system of interest n_u
- Validation data set $\mathcal{D}_\mathrm{val}$ with a continuous trajectory of input $u(k)$, output $y(k)$, and scheduling variable $p(k)$.
- Success Criteria for identification $0\% < \mathrm{SC} < 100\%$

Ensure: $\mathrm{BFR} = 0\%$
while $\mathrm{BFR} \leq \mathrm{SC}$ **do**
Construct state-space OBF representation w.r.t. basis poles ($\{\lambda_i\}_{i=1}^{n_\mathrm{b}}$), number of basis expansion (n_e), and input channel n_u (i.e. Eq (2.64))
Conduct n times LTI-OBF identification in PEM setting for each $\mathcal{D}_{N_n}^{(n)}$ (See Section 4.3.1)
Collect the initial coefficient of the LTV-OBF model θ_o for each output
Simulate the LTV-OBF model with respect to the other part of the global data set $\mathcal{D}_{N_g}$ (validation step)
Compute *Best Fit Ratio*(Ljung (2006)) of the identified LTI-OBF model:

$$\mathrm{BFR} = 100\% \cdot \max\left(1 - \frac{\|y(k) - \hat{y}(k)\|_2}{\|y(k) - \bar{y}\|_2}, 0\right), \tag{5.37}$$

if $\mathrm{BFR} < \mathrm{SC}$ **then**
Set $n_\mathrm{e} \leftarrow n_\mathrm{e} + 1$
end if
end while
Collect initial coefficient of LTI-OBF model $\{\theta(\bar{p}^{(n)})\}_{n=1}^{n_\mathrm{op}}$
Ensure: $\mathrm{BFR} = 0\%$
while $\mathrm{BFR} \leq \mathrm{SC}$ **do**
Construct regression matrix of Eq. (5.4) w.r.t. selected parameterization $\{\psi_s\}_{s=1}^{n_\psi}$ for each output channels
Solve the LPV-OBF local estimation problem of Eq.(5.5)
Collect the LPV-OBF model coefficient $\{\vartheta_s\}_{s=1}^{n_\psi}$ for each output channels
Construct the LPV-OBF model w.r.t. $\{\vartheta_s\}_{s=1}^{n_\psi}$
Simulate the LPV-OBF model w.r.t. validation data set $\mathcal{D}_\mathrm{val}$
Compute the *Best Fit Ratio* of LPV-OBF model (i.e. Eq.5.37)
if $\mathrm{BFR} < \mathrm{SC}$ **then**
Select new parameterization $\{\psi_s\}_{s=1}^{n_\psi}$
end if
end while
Collect the final LPV-OBF model

Algorithm 9 LPV-OBF model identification using the global approach

Require :

- Basis poles for the system of interest ($\{\lambda_i\}_{i=1}^{n_\mathrm{b}}$) (see Chapter 3 for basis selection methodology)
- Coefficient parameterization $\{\psi_s\}_{s=1}^{n_\psi}$ (e.g. monomial basis of Eq.(5.3))
- Selected number of basis expansion n_e
- Number of input channels of the system of interest n_u
- Global identification data set $\mathcal{D}_{N_g}$ with a continuous trajectory of input $u(k)$, output $y(k)$, and scheduling variable $p(k)$
- Validation data set $\mathcal{D}_\mathrm{val}$ with a continuous trajectory of input $u(k)$, output $y(k)$, and scheduling variable $p(k)$.
- Success Criteria for identification $0\% < \mathrm{SC} < 100\%$

Ensure: $\mathrm{BFR} = 0\%$
while $\mathrm{BFR} \leq \mathrm{SC}$ **do**
Construct a state-space OBF representation w.r.t. basis poles ($\{\lambda_i\}_{i=1}^{n_\mathrm{b}}$), number of basis expansion (n_e), and input channel n_u (i.e. Eq (2.64))
Simulate the state evolution $x(k)$ of the SS-OBF w.r.t. global data set $\mathcal{D}_{N_g}$
Construct prediction matrix Eq.(5.6) w.r.t. state evolution $x(k)$ and selected parameterization $\{\psi_s\}_{s=1}^{n_\psi}$
Construct cost function of LPV-PEM identification criterion (i.e. Eq. (5.7))
Solve the LPV-PEM identification problem
Construct the LPV-OBF model with model coefficients $\{\vartheta_s\}_{s=1}^{n_\psi}$
Simulate the LPV-OBF model w.r.t. the validation data set $\mathcal{D}_\mathrm{val}$
Compute the *Best Fit Ratio* of LPV-OBF model (i.e. Eq.5.37)
if $\mathrm{BFR} < \mathrm{SC}$ **then**
Set $n_\mathrm{e} \leftarrow n_\mathrm{e} + 1$ or consider new parameterization $\{\psi_s\}_{s=1}^{n_\psi}$.
end if
end while
Collect the final LPV-OBF model

With the LPV-OBF model at hand, the next step is to find stabilizing linear controller. As described in Section 5.4.3, we only need a single local controller for the LPV-OBF MPC. A standard LQR control synthesis algorithm is as follows:

Algorithm 10 Finding a stabilizing LQR control for LPV-OBF MPC

Require :

- LPV-OBF model of the system of interest (Result from Algorithm 8/9)
- Control matrices Q, and R.

Construct LMI of:

$$\begin{pmatrix} S & (AS+BT)^\top & S & T^\top \\ AS+BT & S & 0 & 0 \\ S & 0 & Q^{-1} & 0 \\ T & 0 & 0 & R^{-1} \end{pmatrix} \succeq 0, \tag{5.38}$$

Solve LMI
Compute matrices $P = S^{-1}$, $K = TP$

The value of $Q = I^{n_\mathrm{x} \times n_\mathrm{x}}$ should be selected in most cases since Q in the LPV-OBF case affects different state elements where each corresponds to a different OBFs (See Eq.(5.1)). This leads to a less intuitive tuning parameter compared to the LTV-OBF case since there is no physical interpretation of the state for the LPV-OBF model. It is also possible to scale down the Q matrix w.r.t. the control action matrix R to make the control action more aggressive. The role of weighting the output channels is now governed by matrix T which is not used for the LQR synthesis but only for the MPC scheme. The online execution of the LPV-OBF MPC scheme is written in this following algorithm:

Another notable point in the online control algorithm is that we require future information on scheduling variables/trajectories up to N step ahead. This is requirement is driven by Definition 5.3. We consider the value at the end of prediction horizon since the reference r is considered to be constant or at most piece wise affine. This type of reference is a common setup for process industry applications. In the next section, we describe the cost function of the LPV-OBF MPC.

Regarding the stability of the LPV-OBF MPC scheme, as given by Theorem 5.2, the stability holds during the commissioning of the proposed MPC scheme. We can show the stability by plotting the evolution of the target function $V_o(y_s - r)$ (Eq. (5.17)). The reason is that it is the last condition of stability where the value of $V_o(y_s - r)$ at time $k+1$ should be less or equal to the value at time k. This value also indicates that the targeted reference r can be fully tracked by the target steady-state output y_s and the change of system dynamics w.r.t. the change operating points can also be captured by the LPV-OBF model.

Remark 5.6 *For the EKF, although not directly mentioned in the algorithm, if we notice unsatisfactory control performance, we can lower the relative ratio between Q_E and R_E.*

Algorithm 11 LPV-OBF MPC online control

Require :

- LPV-OBF model of the system of interest (Result from Algorithm 8/9)
- Stabilizing LQR controller matrices P and K
- Control Matrices Q, R, and T (use the same Q and R that are used for LQR control synthesis)
- Prediction-Control horizon N (value needs to be larger than the settling time of the system dynamics)
- Commissioned data set $\mathcal{D}_k$ consisting of current value of input $u(k)$, output $y(k)$, and scheduling variable $p(k)$. For scheduling variable up to N step ahead are required.
- EKF matrices Q_E and R_E (See Section 5.5 for a typical value of EKF)

Initialize state of LTV-OBF model $x(k)$ w.r.t. the Commissioned data set $\mathcal{D}_k$ (See Section 4.3.3)
while MPC control is online **do**
Compute the steady-state null space M_ξ (i.e. Eq. (5.13)&(5.14))
Initialize state of LPV-OBF model w.r.t. the data set $\mathcal{D}_k$ (See Section 4.3.3)
Calculate LPV model coefficient w.r.t. the data set $\mathcal{D}_k$
Run EKF calculation to update the state of the LPV-OBF model $x(k)$(i.e. Eq.5.36)
Construct the MPC problem of Eq. (5.18)
Solve the MPC problem (Always solvable due to recursive feasibility Theorem 5.1)
Apply control action $u_{\mathrm{MPC}}(k)$
Update the data set $\mathcal{D}_k$ with the output $y(k)$
if Control Performance is not satisfying (e.g MSE of tracking performance, etc) **then**
Tune Q,R, and T matrices
Re-run LQR control synthesis (i.e. Algorithm 10)
Update P and K matrices
end if
end while

A small value of Q_E also means that we are also less confident in the prediction capability of our model.

5.7 Simulation study

The proposed control scheme is tested on a binary distillation column benchmark model that is based on a liquid-vapor flow configuration. The model is also used in Chapter 4 and is detailed in Skogestad (1997). A description of the benchmark model is firstly given and then followed by the steps mentioned in the Algorithms of Section 5.6. The goal of this study is to test the ability of the LPV-OBF MPC scheme to track the change in the system while maintaining a low deviation from the given reference point.

5.7.1 Distillation column case

A linearization of the model is established for the operating condition of 0.5 and 0.95 (mole fraction) of the bottom and top composition levels respectively, with corresponding liquid and vapor flows of 521 kmol/min (kilo-mole per minute) and 664 kmol/min. The sampling time of the system is chosen to be 5 minutes while the settling time of the system is 170 minutes (34 time steps). The MIMO LTI model in deviation variables is given as follows:

$$G(z) = \begin{bmatrix} \frac{0.001357z-0.0009633}{z^2-1.528z+0.5679} & \frac{-0.0009023z+0.000597}{z^2-1.528z+0.5679} \\ \frac{0.001174z-0.0009952}{z^2-1.528z+0.5679} & \frac{-0.0003762z+0.0002929}{z^2-1.528z+0.5679} \end{bmatrix}.$$

5.7.2 LPV identification and open-loop validation

This represents a 2x2 LTI system with liquid and vapor flow as the inputs (manipulated variables) and bottom and top composition as the output (controlled variables) respectively. The generated measurements from this system are corrupted by a discrete-time output additive white noise with *signal-to-noise ratio*[3] (SNR) of 15 dB. The LPV-OBF MPC scheme will be designed and commissioned on this system with $n_{\mathrm{g}} = 4$ (i.e. $n_{\mathrm{b}} = 2$ basis poles and $n_{\mathrm{u}} = 2$ input) basis functions that are generated from the poles of the system. This pole generating mechanism also means zero approximation error i.e. $\| \varepsilon_{\mathrm{n_b}}^{m,n} \|_{\mathcal{RH}_2} = 0$. After the commissioning of the MPC, the change in plant dynamics is induced as an effect of a rotation matrix:

$$G_{\mathrm{new}}(z) = \begin{bmatrix} \cos(p(k)) & -\sin(p(k)) \\ \sin(p(k)) & \cos(p(k)) \end{bmatrix} G(z), \tag{5.39}$$

where $-\pi/5 < p(k) < 0$ is the rotation coefficient and also the selected scheduling variable that drives the change in the system dynamics.

[3]The signal-to-noise ratio is defined as $\mathrm{SNR} := 10 \cdot \log_{10}\left(\frac{\|y-v\|_2^2}{\|v\|_2^2}\right)$.

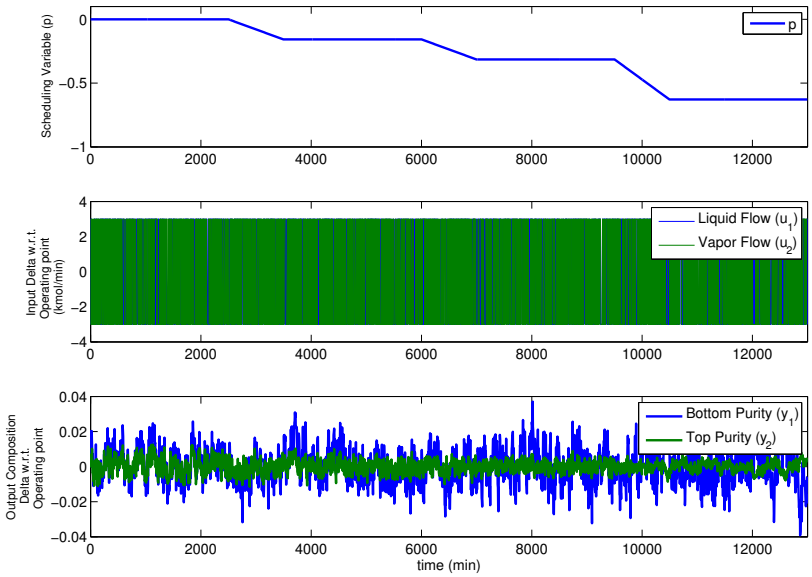

Figure 5.1: Scheduling variable and identification data set for both LPV identification approaches.

Two strategies to do LPV-OBF identification in the PEM setting are presented in Section 5.3 and Algorithm 8,9. In order to have a fair comparison between both approaches, we use the same data set for identification namely $\mathcal{D}_{\text{global}}$. The data set is obtained by exciting the system with PRBS input with a magnitude of $+-3$ kmol/min for 13000 minutes (217 hours) through different scheduling variables $p(k)$. The data set is depicted in Fig 5.1. The identification goal is to obtain $\{\vartheta_i\}_{i=1}^{n_\psi}$ as coefficient of linearly parameterized $\theta(p(k))$ using polynomial basis of $\{\psi_i(p(k))\}_{i=1}^{n_\psi}$. After obtaining the LPV model for both approaches, the model is validated on a separate data set $\mathcal{D}_{\text{val}}$ which is also used in the validation of LTV identification in the previous Chapter. The validation data set have a length of 23000 minutes (383 hours).

LPV-OBF Local approach

For the local approach, we are splitting the identification data set into 4 smaller batches namely $\mathcal{D}_{\text{local}}^{(1)}$,$\mathcal{D}_{\text{local}}^{(2)}$,$\mathcal{D}_{\text{local}}^{(3)}$, and $\mathcal{D}_{\text{local}}^{(4)}$ where each has 2000 minutes (34 hours) length of data. The local data set corresponds to 4 distinct operating points $\bar{p}^{(1)} = 0$, $\bar{p}^{(2)} = -\pi/20$, $\bar{p}^{(3)} = -\pi/10$, and $\bar{p}^{(4)} = -\pi/5$. For each data set, separate linear identifications (LTI-PEM) are used and the resulting BFR for each identification are in the vicinity of $98 - 99\%$. The coefficients of the LTI-PEM are then used to estimate the LPV model coefficient $\{\vartheta_s\}_{s=1}^{n_\psi}$ with a selected polynomial of

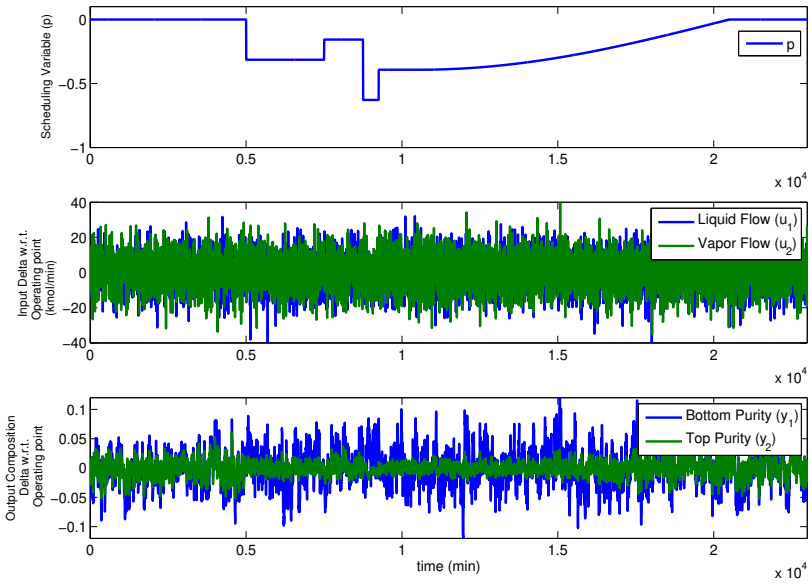

Figure 5.2: Scheduling variable and validation data set in the open-loop setting.

order 2 (i.e. $n_\psi = 3$). The estimated LPV coefficient $\{\vartheta_s\}_{s=1}^{3}$ for each output can be found in Appendix A.9.

LPV-OBF Global approach

For the global approach, we do direct identification LPV-OBF model coefficients using $\mathcal{D}_{\text{global}}$. The linear parameterization use up to 3rd order polynomial and result in $n_\psi = 16$ (since $n_{\text{g}} = 4$ is used). The estimated LPV coefficients $\{\vartheta_s\}_{s=1}^{16}$ can be found in Appendix A.9.

Validation result

The open-loop validation w.r.t. $\mathcal{D}_{\text{val}}$ is captured in Table 5.1. From this table, we can see that the global approach has slightly outperformed the local approach. Notice as well that the BFR validation error of the local approach is lower compared to the result obtained by the LTI-PEM of local identification. The loss of accuracy is not due to the selection of the polynomial parameterization but rather due to the transient dynamics that are captured in the validation data set. This is also the reason why the global approach gives better performance since the identification of the global approach takes into account the transient behavior captured in $\mathcal{D}_{\text{global}}$. Although the transient dynamics between identification and validation data sets are different, the validation result shows that the content is sufficient to

Table 5.1: Validation result for local identification and both LPV identification approaches.

	Bottom product composition (y_1)	Top product composition (y_2)
	BFR	BFR
Local approach	97.99 %	97.70 %
Global approach	98.34 %	98.52 %

Table 5.2: Closed-loop performance of the investigated MPC approaches with respect to the given reference ($r_1 = 0.02, r_2 = 0.98$).

	Bottom product composition (y_1)	Top product composition (y_2)
	MSE	MSE
Local approach	$1.4673e-06$	$2.7747e-06$
Global approach	$1.3466e-06$	$2.5228e-06$

explain the variation in system dynamics. The result also proves that polynomial parameterization is a correct choice for this usecase.

5.7.3 Closed loop experiment

With the parameters available from Section 5.7.2, the LPV-OBF MPC for each approach is commissioned on the system in a separate closed-loop simulation. The control task is to follow a set point of $r_1 = 0.02$ and $r_2 = 0.98$ for each of the output channels under the effect of the rotation coefficient that is depicted in Fig. 5.2. LPV-OBF MPC synthesis follows the algorithm described in Section 5.6 and for the controller of each case, we select the control-prediction horizon values of $N = 34$ which is based on the slowest step response of the system, while the control matrices are selected as

$$Q = I^{n_x \times n_x} \quad R = \begin{bmatrix} 1/521 & 0 \\ 0 & 1/664 \end{bmatrix} \quad T = 100 \cdot \begin{bmatrix} 1/0.05 & 0 \\ 0 & 1/0.95 \end{bmatrix} \tag{5.40}$$

The value of R and T correspond to the normalization of the magnitude of the inputs and outputs of the system while Q is set to be identity as recommended in the Algorithm 10. The P and K matrices for the LQR synthesis can be found in Appendix A.9.

For the EKF, two matrices which are the Q_E and R_E (of Eq.(5.36)) need to be selected before we can commission the MPC. The matrix R_E describes the confidence of your measurement while the matrix Q_E describes the confidence of the prediction. The EKF matrices are given as follows:

$$Q_E = 7.7458 \cdot 10^{-3}.I^{n_x \times n_x} \quad R_E = \begin{bmatrix} 1.3912 \cdot 10^{-2} & 0 \\ 0 & 7.7458 \cdot 10^{-3} \end{bmatrix}. \tag{5.41}$$

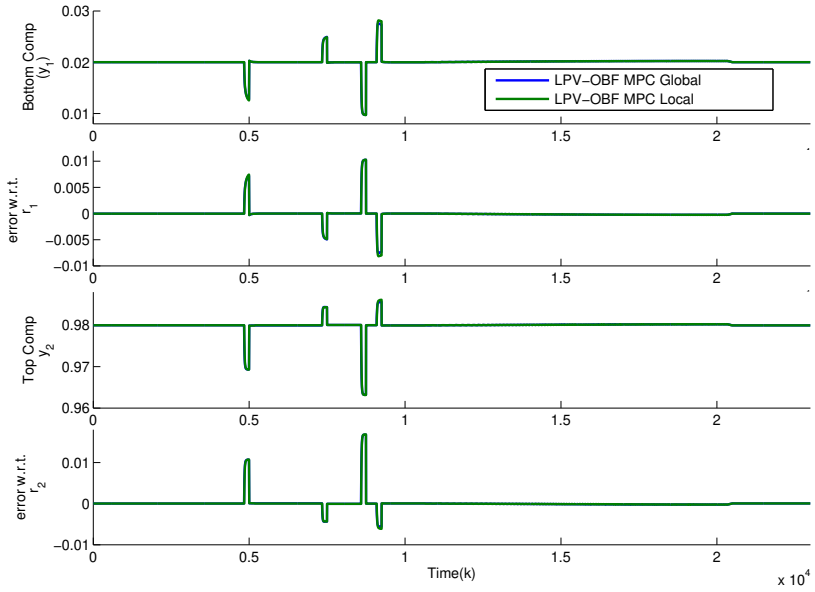

Figure 5.3: Tracking performance of both LPV-OBF MPC approaches under rotation scenario.

With both LQR and EKF matrices, each of the LPV-OBF MPC is commissioned to the system and the result of the closed-loop experiment can be seen in Fig. 5.3 and in Table 5.3. The result shows that both LPV-OBF MPC approaches can achieve the goal of tracking the given reference through the change in system dynamics. Also notice a very close performance of the local and global approaches, with slightly better MSE value for the global approach. This better performance can be better seen in the zoomed in version of the performance in Fig. 5.4 where a small offset can be seen during transient dynamics. It is expected since the global approach can capture the transient dynamics better than the local approach. Related to the stability of the LPV-OBF MPC, although not depicted in any figure, the value of $V_o(y_s - r)$ is zero for all time steps. This constant zero value is also expected due to the outstanding tracking performance of both LPV-OBF MPC schemes.

5.8 Summary

A parameter-varying MPC scheme that is based on an LPV-OBF prediction model is presented in this chapter. The prediction model describes variations in the dynamics of the system of interest that can be characterized by an external signal called the scheduling variable. Two LPV identification approaches are provided to identify the LPV-OBF model before the MPC is commissioned. The local LPV

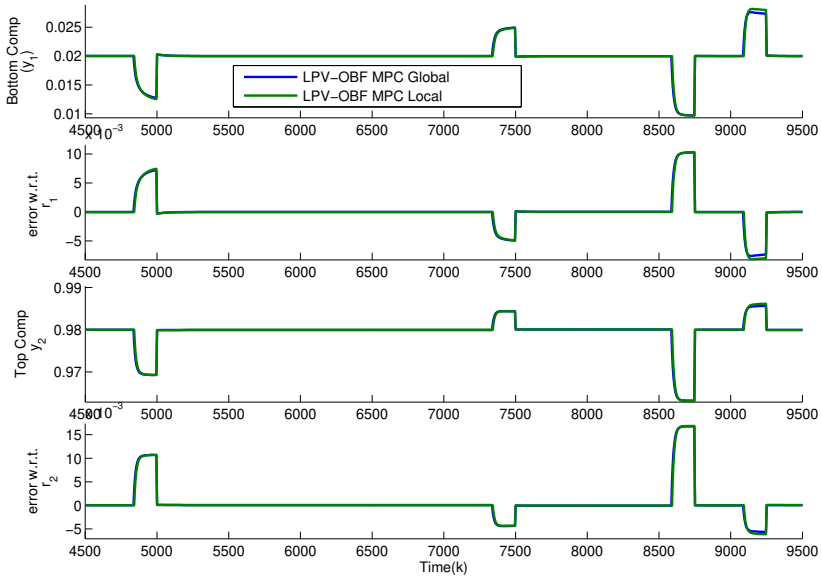

Figure 5.4: Zoom in version of Figure 5.3.

identification approach can be seen as an interpolation of the dynamical behavior of the system, while the global LPV identification approach is a direct identification method based on a single data set that is measured from the system. Afterwards, the LPV-OBF MPC scheme is formulated. The MPC scheme utilizes a designated steady-state target and extra penalty term for tracking purposes. The space of the steady-state pair is characterized by a vector which is used as an argument of minimization for the MPC problem. Such setting helps us in establishing feasibility and stability guarantees of the MPC scheme. In both the feasibility and stability theorems, it is shown that the effect of the parameter variation on the MPC scheme is minimal. The MPC scheme is aided by an EKF to address unaccounted changes in system dynamics from the identification of the LPV-OBF model. Lastly, by conducting a simulation study, we show that the proposed method can capture the parameter-varying dynamics of a given system and manage to achieve the goal of set-point tracking.

6 CHAPTER

Case Study

This chapter is devoted to demonstrate the proposed MPC schemes of this thesis in two simulated industrial case studies. The first case, a high purity distillation column system, is covered in Section 6.2. This system exhibits variations of the input-output dynamics under operating condition changes. In particular, where *directionality* effects become more dominant as one of the outputs reaches higher purity levels. The proposed LTV-OBF MPC and LPV-OBF MPC based controller design approaches of Chapter 4 and 5 are used to solve the reference tracking problem of the high purity distillation column over a designated operating regime. As a second case study, a dual distillation column system is investigated in Section 6.3. In this study, the column dynamics gradually drift from the model of the system that was initially identified at the time of commissioning the controller. Since such drifts cannot be characterized by any measured parameters, the LTV-OBF MPC scheme is applied in this case study. It is shown that the proposed LTV-OBF MPC scheme maintains the given set point despite the drift.

6.1 Introduction

Chemical processes often exhibit a significant nonlinear behavior when operated over a wide range of operating conditions. Despite the advances in model-based control technologies, it remains a challenge to realize high-performance operation of nonlinear chemical processes (in terms of product quality and process productivity) using a single *linear time-invariant* (LTI) model-based controller. For example, when a chemical process is operated under transient conditions (e.g., set-point changes and start-up procedures), the nonlinear behavior of the process becomes more dominant, which makes the use of a single LTI model inadequate to describe the system dynamics over the entire operating window. Distillation columns are a representative example of process systems that exhibit nonlinear dynamics and gain directionality in their operating window (Skogestad et al. 1988; Skogestad

and Morari 1988; Finco et al. 1989; Gokhale et al. 1996). In this chapter, we show that the proposed OBF-based MPC schemes are able to tackle the challenge to realize high-performance operation of industrial distillation column systems. Two case studies are presented on different type of distillation columns. The first case is a high purity distillation column which exhibit variations of the input-output dynamics when operated in the high-purity region. The second case is a dual distillation column system which is affected by an unknown dynamical drift after the controller has been commissioned.

Each distillation column case study is presented in separate sections where the following item are discussed:

- Problem setting of the case studies: Describing the background and underlying information of the system of interest, as well as the experimental setup and the control objective of the experiment.
- OBF modeling of the case studies : Step by step explanation of the OBF modeling procedure which consist of basis pole selection, required parameters for identification, and the resulting OBF-based model of the case studies.
- Control synthesis: Explaining the necessary ingredients and parameters to commission either an LPV-OBF MPC or an LTV-OBF MPC based on the identified model.
- Result and discussion: Presenting the results of the commissioned OBF-based MPC control and analyzing the behavior that can be observed in the closed-loop system.

6.2 Case Study: High-purity distillation column

6.2.1 Problem Setting

High-purity distillation columns are well-known for their *nonlinear dynamics* and *directionality characteristics*, which become more significant as the operating conditions approaches the *high-purity* region Jacobsen et al. (1991),Waller (2003). Due to directionality effects, the system response is dominated by the high-gain direction (i.e., only one product composition can be controlled effectively). The dynamics of the a distillation column can be described by a set of nonlinear, *differential algebraic equations* (DAEs), whose numerical complexity (in terms of the number of equations) can increase significantly with the number of theoretical trays, which can be in the order of hundreds in the high-purity case. The system of interest in this section is a DAE model of a distillation column which is described in the work of Skogestad et al. (1988).

The primary assumptions for the DAE model are as follows:

1. Phase equilibrium on each tray;
2. A binary mixture feed;

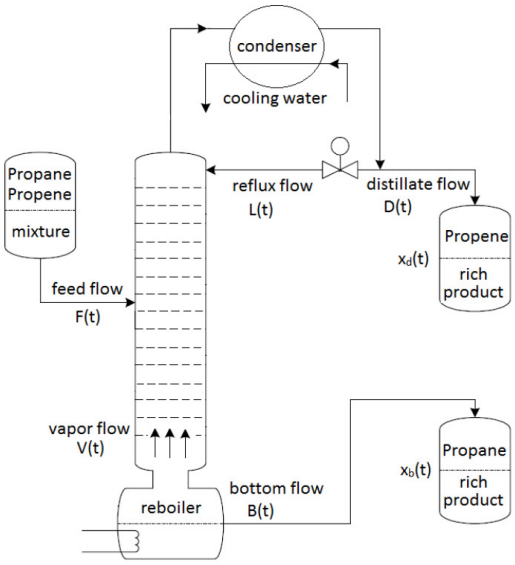

Figure 6.1: Schematics of a typical PP-splitter (binary distillation column).

3. Constant relative volatility along the column;

4. Constant molar flows;

5. Top and bottom flows are ideally controlled (i.e., changes of the vapor and liquid flows have instantaneous effect on the top and bottom flows).

The physical-chemical phenomena are expressed by a set of *differential algebraic equations* (DAEs), which describe the component concentrations, as well as the vapor and liquid flows along the distillation column. The following equations describe the component mass balances on the various trays that are numbered from the bottom tray b, through the feed tray f, and ends at the top tray d $(b, 2, \ldots, n, \ldots, f-1, f, f+1, \ldots, m, \ldots, d)$:

$$
\begin{aligned}
VE_{Top} &: \frac{d(M_d x_d)}{dt} = V_{d-1}y_{d-1} - L_d x_d - D x_d, \\
VE_{m} &: \frac{d(M_m x_m)}{dt} = V_{m-1}y_{m-1} + L_{m+1}x_{m+1} - V_m y_m - L_m x_m, \\
VE_{Feed} &: \frac{d(M_f x_f)}{dt} = F z_f + V_{f-1}y_{f-1} - L_{f+1}x_{f+1} - V_f y_f - L_f x_f, \\
VE_{n} &: \frac{d(M_n x_n)}{dt} = V_{n-1}y_{n-1} - L_{n+1}x_{n+1} - V_n y_n - L_n x_n, \\
VE_{Reboiler} &: \frac{d(M_b x_b)}{dt} = L_2 x_2 - V_b y_b - B x_b.
\end{aligned}
\tag{6.1}
$$

In (6.1), V_i is the molar flow of the vapor phase, y_i is the mole fraction of the vapor phase, L_i is the molar flow of the liquid phase, x_i is the mole fraction of the liquid phase, F is the feed flow, z_f is the mole fraction of the feed, B is the bottom product flow, and D is the top product (distillate) flow. Moreover, the equation consist of five separate parts that corresponds to the top tray, top section trays, feed tray, bottom section trays, and the bottom trays which. These parts are also known as a section in the *distillation column*. Parameter M indicates the molar holdups of the trays, the reboiler, and the condenser distinguished by the indices (the constant molar holdup value is equal to the liquid amount that can be contained in each trays).

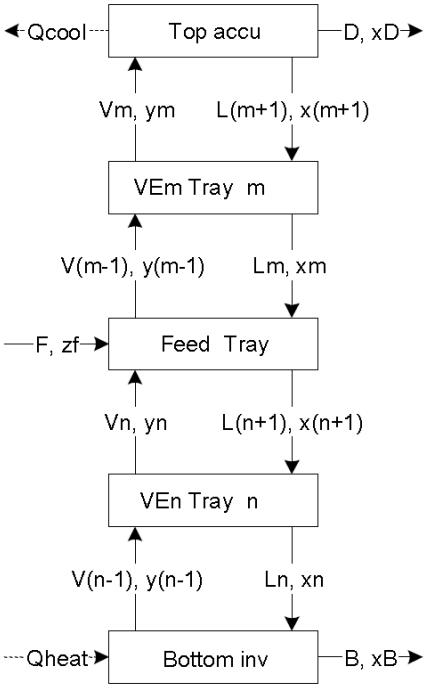

Figure 6.2: Flow diagram of the trays and the accumulators.

It is often assumed that the vapor and liquid flows are constant on each section of the distillation column:

$$\begin{aligned} V_m &= V_n + (1 - q_f)F, \\ V_n &= V_b, \\ L_m &= L_d, \\ L_n &= L_m + q_f F, \end{aligned} \tag{6.2}$$

where q_f is the fraction of liquid in the feed. In reality, the vapor flow depends on the reboiler heat, and the liquid flow depends on the reflux rate in the distillation

Table 6.1: Settings of the high-purity distillation column.

N_{T}	Number of trays	110
N_{F}	Feed stage location	39
α	Relative volatility	1.12
F	Molar feed flow	215 kmol/min
x_{f}	Mole fraction of the feed	0.65
q_{f}	Liquid phase fraction of the feed	1.0
M	Molar holdup (all trays)	30 kmol

tank. However, since we assume that the distillate and bottom flows are ideally controlled, instant change on heat and reflux rate have an instantaneous impact on the vapor and liquid flows. Due to this reason, these flows (L and V) are used as the input channels for the model, while the output channels will be the top and the bottom products composition (x_{d} and x_{b}), and feed properties such as flow, liquid fraction, and mole fraction will act as disturbances.

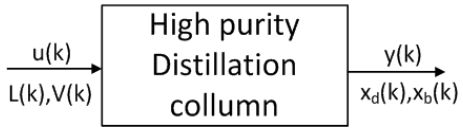

Figure 6.3: Input-Output diagram of the system.

The liquid flow rate L and the vapor flow rate V (manipulated through the reflux rate and re-boiler duty, respectively) are used as the manipulated variables to control the operation of the high-purity distillation column (i.e., $u_1(k) = L(k)$ and $u_2(k) = V(k)$). The system outputs consist of the composition of top (x_{d}) and bottom (x_{b}) products (i.e., $y_1(k) = x_{\mathrm{d}}(k)$ and $y_2(k) = x_{\mathrm{b}}(k)$). The resulting distillation column model describes a large-scale (110^{th} order), nonlinear, 2×2 multi-input multi-output system. The parameters of the high purity distillation column under study are given in Table 6.1 and the anatomy is depicted in Fig. 6.1.

The operating region of distillation column describe the variation of the dynamic behavior of the system. The variables that can describe such a variation are the top and bottom product compositions

$$p(k) = \begin{bmatrix} x_{\mathrm{d}}(k) & x_{\mathrm{b}}(k) \end{bmatrix}^{\top}.$$

The operating region is selected such that it entails a large set of local operating points described by the top and bottom compositions in the region of $\mathbb{P} = [0.95,\ 0.995] \times [0.02,\ 0.1]$. These compositions also serve as the scheduling variable p for the LPV-OBF MPC scheme.

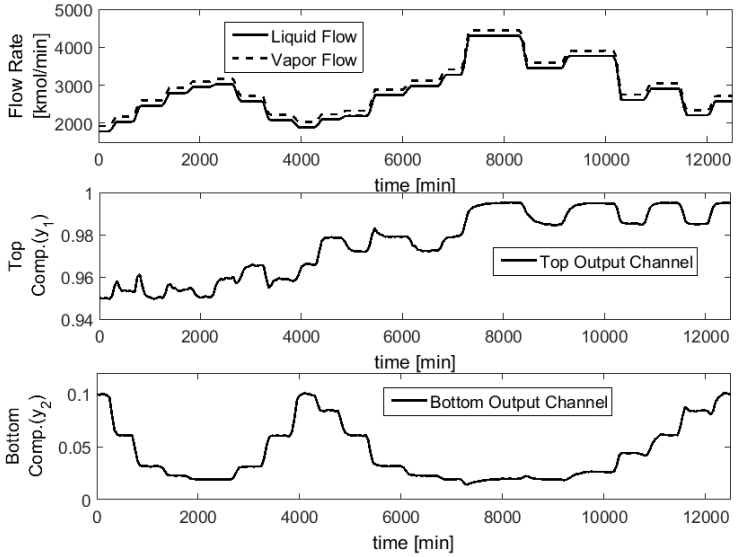

Figure 6.4: Applied excitation signals and measured responses in $\mathcal{D}_{\text{global}}$.

Experimental setup

The core element of the experimental setup for this section is the first principle model of the high purity distillation column. The first-principle model is simulated in continuous-time, while discrete-time input/output data is collected with a sampling time $T_{\text{s}} = 5$ min. This time is chosen 20 times faster than the time constant of the fastest step response of the system for the operating region under investigation (i.e. $\mathbb{P} = [0.95,\ 0.995] \times [0.02,\ 0.1]$). The inputs of the system are manipulated through zero-order-hold actuation synchronized with respect to the sampling time. The generated measurements are corrupted by a discrete-time output additive white noise v with a *signal-to-noise ratio*[1] (SNR) of 15dB. This is a realistic noise level in industrial practice. This first principle model is used in two experiments: an open-loop experiment and a closed-loop experiment.

The open-loop experiment is needed to generate measurement records to accomplish the OBF modeling. In this experiment, two data sets are generated where one serve as the identification data set and the other is used for validation purposes. The first data set $\mathcal{D}_{\text{global}}$ consist of $N = 2500$ samples while the second data set $\mathcal{D}_{\text{val}}$ consists of $N = 6000$ samples. In the real world, this corresponds to 8.7 and 20.8 days of experimentation time. Such a lengthy experiment can either be conducted in a continuous manner or in terms of batches of data depending on the status and usage of the distillation column system. In this experiment, both data sets are continuously generated using an input signal, see Fig.6.4 and Fig.6.5, which were designed to excite the transient behavior of the system when visiting

[1]The signal-to-noise ratio is defined as $\text{SNR} := 10 \cdot \log_{10}\left(\frac{\|y-v\|_2^2}{\|v\|_2^2}\right)$.

several operating points of its operating region. This input signal is a combination of a deterministic component added to a white noise with uniform distribution $\mathcal{U}(-0.5, 0.5)$ corresponding to a standard deviation of $1/\sqrt{12}$. The white noise on the input is intended to excite the "linear" behavior around the operating points.

For the closed-loop experiment, the first principle model is operated with an MPC controller to track a given reference trajectory or output specs within the operating region under investigation. The combination of operating points that were tracked are as follows:

$$\begin{aligned} r_1 &= [0.96; 0.07], \\ r_2 &= [0.98; 0.07], \\ r_3 &= [0.98; 0.05], \\ r_4 &= [0.95; 0.08]. \end{aligned}$$

Each of these references is tracked for 6000 minutes before moving to the subsequent reference. The to be commissioned controller need to ensure the actuation constraints of

$$u_{\min} = [1500, 1500] \text{ kmol/min}; u_{\max} = [5000, 5000] \text{ kmol/min}.$$

Remark 6.1 *The identification of the high-purity distillation column can be performed under closed-loop circumstances, where an operational MPC controller and least-costly experiment design can minimize the loss in production (see Bombois and Scorletti (2012); Larsson et al. (2013)). However, to preserve the simplicity of the discussion, closed-loop identification is not considered in this work.*

6.2.2 OBF modeling of high purity distillation column

There are two major steps of OBF modeling as presented in the earlier chapters of this thesis. As presented in Chapter 3 the first step is the selection of OBF poles while the second step is the choice of identification parameters for each of the LTV-OBF and LPV-OBF model identifications. The OBF poles need to be selected such that the OBF model can describe the variation of the linear dynamics of the system over the operating region under investigation. A group of local LTI models is necessary for this purpose. The second step, presented in Chapter 4 and 5 is the selection of the identification parameter for each of the LTV-OBF and LPV-OBF model w.r.t. identification data set. The resulting identified model can then be validated on a validation data set.

Estimation of local LTI models

For the identification of the local LTI models of the system, we split the identification data set $\mathcal{D}_{\text{global}}$ into 21 groups. These groups are denoted by $\mathcal{D}_{\text{local}}^{(\tau)}$ with $\tau = 1, \ldots, 21$ where each has $N = 80$ samples. From these data sets, LTI models of the local system behavior are estimated using an *output-error* (OE) noise model

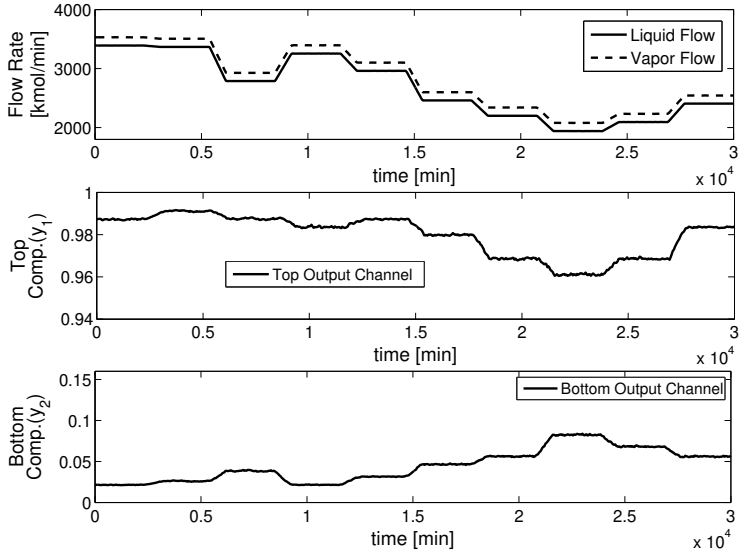

Figure 6.5: Applied excitation signals and measured responses in $\mathcal{D}_{\text{val}}$.

.

structure. In particular, the models have been estimated using *canonical variate analysis* (CVA) based subspace identification (using the `n4sid` implementation in MATLAB) and the orders $(n_{\text{a}}, n_{\text{b}})$ of the OE models have been chosen to be $(2, 2)$ based on BIC-based cross-correlation analysis conducted on the available local data sets Ljung (1999).

The resulting models have been evaluated in terms of the *best fit rate* (BFR) Ljung (2006)

$$\text{BFR} = 100\% \cdot \max\left(1 - \frac{\|y(k) - \hat{y}(k)\|_2}{\|y(k) - \bar{y}\|_2}, 0\right), \tag{6.3}$$

where $\bar{y}$ is the mean of the noise-free output y of the original system and $\hat{y}$ is the simulated output of the model calculated on validation data. The BFR is computed on a 80 samples long step-response (separate step test for each transfer channel with amplitude $5 \cdot 10^{-3}$ divided by the local DC gain) data generated by the linearization of the first principle model at the corresponding operating points. The average value of BFR from all of the 21 identified local models is $(94.95\%, 93.47\%)$ for $u_1 \to (y_1, y_2)$ and $(95.14\%, 93.33\%)$ for $u_2 \to (y_1, y_2)$.

Pole selection for the OBF model

By using the information of pole location from the collected local LTI models, we can start the OBF pole selection procedure. First step is to select the configuration of real and complex conjugate OBF pole w.r.t. the observed the distribution of the local model poles in the unit disk (depicted in Fig. 6.6). From the distribution we can see that the local models consists of real poles which can be roughly

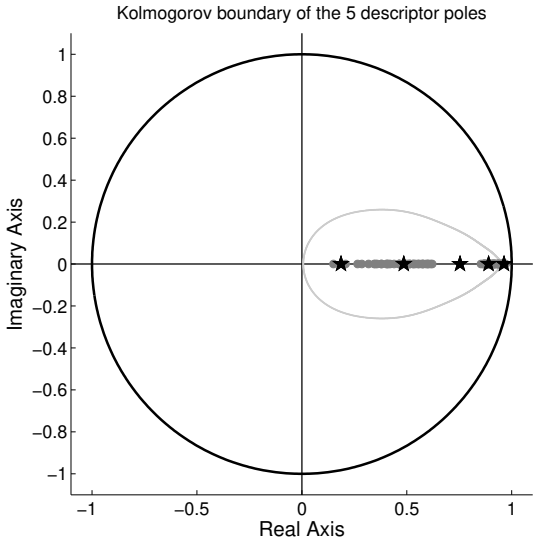

Figure 6.6: Results of the basis selection: sampled poles (○), resulting pole locations of the basis (★), and the corresponding perimeter line (bold grey).

separated in 3 groups. Hence, pole configuration of 3, 5, and 7 real poles are possible candidate for OBF pole. Since the number of basis is considered to be small and moderate, SQP based pole selection algorithm (See Sec 3.4.1 for details) is the preferred selection method. This methodology guarantees optimality while still maintains tractable computation for low to moderate number of OBF pole configurations. We then compare the normalized upperbound $\tilde{\gamma}_{n_\mathrm{b}}$ (proposed in Section 3.6) and the result is shown in table 6.2. From this result, we can see that $n_\mathrm{b} = 5$ with the corresponding set of OBF poles of

$$\{\lambda_l\}_{l=1}^{5} = \{0.3745 \;\; 0.6273 \;\; 0.7127 \;\; 0.8597 \;\; 0.8871\}$$

gives us the lowest normalized bound compared to the other pole configurations and hence gives optimal approximation vs complexity tradeoff. The pole location and the corresponding perimeter line[2] are depicted in Fig. 6.6. This result implies that (i) the selected basis functions have a small representation error w.r.t. the local LTI models and (ii) further reduction of the error introduced by the series expansion would require a significantly larger number of basis poles, which only have a relatively small benefit for the local models identified at the boundary of the operating region. Hence, we can use the aforementioned set of poles as the OBF pole for the LTV-OBF and LPV-OBF models of the distillation column.

Identification of LTV-OBF and LPV-OBF models

In Chapter 4, we presented two strategies to do iterative identification of the LTV-OBF model. These are the *Recursive Least square* (RLS) and the *weighted least square*

[2]Elements on the unit disc with equal value of γ from a given basis poles

Table 6.2: Comparison of the normalized upperbound $\tilde{\gamma}_{n_\mathrm{b}}$ for selected pole configurations.

	3 real	5 real	7 real
Normalized upperbound $\tilde{\gamma}_{n_\mathrm{b}}$	0.384	0.210	0.265

(WLS) methods. Both strategies require us to select the identification parameters or weights in which the guideline is presented in Section 4.3.6. Both have the same purpose to allow adaptation of a linear model with little information on future variation of the to be controlled system. Since we have shown in Section 4.8 that the performance for well-tuned RLS based and WLS based LTV model are comparable, we only use the RLS based LTV-OBF models since the selection of its weight is more straight forward. Based on the measurement data $\mathcal{D}_{\text{global}}$, we found the weight of $W_{\mathrm{RLS}} = 0.945$ corresponds to the minimal BFR (i.e. Eq. 6.3). The validation results for LTV-OBF model is presented together with LPV-OBF model in figure 6.7.

Two strategies to do the identification of the LPV-OBF model are presented in Chapter 5. These strategies are the local and global approaches. The latter tend to be better at capturing the varying dynamics of the system compared to the local approach. Since we have the identification data set $\mathcal{D}_{\text{global}}$ which contains the valuable information on the transient behavior of the system, we only use the global approach to do LPV-OBF model identification. The parametrization of model coefficients (5.8) is done using a 2-variable polynomial function of order n (i.e., $\Psi_s(p(k)) = p_1^i(k)p_2^j(k)$ such that $i, j \in \mathbb{I}_0^n$, $i \cdot j > 0$ and $s = i \cdot (n+1) + j$). By conducting a simple trial and error experiment with an increasing polynomial order, the value of $n = 3$ has been chosen for the LPV-OBF model since increasing the order bring less improvement while rapidly increasing complexity of the model.

The validation results for both LTV and LPV OBF models w.r.t. validation data set $\mathcal{D}_{\text{val}}$ are presented in Fig. 6.7 and Table 6.3 where the *mean squared error* (MSE)

$$\mathrm{MSE} = \|y(k) - \hat{y}(k)\|_2^2, \tag{6.4}$$

and the BFR of the simulation error are provided for quantitative comparison purposes. From these results, we can see comparable identification results with the LPV-OBF model slightly outperforming the LTV-OBF model. This is expected since the LPV model is more well-equipped to describe the variation of system dynamics which can be explained or driven by the scheduling variable. However, we see a slight offset on the LPV model validation result (with the magnitude of $\leq \pm 1.10^{-3}$) that is observed in time span of $t = 6000\ m$ until $t = 13000\ m$ and after $t = 26000\ m$ in the figure of error w.r.t. y_1. The offset occurs since the operating point in the validation data set are not exactly equal to the operating points used in the identification data set. This intermediary point cannot be perfectly described by the selected 3rd order polynomial. As for the LTV-OBF model result, we can see more variation in the model output since the recursive estimation is

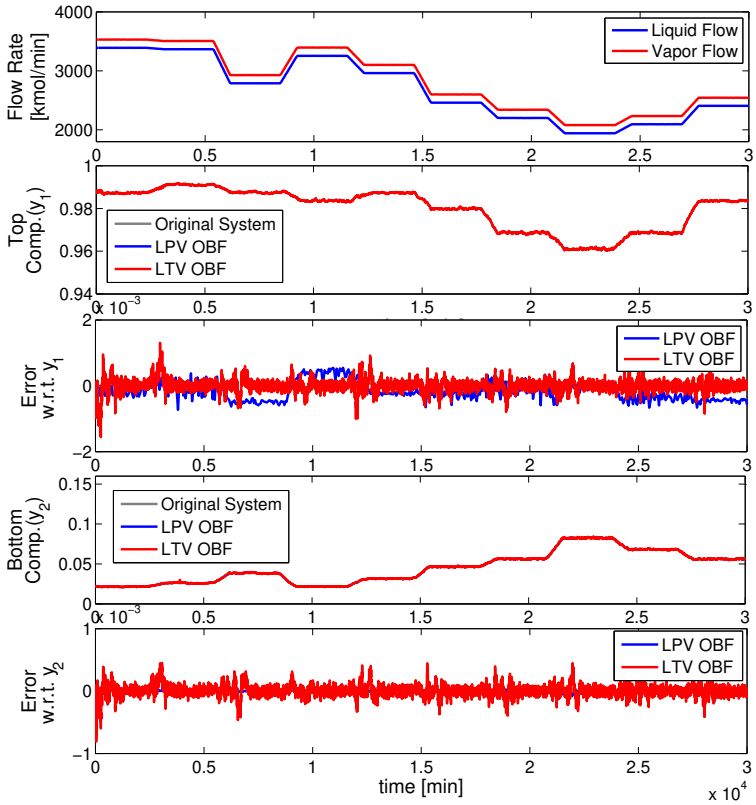

Figure 6.7: Validation results of the identified LPV-OBF and the LTV-OBF models using $\mathcal{D}_{\text{val}}$.

Table 6.3: BFR and MSE of LPV-OBF and LTV-OBF model w.r.t. validation data $\mathcal{D}_{\text{val}}$.

		LTV Model	LPV Model
y_1	BFR	96.89%	97.68%
	MSE	$1.02 \cdot 10^{-7}$	$5.14 \cdot 10^{-8}$
y_2	BFR	98.90%	99.90%
	MSE	$9.07 \cdot 10^{-8}$	$3.79 \cdot 10^{-10}$

affected by the measurement noise. Since both OBF models yield high BFR validation results, we are confident to use the LTV-OBF and LPV-OBF model for each of their corresponding MPC schemes.

6.2.3 Control synthesis

After we have obtained the LTV and LPV model at hand, we can start synthesizing the MPC. The proposed LTV-OBF MPC scheme and synthesis are described in the algorithms of Section 4.7 while the LPV-OBF MPC scheme is described in Section 5.6. The goal for both control schemes is to maintain reference tracking through 4 selected operating points as mentioned in the problem setting section. Essential steps to synthesize both the LTV-OBF MPC and the LPV-OBF MPC as well as their key control parameters are given in this section.

LTV-OBF MPC synthesis

The synthesis of the LTV-OBF MPC scheme start with Algorithm 6 and followed with Algorithm 7. These algorithms requires the control matrices (Q and R) and prediction-control horizons N. The main purpose of the control matrices is to put more weight on a particular output-input channel. These matrices also serve as the tuning parameter that can be used to configure the control performance of the closed-loop system. We use a value of

$$Q = \begin{bmatrix} 1/0.965 & 0 \\ 0 & 1/0.065 \end{bmatrix} \quad R = \begin{bmatrix} 1/3250 & 0 \\ 0 & 1/3250 \end{bmatrix} \tag{6.5}$$

which correspond to the normalization of the magnitude of the input and output of the system. The normalization also meant to give equal importance for both output and input channels.

The value of Q and R matrices, along with the set of possible model coefficients Θ (Eq.(4.19)), will influence the existence of stabilizing LQR controller K and also the invariant set ($\mathcal{X}_f$). These two elements are of paramount importance to the recursive feasibility and stability of the MPC scheme. The reason is the stability that is attached to the existence of stabilizing LQR controller and the corresponding invariant set. For the LTV-OBF case, this condition needs to be achieved for

all possible model parameter θ_k that is recursively updated in the closed-loop setting (See Section 4.6 for details). The LQR is synthesized by solving the LMIs of (Eq.(4.58))

$$\begin{pmatrix} S & (AS+BT)^\top & S\tilde{\theta}_i^\top & T^\top \\ AS+BT & S & 0 & 0 \\ \tilde{\theta}_i S & 0 & Q^{-1} & 0 \\ T & 0 & 0 & R^{-1} \end{pmatrix} \succeq 0, \tag{6.6}$$

for each of the vertices $\tilde{\theta}_i$ of polytope approximation of model set Θ (Eq.(4.18)). As described in the algorithm, we also inject uniform white noise of $\mathcal{U}(-0.5, 0.5)$ on top of the control action of the MPC. The purpose of this extra excitation is to not only maintain the persistency of excitation of the data for model estimation but also to define the set of possible model coefficients Θ in which the LQR controller is synthesized. The LQR control remains valid if the evolution of model coefficient θ_k remains inside of the polytope. As indicated in Algorithm 7, when the identified model travels outside this polytope, then we need to redo the LQR synthesis. A simple convex hull check can be done to check if θ_k remains inside the polytope. The vertices $\{\tilde{\theta}_i\}_{i=1}^n$ that are used for LQR synthesis as well as the solution of the LMI (P and K matrices) can be found in Appendix A.10.

Note that the evolution of model coefficient θ_k also related to the condition (Eq.(4.53)) which is the last element of the stability of the LTV-OBF MPC scheme (See Theorem4.4):

$$\theta_{k+1} Q_{k+1}(i) \theta_{k+1}^\top \preceq \theta_k Q_k(i) \theta_k^\top \quad \forall k \in \mathbb{Z}, i \in \mathbb{N}. \tag{6.7}$$

As described in the Section 4.7, the condition can be monitored to show whether we can attain close loop stability.

For the prediction-control horizon of the MPC, as described in Section 4.5, our proposed MPC scheme denotes the horizon as a single term N. The length of the time horizon will affect the calculation time to solve the MPC problem (4.45). The length of time horizon will affect the calculation time to solve the MPC problem (4.45). Sensible selection would be more than the settling time of the LTV-OBF model, but not long enough such that it burdens the computation of the MPC problem. For these reason, we select $N = 20$ samples (i.e. 100minutes) which is slightly more than the average step response of the distillation column system for the operating region under investigation (i.e. $\mathbb{P} = [0.95,\ 0.995] \times [0.02,\ 0.1]$).

LPV-OBF MPC synthesis

The synthesis of the LPV-OBF MPC scheme follows the Algorithm 10 and 11. These algorithm requires the control matrices (Q, R, and T), MPC horizons N, the steady-state null space M_ξ M_ξ, and a locally stabilizing LQR controller. For the control matrix of LPV-OBF MPC, we select:

$$Q = I^{n_{\mathrm{x}} \times n_{\mathrm{x}}} \quad R = \begin{bmatrix} 1/3250 & 0 \\ 0 & 1/3250 \end{bmatrix} \quad T = 100 \cdot \begin{bmatrix} 1/0.965 & 0 \\ 0 & 1/0.065 \end{bmatrix}, \tag{6.8}$$

while the MPC horizon is selected to be $N = 20$ samples. Notice that the choice of the R matrix and the N parameter are the same as for the LTV-OBF case due to similar usage of this two parameters. The value of $Q = I^{n_x \times n_x}$ should be selected in most cases since Q in the LPV-OBF case affect different state elements where each correspond to different OBFs (See Eq.(5.1)). This lead to less intuitive tuning parameter compared to the LTV-OBF case since there is no physical interpretation of the state for the LPV-OBF model. It is also possible to scale down the Q matrix w.r.t. the control action matrix R to make the control action more aggressive. The role of weighting the output channels is now governed by matrix T. Note that the matrix T does not exist in the LTV-OBF case (see Section 5.4.2 for details) and this matrix need to be selected to be significantly bigger than matrix Q and R. The reason why we need a big matrix T is to strongly affect the LPV-OBF MPC cost function (i.e. Eq.(5.16)) such that it gravitates towards reference tracking via the tracking cost function:

$$V_o(y_s - r) = \|y_s - r\|_T^2, \tag{6.9}$$

where y_s is the steady state output and r is the reference. The value of y_s is governed by the coefficient matrix of the LPV-OBF model (See Eq.(5.15)) while the target steady-state x_s is selected from the steady-state null space M_ξ by the variable ξ which is one of the arguments of the LPV-OBF MPC cost function.

For the LQR synthesis, although the MPC is synthesized for LPV-OBF model, there is actually no varying terms in the stability guarantee (See Theorem 5.2):

$$(A + BK)^\top P(A + BK) - P \succeq Q + K^\top RK. \tag{6.10}$$

Hence only a single LQR synthesis problem needs to be solved to obtain P and K. The calculated value of P and K is shown in the Appendix A.11.

Besides the controller part, as described in the Algorithms in Section 5.6, there are two extra elements that are not directly linked with the MPC scheme but will inherently affect the LPV-OBF model. These two elements are the information of scheduling trajectory up to N step ahead ($p(k + N)$) and the *Extended Kalman Filter* (EKF) for the LPV-OBF model. It is mentioned in the problem settings that the top and bottom composition define the system dynamics. Since our goal is to track the reference for both of these outputs, we can directly use the reference as the scheduling variable of the LPV-OBF model. For the EKF, two matrices which are the Q_E and R_E (of Eq.(5.36)) need to be selected before we can commission the MPC. The matrix R_E describes the confidence of your measurement while the matrix Q_E describes the confidence of the prediction. The EKF matrices are given as follows:

$$Q_E = 7.3691 \cdot 10^{-5}.I^{n_x \times n_x} \quad R_E = \begin{bmatrix} 7.3691 \cdot 10^{-5} & 0 \\ 0 & 1.3581 \cdot 10^{-4} \end{bmatrix}. \tag{6.11}$$

Notice that we select the entries of R_E to be equal to the variance of the measurement noise (v_1 and v_2), while the Q_E matrix has the lowest value of R_E for each of the elements of this matrix. Reason of the Q_E matrix selection is the good fit result in the identification step (i.e. Table 6.3). If we notice unsatisfactory control performance, we can lower the value of Q_E. The relative value between Q_E

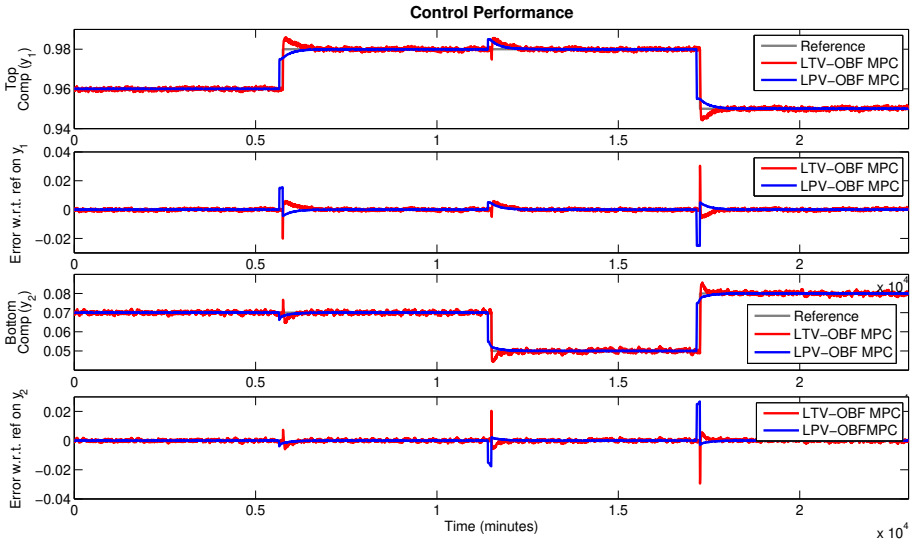

Figure 6.8: Tracking performance of the LTV MPC and the LPV MPC through all tracked operating points.

and R_E is the defining condition for the EKF and a low Q_E value also means that we are less confident in the prediction capability of our model.

6.2.4 Results and discussion

After we synthesize both the LTV-OBF MPC and LPV-OBF MPC, we can use the MPCs to control the first principle model of the distillation column. The goal is to track the reference through a selected combination of operating points as mentioned in the problem setting section. The resulting tracking performance is captured in Figure 6.8 while the computed MSE can be found in Table 6.4. By looking at Figure 6.8, we can say that both controllers achieve tracking performance with the LPV-OBF MPC slightly outperforms the LTV-OBF MPC. This result is understandable since the fit ratio of the LPV-OBF model also outperforms the LTV-OBF model (See table 6.3). Judging from this result, we do not need to change our control parameters and matrices for either of the controllers. However, If we look closely at this figure, several items can be observed:

- LPV-OBF MPC output already start moving to the next operating points even before the reference moves to the next operating points
- LTV-OBF MPC output has higher variance compared to LPV-OBF MPC
- LTV-OBF MPC output has bigger transient behavior compared to LPV-OBF MPC

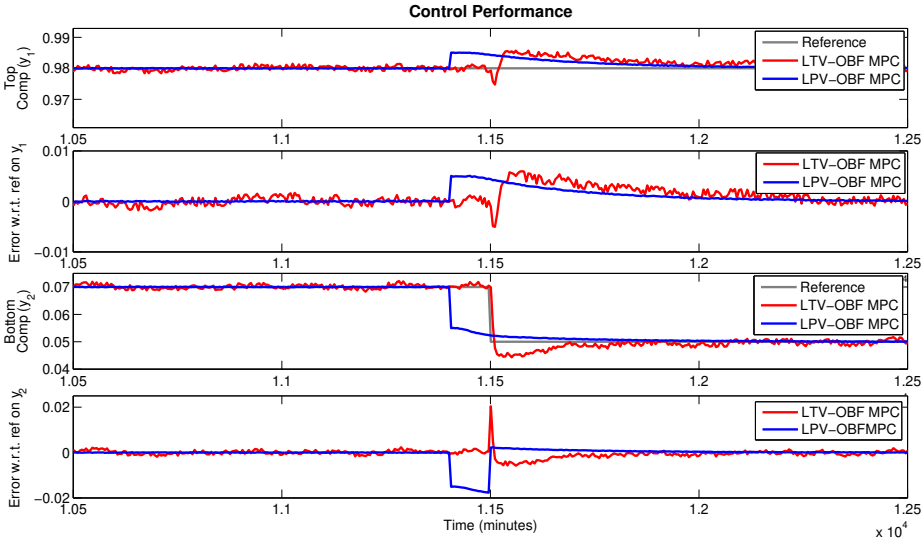

Figure 6.9: Tracking performance at the point of interest.

Table 6.4: Control performance of LTV-OBF and LPV-OBF MPC w.r.t. reference.

		LTV-OBF MPC	LPV-OBF MPC
y_1	MSE	$1.8014 \cdot 10^{-6}$	$1.3554 \cdot 10^{-6}$
y_2	MSE	$1.3852 \cdot 10^{-6}$	$1.0075 \cdot 10^{-6}$

These items are more apparent in the zoomed version of the result that is depicted in Figure 6.9.

The first item is an expected behavior due to the target output y_s (Definition 5.3) of the MPC cost function is described as $y_s = C(p(k+N))x_s$. Since we use the reference as our scheduling variable (i.e. $p(k) = r(k)$), then the targeted output of the closed-loop system at time k is the reference at time $k+N$. Due to this behavior, we can say that the LPV-OBF MPC is an *anticipative* controller. We can delay this anticipation by lowering the value of N. The only expected drawback is potentially more aggressive transient behavior of the closed-loop system due to the shorter horizon. Alternatively, we can modify the definition of the target output to be dependent on the scheduling variable at time k. From this modification, we can expect a closer closed-loop system behavior to the one that is controlled by the LTV-OBF MPC.

The second point of interest, the higher output variance of the closed-loop system output, can be explained due to the injected noise in the input to maintain the iterative identification of the LTV-OBF model. If the variance is not satisfactory and leads to deterioration of tracking performance, then we can lower the injected noise. But this also means that the covariance matrix will be bigger and hence might lead to difficulties in the LQR control synthesis.

The third point of interest, the slower transient behavior of the LTV-OBF model, is simply the result of the LTV-OBF model trying to find a new coefficient θ_k when the reference jumps to the new operating points. The evolution of model coefficient of LTV-OBF model is also part of the stability that is written in Theorem 4.4 (i.e. the condition of (4.53)/(6.7)).

In order to show the stability of the closed loop system, as described in Section 4.7 and 5.6, we monitor the evolution of

$$x^\top(k+1)\theta_{k+1}Q_{k+1}(i)\theta_{k+1}^\top x(k+1) \leq x(k)\theta_k Q_k(i)\theta_k^\top x(k) \quad \forall k \in \mathbb{Z}, i \in \mathbb{N}. \quad (6.12)$$

for LTV-OBF MPC case and the target cost function of $V_o(y_s - r)$ for LPV-OBF MPC case. The evolution for these parameters can be observed in figure 6.10.

For the LTV-OBF MPC case, we see that there are three jumping points where the stability condition is also jumping. These jumping points exactly correspond to the steep change of the coefficient θ_k. For this case, the steep change even drives the coefficient to venture outside the polytope approximation of the model set Θ. This triggers the necessity of redoing LQR control synthesis (See Algorithm7). Since a stabilizing LQR is found, the stability of the closed-loop system is then re-guaranteed, and the stability condition decay to the reference state x_{rk}. Note that the non-smoothness of the LTV-OBF stability parameter is due to the measurement noise and the induced excitation to maintain persistent excitation for system identification. The non-smoothness does not impact the stability of the closed-loop system.

For the LPV-OBF stability, we see a constant value of 0 throughout the experiment. This can be interpreted that the targeted reference r can be fully tracked by the target steady-state output y_s and the change of system dynamics w.r.t. the change operating points can also be captured by the LPV-OBF model.

From these observations, we can conclude that the LPV-OBF MPC scheme in this scenario outperforms the LTV-OBF MPC scheme in both tracking performance and guarantee of stability for the high purity distillation column case.

6.3 Case Study: Dual distillation columns

6.3.1 Problem Setting

In the second case study, we use a simulated industrial example of a dual distillation column system. Similar to the first case study, the main purpose of the dual distillation column is to separate chemical products. However, instead of splitting into binary products, the additional column act as an intermediary outlet that can produce a middle cut with a designated purity level. The diagram of the dual distillation columns can be found in Figure 6.11.

For this study, two identified models of the system from a different moments in time are provided by the industry. The separate identification instances correspond to the initial commissioning of the *Advanced Process Control* (APC) and re-commissioning of the APC. Each of the two identified models are 5×5 MIMO discrete *Finite Input Response* (FIR) models of order 300 with sampling time $T_s = 1$

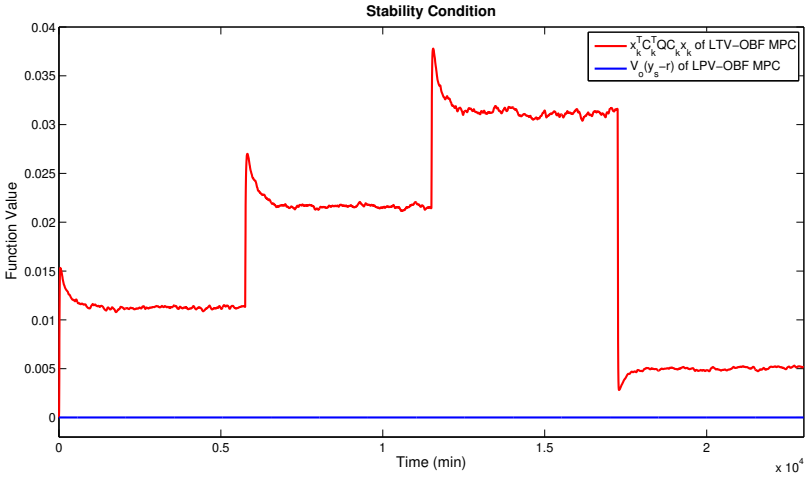

Figure 6.10: Stability condition for LTV-OBF MPC and LPV-OBF MPC scheme.

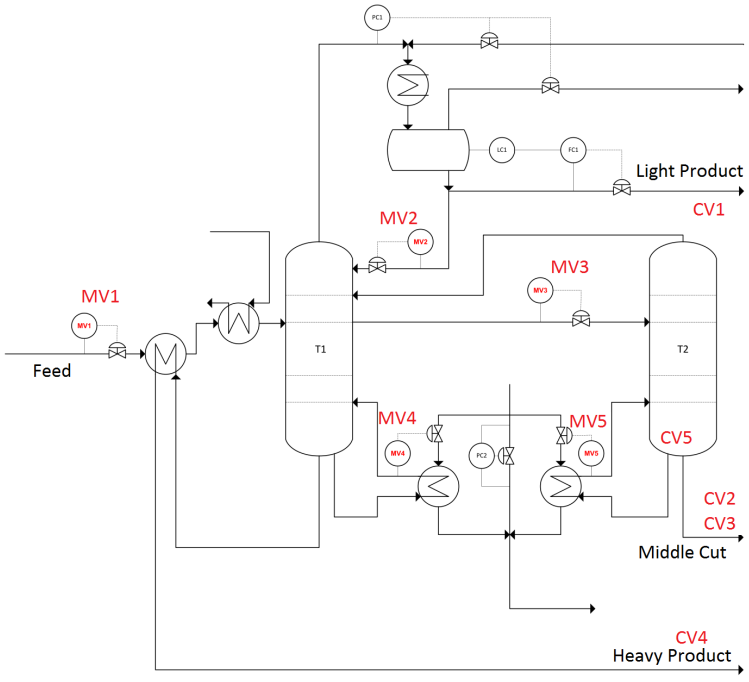

Figure 6.11: Operational flow diagram of the studied of dual distillation columns.

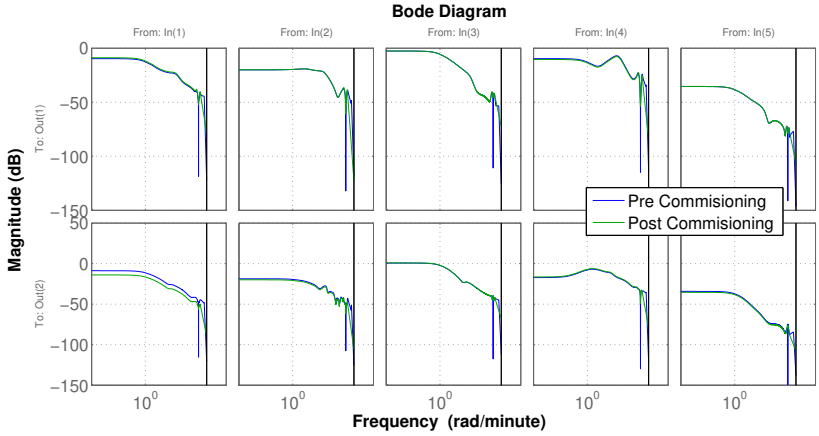

Figure 6.12: Frequency Response of dual distillation column FIR model

minute. It is not necessary to use all of 5×5 FIR model since the output of interest (Controlled variable) for the case study are the light product (CV1) and the middle cut (CV2). Hence, only the corresponding 2x5 FIR models are used for this case study. This also means that our system is non-square in this case study. The frequency responses for each model are given in Figure 6.12.

If we look at Figure 6.12, the differences between the frequency responses of the two models already give a hint why the APC needed to be re-commissioned. Commonly used linear APC will have difficulty maintaining the performance (e.g. reference tracking) when the controlled system changes/drift during the APC lifetime. This drift frequently comes due to the wear of the system actuators (pumps, valve, etc) and or change in the related thermochemical processes (Material variation, seasonal change, etc). The inevitable performance deterioration due to such drift is a prominent problem in the industry. Hence, our goal is to show that the proposed MPC schemes in this thesis can maintain control performance through the drift and consequently avoid the necessity of APC re-commissioning. Since the drift cannot be characterized by any measured parameters, only the LTV-OBF MPC scheme can be realistically applied for this case study.

In order to mimic the drifting behavior, we are using both of the FIR models for the experiment setup. The drift is then induced by interpolation of both models where the interpolation is controlled by a priori chosen weighting which will not be taken into account during the modeling and commissioning of our proposed LTV-OBF MPC scheme. This way we emulate the drift where dual distillation columns slowly moves from the initial commissioning to the re-commissioning state. The experimental setup is depicted in Figure 6.13 while the interpolation weight is shown in 6.14. Interpolation of the two given models is what we consider as the system of interest for this section. Lastly, from the information on sensor noise determined based on the instrumentation of the real plant, the generated measurements of the experimental setup are corrupted by a discrete-time output additive white noise v with a *signal-to-noise ratio*[3] (SNR) of 25dB. We syn-

[3]The signal-to-noise ratio is defined as $\mathrm{SNR} := 10 \cdot \log_{10}\left(\frac{\|y-v\|_2^2}{\|v\|_2^2}\right)$.

thetically add this noise to the output measurement for our experiment setup.

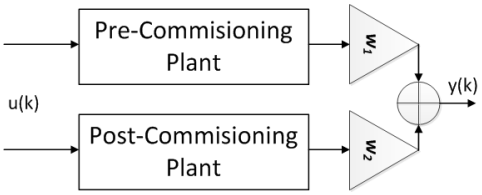

Figure 6.13: Data generating system

The objective of the experiment is to show sustained control performance of reference tracking from the nominal operating point of light product (y_1) and middle cut (y_2) through the unknown drift. The selected reference is $r = [0.01 \quad -0.01]$ which is an example of a possible operating point used by the industry when operating the column. The information on the drift is not used for the model update or during the commissioning of the controller. Last but not least, the designed controller need to obey operating constraint for all of its input $-10 \leq u_i \leq 10; \forall \ \ i = 1, \ldots, 5$.

6.3.2 OBF modeling of the dual distillation column

The first step to deploying any of the proposed OBF MPC schemes is to get the OBF model of the system of interest. For this case study, although we have both pre and post commissioned models of the system at hand, we are going to deriver the LTV-OBF model only from the information of the pre-commissioned plant. The rationale to use only the information of the pre- commissioned plant is to show the benefit of using the LTV-OBF MPC scheme to maintain control performance irrespective of unknown drift that will happen to the system.

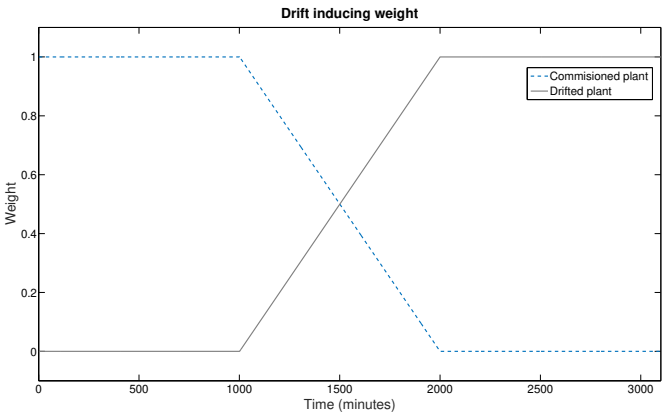

Figure 6.14: Drift inducing weight.

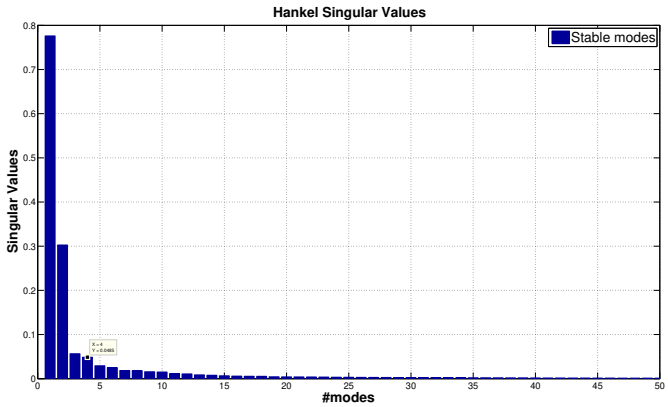

Figure 6.15: Hankel singular values of FIR model.

Getting the OBF model

Since we have the FIR model for the pre-commissioned plant, the basis pole can be inferred directly from the FIR model. This is in a different flavor compared to calculating the basis pole from a union of local LTI model poles as shown in the previous case study. Since the OBF construction itself can span the full space of a stable LTI system, we can always extend the expansion of the OBFs as mentioned in Section 2.5.2. Such expansion is only necessary if the online iterative identification does not yield a good fit to the latest measurement data set.

In order to obtain the pole information from the FIR model of the data generating system, we are going to transform and reduced the full order model of the DDC system. The first step is to check the *Hankel singular values* of the system which is depicted in Figure 6.15. From this observation, we can see that the singular values drop rapidly from the 2nd and the 4th order. The singular value information is in line with the initial observation of the frequency response shown in Figure 6.16. It can be seen that the dominant dynamics for most of the input-output combinations have 2nd order behavior while the 4th input to 1st and 2nd output have at least 4th order dominant dynamics. From these observations, we can use the model order reduction technique to obtain 4th order system representation from the original 300th order FIR model. For this purpose, we use balance reduction since this method yields us an asymptotically stable minimal realization in which the controllability and observability Gramians are equal. The balanced form is comparable to the OBF construction as defined in Definition 2.20. The resulting reduced-order model frequency behavior is shown in Figure 6.16. The reduced order model captures the low-frequency behavior of the full order model while the higher frequency is decently captured since the delta is limited at -40dB. With these results, we can use the reduced- order model poles of

$$\{\lambda_l\}_{l=1}^{4} = \{0.8901 \pm i0.1873, 0.9778, 0.9705\}$$

as our OBF poles.

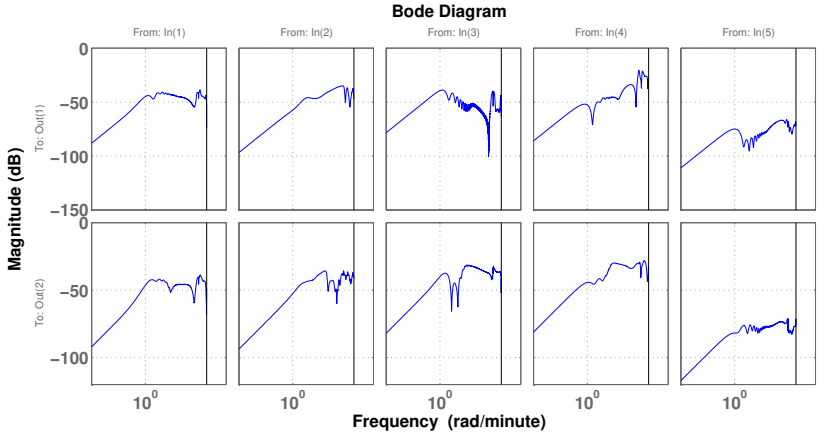

Figure 6.16: Delta of frequency response between full order and reduced order

With the OBF model at hand, we can start the LTI identification exercise to determine the initial coefficient of the LTV-OBF model. This exercise can be done by feeding each of the inputs of the pre-commissioned data-generating system with a uniform white noise of $\mathcal{U}(-0.01, 0.01)$ corresponding to a standard deviation of 0.003 with the length of N=400. The selected value corresponds to twice of settling time of the slowest dynamics in the data generating system while the input magnitude is sufficient to get the system dynamics around the linear operating point. As a short reminder, the input magnitude is going to directly impact the state evolution of the OBF model which then affects the covariance matrix of the identification and also the LQR synthesis (See Section 4.3.4 for details). Lastly, measurement is corrupted by Gaussian white noise with 25dB SNR similarly to the experiment setting mentioned in the previous section.

For the LTV-OBF model, we are going to explore both the *Weighted Least Square* (WLS) and *Recursive Least Square* (RLS) iterative identification strategies. We need to select the weighting for each of these methods as written in (4.22) and (4.23). The initial value that we use are $W_{\mathrm{RLS}} = 1$ for RLS method and $\beta = 2$ with $N_{WLS} = 400$ for the WLS method. Since this is an LTI identification, it is expected that both methods yield the same best fit ratio (Eq (6.3)) and model coefficients. The BFR are 88% for top output and 86% for middle cut output.

Setting up LTV model parameters

The last step of the LTV-OBF model is to select the weight of RLS and WLS identification strategy. By using the information that we got from the previous identification exercise we use $\beta = 2$ with $N_{WLS} = 400$ for the WLS method while for the RLS method we tune down the weight to $W_{\mathrm{RLS}} = 0.995$. The weight for both WLS and RLS are meant to allow smooth but continuous adaptation of the LTV-OBF model coefficient when the system is drifting. In case of deterioration is seen in control performance after the LTV-OBF MPC has been commissioned, we can readjust the RLS and WLS weight.

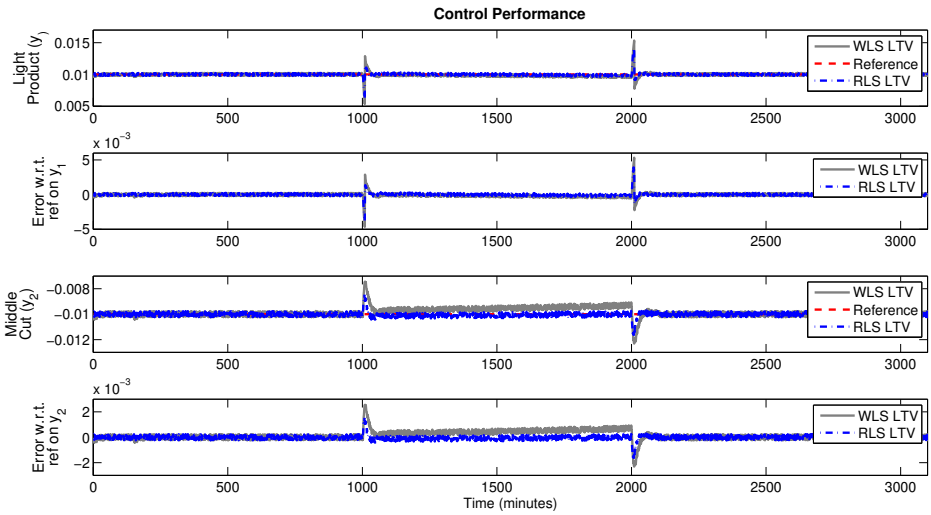

Figure 6.17: Control performance of LTV MPC with WLS and RLS based models.

6.3.3 LTV Control synthesis

Similar to the previous case study, we start with the selection of the MPC scheme control matrices (i.e. Q and R matrices for LTV-OBF MPC scheme). We select control matrices as

$$Q = \begin{bmatrix} 100 & 0 \\ 0 & 100 \end{bmatrix} \quad R = I^{n_{\mathrm{u}} \times n_{\mathrm{u}}} \tag{6.13}$$

due to the magnitude of the output of the system and the information that the FIR model input channels are already normalized.

Following the LTV-OBF MPC algorithm 6 and 7, we re-iterate a similar procedure as in the first case study. Uniform white noise of $\mathcal{U}(-0.01, 0.01)$ is injected in all input channels and a polytopic approximation is constructed for the covariance matrix. The vertices of the polytope are then used to construct the set of LMIs to synthesize the LQR controller. This setup yields solvable LMIs that guarantee the existence of stabilizing LQR controller matrices P and K. The resulting values related to the LQR control synthesis can be found in Appendix A.12.

Similar to the previous case, we are monitoring the condition of Eq.(4.53)/ (6.7) to see whether the close loop stability is attained or not. In case the tracking performance does not meet the expectation and/or covariance matrix needs to be updated, as described in Section 4.7, we can also adjust the value of Q and R to put more emphasis on one of the output and/or to weight down the input if it is too aggressive. Lastly, we select $N = 150$ minutes as the MPC horizon. This value is slightly more than the settling time of the system of interest.

Table 6.5: Control performance of LTV MPC with WLS and RLS based models

		RLS adaptation	WLS adaptation
y_1	MSE	$9.9921 \cdot 10^{-8}$	$1.0068 \cdot 10^{-7}$
y_2	MSE	$3.2953 \cdot 10^{-8}$	$1.3179 \cdot 10^{-7}$

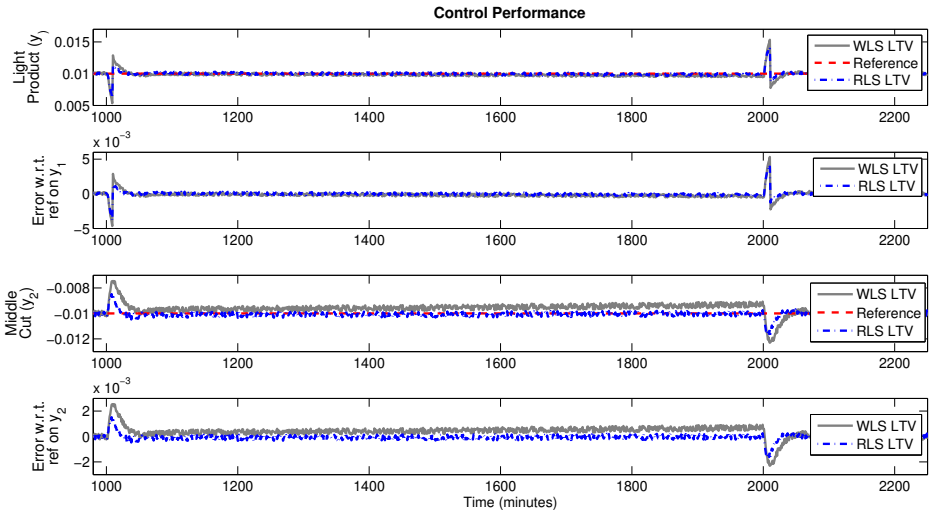

Figure 6.18: Control performance in the highlighted drift period.

6.3.4 Results and discussion

With all the ingredients for the LTV-OBF MPC at hand, we can commission our controller in the experimental setup of the dual distillation column. The control goal is to maintain reference tracking of $r = [0.01 \quad -0.01]$ from the nominal operating point of light product (y_1) and middle cut (y_2) through the unknown drift. Note that the information of the drift is not used for the model update or the control synthesis. The result of the experiment can be found in Fig. 6.17 while the computed MSE can be found in Table 6.5

From these result, we can see that the LTV-OBF MPC perform its job of tracking the reference for both outputs through the drift scenario as mentioned in the problem setting section. The RLS-based LTV-OBF MPC has a slightly better MSE value compared to the WLS-based strategy especially in the middle cut output (y_2). If we look closely to figure 6.17, there are at least two points of interest from this figure. The first point of interest is the two transient behaviors when the drift starts to be induced at $T = 1000$ minutes and when the system settled to the second linear dynamics at $T = 2000$ minutes while the second point of interest is that WLS has a slight offset on the middle cut during the drift. These can be easier to see through the zoomed in version of the results depicted in Figure 6.18.

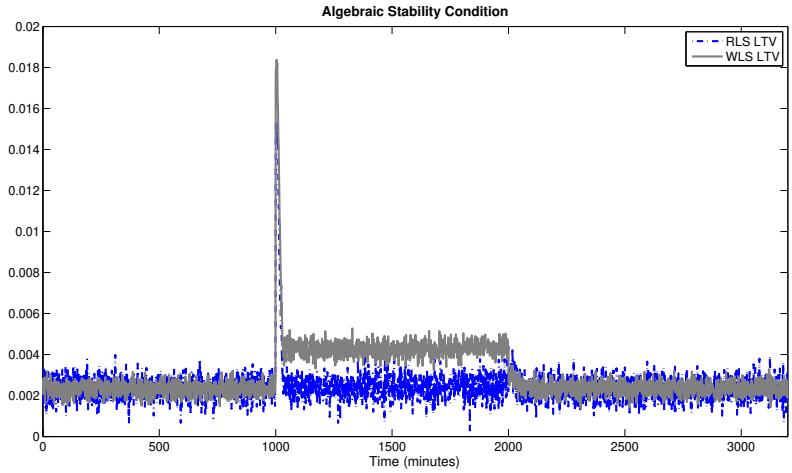

Figure 6.19: LTV Stability condition.

The first observed behavior is understandable since when the drift starts to happen, output measurements will change and hence lead to an abrupt change in the identified model coefficient. At the same time, the MPC control action also starts to move away from the nominal point to provide a countermeasure of the detected change in the system. This action further excites the identification and provides a distinct spike to drive the coefficient further out from its initial value. We can tune down WLS and RLS identification weights if the spike in the output is getting close to the operation constraint. For RLS identification we can increase the W_{RLS} to be very close to $W_{\mathrm{RLS}} = 1$. However, with such a weighting value, the model update will be slowed down significantly. A similar thing can be done for the WLS identification strategy where we can slow down the model update by taking more points (i.e. increasing N_{WLS}) and reducing the value of W_{LS}. Note that updating the WLS parameter will have a potential drawback on control performance.

The second observed behavior is the slight tracking offset for LTV-OBF MPC with WLS adaptation during the drift. This can be explained since WLS takes into account older state evolution and measurement of the system and hence will have a problem when a continuous drift is happening on the system. This is validated since the control performance becomes better when the system settled into the post-commissioned behavior. So the weighting parameter of the WLS identification strategy is a sensitive tuning parameter. By trying to reduce the transient behavior of the control action when the drift start and ends can lead to an offset in tracking performance during the drift.

The last observed behavior is the stability of the closed-loop system. We are monitoring the value of Eq.(6.12) for both WLS and RLS cases in Figure 6.19 (see Section 4.7 for details). From this figure, non-smooth stability condition similar to the first case study is also observed. The root cause of this behavior is the noise of measurement and induced excitation to maintain persistent excitation. If we filter out the noisy part of Figure 6.19, we see a stable and non-increasing trend which

shows the closed-loop system is stable throughout a large part of the experiment. The only two points where the stability is compromised are when the model coefficient suddenly moved outside of its initial value when the first drift happen and when it settled down to the post-commissioned behavior. Another important behavior that can be observed from the figure is that we also see a similar offset in the stability condition of the WLS strategy as seen in the tracking performance. Since the closed-loop system is unable to track the reference, a slight offset also appears in the stability condition. This value goes down to a lower value as soon as the system settled into the post-commissioned behavior ($t \geq 2000$ min). From this result, we can conclude that for this particular case RLS identification strategy outperforms the WLS strategy in terms of tracking the performance and stability of the closed-loop system.

6.4 Summary

The proposed LTV-OBF MPC and LPV-OBF MPC have been demonstrated in two industrial case studies. LPV-OBF MPC shows better performance compared to LTV-OBF MPC in the high purity distillation column case study and also a better stability guarantee. The LPV scheme itself requires an explicit signal, namely the scheduling variable, that can describe different system dynamics of the interested operating regime. Additionally, the LPV-OBF MPC also need longer experiment time to get correct description on the varying dynamics. On the other hand, the LTV-OBF MPC does not need explicit signal to describe different system dynamics. This scheme is not only able to tackle varying reference on high purity distillation case, but also maintain reference tracking under unknown drift on the dual distillation column case. It requires less resources for the identification, but tuning of the identification parameter can be less intuitive. The slight drawback for the LTV-OBF MPC scheme is the higher variance due to necessity of extra excitation to maintain the model update. Note that if we are confident that the plant dynamics remain in the linear regime, the iterative identification of the LTV-OBF model can be turned off. This also means that we are controlling the system similar to the standard LTI MPC. After the testing both method in the case study, we can conclude that LPV-OBF MPC is better for the case when the variations of system dynamics are known, while LTV-OBF is better when the variations are not known.

7 CHAPTER

Conclusion

This chapter presents the concluding remarks on the research presented in this thesis. We first revisit the research question posed in the introduction section and verify whether the results given in this thesis give a sufficient answer to the question. We then further list the contributions of this thesis before concluding the chapter with several potential future research directions related.

7.1 Answer to the Research Objective

This thesis has been driven by the growing demand in the process industry where the standard way of linear control is not enough to maintain the high control performance through its operational period. This problem is embodied in the research objective that is given at the beginning of the thesis:

- Primary research question -

How to reduce the discrepancy between the prediction model in MPC and the process of interest so as to sustain high performance of the controller? In particular, how and when should the update of the controller and model take place?

Throughout this thesis, we have shown that it is possible to improve the performance of APC by taking into account model inaccuracy and variation of process dynamics that are causing the plant-model mismatch. The solution stems from the usage of the *Orthonormal Basis Function* as the foundation to capture the broad variation of linear system dynamics around a given and even multiple operating points. With the OBF model at hand, we then employ two paradigms of LTV and LPV in order to capture the variation in process dynamics. The OBF

model coefficient is updated iteratively in each time step either with or without information about its operational trajectory. In order to establish MPC schemes for each paradigm, we construct the theoretical foundation that is essential for the control scheme. Lastly, we have demonstrated that the proposed algorithm can maintain the control performance in two industrial case studies. After examining both methods in a simulation environment, we observed that LPV-OBF MPC is more suited for the case when the variations of system dynamics are known, while LTV-OBF MPC is more practical when the variations are not known. With these findings, we conclude that the research objective of the thesis is sufficiently answered.

7.2 Summary of the Thesis Contribution

In this section we are summarizing the Thesis contribution that help construct the answer towards the research objective.

In Chapter 2, we provide a concise overview of established theories and their respective notations that are used throughout this thesis. The includes representation of LTI, LTV, and LPV system which are the basis framework to describe system dynamics of interest. Afterward, we introduce the foundational theories for the OBFs which are key ingredients of understanding OBFs and also constructing OBF-based model. Lastly, we provide notion of optimality on the selection of OBFs which then become the bridge to the next chapter.

In Chapter 3, we turn the optimality notion described in Chapter 2 into an OBF pole selection problem. We then propose three different basis pole selection algorithms to solve this problem:

- The *Sequential Quadratic Programming* (SQP) algorithm utilize direct computation of the gradient
- The *Randomized Algorithm* (RA) provides an alternative selection technique for where the result can be interpreted in probabilistic sense
- The *Sum of Squares* (SOSP) algorithm provides a convex global solution to the relaxed problem definition

Each of the proposed algorithm have a small number of tuning parameters which is intuitive for the user. We then extend the basis selection problem for a model of system that is obtained via system identification procedure. Throughout academic examples we demonstrate the performance and computational load of the proposed methods. The SQP algorithm excels for a small-medium number of basis poles while RA algorithm is computationally more efficient for a large number of basis poles. Due to the relaxation of the SOSP algorithm, it is more suited as a tool to assess the result of the other two algorithms. With the OBF pole selection at hand, we can start the next chapters on constructing OBF-based model in LTV and LPV framework as well as the MPC control synthesis of those models.

In Chapter 4, we are interested in solving the plant-model mismatch problem of predictive control in case the cause of the changes in the plant dynamics is not known. We first formulate LTI-OBF and LTV-OBF based model identification in the PEM identification settings. Two methods to do iterative identification of LTV-OBF are proposed:

- *Weighted Least Square* (WLS) estimation has the advantages of using past data for estimation
- *Recursive Least Square* (RLS) do not use the full past data set but has the ease of tuning parameter selection

With the model at hand, we construct the MPC problem with OBF model as its prediction model. We start establishing classical feasibility and stability theorems in the LTI framework and extend it to the LTV framework. In the LTV theorems, we propose an extra condition to guarantee the stability of the LTV-OBF MPC controlled system, where the stability of the controlled system can be established from both the control synthesis and the identification side. The proposed LTV-OBF MPC is then demonstrated in an academic case study. We shows comparable performance between WLS and RLS method, with RLS having slightly better performance in the experimental study.

In Chapter 5, we are focusing on solving the plant-model mismatch problem in case the cause of the changes in the plant dynamics is known and measurable. We first formulate LPV-OBF based model identification in the PEM identification settings. Two approaches to estimate the LPV-OBF model coeffiecient are introduced:

- Local LPV identification approach can be seen as an interpolation of the dynamical behavior of the system
- Global LPV identification approach is a direct identification method based on a single data set that is measured from the system

For the construction of LPV-OBF MPC problem, we utilizes designated steady-state target and extra penalty term for tracking purposes. The space of the steady-state pair is characterized by a vector which is used as an argument of minimization for the MPC problem. Such formulation leads to a straightforward formulation of feasibility and stability theorems where the effect of the parameter variation on the MPC scheme is minimal. We then utilize *Extended Kalman Filter* to address unaccounted changes in system dynamics from the identification of the LPV-OBF model. The proposed LPV-OBF MPC is then demonstrated in an academic case study where the global approach slightly outperform the local approach but require more longer experiment time to obtain the model.

In Chapter 6, we test the performance of both LTV-OBF MPC and LPV-OBF MPC in realistic industrial case studies that are based on distillation column. The first case we use first principle model of *High Purity Distillation Column*, while the second case we show scenario of drifting on *Dual Distillation Column* model with

two identified FIR systems from different time instances. Some observation was made during the experiment:

- For HPDC case study, the LTV-OBF MPC output has a higher variance compared to LPV-OBF MPC
- The Variance comes from extra excitation signals, but can be turned off if the model does not need to be updated (i.e. control in LTI-OBF mode)
- LPV-OBF MPC scheme in this scenario outperforms the LTV-OBF MPC scheme in both tracking performance and guarantee of stability for the high purity distillation column case
- For DDC case study, since the drift cannot be characterized by any measured parameters, only the LTV-OBF MPC scheme can be realistically applied for this case study
- For DDC case study, RLS identification strategy outperform the WLS strategy in terms of tracking performance and stability of the closed-loop system

Throughout this experiment, we are sure that the LPV-OBF MPC is better for the case when the variations of system dynamics are known, while LTV-OBF is better when the variations are not known. The LPV-OBF MPC is more of an *anticipative* controller where the anticipation time can be lowered by tuning the value of N.

7.3 Recommendations for Future Research

Below are several recommendations for possible future research related to the topic of this thesis

- Improvement of the basis pole selection: Due to the growth of computation power over the past year, new computationally expensive approaches for selection can be explored.
- Utilization of Instrumental Variable or other closed lood identification method: In the closed loop setting, OE noise model will always be biased. Introduction of IV to deal with this biased estimate can be explored. It is also interesting to see the impact of the IV for the whole OBF MPC algorithm.
- Extension of the LTV-OBF MPC algorithm with an iterative update on Q_k: As indicated in the remark of Section 4.7, this direction can be explored to simultaneously establish the closed-loop stability from both the control synthesis and the identification side.
- Reformulation of the LTV-OBF MPC scheme: Notice that the LTV-OBF MPC scheme presented in this thesis has a different formulation than the LPV-OBF MPC scheme with target output and target penalty function. The difference on the formulation stem from the intention of exploring both method

and obtain the learning from both formulation. Not until the later phase of the research that we found out that the LPV-OBF MPC formulation gives ease of formulation and more straight forward stability construction. Due to this, reformulation of the LTV-OBF MPC scheme can be worked out to be closer to the LPV-OBF scheme.

- Explore possibilty to implement EKF in the LTV-OBF setting: although the coefficients of the LTV model are updated for each time step, incorporating EKF in the total solution can provide extra tool to tackle plant-model mismatch in the LTV setting.
- Extend the LPV-OBF model structure: the LPV-OBF model constructed in this thesis is based on piece wise affine assumption of the system dynamic. Hence, possible extension of the model structure by relaxing this assumption can be explored.
- Comparison with non OBF MPC scheme: This thesis is focusing on the different settings (time and parameter varying) in which OBF MPC can be used. Practical or theoretical comparison to other well established MPC scheme can be explored. This will be usefull to give better comparative overview on the OBF MPC scheme.

A APPENDIX

Appendix

In this appendix, derivation of expressions as well as proofs of the theories and lemmas of this thesis are presented. The notation of the appendix correspond to their respective chapters.

A.1 Derivation of gradients in Chapter 3

Each of the n_z number of gradient in (3.24) can be distinguished based on that the gradient elements is required to be computed for a real pole parameter or the parameters of a complex conjugate pairs of basis poles. For a real pole parameter, the j-th inequality results in:

$$\frac{d\tilde{J}_j}{d\bar{a}_i} = \frac{dNr}{d\bar{a}_i}\prod_{i=1}^{n} Nc_i - \rho^2 \frac{dDr}{d\bar{a}_i}\prod_{i=1}^{n} Dc_i, \tag{A.1}$$

with

$$\frac{dNr}{d\bar{a}_i} = \frac{dNr_i}{d\bar{a}_i}\prod_{k=1,k\neq i}^{n} (Nr_k), \tag{A.2}$$

$$\frac{dDr}{d\bar{a}_i} = \frac{dDr_i}{d\bar{a}_i}\prod_{k=1,k\neq i}^{n} (Dr_k), \tag{A.3}$$

and

$$\frac{dNr_i}{d\bar{a}_i} = \bar{a}_i - 2x_j, \tag{A.4}$$

$$\frac{dDr_i}{d\bar{a}_i} = 2\bar{a}_i y_j^2 + 2x_j(\bar{a}_i x_j - 1). \tag{A.5}$$

For the complex conjugate parts:

$$\frac{d\tilde{J}_j}{da_i} = \prod_{i=1}^{n} Nr_i \frac{dNc}{da_i} - \rho^2 \prod_{i=1}^{n} Dr_i \frac{dDc}{da_i}, \tag{A.6}$$

$$\frac{d\tilde{J}_j}{db_i} = \prod_{i=1}^{n} Nr_i \frac{dNc}{db_i} - \rho^2 \prod_{i=1}^{n} Dr_i \frac{dDc}{db_i}, \tag{A.7}$$

where the derivatives w.r.t. a_i are given by:

$$\frac{dNc}{da_i} = \frac{dNc_i}{da_i} \prod_{k=1,k\neq i}^{n} (Nc_k), \tag{A.8}$$

$$\frac{dDc}{da_i} = \frac{dDc_i}{da_i} \prod_{k=1,k\neq i}^{n} (Dc_k), \tag{A.9}$$

with

$$\begin{aligned}\frac{dNc_i}{da_i} &= ((b_i + y_j)^2 + (a_i - x_j)^2)(2a_i - 2x_j) + \dots \\ &\qquad ((a_i - x_j)^2 + (b_i - y_j)^2)(2a_i - 2x_j),\end{aligned} \tag{A.10}$$

$$\begin{aligned}\frac{dDc_i}{da_i} &= (2x_j(a_i x_j + b_i y_j - 1) + 2y_j(a_i y_j - b_i x_j)) \dots \\ &\qquad ((a_i y_j + b_i x_j)^2 + (b_i y_j - a_i x_j + 1)^2) - \dots \\ &\qquad (2x(b_i y_j - a_i x_j + 1) - 2y(a_i y_j + b_i x_j)) \dots \\ &\qquad ((a_i y_j - b_i x_j)^2 + (a_i x_j + b_i y_j - 1)^2),\end{aligned} \tag{A.11}$$

and the derivatives w.r.t b_i are given by:

$$\frac{dNc_i}{db_i} = \frac{dNc_i}{db_i} \prod_{k=1,k\neq i}^{n} (Nc_k), \tag{A.12}$$

$$\frac{dDc_i}{db_i} = \frac{dDc_i}{db_i} \prod_{k=1,k\neq i}^{n} (Dc_k), \tag{A.13}$$

with

$$\begin{aligned}\frac{dNc_i}{db_i} &= ((b_i + y_j)^2 + (a_i - x_j)^2)(2b_i - 2y_j) + \dots \\ &\qquad ((a_i - x_j)^2 + (b_i - y_j)^2)(2b_i + 2y_j),\end{aligned} \tag{A.14}$$

$$\begin{aligned}\frac{dDc_i}{db_i} &= (2x_j(a_i y_j + b_i x_j) + 2y_j(b_i y_j - a_i x_j + 1)) \dots \\ &\qquad ((a_i y_j - b_i x_j)^2 + (a_i x_j + b_i y_j - 1)^2) - \dots \\ &\qquad (2x(a_i y_j - b_i x_j) - 2y(a_i x_j + b_i y_j - 1)) \dots \\ &\qquad ((a_i y_j + b_i x_j)^2 + (b_i y - a_i x_j + 1)^2).\end{aligned} \tag{A.15}$$

A.2 Proof of Theorem 4.1

Proof: Supposed that $K^{(k)}$ or K exist such that all the conditions in Theorem 4.1 are satisfied. The first condition of Theorem 4.1 guarantees the existence of optimal input sequence $\{u^*(i|k)\}_{i=0}^{N}$ and the existence of $u_{\mathrm{MPC}}(k)$ as the control law. Such control law lead to a state $x(k+1) = x(i+1|k)$ for the MPC problem at $k+1$. At time $k+1$, the previous optimal input sequence at time k can be used as the candidate solution for $i = 0, 1, \ldots, N-1$:

$$\{u(i|k+1)\}_{i=0}^{N-1} = \{u^*(i|k)\}_{i=1}^{N}. \tag{A.16}$$

This solution is not necessary the minimum of (4.29) at time $k+1$, but the feasibility is guaranteed since both operational constraints and stability constraints for $i = 0, 1, \ldots, N-1$ are satisfied by using such an input sequence. Next, we need to show that both of these constraints are also satisfied for $i = N$. In order to show the satisfaction of both constraints, we utilize the definition of extended input u_{ext} of (4.33) which also means that we have a full candidate of input sequence

$$\{u(i|k+1)\}_{i=0}^{N} = \{u_{\mathrm{ext}}(i|k)\}_{i=1}^{N+1}. \tag{A.17}$$

By using sequence (A.17) we have $x(N-1|k+1) = x(N|k)$. Supposed that the second condition of Theorem 4.1 is satisfied, then we have

$$\begin{aligned} x(N|k+1) &= Ax(N|k) + Bu_{\mathrm{ext}}(N|k) \\ &= (A + BK^{(k)})x(N|k) + (I - A - BK^{(k)})x_r \in \mathcal{X}_f \end{aligned} \tag{A.18}$$

which shows that the stability constraint at $i = N$ for time instance $k+1$ is satisfied. Lastly, by using sequence (A.17) we know that $u(N|k+1) = K^{(k)}(x(N|k))$. Since we know that $x(N|k) \in \mathcal{X}_f$, the condition that is required to ensure that the operational constraint

$$u_{min} \quad \leq u(N|k+1) \quad \leq u_{max}, \tag{A.19}$$

is satisfied, is the third condition of Theorem 4.1:

$$u_{min} - u_r \leq K^{(k)}(\mathcal{X}_f \ominus x_r) \leq u_{max} - u_r. \tag{A.20}$$

These arguments ensure that the feasibility of MPC problem (4.29) at time k leads to the feasibility of MPC problem (4.29) at time $k+1$. This reasoning can be repeated for all k, which also implies the recursive feasibility of the MPC problem. □

A.3 Proof of Theorem 4.2

Proof: According to definition 4.14, there are three conditions that need to be satisfied to state that V_N is a control Lyapunov function. The conditions are

1. $V_N(x(k)) \geq \alpha_1(\|x(k) - x_r\|), \quad \forall k \in \mathbb{Z},$
2. $V_N(x(k)) \leq \alpha_2(\|x(k) - x_r\|), \quad \forall k \in \mathbb{Z},$
3. $V_N(Ax(k)+Bu_{\mathrm{MPC}}(k)) \leq V_N(x(k))-\alpha_3(\|Ax(k) + Bu_{\mathrm{MPC}}(k) - x_r\|), \ \forall k \in \mathbb{Z}.$

The first condition is trivial to show since selecting

$$\alpha_1(\|x(k) - x_r\|) = \sum_{k=0}^{N} (x(k) - x_r)^\top C^\top Q C (x(k) - x_r), \tag{A.21}$$

which is a part of the first element of stage cost $l_i(x, u)$, should satisfy the first condition for all $x \in \mathbb{X}$. Satisfying the second and third conditions require a bit more work and additional requirements. In this proof we also show that a particular selection of these requirements lead to satisfaction of both Control Lyapunov conditions.

By having an MPC problem that is recursively feasible we guarantee the existence of the MPC control law for all k. Similar to (A.17), at time $k + 1$ we have a candidate optimal sequence

$$\{u(i|k + 1)\}_{i=0}^{N} = \{u_{\mathrm{ext}}(i|k)\}_{i=1}^{N+1}, \tag{A.22}$$

which is not necessary optimal at time $k + 1$. Now denote $\tilde{V}_N(k + 1)$ as the cost function of the MPC problem that utilizes the candidate optimal sequence (A.22):

$$\tilde{V}_N(k + 1) := V_N(\{u(i|k + 1)\}_{i=0}^{N}, x(k + 1)). \tag{A.23}$$

We utilize $V_N^*(k)$ in Definition 4.2 as the primal optimization of the MPC problem at time k and without loss of generality we use K instead of $K^{(k)}$ to simplify notation. Now the relation of $V_N^*(k)$ and $\tilde{V}_N(k + 1)$ is given as follows:

$$\begin{aligned}\tilde{V}_N(k + 1) = V_N^*(k) &- l_0\big(x(0|k), u_{\mathrm{MPC}}(k), x(k)\big) \\ &- V_f\big(x(N|k)\big) + V_f\big((A + BK)x(N|k) + (I - A - BK^{(k)})x_r\big) \\ &+ l_N\big(x(N|k), Kx(N|k)\big).\end{aligned} \tag{A.24}$$

In order to show the third condition, first we need to have $\tilde{V}_N(k+1) \leq V_N^*(k)x(k)-l_0\big(x(0|k), u_{\mathrm{MPC}}(k), x(k)\big)$. This can be achieved if

$$V_f\big((A+BK)x(N|k)+(I-A-BK^{(k)})x_r\big)-V_f\big(x(N|k)\big)+l_N\big(x(N|k), Kx(N|k)\big) \leq 0. \tag{A.25}$$

With this equation it can be seen that the selection of the terminal cost V_f is crucial to guarantee satisfaction of (A.25) and making V_f a control Lyapunov function with control law K and invariant set $\mathcal{X}_f$. One possible selection of the terminal cost to achieve (A.25) is

$$V_f\big(x\big) = (x - x_r)^\top P (x - x_r), \tag{A.26}$$

with $P \succ 0$. Substituting (A.26) into (A.25) lead to

$$(x(N|k)-x_r)^\top \big((A+BK)^\top P(A+BK)-P+C^\top QC+K^\top RK\big)(x(N|k)-x_r) \leq 0. \tag{A.27}$$

Now this particular selection of terminal cost is interesting since it also provides a method to select a stabilizing linear controller K as a solution for LQR control synthesis

$$(A+BK)^\top P(A+BK) - P \preceq -(C^\top QC + K^\top RK) \tag{A.28}$$

which is a uniformly stabilizing linear controller. The invariant set of such controller is equivalent to the level set of (A.26)

$$\mathcal{X}_f = \{x | V_f(x) \leq \gamma\} \tag{A.29}$$

with $0 < \gamma \leq 0$. A method to find the value of γ and the related LQR control synthesis is elaborated further in Section 4.6.

By selecting V_f as (A.26), the first and the second conditions of Theorem 4.2 are achieved. However, since we only have

$$\tilde{V}_N(k+1) \leq V_N^*(k) - l_0\big(x(0|k), u_{\mathrm{MPC}}(k)\big) \tag{A.30}$$

the third Control Lyapunov condition is not yet achieved since we only have a possible cost function of $\tilde{V}_N(k+1)$ and not the primal optimum of $V_N^*(k+1)$. The last step that is required to complete the proof follows through the optimality principle where it is stated that

$$V_N^*(k+1) \leq \tilde{V}_N(k+1). \tag{A.31}$$

This relation satisfies the second control Lyapunov condition and as well the third condition of

$$V_N^*(k+1) \leq V_N^*(k) - l_0\big(x(0|k), u_{\mathrm{MPC}}(k)\big). \tag{A.32}$$

□

A.4 Proof of Theorem 4.3

Proof: The variation of C_k does not violate any of the constraints of MPC problem for a candidate solution on the next time instant $k+1$ which is denoted by $\{u(i|k+1)\}_{i=0}^{N}$:

- The operational constraint remains unchanged for $K^{(k)}$ or K that is invariant with the variation of C_k,
- The stability constraint remains unchanged since $\mathcal{X}_f$ is invariant under the variation of C_k.

Hence, same proof such as written in Theorem 4.1 can be directly applied for the adaptive case. □

A.5 Proof of Theorem 4.4

Proof: We follow the same line of reasoning of the stability proof written in Theorem 4.2 to show that $V_{N|k}(\cdot)$ admits a control Lyapunov function. The recursive feasibility is needed to guarantee the existence of a solution to the MPC problem (4.45) for all k. This condition also implies that the constraints of the MPC problem are also satisfied for all k. The same terminal cost

$$V_f(x) = (x - x_{rk})^\top P(x - x_{rk}) \tag{A.33}$$

is being employed to satisfy the control Lyapunov conditions. The condition on the controller K is updated based on (4.48).

As a replacement of the optimality principle of (A.31), the relation

$$V_{N|k}(k+1) \leq \tilde{V}_{N|k}(k) - l_0\big(x(0|k), u_{\mathrm{MPC}}(k)\big) \tag{A.34}$$

is guaranteed by satisfying

$$\sum_{i=0}^{N} \|{C_{k+1}}^\top (x(i|k+1) - x_{rk})\|_{Q_{k+1}} \leq \sum_{i=0}^{N} \|{C_k}^\top (x(i|k+1) - x_{rk}))\|_{Q_k} \tag{A.35}$$

The difference between the value function $V_{N|k}$ at time k and $k+1$ is only governed by the summation of the stage cost $l_{i|k}$. The right hand side of (A.35) can be iteratively computed for each time step k. For arbitrary value of $x(i|k+1), i = 1, \ldots, n$ and x_r, the condition (A.35) is achieved by satisfying the condition (4.53):

$${C_{k+1}}^\top Q_{k+1}(i) C_{k+1} \preceq C_k^\top Q_k(i) C_k \quad \forall k \in \mathbb{Z}, i \in \mathbb{N}.$$

At the next time instance $k+1$, this condition can be achieved by adjusting the sequence of weighting matrices $Q_{k+1}(i)$ for all i and/or restricting the value of C_{k+1} which comes from the iterative identification of model coefficient θ_{k+1}. Suppose that $Q_k(i)$ is independent of i, then only a single matrix Q_{k+1} that needs to be adjusted with respect to C_{k+1}.

□

A.6 Proof of Theorem 5.1

Proof: The feasibility of the MPC problem (5.18) is straightforward to show. By selecting $\mathcal{X}_f^w = \mathrm{Proj}_{\mathbb{X}}(\mathcal{O}_{\infty,\eta}^{K,w})$ we get (5.29). If $P_{\mathrm{PV-MPC}}$ is feasible at time k then there exist a solution $(u_{\mathrm{ext}}(i|k), \xi)$ that achieves

$$(x(i|k), u_{\mathrm{ext}}(i|k)) \in \mathcal{Z}, \quad \text{for all } i \in \mathbb{N}$$

and

$$(x(N|k), \xi) \in \mathcal{X}_f^w.$$

The admissible set $\mathcal{Z}$ does not depend on the target r or the scheduling variable p thanks to Assumption 5.1. In the next time step k, the existence of a solution for (5.18) is guaranteed since we can use

$$(u_{\text{ext}}(i|k+1), \xi) = (u_{\text{ext}}(i+1|k), \xi), \quad \text{for all } i \in \mathbb{N}.$$

Since the set (5.28) is constructed based on (5.27) we get

$$(x(i|k+1), u_{\text{ext}}(i|k+1)) \in \mathcal{Z}, \quad \text{for all } i \in \mathbb{N}, \tag{A.36}$$

and

$$(x(N|k+1), \xi) \in \mathcal{X}_f^w, \tag{A.37}$$

for free. As mentioned in Section 5.4.3 the only condition that is needed for this purpose is that the matrix $A + BK$ is Hurwitz. Note that the local controller K is independent of the scheduling variable p, and the invariant set $\mathcal{O}_{\infty,\eta}^{K,w}$ is also independent of p and remains the same for a selected control law K. Hence, as long as $P_{\text{PV}-\text{MPC}}$ is feasible at time k the problem is feasible and remains feasible for future time instances. □

A.7 Proof of Theorem 5.2

Proof: According to Definition 4.14 there are three conditions that need to be satisfied to state that V_N is a control Lyapunov function. The conditions are

1. $V_N(x(k)) \geq \alpha_1(\|x(k) - x_s\|), \quad \forall k \in \mathbb{Z},$
2. $V_N(x(k)) \leq \alpha_2(\|x(k) - x_s\|), \quad \forall k \in \mathbb{Z},$
3. $V_N(Ax(k)+Bu_{\text{MPC}}(k)) \leq V_N(x(k))-\alpha_3(\|Ax(k) + Bu_{\text{MPC}}(k) - x_s\|), \quad \forall k \in \mathbb{Z}.$

The first condition is trivial to show since selecting

$$\alpha_1(\|x(k) - x_s\|) = \sum_{i=1}^{N} \|x(i|k) - x_s\|_Q^2, \tag{A.38}$$

which is a part of the cost function (5.16), should satisfy the first condition for all $x \in \mathbb{X}$. Satisfying the second and third conditions require a bit more work and additional requirements. In this proof we also show that a particular selection of these requirements lead to the satisfaction of both Control Lyapunov conditions.

By having an MPC problem that is recursively feasible, we guarantee the existence of the MPC control law for all k. Hence, at time $k + 1$ we have a candidate optimal sequence

$$\{u(i|k+1)\}_{i=0}^{N} = \{u_{\text{ext}}(i|k)\}_{i=1}^{N+1}, \tag{A.39}$$

which is not necessary optimal at time $k+1$. Now denote $\tilde{V}_N(k+1)$ as the cost function of the MPC problem that utilizes the candidate optimal sequence (A.39):

$$\tilde{V}_N(k+1) := V_N(\{u(i|k+1)\}_{i=0}^{N}, x(k+1)). \tag{A.40}$$

Now consider $V_N^*(k)$ in Definition 5.4 as the primal optimal cost of the MPC problem at time k. Now the relation of $V_N^*(k)$ and $\tilde{V}_N(k+1)$ is given as follows:

$$\begin{aligned}\tilde{V}_N(k+1) = V_N^*(k) - \|x(0|k) - x_s\|_Q^2 - \|u(0|k) - u_s\|_R^2 \\ - \|x(N|k) - x_s\|_P^2 + \|(A+BK)x(N|k) - x_s\|_P^2 \\ + \|x(N|k) - x_s\|_Q^2 + \|u(N|k) - u_s\|_R^2.\end{aligned} \tag{A.41}$$

In order to show the third condition, first we need to have $\tilde{V}_N(k+1) \leq V_N^*(k) - \|x(0|k) - x_s\|_Q^2 - \|u(0|k) - u_s\|_R^2$. This can be achieved if

$$\|(A+BK)x(N|k) - x_s\|_P^2 - \|x(N|k) - x_s\|_P^2 + \|x(N|k) - x_s\|_Q^2 + \|u(N|k) - u_s\|_R^2 \leq 0. \tag{A.42}$$

The left hand side of (A.42) can be collected into

$$(x(N|k) - x_s)^\top \big((A+BK)^\top P(A+BK) - P + Q + K^\top RK\big)(x(N|k) - x_s). \tag{A.43}$$

This relation also provide a method to select a stabilizing linear controller K as a solution of the LQR control synthesis problem

$$(A+BK)^\top P(A+BK) - P \preceq -(Q + K^\top RK) \tag{A.44}$$

which is the second condition of this theorem.

However, since we only have

$$\tilde{V}_N(k+1) \leq V_N^*(k) - \|x(0|k) - x_s\|_Q^2 - \|u(0|k) - u_s\|_R^2, \tag{A.45}$$

the third Control Lyapunov condition is not yet achieved since we only have possible cost function value $\tilde{V}_N(k+1)$ and not the primal optimum of $V_N^*(k+1)$. The last step that needs to be done to complete the proof is to use the optimality principle

$$V_N^*(k+1) \leq \tilde{V}_N(k+1). \tag{A.46}$$

In the parameter-varying case, this optimality principle holds if the third condition of

$$\tilde{V}_o(y_s - r) - V_o(y_s - r) \leq 0, \tag{A.47}$$

is satisfied. From this condition, we can see that the target penalty function V_o have additional role in stability beside dictating the selection of ξ for tracking. This condition also implies the required situation for the end value of $p(N)$, or the trajectory of $p(k)$ (Assumption 5.1), such that a stability statement can be made.

By using (A.46), the second and third control Lyapunov condition of

$$V_N^*(k+1) \leq V_N^*(k) - \|x(0|k) - x_s\|_Q^2 - \|u(0|k) - u_s\|_R^2, \tag{A.48}$$

are satisfied. □

A.8 Matrices and parameters used in the simulation study of Chapter 4

Vertices considered for the LQR problem of the Oracle-MPC

$$\tilde{\theta}_{\text{orc1}} = \begin{bmatrix} 0.0217 & -0.0154 & -0.0289 & 0.0191 \\ 0.0188 & -0.0159 & 0.0120 & 0.0094 \end{bmatrix} \tag{A.49}$$

$$\tilde{\theta}_{\text{orc2}} = \begin{bmatrix} 0.0265 & -0.0196 & -0.0312 & 0.0211 \\ 0.0112 & 0.0104 & -0.0025 & 0.0030 \end{bmatrix} \tag{A.50}$$

$$\tilde{\theta}_{\text{orc3}} = \begin{bmatrix} 0.0244 & -0.0177 & -0.0304 & 0.0203 \\ 0.0152 & -0.0133 & 0.0074 & 0.0063 \end{bmatrix} \tag{A.51}$$

$$\tilde{\theta}_{\text{orc4}} = \begin{bmatrix} 0.0286 & -0.0218 & -0.0304 & 0.0210 \\ 0.0024 & 0.0038 & 0.0072 & -0.0036 \end{bmatrix} \tag{A.52}$$

$$\tilde{\theta}_{\text{orc5}} = \begin{bmatrix} 0.0272 & -0.0203 & -0.0313 & 0.0212 \\ 0.0090 & -0.0088 & -0.0001 & 0.0013 \end{bmatrix} \tag{A.53}$$

LQR solution of the Oracle-MPC

$$P_{\text{orc}} = \begin{bmatrix} 0.0664 & -0.0107 & -0.0006 & 0.0001 \\ -0.0107 & 0.0380 & 0.0003 & 0.0003 \\ 0.0006 & 0.0003 & 0.0670 & -0.0108 \\ 0.0001 & 0.0003 & -0.0108 & 0.0381 \end{bmatrix} \tag{A.54}$$

$$K_{\text{orc}} = \begin{bmatrix} 0.4845 & -0.6373 & 0.1831 & -0.3991 \\ 0.1369 & -0.3235 & -0.4475 & -0.4903 \end{bmatrix} .10^{-3} \tag{A.55}$$

Vertices considered for the LQR problem of the Fixed-MPC

$$\tilde{\theta}_{\text{fixed1}} = \begin{bmatrix} 0.0217 & -0.0154 & -0.0289 & 0.0191 \\ 0.0188 & -0.0159 & 0.0120 & 0.0094 \end{bmatrix}$$

LQR solution of the Fixed-MPC

$$P_{\text{fixed}} = \begin{bmatrix} 0.0739 & -0.0118 & 0 & -0.0002 \\ -0.0118 & 0.0432 & -0.0001 & 0.0006 \\ 0 & 0.0001 & 0.0741 & -0.0117 \\ -0.0002 & 0.0006 & -0.0117 & 0.0431 \end{bmatrix} \tag{A.56}$$

$$K_{\text{fixed}} = \begin{bmatrix} -0.4167 & -1.0147 & 0.1588 & -0.3600 \\ 0.1176 & -0.2915 & -0.4349 & 0.7456 \end{bmatrix} .10^{-3} \tag{A.57}$$

Vertices considered for the LQR problem of the LPV-OBF MPC WLS and the RLS

$$\tilde{\theta}_{\text{wls1}} = \tilde{\theta}_{\text{rls1}} = \begin{bmatrix} 0.0604 & 0.6978 & -0.0588 & 0.7091 \\ 0.1603 & 0.6167 & -0.720 & 0.7265 \end{bmatrix} \tag{A.58}$$

$$\tilde{\theta}_{\text{wls2}} = \tilde{\theta}_{\text{rls2}} = \begin{bmatrix} 0.0947 & -0.7160 & -0.0490 & 0.7090 \\ 0.1946 & -0.7971 & -0.0622 & 0.7264 \end{bmatrix} \tag{A.59}$$

$$\tilde{\theta}_{\text{wls3}} = \tilde{\theta}_{\text{rls3}} = \begin{bmatrix} -0.6282 & -0.0311 & -0.7654 & 0.0054 \\ -0.5283 & -0.1122 & -0.7786 & 0.0228 \end{bmatrix} \tag{A.60}$$

$$\tilde{\theta}_{\text{wls4}} = \tilde{\theta}_{\text{rls4}} = \begin{bmatrix} 0.7856 & 0.0032 & -0.7652 & 0.0072 \\ 0.8855 & 0.0778 & 0.7785 & 0.0246 \end{bmatrix} \tag{A.61}$$

$$\tilde{\theta}_{\text{wls5}} = \tilde{\theta}_{\text{rls5}} = \begin{bmatrix} 0.0622 & 0.6979 & -0.0675 & -0.7051 \\ 0.1622 & 0.6168 & -0.0807 & -0.6878 \end{bmatrix} \tag{A.62}$$

$$\tilde{\theta}_{\text{wls6}} = \tilde{\theta}_{\text{rls6}} = \begin{bmatrix} 0.7852 & 0.0130 & 0.6489 & -0.0015 \\ 0.8851 & -0.0681 & 0.6357 & 0.0159 \end{bmatrix} \tag{A.63}$$

$$\tilde{\theta}_{\text{wls7}} = \tilde{\theta}_{\text{rls7}} = \begin{bmatrix} -0.6286 & 0.0213 & 0.6487 & -0.0033 \\ -0.5287 & -0.1024 & 0.6355 & 0.0141 \end{bmatrix} \tag{A.64}$$

$$\tilde{\theta}_{\text{wls8}} = \tilde{\theta}_{\text{rls8}} = \begin{bmatrix} -0.0966 & 0.7159 & 0.0577 & -0.7052 \\ 0.1965 & -0.7970 & 0.0709 & 0.6878 \end{bmatrix} \tag{A.65}$$

LQR solution of the LPV-OBF MPC WLS and the RLS

$$P_{\text{wls}} = P_{\text{rls}} = \begin{bmatrix} 8.5660 & 0.3724 & -0.2216 & 0.0003 \\ 0.3724 & 1.8737 & 0.0294 & 0.0035 \\ -0.2216 & 0.0294 & 8.4983 & 0.4488 \\ 0.0003 & 0.0035 & 0.4488 & 1.8478 \end{bmatrix} \tag{A.66}$$

$$K_{\text{wls}} = K_{\text{rls}} = \begin{bmatrix} -9.6388 & 1.3569 & -0.2382 & 0.0737 \\ -0.1744 & 0.0882 & -8.7961 & 1.0285 \end{bmatrix} .10^{-3} \tag{A.67}$$

A.9 Matrices and parameters used in the simulation study of Chapter 5

LPV-OBF model coefficients $\{\vartheta_s\}_{s=1}^{3}$ of local approach for y_1

$$\{\vartheta_s\}_{s=1}^{3} = \begin{bmatrix} 7.6799 & -0.8861 & -5.7001 & 0.1920 \\ -0.4854 & 1.6811 & -1.0636 & -0.3600 \\ -0.2109 & 0.3089 & -0.0928 & -0.0662 \end{bmatrix} .10^{-2} \tag{A.68}$$

LPV-OBF model coefficients $\{\vartheta_s\}_{s=1}^{3}$ of local approach for y_2

$$\{\vartheta_s\}_{s=1}^{3} = \begin{bmatrix} 17.8533 & -9.0150 & -7.1565 & 1.9351 \\ 31.8995 & -3.7210 & -23.6405 & 0.8064 \\ -3.9230 & 3.7467 & 0.0253 & -0.8032 \end{bmatrix} .10^{-2} \tag{A.69}$$

Transposed LPV-OBF model coefficient for global approach $\{\vartheta_s\}_{s=1}^{16}$

$$\{\vartheta_s\}_{s=1}^{16}{}^{\top} = \begin{bmatrix} 2.4925 & 1.4487 \\ -1.8914 & 2.4762 \\ -2.4864 & -0.7387 \\ -0.5793 & -0.1517 \\ -0.3048 & -0.7413 \\ 0.5851 & -0.3332 \\ -0.3664 & 0.1967 \\ -0.5176 & -0.0560 \\ -1.8523 & -0.5759 \\ 0.8968 & -1.8233 \\ 1.8943 & 0.4051 \\ 0.6854 & 0.3010 \\ 0.0704 & 0.1590 \\ -0.0882 & 0.0621 \\ 0.1456 & -0.1061 \\ 0.0575 & -0.1331 \end{bmatrix} \tag{A.70}$$

LQR of both LPV-OBF MPC local and global

$$P = \begin{bmatrix} 4.9043 & 1.4766 & 0.0000 & 0.0000 \\ 1.4766 & 1.5595 & 0.0000 & 0.0000 \\ 0.0000 & 0.0000 & 4.9038 & 1.4767 \\ 0.0000 & 0.0000 & 1.4767 & 1.5594 \end{bmatrix} \tag{A.71}$$

$$K = \begin{bmatrix} 1.1463 & -0.3020 & 0.0000 & 0.0000 \\ 0.0000 & 0.0000 & 1.1469 & 0.3022 \end{bmatrix} \tag{A.72}$$

A.10 Matrices and parameters for LTV-OBF MPC in Chapter 6 HPDC/case1

P matrix is truncated due to limited paper space

$$P = [P_{LTV1} \;\; P_{LTV2}] \tag{A.73}$$

$$P_{LTV1} = \begin{bmatrix} 13.8691 & 10.6177 & 4.4313 & 1.7764 & 0.3047 \\ 10.6177 & 15.5923 & 9.8897 & 3.9008 & 0.1735 \\ 4.4313 & 9.8897 & 12.6860 & 7.0918 & 0.2188 \\ 1.7764 & 3.9008 & 7.0918 & 8.9553 & 2.4466 \\ 0.3047 & 0.1735 & 0.2188 & 2.4466 & 2.6758 \\ -0.3245 & -0.7472 & -0.3448 & 0.0851 & -0.0620 \\ -0.7325 & -0.9323 & -0.8576 & 0.0729 & 0.1484 \\ -0.6317 & -0.9986 & -0.9977 & -0.2441 & 0.2367 \\ 0.1885 & -0.1525 & -0.5104 & -0.3522 & 0.0152 \\ 0.3234 & 0.2892 & 0.1089 & 0.0090 & 0.0624 \end{bmatrix} \tag{A.74}$$

$$P_{LTV2} = \begin{bmatrix} -0.3245 & -0.7325 & -0.6317 & 0.1885 & 0.3234 \\ -0.7472 & -0.9323 & -0.9986 & -0.1525 & 0.2892 \\ -0.3448 & -0.8576 & -0.9977 & -0.5104 & 0.1089 \\ 0.0851 & 0.0729 & -0.2441 & -0.3522 & 0.0090 \\ -0.0620 & 0.1484 & 0.2367 & 0.0152 & 0.0624 \\ 11.4632 & 7.1726 & 2.1544 & 0.3611 & -0.2745 \\ 7.1726 & 11.9976 & 6.4368 & 1.4989 & -0.4208 \\ 2.1544 & 6.4368 & 9.5335 & 4.8755 & -0.2866 \\ 0.3611 & 1.4989 & 4.8755 & 7.8836 & 2.1488 \\ -0.2745 & -0.4208 & -0.2866 & 2.1488 & 2.8980 \end{bmatrix} \tag{A.75}$$

K matrix and the vertices are transposed due to limited paper space

$$K^\top = \begin{bmatrix} -6.4533 & 0.8045 \\ -6.3846 & 1.0416 \\ -4.5186 & 0.8562 \\ -2.4405 & 0.5849 \\ -0.1864 & 0.1268 \\ -1.6258 & -1.7889 \\ -2.0516 & -0.5892 \\ -2.1794 & 0.2923 \\ -2.1298 & 0.3729 \\ -0.6427 & 0.0682 \end{bmatrix} .10^{-3} \tag{A.76}$$

$$\tilde{\theta}_{\text{tv1}}^\top = \begin{bmatrix} -0.0561 & -0.0574 \\ 0.2889 & 0.2880 \\ -0.0914 & -0.0916 \\ -0.0207 & -0.0205 \\ -0.1224 & -0.1225 \\ -0.5166 & -0.5153 \\ -0.6298 & -0.6289 \\ -0.3699 & -0.3697 \\ -0.2286 & -0.2288 \\ -0.1872 & -0.1871 \end{bmatrix} \tilde{\theta}_{\text{tv2}}^\top = \begin{bmatrix} -0.1168 & -0.1180 \\ 0.2815 & 0.2806 \\ 0.0524 & 0.0521 \\ -0.0681 & -0.0679 \\ 0.1325 & 0.1324 \\ 0.6608 & 0.6621 \\ 0.0469 & 0.0478 \\ -0.3765 & -0.3763 \\ -0.4280 & -0.4282 \\ -0.3432 & -0.3430 \end{bmatrix} \tilde{\theta}_{\text{tv3}}^\top = \begin{bmatrix} -0.2083 & -0.2095 \\ 0.0601 & 0.0592 \\ 0.1758 & 0.1756 \\ 0.0422 & 0.0424 \\ 0.2841 & 0.2839 \\ -0.4798 & -0.4785 \\ 0.4709 & 0.4718 \\ 0.2549 & 0.2552 \\ -0.3652 & -0.3654 \\ -0.4361 & -0.4359 \end{bmatrix} \tag{A.77}$$

$$\tilde{\theta}_{\text{tv4}}^\top = \begin{bmatrix} -0.2004 & -0.2016 \\ -0.3122 & -0.3131 \\ 0.0196 & 0.0194 \\ 0.0267 & 0.0268 \\ 0.0385 & 0.0384 \\ 0.2104 & 0.2117 \\ -0.4662 & -0.4654 \\ 0.4262 & 0.4265 \\ 0.2399 & 0.2397 \\ -0.5981 & -0.5979 \end{bmatrix} \tilde{\theta}_{\text{tv5}}^\top = \begin{bmatrix} 0.0024 & 0.0012 \\ 0.1029 & 0.1020 \\ -0.1826 & -0.1828 \\ -0.0042 & -0.0040 \\ -0.1746 & -0.1747 \\ -0.1026 & -0.1013 \\ 0.3605 & 0.3613 \\ -0.4395 & -0.4393 \\ 0.6226 & 0.6224 \\ -0.4504 & -0.4503 \end{bmatrix} \tilde{\theta}_{\text{tv6}}^\top = \begin{bmatrix} 0.2329 & 0.2316 \\ 0.2147 & 0.2138 \\ -0.4149 & -0.4151 \\ -0.5979 & -0.5977 \\ 0.5709 & 0.5707 \\ -0.0246 & -0.0233 \\ -0.0615 & -0.0606 \\ 0.1432 & 0.1434 \\ 0.1295 & 0.1293 \\ 0.0028 & 0.0029 \end{bmatrix} \tag{A.78}$$

$$\tilde{\theta}_{\text{tv7}}^{\top} = \begin{bmatrix} 0.2643 & 0.2631 \\ 0.3617 & 0.3608 \\ 0.1458 & 0.1455 \\ 0.6769 & 0.6771 \\ 0.4960 & 0.4958 \\ 0.0339 & 0.0352 \\ -0.1279 & -0.1271 \\ 0.0267 & 0.0269 \\ 0.2335 & 0.2333 \\ 0.0156 & 0.0157 \end{bmatrix} \quad \tilde{\theta}_{\text{tv8}}^{\top} = \begin{bmatrix} 0.1826 & 0.1813 \\ -0.1897 & -0.1906 \\ 0.8009 & 0.8006 \\ -0.3613 & -0.3612 \\ 0.2108 & 0.2106 \\ -0.0694 & -0.0681 \\ -0.0929 & -0.0920 \\ -0.2638 & -0.2635 \\ 0.1701 & 0.1699 \\ -0.0072 & -0.0070 \end{bmatrix} \quad \tilde{\theta}_{\text{tv9}}^{\top} = \begin{bmatrix} 0.4447 & 0.4434 \\ -0.6704 & -0.6712 \\ -0.2796 & -0.2799 \\ 0.1999 & 0.2001 \\ 0.2137 & 0.2135 \\ -0.0591 & -0.0577 \\ 0.0160 & 0.0169 \\ -0.3143 & -0.3141 \\ -0.2586 & -0.2588 \\ -0.1471 & -0.1470 \end{bmatrix} \tag{A.79}$$

$$\tilde{\theta}_{\text{tv10}}^{\top} = \begin{bmatrix} 0.7377 & 0.7365 \\ 0.2500 & 0.2492 \\ 0.1051 & 0.1049 \\ -0.0760 & -0.0759 \\ -0.4373 & -0.4374 \\ 0.0359 & 0.0372 \\ 0.0452 & 0.0461 \\ 0.3023 & 0.3025 \\ -0.1378 & -0.1380 \\ -0.2672 & -0.2671 \end{bmatrix} \quad \tilde{\theta}_{\text{tv11}}^{\top} = \begin{bmatrix} 0.0559 & 0.0547 \\ -0.2911 & -0.2920 \\ 0.0904 & 0.0902 \\ 0.0229 & 0.0231 \\ 0.1211 & 0.1209 \\ 0.5168 & 0.5181 \\ 0.6320 & 0.6329 \\ 0.3708 & 0.3711 \\ 0.2264 & 0.2262 \\ 0.1885 & 0.1887 \end{bmatrix} \quad \tilde{\theta}_{\text{tv12}}^{\top} = \begin{bmatrix} 0.1166 & 0.1153 \\ -0.2837 & -0.2845 \\ -0.0533 & -0.0536 \\ 0.0704 & 0.0706 \\ -0.1338 & -0.1340 \\ -0.6607 & -0.6593 \\ -0.0447 & -0.0438 \\ 0.3774 & 0.3777 \\ 0.4258 & 0.4256 \\ 0.3445 & 0.3446 \end{bmatrix} \tag{A.80}$$

$$\tilde{\theta}_{\text{tv13}}^{\top} = \begin{bmatrix} 0.2081 & 0.2068 \\ -0.0623 & -0.0631 \\ -0.1768 & -0.1770 \\ -0.0400 & -0.0398 \\ -0.2853 & -0.2855 \\ 0.4800 & 0.4813 \\ -0.4687 & -0.4678 \\ -0.2541 & -0.2538 \\ 0.3630 & 0.3628 \\ 0.4373 & 0.4375 \end{bmatrix} \quad \tilde{\theta}_{\text{tv14}}^{\top} = \begin{bmatrix} 0.2002 & 0.1989 \\ 0.3100 & 0.3092 \\ -0.0206 & -0.0208 \\ -0.0244 & -0.0242 \\ -0.0398 & -0.0400 \\ -0.2102 & -0.2089 \\ 0.4685 & 0.4694 \\ -0.4254 & -0.4251 \\ -0.2421 & -0.2422 \\ 0.5994 & 0.5995 \end{bmatrix} \quad \tilde{\theta}_{\text{tv15}}^{\top} = \begin{bmatrix} -0.0026 & -0.0039 \\ -0.1051 & -0.1059 \\ 0.1816 & 0.1814 \\ 0.0064 & 0.0066 \\ 0.1733 & 0.1731 \\ 0.1027 & 0.1041 \\ -0.3582 & -0.3574 \\ 0.4404 & 0.4407 \\ -0.6248 & -0.6250 \\ 0.4517 & 0.4519 \end{bmatrix} \tag{A.81}$$

$$\tilde{\theta}_{\text{tv16}}^{\top} = \begin{bmatrix} -0.2331 & -0.2343 \\ -0.2169 & -0.2178 \\ 0.4139 & 0.4137 \\ 0.6001 & 0.6003 \\ -0.5722 & -0.5724 \\ 0.0248 & 0.0261 \\ 0.0637 & 0.0646 \\ -0.1423 & -0.1420 \\ -0.1317 & -0.1319 \\ -0.0015 & -0.0013 \end{bmatrix} \tilde{\theta}_{\text{tv17}}^{\top} = \begin{bmatrix} -0.2645 & -0.2657 \\ -0.3639 & -0.3647 \\ -0.1467 & -0.1469 \\ -0.6747 & -0.6745 \\ -0.4973 & -0.4974 \\ -0.0337 & -0.0324 \\ 0.1302 & 0.1310 \\ -0.0258 & -0.0255 \\ -0.2357 & -0.2359 \\ -0.0143 & -0.0141 \end{bmatrix} \tilde{\theta}_{\text{tv18}}^{\top} = \begin{bmatrix} -0.1828 & -0.1840 \\ 0.1875 & 0.1866 \\ -0.8018 & -0.8020 \\ 0.3636 & 0.3638 \\ -0.2121 & -0.2122 \\ 0.0696 & 0.0709 \\ 0.0951 & 0.0960 \\ 0.2647 & 0.2649 \\ -0.1723 & -0.1725 \\ 0.0085 & 0.0086 \end{bmatrix} \tag{A.82}$$

$$\tilde{\theta}_{\text{tv19}}^{\top} = \begin{bmatrix} -0.4449 & -0.4461 \\ 0.6681 & 0.6673 \\ 0.2787 & 0.2784 \\ -0.1976 & -0.1974 \\ -0.2150 & -0.2152 \\ 0.0592 & 0.0605 \\ -0.0138 & -0.0129 \\ 0.3152 & 0.3154 \\ 0.2564 & 0.2562 \\ 0.1484 & 0.1485 \end{bmatrix} \tilde{\theta}_{\text{tv20}}^{\top} = \begin{bmatrix} -0.7379 & -0.7392 \\ -0.2522 & -0.2531 \\ -0.1061 & -0.1063 \\ 0.0783 & 0.0785 \\ 0.4360 & 0.4358 \\ -0.0358 & -0.0344 \\ -0.0430 & -0.0421 \\ -0.3014 & -0.3012 \\ 0.1356 & 0.1354 \\ 0.2685 & 0.2686 \end{bmatrix} \tag{A.83}$$

A.11 Matrices and parameters for LPV-OBF MPC in Chapter 6 HPDC/case1

LPV-OBF model coefficient for global approach $\{\vartheta_s\}_{s=1}^{120}$

$$\{\vartheta_s\}_{s=1}^{120}{}^{\top} = \begin{bmatrix} -1.8545 & 8.9413 \\ 1.6703 & 8.2037 \\ 5.6753 & -27.5218 \\ 0.5173 & 1.9983 \\ -3.4866 & -16.5507 \\ -5.7889 & 28.1644 \\ -0.9305 & -3.3733 \\ -0.3754 & -1.3838 \\ 1.8103 & 8.3121 \\ 1.9682 & -9.5838 \\ -0.1149 & -3.4547 \\ -0.0409 & -1.3333 \\ 0.3702 & 11.2011 \\ 0.4964 & 0.5162 \\ 0.0349 & 2.9097 \\ -0.3948 & -12.0596 \\ 0.8937 & -0.0942 \\ -0.6752 & -0.4249 \\ 0.0153 & -1.5894 \\ 0.1394 & 4.3131 \\ 1.5948 & -11.3540 \\ -0.7791 & -11.5456 \\ -4.9133 & 35.6576 \\ -0.2896 & -5.6312 \\ 1.6484 & 24.8830 \\ 5.0450 & -37.3098 \\ -0.0652 & 6.3492 \\ 0.3144 & 4.5060 \\ -0.8723 & -13.2861 \\ -1.7264 & 13.0053 \\ 0.3347 & -4.6877 \\ -0.1965 & -12.2092 \\ -0.9850 & 14.8794 \\ 0.2702 & 2.0692 \\ 0.3875 & 25.2058 \\ 0.9649 & -15.7202 \\ 0.0899 & 7.9549 \\ -0.2990 & -3.5602 \\ -0.1894 & -12.9220 \\ -0.3146 & 5.5273 \\ -0.6004 & 5.9958 \\ \vdots & \vdots \end{bmatrix} \begin{bmatrix} \vdots & \vdots \\ -0.3346 & 7.1825 \\ 1.8393 & -19.3085 \\ -0.2694 & 0.6224 \\ 0.7205 & -14.9486 \\ -1.8781 & 20.7110 \\ -0.1225 & -6.0411 \\ 0.3038 & 0.4272 \\ -0.3888 & 7.7256 \\ 0.6392 & -7.3990 \\ 1.6857 & -5.6382 \\ -1.2038 & -8.8765 \\ -5.1747 & 17.3465 \\ -0.6166 & -2.3771 \\ 2.5457 & 18.0730 \\ 5.2945 & -17.7157 \\ 0.8737 & 3.5084 \\ 0.4879 & 1.7178 \\ -1.3365 & -9.1581 \\ -1.8056 & 6.0073 \\ 0.1506 & 2.3449 \\ -0.1817 & 1.1507 \\ -0.4713 & -7.7450 \\ -0.3963 & -0.0889 \\ 0.4108 & -2.5222 \\ 0.4900 & 8.4729 \\ -0.9120 & -0.2265 \\ 0.5748 & 0.0484 \\ -0.2384 & 1.3820 \\ -0.1691 & -3.0728 \\ -1.5494 & 12.2249 \\ 0.8712 & 11.6453 \\ 4.7698 & -38.3742 \\ 0.2195 & 5.2509 \\ -1.8273 & -25.0424 \\ -4.8942 & 40.1325 \\ 0.1027 & -6.1296 \\ -0.2479 & -4.1575 \\ 0.9591 & 13.3472 \\ \vdots & \vdots \end{bmatrix} \begin{bmatrix} \vdots & \vdots \\ -0.3944 & 3.7267 \\ 0.1653 & 11.9115 \\ 1.1698 & -11.9022 \\ -0.2439 & -1.5877 \\ -0.3275 & -24.6485 \\ -1.1553 & 12.6472 \\ -0.1118 & -8.0813 \\ 0.2752 & 3.0931 \\ 0.1604 & 12.6618 \\ 0.3800 & -4.4704 \\ 0.6067 & -5.7882 \\ 0.3363 & -7.2297 \\ -1.8588 & 18.6670 \\ 0.2705 & -0.6482 \\ -0.7239 & 15.0471 \\ 1.8982 & -20.0506 \\ 0.1244 & 6.0250 \\ -0.3052 & -0.3983 \\ 0.3906 & -7.7772 \\ -0.6461 & 7.1723 \\ 1.3505 & 3.1441 \\ 0.9164 & 4.0498 \\ -4.2046 & -9.7770 \\ -0.4816 & -2.3289 \\ -1.8208 & -8.1129 \\ 4.3606 & 10.1297 \\ -0.1614 & -0.8691 \\ 0.5251 & 2.5231 \\ 0.9018 & 4.0542 \\ -1.5065 & -3.4968 \\ -1.1822 & -5.9759 \\ -1.2249 & -2.1218 \\ 3.6999 & 18.4622 \\ 0.4981 & 1.5237 \\ 2.4511 & 4.2220 \\ -3.8566 & -19.0089 \\ 0.2379 & 1.1967 \\ -0.5553 & -1.7336 \\ -1.2230 & -2.0915 \\ 1.3388 & 6.5226 \end{bmatrix} \tag{A.84}$$

LQR of LPV-OBF MPC

$$P = \begin{bmatrix} P_{LPV} & 0 \\ 0 & P_{LPV} \end{bmatrix} \tag{A.85}$$

with

$$P_{LPV} = \begin{bmatrix} 4.3955 & 3.6629 & 1.3480 & 0.5804 & 0.0411 \\ 3.6629 & 9.2355 & 6.1262 & 2.2505 & 0.1534 \\ 1.3480 & 6.1262 & 10.1923 & 6.4840 & 0.4077 \\ 0.5804 & 2.2505 & 6.4840 & 11.1608 & 4.1273 \\ 0.0411 & 0.1534 & 0.4077 & 4.1273 & 4.6916 \end{bmatrix} \tag{A.86}$$

Transposed K matrix

$$K^\top = \begin{bmatrix} 0.8124 & 0.0000 \\ 0.4735 & 0.0000 \\ 0.2050 & 0.0000 \\ 0.0915 & 0.0000 \\ 0.0066 & 0.0000 \\ 0.0000 & 0.8124 \\ 0.0000 & 0.4735 \\ 0.0000 & 0.2050 \\ 0.0000 & 0.0915 \\ 0.0000 & 0.0066 \end{bmatrix} \tag{A.87}$$

A.12 Matrices and parameters for MPC in Chapter 6 DDC/case2

$$P_{LTV} = [P_{LTV1} \;\; P_{LTV2} \;\; P_{LTV3}] \tag{A.88}$$

P matrix is truncated due to limited paper space

$$P_{LTV1} = \begin{bmatrix} 3.1251 & -2.5563 & 6.5102 & -0.6443 & -6.1922 & -2.8919 & -0.0951 \\ -2.5563 & 8.0741 & -11.6502 & 2.4152 & 17.0408 & 7.8433 & 0.0501 \\ 6.5102 & -11.6502 & 22.0498 & -2.4284 & -26.4909 & -11.5793 & -2.1235 \\ -0.6443 & 2.4152 & -2.4284 & 1.5239 & 4.9286 & 2.6861 & -1.4085 \\ -6.1922 & 17.0408 & -26.4909 & 4.9286 & 38.4591 & 17.2567 & 1.7655 \\ -2.8919 & 7.8433 & -11.5793 & 2.6861 & 17.2567 & 8.5027 & -0.6176 \\ -0.0951 & 0.0501 & -2.1235 & -1.4085 & 1.7655 & -0.6176 & 5.4133 \\ 3.2262 & -7.9782 & 11.7641 & -3.0026 & -17.0983 & -8.3358 & 1.9167 \\ -1.1387 & -0.6018 & -0.5062 & -0.2543 & -1.2967 & -0.4151 & -0.2092 \\ 2.2854 & -6.3167 & 9.5505 & -1.8553 & -13.4611 & -6.3214 & -0.0892 \\ -16.0032 & 29.9766 & -54.3126 & 6.8850 & 68.0791 & 29.9918 & 5.0946 \\ -8.3371 & 13.2762 & -26.7091 & 1.9820 & 30.6309 & 12.4664 & 4.6002 \\ 22.1701 & -59.8377 & 91.9137 & -17.2589 & -130.7269 & -59.6597 & -2.2402 \\ 4.0412 & 3.0075 & -0.6391 & 1.0372 & 6.8454 & 1.0067 & 1.3692 \\ -5.6317 & 14.7433 & -26.0848 & 2.5443 & 35.5520 & 14.7473 & 8.0326 \\ 7.8798 & -24.9533 & 31.6067 & -11.5594 & -51.9822 & -27.0827 & 10.4623 \\ -0.9352 & 2.2575 & -2.8374 & 1.2630 & 4.5170 & 2.5501 & -1.7751 \\ -0.0342 & 0.3974 & -0.4762 & 0.1645 & 0.8187 & 0.3579 & -0.1336 \\ -3.6775 & 9.7404 & -13.2826 & 4.2874 & 20.3219 & 10.4394 & -3.9640 \\ -0.6151 & 1.9030 & -2.4246 & 0.8853 & 3.9313 & 2.0730 & -0.9034 \end{bmatrix} \tag{A.89}$$

$$P_{LTV2} = \begin{bmatrix} 3.2262 & -1.1387 & 2.2854 & -16.0032 & -8.3371 & 22.1701 & 4.0412 \\ -7.9782 & -0.6018 & -6.3167 & 29.9766 & 13.2762 & -59.8377 & 3.0075 \\ 11.7641 & -0.5062 & 9.5505 & -54.3126 & -26.7091 & 91.9137 & -0.6391 \\ -3.0026 & -0.2543 & -1.8553 & 6.8850 & 1.9820 & -17.2589 & 1.0372 \\ -17.0983 & -1.2967 & -13.4611 & 68.0791 & 30.6309 & -130.7269 & 6.8454 \\ -8.3358 & -0.4151 & -6.3214 & 29.9918 & 12.4664 & -59.6597 & 1.0067 \\ 1.9167 & -0.2092 & -0.0892 & 5.0946 & 4.6002 & -2.2402 & 1.3692 \\ 9.2064 & 0.2328 & 6.3572 & -30.3898 & -12.9063 & 60.3364 & -1.7345 \\ 0.2328 & 2.7679 & 0.5415 & 4.1166 & 1.5645 & 4.3995 & -4.5095 \\ 6.3572 & 0.5415 & 5.4649 & -24.6965 & -11.3205 & 47.9840 & -1.0762 \\ -30.3898 & 4.1166 & -24.6965 & 149.7394 & 72.9015 & -239.6697 & -1.9930 \\ -12.9063 & 1.5645 & -11.3205 & 72.9015 & 39.6453 & -110.6774 & -2.3403 \\ 60.3364 & 4.3995 & 47.9840 & -239.6697 & -110.6774 & 465.5145 & -14.6373 \\ -1.7345 & -4.5095 & -1.0762 & -1.9930 & -2.3403 & -14.6373 & 30.7797 \\ -12.3852 & 0.9023 & -11.4550 & 67.0327 & 29.6612 & -108.8341 & 7.5582 \\ 29.6112 & 2.3749 & 19.3144 & -78.4178 & -27.0700 & 181.2225 & -9.5438 \\ -3.0866 & -0.1913 & -1.8055 & 6.8036 & 2.2520 & -16.4570 & 0.5066 \\ -0.4572 & -0.1185 & -0.3164 & 1.1382 & 0.4647 & -2.8673 & 0.8612 \\ -11.6690 & -0.7741 & -7.6749 & 32.7248 & 12.5593 & -72.1580 & 2.6702 \\ -2.3062 & -0.2258 & -1.4684 & 5.6863 & 1.8787 & -13.7601 & 0.7179 \end{bmatrix} \tag{A.90}$$

$$P_{LTV3} = \begin{bmatrix} -5.6317 & 7.8798 & -0.9352 & -0.0342 & -3.6775 & -0.6151 \\ 14.7433 & -24.9533 & 2.2575 & 0.3974 & 9.7404 & 1.9030 \\ -26.0848 & 31.6067 & -2.8374 & -0.4762 & -13.2826 & -2.4246 \\ 2.5443 & -11.5594 & 1.2630 & 0.1645 & 4.2874 & 0.8853 \\ 35.5520 & -51.9822 & 4.5170 & 0.8187 & 20.3219 & 3.9313 \\ 14.7473 & -27.0827 & 2.5501 & 0.3579 & 10.4394 & 2.0730 \\ 8.0326 & 10.4623 & -1.7751 & -0.1336 & -3.9640 & -0.9034 \\ -12.3852 & 29.6112 & -3.0866 & -0.4572 & -11.6690 & -2.3062 \\ 0.9023 & 2.3749 & -0.1913 & -0.1185 & -0.7741 & -0.2258 \\ -11.4550 & 19.3144 & -1.8055 & -0.3164 & -7.6749 & -1.4684 \\ 67.0327 & -78.4178 & 6.8036 & 1.1382 & 32.7248 & 5.6863 \\ 29.6612 & -27.0700 & 2.2520 & 0.4647 & 12.5593 & 1.8787 \\ -108.8341 & 181.2225 & -16.4570 & -2.8673 & -72.1580 & -13.7601 \\ 7.5582 & -9.5438 & 0.5066 & 0.8612 & 2.6702 & 0.7179 \\ 53.9739 & -31.5931 & 1.1271 & 0.4170 & 11.6224 & 2.2308 \\ -31.5931 & 109.2799 & -11.7810 & -1.6250 & -41.4615 & -8.5630 \\ 1.1271 & -11.7810 & 1.7444 & 0.2417 & 4.9048 & 0.9282 \\ 0.4170 & -1.6250 & 0.2417 & 0.1531 & 0.6390 & 0.1148 \\ 11.6224 & -41.4615 & 4.9048 & 0.6390 & 16.9231 & 3.4791 \\ 2.2308 & -8.5630 & 0.9282 & 0.1148 & 3.4791 & 0.8819 \end{bmatrix} \tag{A.91}$$

K matrix and the vertices are transposed due to limited paper space

$$K_{\text{orc}}^{\top} = \begin{bmatrix} -0.1033 & 0.7975 & 0.0095 & -0.1159 & 0.2188 \\ -0.3178 & -0.6997 & 0.1590 & -0.1544 & -0.1494 \\ -0.0344 & 1.5379 & -0.1247 & 0.0450 & 0.1790 \\ -0.0801 & -0.1815 & 0.0027 & -0.0643 & -0.1912 \\ -0.2987 & -1.6836 & 0.1419 & -0.3020 & -0.1828 \\ -0.2267 & -1.0637 & 0.0556 & -0.1112 & -0.2476 \\ 0.0848 & -0.0939 & 0.0531 & -0.0158 & 0.5444 \\ 0.1672 & 0.8246 & -0.0722 & 0.1023 & 0.4096 \\ 0.0156 & -0.3838 & -0.4049 & 0.1427 & -0.0887 \\ 0.2187 & 0.7477 & -0.2899 & 0.0830 & 0.1572 \\ -0.3576 & -4.3226 & -0.2709 & 0.0773 & -0.4473 \\ -0.0695 & -2.0111 & 0.2715 & 0.1621 & -0.1020 \\ 1.8045 & 6.2185 & -1.2508 & 0.7748 & 1.2618 \\ 0.6537 & 3.0831 & -0.1449 & -0.7890 & 0.7174 \\ 0.0284 & -1.6813 & -0.5096 & -0.4211 & 0.8286 \\ 0.6643 & 2.1046 & -0.1388 & 0.5729 & 1.6916 \\ -0.0330 & -0.1955 & 0.0394 & -0.0333 & -0.3484 \\ 0.0122 & 0.0527 & 0.0144 & -0.0230 & -0.0669 \\ -0.2126 & -0.8938 & 0.1346 & -0.1650 & -0.8006 \\ -0.0473 & -0.1574 & 0.0193 & -0.0445 & -0.1334 \end{bmatrix} \tag{A.92}$$

$$\tilde{\theta}_{\text{tv1}}^{\top} = \begin{bmatrix} 2.9969 & -1.2892 \\ -10.9441 & 1.5302 \\ 16.2904 & -3.6052 \\ -2.7590 & -0.5226 \\ -22.3824 & 0.6521 \\ -9.1454 & -0.5713 \\ -1.3249 & 1.1479 \\ 10.5804 & -0.6017 \\ 1.8665 & -0.5692 \\ 9.6751 & -2.2213 \\ -39.6454 & 6.4579 \\ -20.2297 & 8.8703 \\ 79.2116 & -8.5846 \\ -12.4640 & 0.6420 \\ -18.0098 & -2.1990 \\ 30.7208 & 3.5098 \\ -2.8073 & 0.2812 \\ -0.3879 & 0.8142 \\ -12.4704 & 0.3193 \\ -2.3078 & -0.2537 \end{bmatrix} \quad \tilde{\theta}_{\text{tv2}}^{\top} = \begin{bmatrix} 3.0029 & -1.2832 \\ -11.0271 & 1.4472 \\ 16.3355 & -3.5601 \\ -2.8823 & -0.6459 \\ -22.5141 & 0.5203 \\ -9.2866 & -0.7125 \\ -1.0332 & 1.4396 \\ 10.9152 & -0.2669 \\ 2.0087 & -0.4270 \\ 8.7256 & -3.1708 \\ -39.3174 & 6.7859 \\ -20.1953 & 8.9047 \\ 79.2441 & -8.5521 \\ -12.2115 & 0.8946 \\ -18.0961 & -2.2854 \\ 31.1574 & 3.9464 \\ -2.5986 & 0.4899 \\ -0.9266 & 0.2755 \\ -12.8027 & -0.0130 \\ -2.3693 & -0.3153 \end{bmatrix} \quad \tilde{\theta}_{\text{tv3}}^{\top} = \begin{bmatrix} 3.0282 & -1.2579 \\ -11.1732 & 1.3011 \\ 16.2733 & -3.6223 \\ -2.7360 & -0.4996 \\ -22.3971 & 0.6374 \\ -9.0028 & -0.4287 \\ -1.1622 & 1.3106 \\ 10.5867 & -0.5954 \\ 2.3875 & -0.0482 \\ 9.3108 & -2.5856 \\ -38.9753 & 7.1280 \\ -20.1032 & 8.9968 \\ 79.0640 & -8.7322 \\ -12.3367 & 0.7693 \\ -18.5438 & -2.7330 \\ 30.8250 & 3.6141 \\ -2.9704 & 0.1181 \\ -1.0714 & 0.1307 \\ -12.0762 & 0.7135 \\ -2.0926 & -0.0386 \end{bmatrix} \tag{A.93}$$

$$\tilde{\theta}_{\text{tv4}}^{\top} = \begin{bmatrix} 2.8801 & -1.4060 \\ -11.2924 & 1.1820 \\ 16.4264 & -3.4692 \\ -2.8514 & -0.6150 \\ -22.3683 & 0.6662 \\ -9.1674 & -0.5933 \\ -1.0833 & 1.3895 \\ 10.5743 & -0.6078 \\ 1.8159 & -0.6198 \\ 9.4683 & -2.4281 \\ -39.2901 & 6.8132 \\ -20.1787 & 8.9213 \\ 79.1510 & -8.6451 \\ -12.3663 & 0.7397 \\ -18.6096 & -2.7989 \\ 30.5564 & 3.3454 \\ -3.0309 & 0.0577 \\ -1.0975 & 0.1046 \\ -13.2362 & -0.4465 \\ -2.0532 & 0.0008 \end{bmatrix} \quad \tilde{\theta}_{\text{tv5}}^{\top} = \begin{bmatrix} 2.8390 & -1.4471 \\ -11.3521 & 1.1222 \\ 15.8108 & -4.0849 \\ -2.6790 & -0.4426 \\ -22.1787 & 0.8558 \\ -9.3059 & -0.7318 \\ -1.2931 & 1.1797 \\ 10.6039 & -0.5782 \\ 1.7906 & -0.6451 \\ 9.4628 & -2.4336 \\ -39.0506 & 7.0527 \\ -20.5433 & 8.5568 \\ 79.2380 & -8.5581 \\ -12.6323 & 0.4737 \\ -17.9658 & -2.1551 \\ 30.9590 & 3.7480 \\ -2.8422 & 0.2463 \\ -1.3177 & -0.1156 \\ -12.6163 & 0.1734 \\ -2.4679 & -0.4138 \end{bmatrix} \quad \tilde{\theta}_{\text{tv6}}^{\top} = \begin{bmatrix} 3.0146 & -1.2715 \\ -11.0470 & 1.4273 \\ 16.3763 & -3.5193 \\ -2.2772 & -0.0408 \\ -22.7869 & 0.2476 \\ -9.3925 & -0.8184 \\ -0.7990 & 1.6738 \\ 10.7650 & -0.4171 \\ 1.9878 & -0.4479 \\ 9.4116 & -2.4849 \\ -39.1611 & 6.9422 \\ -20.2668 & 8.8332 \\ 79.5899 & -8.2062 \\ -12.3496 & 0.7564 \\ -17.9998 & -2.1890 \\ 30.7121 & 3.5011 \\ -3.3506 & -0.2621 \\ -1.0403 & 0.1619 \\ -12.5957 & 0.1939 \\ -2.3439 & -0.2899 \end{bmatrix} \tag{A.94}$$

$$\tilde{\theta}_{\text{tv7}}^{\top} = \begin{bmatrix} 2.6228 & -1.6633 \\ -11.2045 & 1.2698 \\ 16.4018 & -3.4938 \\ -3.0184 & -0.7820 \\ -22.5578 & 0.4767 \\ -9.8277 & -1.2536 \\ -0.9321 & 1.5407 \\ 10.1333 & -1.0488 \\ 2.0536 & -0.3821 \\ 9.2719 & -2.6246 \\ -39.0534 & 7.0499 \\ -20.2407 & 8.8593 \\ 79.1789 & -8.6173 \\ -12.3751 & 0.7309 \\ -18.2175 & -2.4068 \\ 30.6351 & 3.4241 \\ -2.8467 & 0.2418 \\ -0.8233 & 0.3788 \\ -12.5079 & 0.2818 \\ -2.5564 & -0.5023 \end{bmatrix} \tilde{\theta}_{\text{tv8}}^{\top} = \begin{bmatrix} 2.9076 & -1.3785 \\ -10.5238 & 1.9505 \\ 16.3029 & -3.5927 \\ -2.7815 & -0.5452 \\ -21.9136 & 1.1209 \\ -9.6459 & -1.0718 \\ -1.1723 & 1.3006 \\ 10.7992 & -0.3829 \\ 2.1957 & -0.2400 \\ 9.4537 & -2.4428 \\ -39.2238 & 6.8795 \\ -20.2873 & 8.8127 \\ 79.1135 & -8.6827 \\ -12.2448 & 0.8612 \\ -18.3421 & -2.5313 \\ 30.8835 & 3.6726 \\ -3.2480 & -0.1595 \\ -1.0546 & 0.1476 \\ -12.7114 & 0.0783 \\ -2.5163 & -0.4623 \end{bmatrix} \tilde{\theta}_{\text{tv9}}^{\top} = \begin{bmatrix} 3.1484 & -1.1377 \\ -10.9012 & 1.5732 \\ 16.2369 & -3.6587 \\ -2.9077 & -0.6714 \\ -22.3408 & 0.6937 \\ -9.3185 & -0.7445 \\ -1.0682 & 1.4046 \\ 10.6896 & -0.4925 \\ 2.0501 & -0.3856 \\ 9.2078 & -2.6886 \\ -38.6306 & 7.4727 \\ -20.3710 & 8.7290 \\ 79.3715 & -8.4247 \\ -12.9501 & 0.1559 \\ -18.2597 & -2.4489 \\ 30.7880 & 3.5771 \\ -3.0520 & 0.0365 \\ -0.5101 & 0.6920 \\ -12.8224 & -0.0328 \\ -2.2014 & -0.1474 \end{bmatrix} \tag{A.95}$$

$$\tilde{\theta}_{\text{tv10}}^{\top} = \begin{bmatrix} 3.0193 & -1.2668 \\ -11.0003 & 1.4741 \\ 16.2705 & -3.6251 \\ -2.8456 & -0.6093 \\ -22.2627 & 0.7718 \\ -9.2025 & -0.6284 \\ -0.8740 & 1.5989 \\ 10.3991 & -0.7830 \\ 2.1176 & -0.3181 \\ 9.7839 & -2.1125 \\ -38.9058 & 7.1975 \\ -20.2336 & 8.8664 \\ 79.7508 & -8.0453 \\ -12.0689 & 1.0371 \\ -18.2994 & -2.4886 \\ 31.2023 & 3.9914 \\ -2.6534 & 0.4351 \\ -0.8599 & 0.3422 \\ -12.7905 & -0.0008 \\ -2.3421 & -0.2881 \end{bmatrix} \tilde{\theta}_{\text{tv11}}^{\top} = \begin{bmatrix} 3.6418 & -0.6443 \\ -10.8962 & 1.5782 \\ 16.0864 & -3.8092 \\ -2.9109 & -0.6745 \\ -22.3976 & 0.6369 \\ -9.4842 & -0.9102 \\ -1.1201 & 1.3527 \\ 10.3124 & -0.8697 \\ 1.8410 & -0.5947 \\ 9.3619 & -2.5345 \\ -39.0185 & 7.0848 \\ -19.9179 & 9.1822 \\ 79.1253 & -8.6709 \\ -12.2135 & 0.8926 \\ -17.9237 & -2.1129 \\ 30.6533 & 3.4423 \\ -2.9290 & 0.1595 \\ -1.1187 & 0.0835 \\ -12.7005 & 0.0892 \\ -2.1837 & -0.1297 \end{bmatrix} \tilde{\theta}_{\text{tv12}}^{\top} = \begin{bmatrix} 3.5417 & -0.7444 \\ -11.3010 & 1.1734 \\ 16.2256 & -3.6700 \\ -2.9454 & -0.7090 \\ -22.4145 & 0.6200 \\ -9.4483 & -0.8742 \\ -0.9704 & 1.5024 \\ 10.6230 & -0.5591 \\ 2.3255 & -0.1102 \\ 9.3972 & -2.4993 \\ -39.3668 & 6.7365 \\ -20.8878 & 8.2122 \\ 79.2922 & -8.5039 \\ -12.2851 & 0.8209 \\ -18.3790 & -2.5683 \\ 30.6842 & 3.4732 \\ -2.9427 & 0.1459 \\ -0.8857 & 0.3165 \\ -12.6810 & 0.1087 \\ -2.4851 & -0.4311 \end{bmatrix} \tag{A.96}$$

$$\tilde{\theta}_{\text{tv13}}^{\top} = \begin{bmatrix} 3.1504 & -1.1357 \\ -10.9842 & 1.4901 \\ 16.5510 & -3.3446 \\ -2.3257 & -0.0893 \\ -22.4115 & 0.6230 \\ -9.2562 & -0.6822 \\ -1.4238 & 1.0490 \\ 10.0601 & -1.1220 \\ 1.9629 & -0.4728 \\ 9.1885 & -2.7079 \\ -39.0236 & 7.0797 \\ -20.5835 & 8.5166 \\ 79.0573 & -8.7389 \\ -12.2628 & 0.8432 \\ -18.2657 & -2.4550 \\ 31.1299 & 3.9189 \\ -3.0395 & 0.0490 \\ -0.8269 & 0.3753 \\ -12.8170 & -0.0273 \\ -2.3690 & -0.3150 \end{bmatrix} \quad \tilde{\theta}_{\text{tv14}}^{\top} = \begin{bmatrix} 3.0350 & -1.2511 \\ -11.0184 & 1.4560 \\ 16.6145 & -3.2811 \\ -3.1566 & -0.9203 \\ -22.8471 & 0.1874 \\ -9.3643 & -0.7902 \\ -1.5670 & 0.9059 \\ 10.8380 & -0.3441 \\ 2.0221 & -0.4136 \\ 9.6866 & -2.2099 \\ -38.8666 & 7.2367 \\ -20.4315 & 8.6685 \\ 79.1656 & -8.6306 \\ -12.2660 & 0.8400 \\ -18.0647 & -2.2539 \\ 30.9493 & 3.7384 \\ -3.0068 & 0.0817 \\ -1.0789 & 0.1233 \\ -12.6933 & 0.0964 \\ -2.3853 & -0.3313 \end{bmatrix} \quad \tilde{\theta}_{\text{tv15}}^{\top} = \begin{bmatrix} 3.1169 & -1.1692 \\ -11.5992 & 0.8751 \\ 16.4797 & -3.4159 \\ -2.8669 & -0.6305 \\ -22.1362 & 0.8982 \\ -9.5453 & -0.9713 \\ -1.0511 & 1.4217 \\ 10.6188 & -0.5633 \\ 2.2191 & -0.2166 \\ 9.4738 & -2.4227 \\ -39.1696 & 6.9338 \\ -20.1076 & 8.9924 \\ 79.1003 & -8.6958 \\ -12.3722 & 0.7338 \\ -17.8936 & -2.0829 \\ 31.2567 & 4.0458 \\ -3.3120 & -0.2234 \\ -0.7371 & 0.4650 \\ -12.7407 & 0.0489 \\ -2.1219 & -0.0679 \end{bmatrix} \tag{A.97}$$

$$\tilde{\theta}_{\text{tv16}}^{\top} = \begin{bmatrix} 3.0469 & -1.2392 \\ -11.0471 & 1.4272 \\ 16.9010 & -2.9946 \\ -2.8113 & -0.5749 \\ -21.9737 & 1.0608 \\ -9.2713 & -0.6973 \\ -0.9503 & 1.5225 \\ 10.6093 & -0.5728 \\ 1.8872 & -0.5485 \\ 9.3345 & -2.5619 \\ -39.0022 & 7.1011 \\ -20.5906 & 8.5094 \\ 79.3093 & -8.4868 \\ -12.3474 & 0.7586 \\ -17.8643 & -2.0536 \\ 30.5904 & 3.3795 \\ -2.7455 & 0.3430 \\ -1.0979 & 0.1043 \\ -12.4875 & 0.3022 \\ -2.0681 & -0.0141 \end{bmatrix} \quad \tilde{\theta}_{\text{tv17}}^{\top} = \begin{bmatrix} 3.0675 & -1.2186 \\ -10.9606 & 1.5138 \\ 16.4781 & -3.4175 \\ -2.6423 & -0.4059 \\ -22.4740 & 0.5605 \\ -9.1788 & -0.6047 \\ -0.9131 & 1.5597 \\ 10.4816 & -0.7005 \\ 2.5771 & 0.1414 \\ 9.5901 & -2.3063 \\ -39.1764 & 6.9269 \\ -20.1899 & 8.9101 \\ 78.9348 & -8.8613 \\ -12.7336 & 0.3724 \\ -17.9099 & -2.0992 \\ 30.8245 & 3.6136 \\ -2.6766 & 0.4120 \\ -1.1298 & 0.0723 \\ -12.9651 & -0.1754 \\ -2.5106 & -0.4566 \end{bmatrix} \quad \tilde{\theta}_{\text{tv18}}^{\top} = \begin{bmatrix} 3.0267 & -1.2594 \\ -11.0015 & 1.4728 \\ 16.4409 & -3.4547 \\ -3.1332 & -0.8969 \\ -22.3198 & 0.7147 \\ -9.1014 & -0.5274 \\ -1.3556 & 1.1172 \\ 10.2217 & -0.9604 \\ 2.2756 & -0.1601 \\ 9.1571 & -2.7393 \\ -39.4080 & 6.6953 \\ -20.2472 & 8.8529 \\ 79.7459 & -8.0503 \\ -12.5915 & 0.5146 \\ -18.0283 & -2.2176 \\ 30.8596 & 3.6486 \\ -3.2586 & -0.1701 \\ -1.1784 & 0.0238 \\ -12.6978 & 0.0919 \\ -2.3691 & -0.3151 \end{bmatrix} \tag{A.98}$$

$$\tilde{\theta}_{\text{tv19}}^{\top} = \begin{bmatrix} 3.0865 & -1.1996 \\ -11.3535 & 1.1208 \\ 16.4084 & -3.4872 \\ -2.7074 & -0.4710 \\ -22.1423 & 0.8922 \\ -9.0663 & -0.4923 \\ -1.3257 & 1.1471 \\ 10.6780 & -0.5040 \\ 2.1625 & -0.2732 \\ 9.2730 & -2.6235 \\ -38.8535 & 7.2498 \\ -20.0828 & 9.0173 \\ 79.3286 & -8.4676 \\ -12.1087 & 0.9974 \\ -18.0417 & -2.2309 \\ 30.4696 & 3.2587 \\ -3.0119 & 0.0766 \\ -0.7553 & 0.4469 \\ -12.8019 & -0.0123 \\ -2.8956 & -0.8416 \end{bmatrix} \quad \tilde{\theta}_{\text{tv20}}^{\top} = \begin{bmatrix} 3.2440 & -1.0420 \\ -11.0716 & 1.4028 \\ 16.5782 & -3.3174 \\ -3.0100 & -0.7736 \\ -22.3479 & 0.6866 \\ -9.0350 & -0.4610 \\ -0.7401 & 1.7327 \\ 10.5184 & -0.6637 \\ 1.6345 & -0.8012 \\ 9.4460 & -2.4504 \\ -39.1558 & 6.9475 \\ -20.2240 & 8.8760 \\ 79.0648 & -8.7313 \\ -12.5826 & 0.5235 \\ -18.3178 & -2.5071 \\ 31.0954 & 3.8845 \\ -3.1618 & -0.0732 \\ -1.0217 & 0.1804 \\ -12.5125 & 0.2772 \\ -2.8290 & -0.7750 \end{bmatrix} \quad \tilde{\theta}_{\text{tv21}}^{\top} = \begin{bmatrix} 3.0277 & -1.2584 \\ -11.1543 & 1.3200 \\ 16.3280 & -3.5676 \\ -2.9748 & -0.7384 \\ -22.3669 & 0.6675 \\ -9.2851 & -0.7110 \\ -0.7622 & 1.7107 \\ 10.4678 & -0.7143 \\ 2.2783 & -0.1574 \\ 9.0688 & -2.8277 \\ -38.5414 & 7.5619 \\ -20.4873 & 8.6127 \\ 79.1689 & -8.6272 \\ -12.1639 & 0.9422 \\ -18.1557 & -2.3449 \\ 30.9498 & 3.7388 \\ -3.2736 & -0.1851 \\ -1.4470 & -0.2449 \\ -12.9447 & -0.1550 \\ -2.3827 & -0.3286 \end{bmatrix}$$

(A.99)

$$\tilde{\theta}_{\text{tv22}}^{\top} = \begin{bmatrix} 3.0218 & -1.2643 \\ -11.0714 & 1.4030 \\ 16.2830 & -3.6126 \\ -2.8515 & -0.6151 \\ -22.2352 & 0.7993 \\ -9.1439 & -0.5698 \\ -1.0539 & 1.4189 \\ 10.1330 & -1.0491 \\ 2.1362 & -0.2995 \\ 10.0183 & -1.8782 \\ -38.8694 & 7.2339 \\ -20.5217 & 8.5783 \\ 79.1364 & -8.6597 \\ -12.4164 & 0.6896 \\ -18.0693 & -2.2586 \\ 30.5131 & 3.3022 \\ -3.4823 & -0.3938 \\ -0.9083 & 0.2938 \\ -12.6124 & 0.1773 \\ -2.3211 & -0.2671 \end{bmatrix} \quad \tilde{\theta}_{\text{tv23}}^{\top} = \begin{bmatrix} 2.9965 & -1.2896 \\ -10.9252 & 1.5491 \\ 16.3452 & -3.5505 \\ -2.9978 & -0.7614 \\ -22.3522 & 0.6822 \\ -9.4277 & -0.8536 \\ -0.9249 & 1.5480 \\ 10.4614 & -0.7206 \\ 1.7574 & -0.6783 \\ 9.4331 & -2.4633 \\ -39.2115 & 6.8918 \\ -20.6138 & 8.4862 \\ 79.3166 & -8.4796 \\ -12.2912 & 0.8148 \\ -17.6217 & -1.8110 \\ 30.8455 & 3.6345 \\ -3.1105 & -0.0220 \\ -0.7635 & 0.4387 \\ -13.3389 & -0.5492 \\ -2.5978 & -0.5438 \end{bmatrix} \quad \tilde{\theta}_{\text{tv24}}^{\top} = \begin{bmatrix} 3.1446 & -1.1415 \\ -10.8061 & 1.6682 \\ 16.1920 & -3.7036 \\ -2.8824 & -0.6460 \\ -22.3810 & 0.6535 \\ -9.2631 & -0.6890 \\ -1.0037 & 1.4691 \\ 10.4739 & -0.7082 \\ 2.3290 & -0.1067 \\ 9.2756 & -2.6209 \\ -38.8967 & 7.2066 \\ -20.5383 & 8.5617 \\ 79.2295 & -8.5667 \\ -12.2615 & 0.8445 \\ -17.5558 & -1.7451 \\ 31.1141 & 3.9032 \\ -3.0501 & 0.0384 \\ -0.7374 & 0.4648 \\ -12.1789 & 0.6108 \\ -2.6372 & -0.5832 \end{bmatrix}$$

(A.100)

$$\tilde{\theta}_{\text{tv25}}^{\top} = \begin{bmatrix} 3.1857 & -1.1004 \\ -10.7464 & 1.7280 \\ 16.8077 & -3.0879 \\ -3.0548 & -0.8184 \\ -22.5707 & 0.4638 \\ -9.1246 & -0.5505 \\ -0.7940 & 1.6789 \\ 10.4443 & -0.7378 \\ 2.3543 & -0.0814 \\ 9.2811 & -2.6154 \\ -39.1362 & 6.9671 \\ -20.1738 & 8.9263 \\ 79.1425 & -8.6537 \\ -11.9956 & 1.1104 \\ -18.1996 & -2.3889 \\ 30.7115 & 3.5006 \\ -3.2387 & -0.1502 \\ -0.5172 & 0.6849 \\ -12.7988 & -0.0091 \\ -2.2226 & -0.1686 \end{bmatrix} \quad \tilde{\theta}_{\text{tv26}}^{\top} = \begin{bmatrix} 3.0101 & -1.2760 \\ -11.0514 & 1.4229 \\ 16.2421 & -3.6535 \\ -3.4566 & -1.2202 \\ -21.9625 & 1.0720 \\ -9.0380 & -0.4639 \\ -1.2881 & 1.1848 \\ 10.2832 & -0.8989 \\ 2.1570 & -0.2787 \\ 9.3323 & -2.5641 \\ -39.0257 & 7.0776 \\ -20.4502 & 8.6498 \\ 78.7906 & -9.0056 \\ -12.2783 & 0.8278 \\ -18.1657 & -2.3550 \\ 30.9585 & 3.7475 \\ -2.7304 & 0.3582 \\ -0.7947 & 0.4075 \\ -12.8193 & -0.0297 \\ -2.3465 & -0.2925 \end{bmatrix} \quad \tilde{\theta}_{\text{tv27}}^{\top} = \begin{bmatrix} 3.4019 & -0.8842 \\ -10.8939 & 1.5804 \\ 16.2167 & -3.6790 \\ -2.7154 & -0.4790 \\ -22.1916 & 0.8429 \\ -8.6028 & -0.0287 \\ -1.1550 & 1.3179 \\ 10.9149 & -0.2672 \\ 2.0913 & -0.3444 \\ 9.4720 & -2.4244 \\ -39.1335 & 6.9699 \\ -20.4763 & 8.6237 \\ 79.2016 & -8.5945 \\ -12.2528 & 0.8533 \\ -17.9479 & -2.1372 \\ 31.0354 & 3.8245 \\ -3.2343 & -0.1457 \\ -1.0116 & 0.1906 \\ -12.9072 & -0.1175 \\ -2.1341 & -0.0800 \end{bmatrix} \tag{A.101}$$

$$\tilde{\theta}_{\text{tv28}}^{\top} = \begin{bmatrix} 3.1171 & -1.1690 \\ -11.5747 & 0.8997 \\ 16.3156 & -3.5801 \\ -2.9523 & -0.7159 \\ -22.8357 & 0.1988 \\ -8.7846 & -0.2105 \\ -0.9148 & 1.5580 \\ 10.2490 & -0.9331 \\ 1.9491 & -0.4866 \\ 9.2902 & -2.6062 \\ -38.9630 & 7.1403 \\ -20.4297 & 8.6703 \\ 79.2670 & -8.5291 \\ -12.3831 & 0.7230 \\ -17.8234 & -2.0126 \\ 30.7870 & 3.5760 \\ -2.8330 & 0.2555 \\ -0.7803 & 0.4218 \\ -12.7037 & 0.0860 \\ -2.1741 & -0.1201 \end{bmatrix} \quad \tilde{\theta}_{\text{tv29}}^{\top} = \begin{bmatrix} 2.8763 & -1.4098 \\ -11.1973 & 1.2770 \\ 16.3815 & -3.5141 \\ -2.8261 & -0.5897 \\ -22.4085 & 0.6260 \\ -9.1119 & -0.5379 \\ -1.0189 & 1.4539 \\ 10.3586 & -0.8235 \\ 2.0948 & -0.3409 \\ 9.5361 & -2.3604 \\ -39.5562 & 6.5471 \\ -20.3460 & 8.7540 \\ 79.0090 & -8.7871 \\ -11.6777 & 1.4283 \\ -17.9058 & -2.0950 \\ 30.8825 & 3.6716 \\ -3.0290 & 0.0596 \\ -1.3248 & -0.1227 \\ -12.5926 & 0.1970 \\ -2.4890 & -0.4350 \end{bmatrix} \quad \tilde{\theta}_{\text{tv30}}^{\top} = \begin{bmatrix} 3.0053 & -1.2808 \\ -11.0982 & 1.3761 \\ 16.3480 & -3.5477 \\ -2.8881 & -0.6518 \\ -22.4866 & 0.5479 \\ -9.2280 & -0.6539 \\ -1.2131 & 1.2597 \\ 10.6491 & -0.5330 \\ 2.0273 & -0.4084 \\ 8.9600 & -2.9365 \\ -39.2810 & 6.8223 \\ -20.4834 & 8.6166 \\ 78.6297 & -9.1665 \\ -12.5590 & 0.5470 \\ -17.8661 & -2.0553 \\ 30.4682 & 3.2572 \\ -3.4275 & -0.3390 \\ -0.9750 & 0.2271 \\ -12.6246 & 0.1651 \\ -2.3483 & -0.2943 \end{bmatrix} \tag{A.102}$$

$$\tilde{\theta}_{\text{tv31}}^{\top} = \begin{bmatrix} 2.3829 & -1.9032 \\ -11.2023 & 1.2720 \\ 16.5320 & -3.3636 \\ -2.8229 & -0.5865 \\ -22.3518 & 0.6827 \\ -8.9462 & -0.3722 \\ -0.9670 & 1.5058 \\ 10.7358 & -0.4463 \\ 2.3039 & -0.1318 \\ 9.3820 & -2.5145 \\ -39.1684 & 6.9349 \\ -20.7992 & 8.3009 \\ 79.2552 & -8.5409 \\ -12.4144 & 0.6916 \\ -18.2418 & -2.4310 \\ 31.0173 & 3.8063 \\ -3.1520 & -0.0635 \\ -0.7162 & 0.4859 \\ -12.7146 & 0.0751 \\ -2.5067 & -0.4527 \end{bmatrix} \quad \tilde{\theta}_{\text{tv32}}^{\top} = \begin{bmatrix} 2.3829 & -1.9032 \\ -11.2023 & 1.2720 \\ 16.5320 & -3.3636 \\ -2.8229 & -0.5865 \\ -22.3518 & 0.6827 \\ -8.9462 & -0.3722 \\ -0.9670 & 1.5058 \\ 10.7358 & -0.4463 \\ 2.3039 & -0.1318 \\ 9.3820 & -2.5145 \\ -39.1684 & 6.9349 \\ -20.7992 & 8.3009 \\ 79.2552 & -8.5409 \\ -12.4144 & 0.6916 \\ -18.2418 & -2.4310 \\ 31.0173 & 3.8063 \\ -3.1520 & -0.0635 \\ -0.7162 & 0.4859 \\ -12.7146 & 0.0751 \\ -2.5067 & -0.4527 \end{bmatrix} \quad \tilde{\theta}_{\text{tv33}}^{\top} = \begin{bmatrix} 2.8743 & -1.4118 \\ -11.1142 & 1.3601 \\ 16.0675 & -3.8282 \\ -3.4081 & -1.1717 \\ -22.3378 & 0.6967 \\ -9.1742 & -0.6002 \\ -0.6632 & 1.8096 \\ 10.9881 & -0.1940 \\ 2.1820 & -0.2537 \\ 9.5554 & -2.3411 \\ -39.1633 & 6.9400 \\ -20.1335 & 8.9665 \\ 79.3232 & -8.4729 \\ -12.3650 & 0.7410 \\ -17.8997 & -2.0890 \\ 30.5407 & 3.3297 \\ -3.0415 & 0.0470 \\ -1.0080 & 0.1941 \\ -12.5981 & 0.1916 \\ -2.3214 & -0.2674 \end{bmatrix} \tag{A.103}$$

$$\tilde{\theta}_{\text{tv34}}^{\top} = \begin{bmatrix} 2.9896 & -1.2965 \\ -11.0801 & 1.3942 \\ 16.0040 & -3.8916 \\ -2.5772 & -0.3408 \\ -21.9023 & 1.1322 \\ -9.0662 & -0.4921 \\ -0.5201 & 1.9527 \\ 10.2102 & -0.9719 \\ 2.1228 & -0.3129 \\ 9.0573 & -2.8391 \\ -39.3203 & 6.7830 \\ -20.2855 & 8.8145 \\ 79.2149 & -8.5812 \\ -12.3618 & 0.7442 \\ -18.1008 & -2.2900 \\ 30.7212 & 3.5102 \\ -3.0741 & 0.0144 \\ -0.7561 & 0.4461 \\ -12.7218 & 0.0679 \\ -2.3051 & -0.2511 \end{bmatrix} \quad \tilde{\theta}_{\text{tv35}}^{\top} = \begin{bmatrix} 2.9078 & -1.3783 \\ -10.4992 & 1.9751 \\ 16.1388 & -3.7569 \\ -2.8669 & -0.6305 \\ -22.6131 & 0.4214 \\ -8.8851 & -0.3111 \\ -1.0360 & 1.4368 \\ 10.4294 & -0.7527 \\ 1.9258 & -0.5099 \\ 9.2701 & -2.6263 \\ -39.0173 & 7.0860 \\ -20.6094 & 8.4906 \\ 79.2802 & -8.5160 \\ -12.2557 & 0.8503 \\ -18.2718 & -2.4611 \\ 30.4138 & 3.2028 \\ -2.7690 & 0.3195 \\ -1.0978 & 0.1044 \\ -12.6743 & 0.1153 \\ -2.5685 & -0.5145 \end{bmatrix} \quad \tilde{\theta}_{\text{tv36}}^{\top} = \begin{bmatrix} 2.9778 & -1.3083 \\ -11.0513 & 1.4230 \\ 15.7174 & -4.1782 \\ -2.9225 & -0.6861 \\ -22.7757 & 0.2588 \\ -9.1591 & -0.5851 \\ -1.1367 & 1.3361 \\ 10.4389 & -0.7432 \\ 2.2577 & -0.1780 \\ 9.4094 & -2.4871 \\ -39.1846 & 6.9187 \\ -20.1264 & 8.9736 \\ 79.0712 & -8.7250 \\ -12.2804 & 0.8256 \\ -18.3011 & -2.4904 \\ 31.0801 & 3.8691 \\ -3.3354 & -0.2469 \\ -0.7371 & 0.4651 \\ -12.9276 & -0.1379 \\ -2.6223 & -0.5683 \end{bmatrix} \tag{A.104}$$

$$\tilde{\theta}_{\text{tv37}}^{\top} = \begin{bmatrix} 2.9572 & -1.3289 \\ -11.1379 & 1.3364 \\ 16.1403 & -3.7553 \\ -3.0915 & -0.8551 \\ -22.2754 & 0.7591 \\ -9.2517 & -0.6776 \\ -1.1740 & 1.2989 \\ 10.5666 & -0.6155 \\ 1.5678 & -0.8679 \\ 9.1538 & -2.7427 \\ -39.0105 & 7.0929 \\ -20.5271 & 8.5729 \\ 79.4457 & -8.3505 \\ -11.8943 & 1.2118 \\ -18.2555 & -2.4448 \\ 30.8460 & 3.6350 \\ -3.4044 & -0.3159 \\ -0.7051 & 0.4971 \\ -12.4500 & 0.3397 \\ -2.1798 & -0.1258 \end{bmatrix} \tilde{\theta}_{\text{tv38}}^{\top} = \begin{bmatrix} 2.9980 & -1.2881 \\ -11.0969 & 1.3774 \\ 16.1776 & -3.7180 \\ -2.6005 & -0.3642 \\ -22.4295 & 0.6050 \\ -9.3290 & -0.7550 \\ -0.7315 & 1.7414 \\ 10.8265 & -0.3556 \\ 1.8693 & -0.5664 \\ 9.5868 & -2.3096 \\ -38.7788 & 7.3245 \\ -20.4699 & 8.6302 \\ 78.6346 & -9.1615 \\ -12.0364 & 1.0696 \\ -18.1371 & -2.3264 \\ 30.8110 & 3.6000 \\ -2.8224 & 0.2661 \\ -0.6565 & 0.5456 \\ -12.7173 & 0.0724 \\ -2.3213 & -0.2673 \end{bmatrix} \tilde{\theta}_{\text{tv39}}^{\top} = \begin{bmatrix} 2.9381 & -1.3480 \\ -10.7449 & 1.7294 \\ 16.2100 & -3.6856 \\ -3.0264 & -0.7900 \\ -22.6070 & 0.4275 \\ -9.3641 & -0.7901 \\ -0.7614 & 1.7115 \\ 10.3701 & -0.8120 \\ 1.9824 & -0.4533 \\ 9.4709 & -2.4255 \\ -39.3333 & 6.7700 \\ -20.6343 & 8.4658 \\ 79.0519 & -8.7442 \\ -12.5192 & 0.5868 \\ -18.1238 & -2.3130 \\ 31.2009 & 3.9899 \\ -3.0691 & 0.0194 \\ -1.0796 & 0.1225 \\ -12.6131 & 0.1765 \\ -1.7948 & 0.2592 \end{bmatrix} \tag{A.105}$$

$$\tilde{\theta}_{\text{tv40}}^{\top} = \begin{bmatrix} 2.7806 & -1.5055 \\ -11.0269 & 1.4474 \\ 16.0402 & -3.8554 \\ -2.7238 & -0.4874 \\ -22.4014 & 0.6330 \\ -9.3954 & -0.8214 \\ -1.3470 & 1.1259 \\ 10.5298 & -0.6523 \\ 2.5103 & 0.0746 \\ 9.2979 & -2.5986 \\ -39.0310 & 7.0723 \\ -20.4930 & 8.6070 \\ 79.3157 & -8.4805 \\ -12.0453 & 1.0607 \\ -17.8477 & -2.0369 \\ 30.5751 & 3.3642 \\ -2.9192 & 0.1693 \\ -0.8132 & 0.3889 \\ -12.9026 & -0.1129 \\ -1.8614 & 0.1926 \end{bmatrix} \tag{A.106}$$

Bibliography

Apkarian, P. and P. Gahinet (1995). A convex characterization of gain-scheduled $\mathcal{H}_\infty$ controllers. *IEEE Trans. on Automatic Control* **40**(5), 853–864.

Åström, K. J. and B. Wittenmark (1990). *Computer controlled systems*. Prentice-Hall.

Bachnas, A. A. (2012). Linear parameter-varying modelling of a high-purity distillation collumn. Master's thesis, Delft University of Technology.

Bachnas, A. A., R. Tóth, A. Mesbah and J. Ludlage (2014). A review on data-driven linear parameter-varying modeling approaches: A high-purity distillation column case study. *Journal of Process Control* **24**, 272–285.

Bachnas, A. A., S. Weiland and R. Tóth (2014). Data driven predictive control based on orthonormal basis functions. In *Proc. of the 23rd ERNSI Workshop in System Identification*, Ostend, Belgium (Sep.).

Bachnas, A. A., S. Weiland and R. Tóth (2015a). Data driven predictive control based on orthonormal basis functions. In *Proc. of the 54th IEEE Conf. on Decision and Control*, Osaka, Japan (Dec.), pp. 3026–3031.

Bachnas, A. A., S. Weiland and R. Tóth (2015b). Other attempts on OBFs pole selection. Technical report, Eindhoven University of Technology.

Bachnas, A. A., X. Yan and S. Weiland (2016). Complexity reduction for uncertain systems: A projection-based approach. In *Proc. of the 55th IEEE Conf. on Decision and Control*, Las Vegas, USA (Dec.), pp. 5769–5774.

Bai, E. W., R. Tempo and M. Fu (1997). Worst-case properties of the uniform distribution and randomized algorithm for robustness analysis. In *Proc. of the 1997 American Control Conference*, pp. 861–865.

Bauer, M. and I. K. Craig (2008). Economic assessment of advanced process control - a survey and framework. *Journal of Process Control* **18**, 2–18.

Beck, C., J. Doyle and K. Glover (1996). Model reduction of multidimensional and uncertain systems. *IEEE Transactions on Automatic Control* **41**(10), 1466–1477.

Bemporad, A., F. Borrelli and M. Morari (2003). Min-max control of constrained uncertain discrete-time linear systems. *IEEE Transactions on Automatic Control* **48**(9), 1600–1606.

Bodin, P., L. Villemoes and B. Wahlberg (1997). An algorithm for selection of best orthonormal rational basis. In *Proc. of the 36th IEEE Conf. on Decision and Control*, San Diego, California, USA (Dec.).

Bombois, X. and G. Scorletti (2012). Design of least costly identification examples - the main philosophy accompanied by illustrative examples. *Journal Européen des Systèmes Automatisés* **46**(6-7), 587–610.

Boyd, S. and L. O. Chua (1985). Fading memory and the problem of approximating nonlinear operators with Volterra series. *IEEE Trans. on Circuits and Systems* **32**(11), 1150–1161.

Boyd, S. and L. Vandenberghe (2004). *Convex Optimization*. Cambridge University Press.

Bronstein, E. M. (2008). Approximation of convex sets by polytopes. *Journal of Mathematical Sciences* **153**(6), 727–762.

Camacho, Eduardo F and Carlos Bordons Alba (2013). *Model predictive control*. Springer Science & Business Media.

Clarke, David W, C Mohtadi and PS Tuffs (1987). Generalized predictive control part i: The basic algorithm. *Automatica* **23**(2), 137–148.

Cutler, Charles R. and Brian L. Ramaker (1979). Dynamic matrix control – a computer control algorithm. *IEEE Transactions on Automatic Control* **17**, 72.

Darwish, M. A. H., G. Pillonetto and R. Tóth (2015). Perspectives of orthonormal basis functions based kernels in Bayesian system identification. In *Proc. of the 54th IEEE Conf. on Decision and Control*, Osaka, Japan (Dec.), pp. 2713–2718.

Darwish, M. A. H., G. Pillonetto and R. Tóth (2018). The quest for the right kernel in bayesian impulse response identification: The use of OBFs. *Automatica* **87**, 318–329.

Di Cairano, S. (2012). An industry perspective on mpc in large volumes applications: Potential benefits and open challenges. *IFAC Proceedings Volumes* **45**(17), 52–59.

Douik, A., J. Ghabi and H. Messaoud (2007). Robust predictive control using a GOBF model for MISO systems. *International Journal of Computers, Communications & Control* **2**(4), 355–366.

Ferramosca, A., D. Limón, I. Alvarado, T. Alamo and E. F. Camacho (2009). Mpc for tracking with optimal closed-loop performance. *Automatica* **45**(8), 1975–1978.

Finco, M. V., W. L. Luyben and R. E. Polleck (1989). Control of distillation columns with low relative volatilities. *Industrial & Engineering Chemistry Research* **28**, 75–83.

Franklin, G. F., J. D. Powell and M. L. Workman (1990). *Digital Control of Dynamic Systems*. Addison-Wesley.

Gelb, A. (1974). *Applied Optimal Estimation*. The MIT Press. ISBN 0262570483, 9780262570480.

Genceli, H. and M. Nikolaou (1996). New approach to constrained predictive control with simultaneous model identification. *AIChE journal* **42**(10), 2857–2868.

Giarré, L., D. Bauso, P. Falugi and B. Bamieh (2006). LPV model identification for gain scheduling control: An application to rotating stall and surge control problem. *Control Engineering Practice* **14**(4), 351–361.

Gilbert, E. G. and K. T. Tan (1991). Linear systems with state and control constraints: The theory and application of maximal output admissible sets. *IEEE Transactions on Automatic control* **36**(9), 1008–1020.

Gokhale, V., S. Hurowitz and J. B. Riggs (1996). A comparison of advanced distillation control techniques for a propylene-propane splitter. *Industrial & Engineering Chemistry Research* **34**, 4413–4419.

Goodwin, G. C., S. F. Graebe and M. E. Salgado (2000). *Control System Design*. Prentice Hall.

Goodwin, G. C., M. M. Seron and J. A. D. Doná (2005). *Constrained Control and Estimation: An Optimisation Approach*. Springer.

Grüne, L. and J. Pannek (2011). Nonlinear model predictive control. In *Nonlinear Model Predictive Control*, pp. 43–66. Springer.

Guillaume, P., J. Schoukens and R. Pintelon (1989). Sensitivity of roots to errors in the coefficient of polynomials obtained by frequency-domain estimation methods. *IEEE Trans. on Instrumentation and Measurement* **38**(6), 1050–1056.

Heirung, T.A.N., B. Foss and B.E. Ydstie (2015). MPC-based dual control with online experiment design. *Journal of Process Control* **32**, 64–76.

Heuberger, P. S. C. (1990). *On Approximate System Identification with System Based Orthonormal Functions*. Ph. D. thesis, Delft University of Technology.

Heuberger, P. S. C., P. M. J. Van den Hof and Bo Wahlberg (2005). *Modeling and Identification with Rational Orthonormal Basis Functions*. Springer-Verlag.

Heuberger, P. S. C., P. M. J. Van den Hof and O. H. Bosgra (1995). A generalized orthonormal basis for linear dynamical systems. *IEEE Trans. on Automatic Control* **40**(3), 451–465.

Hsu, K., T. L. Vincent and K. Poolla (2008). Nonparametric methods for the identification of linear parameter varying systems. In *Proc. of the Int. Symposium on Computer-Aided Control System Design*, San Antonio, Texas, USA (Sept.), pp. 846–851.

Huesman, A. (2011). *Process Dynamics and Control*, Lecture Notes. Delft University of Technology.

Jacobsen, E.W., P. Lundström and S. Skogestad (1991). Modelling and identification for robust control of ill-conditioned plants - a distillation case study. In *Proc. of the American Control Conf.*, Boston, USA (June), pp. 242–248.

Jurre, H., L. Mircea and R. Tóth (2017). Stabilizing tube-based model predictive control: Terminal set and cost construction for LPV systems. *Automatica* **85**, 137–144.

Kautz, W. H. (1954). Transient synthesis in the time domain. *IRE Transactions on Circuit Theory* **1**, 29–39.

Khalate, A. A., X. Bombois, R. Tóth and R. Babuška (2009). Optimal experimental design for LPV identification using a local approach. In *Proc. of the 15th IFAC Symposium on System Identification*, Saint-Malo, France (July), pp. 162–167.

Khalil, H.K. (2002). *Nonlinear Systems*. Pearson Education. Prentice Hall. ISBN 9780130673893.

Kothare, M. V., V. Balakrishnan and M. Morari (1996). Robust constrained model predictive control using linear matrix inequalities. *Automatica* **32**(10), 1361–1379.

Kreyzig, E (1978). *Introductory Functional Analysis with Applications*. John Wiley and Sons.

Kwon, W. H. and S. H. Han (2006). *Receding horizon control: model predictive control for state models*. Springer Science & Business Media.

Larsson, C. A., M. Annergren, H. Hjalmarsson, C. R. Rojas, X. Bombois, A. Mesbah and P. E. Modén (2013). Model predictive control with integrated experiment design for output error systems. In *Proc. of the European Control Conf.*, Zurich, Switzerland.

Laurain, V., R. Tóth, W-X. Zheng and M. Gilson (2012). Nonparametric identification of lpv models under general noise conditions. an ls-svm based approach. In *Proc. of the the 16th IFAC Symposium on System Identification*, Brussels, Belgium (July), pp. 1761–1766.

Lee, J. H. (2014). From robust model predictive control to stochastic optimal control and approximate dynamic programming: A perspective gained from a personal journey. *Computers & Chemical Engineering* **70**, 114–121.

Lee, Y. W. (1932). Synthesis of electric networks by means of the fourier transform of laguerre's functions. *Journal of Mathematical Physics* **2**, 83–113.

Limón, D., I. Alvarado, T. Alamo and E. F. Camacho (2008). Mpc for tracking piecewise constant references for constrained linear systems. *Automatica* **44**(9), 2382–2387.

Ljung, L. (1999). *System Identification, theory for the user* (2nd ed.). Prentice-Hall.

Ljung, L. (2006). *System Identification Toolbox, for use with Matlab*. The Mathworks Inc.

Lu, Y. and Y. Arkun (2000). Quasi-min-max MPC for LPV systems. *Automatica* **36**, 527–540.

Maciejowski, J.M. (2002). *Predictive control: with constraints*. Pearson education.

Marafioti, G., R.R. Bitmead and M. Hovd (2014). Persistently exciting model predictive control. *International Journal of Adaptive Control and Signal Processing* **28**(6), 536–552.

Matlab (2022). Optimization toolbox user's guide.

Mayne, D.Q. (2014). Model predictive control: Recent developments and future promise. *Automatica* **50**(12), 2967–2986.

Mayne, D.Q., J.B. Rawlings, C.V. Rao and P.O.M Scokaert (2000). Constrained model predictive control: Stability and optimality. *Automatica* **36**(6), 789–814.

Mayne, D. Q. (2016). Robust and stochastic model predictive control: Are we going in the right direction? *Annual Reviews in Control* **41**, 184–192.

Mayne, D. Q., E. C. Kerrigan, E. J. van Wyk and P. Falugi (2011). Tube-based robust nonlinear model predictive control. **21**(11), 1341–1353.

Morari, M. and J. H. Lee (1999). Model predictive control: past, present and future. *Computers and Chemical Engineering* **23**(4/5), 667–682.

Ninness, B. and F. Gustafsson (1997). A unifying construction of orthonormal bases for system identification. *IEEE Transactions on Automatic Control* **42**(4), 515–521.

Ninness, B. and F. Gustafsson (1999). The fundamental role of general orthonormal bases in system identification. *IEEE Transactions on Automatic Control* **44**(5), 1384–1407.

Ninness, B. M., J. C. Gómez and S. Weller (1996). MIMO system identification using orthonormal basis functions. In *Proc. of the 34th IEEE Conf. on Decision and Control*, New Orleans, Louisiana, USA (Dec.), pp. 703–708.

Nocedal, J. and S. J. Wright (2006). *Numerical Optimization*. Springer Verlag.

Oliviera e Silva, T. (1996). A n-width result for the generalized orthonormal basis function model. In *Proc. of the 13th IFAC World Congress*, Sydney, Australia (July), pp. 375–380.

Ozkan, L., X.J.A. Bombois, J.H.A. Ludlage, C.R. Rojas, H. Hjalmarsson, P.E. Moden, M. Lundh, A.C.P.M. Backx and P.M.J. Van den Hof (2016). Advanced autonomous model-based operation of industrial process systems (autoprofit): technological developments and future perspectives. *Annual Reviews in Control* **42**, 126–142.

Parrilo, P. A. (2000). *Structured semidefinite programs and semialgebraic geometry methods in robustness and optimization*. Ph. D. thesis, California Institute of Technology.

Patwardhan, S.C. and S.L. Shah (2005). From data to diagnosis and control using generalized orthonormal basis filters. part I: Development of state observers. *Journal of Process Control* **15**(7), 819–835.

Patwardhan, S. C., S. Manuja, S. Narasimhan and S. L. Shah (2006). From data to diagnosis and control using generalized orthonormal basis filters. part II: Model predictive and fault tolerant control. *Journal of Process Control* **16**, 157–175.

Pinkus, A. (1985). *n-Widths in Approximation Theory*. Springer-Verlag.

Pintelon, R. and J. Schoukens (2001). *System identification, a frequency domain approach*. IEEE press.

Polderman, J. W. and J. C. Willems (1991). *Introduction to Mathematical Systems Theory, A Behavioral Approach*. Springer.

Qin, S.J. and T. Badgwell (2003a). A survey of industrial model predictive control technology. *Control engineering practice* **11**(7), 733–764.

Qin, S. J. and T. A. Badgwell (2000). An overview of nonlinear model predictive control applications. In F. Allgöwer and A. Zheng (Eds.), *Nonlinear Predictive Control*, pp. 369–393. Birkhäuser Verlag.

Qin, S. J. and T. A. Badgwell (2003b). A survey of industrial model predictive control technology. *Control Engineering Practice* **11**, 733–764.

Rawlings, J. B. and D. Q. Mayne (2009). *Model predictive control: Theory and design*. Nob Hill Pub.

Richalet, J., A. Rault, J.Testud and J.Papon (1978). Model predictive heuristic control: Applications to industral processes. *Automatica* **14**(5), 413–428.

Rosolia, U. and F. Borrelli (2018). Learning model predictive control for iterative tasks. a data-driven control framework. *IEEE Transactions on Automatic Control* **63**(7), 1883–1896.

Saltik, M.B., L. Özkan, T. Backx, S. Weiland and J.H.A. Ludlage (2017). Moment based model predictive control for systems with additive uncertainty. In *Americal Control Conference, Seattle, Washington*, pp. 1975–1978.

Shamma, J. S. and M. Athans (1991). Guaranteed properties of gain-scheduled control for nonlinear-plants. *Automatica* **27**, 559–564.

Skogestad, S. (1997). Dynamics and control of distillation columns: A tutorial introduction. *Chemical Engineering Research and Design* **75**(6), 539–562.

Skogestad, S. and M. Morari (1988). LV-control of a high-purity distillation column. *Chemical Engineering Science* **43**(1), 33–48.

Skogestad, S., M. Morari and J.C. Doyle (1988). Robust control of ill-conditioned plants: high-purity distillation. *IEEE Trans. on Automatic Control* **33**(12), 1092–1105.

Sontag, E. D. (1998). *Mathematical Control Theory: Deterministic Finite Dimensional Systems (2Nd Ed.)*. New York, NY, USA: Springer-Verlag New York, Inc. ISBN 0-387-98489-5.

Suzuki, H and T. Sugie (2006). Mpc for lpv systems with bounded parameter variation using ellipsoidal set prediction. In *American Control Conference, 2006*, pp. 6–pp. IEEE.

Takatsu, H., T. Itoh and M. Araki (1998). Future needs for the control theory in industries report and topics of the control technology survey in japanese industry. *Journal of Process Control* **8**(5-6), 369–374.

Tanaskovic, M., L. Fagiano, R. Smith and M. Morari (2014). Adaptive receding horizon control for constrained MIMO systems. *Automatica* **50**(12), 3019–3029.

Tempo, R., G. Calafiore and F. Dabbene (2013). *Randomized Algorithms for Analysis and Control of Uncertain Systems*. Springer.

Tóth, R. (2008). *Modeling and Identification of Linear Parameter-Varying Systems, an Orthonormal Basis Function Approach*. Ph. D. thesis, Delft University of Technology.

Tóth, R. (2010). *Modeling and Identification of Linear Parameter-Varying Systems*. Lecture Notes in Control and Information Sciences, Vol. 403. Heidelberg: Springer.

Tóth, R., P. S. C. Heuberger and P. M. J. Van den Hof (2009). Asymptotically optimal orthonormal basis functions for LPV system identification. *Automatica* **45**(6), 1359–1370.

Tran, Q, Leyla Özkan and T Backx (2012). Mpc tuning based on impact of model uncertainty on closed-loop performance. In *AIChE Annual Meeting, Pittsburgh, PA*.

van Donkelaar, E. T. (2000). *Improvement of efficiency in identification and model predictive control of industrial processes, a flexible linear parametrization approach*. Ph. D. thesis, Delft University of Technology.

van Donkelaar, E. T., P. S. C. Heuberger and P. M. J. Van den Hof (1998). Identification of a fluidized catalytic cracking unit: an orthonormal basis functions approach. In *Proc. of the American Control Conf.*, Philadelphia, Pennsylvania, USA (June), pp. 1814–1817.

Vuerinckx, R., R. Pintelon, J. Schoukens and Y. Rolain (2001). Obtaining accurate confidence regions for the estimated zeros and poles in system identification problems. *IEEE Trans. on Automatic Control* **46**(4), 656–659.

Waller, J. B. (2003). *Directionality and Nonlinearity- Challenges in Process Control*. Ph. D. thesis, Åbo Akademi University.

Wang, L. (2009). *Model predictive control system design and implementation using MATLAB®*. Springer Science & Business Media.

Young, P., H. Garnier and M. Gilson (2009). Simple refined IV methods of closed-loop system identification. In *Proc. of the 15th IFAC Symposium on System Identification, SYSID 2009*, pp. 284–289.

Young, P. C. (2008). The refined instrumental variable method: Unified estimation of discrete and continuous-time transfer function models. *Journal Européen des Systèmes Automatisés* **42**, 149–179.

Zerz, E. (2006). An algebraic analysis approach to linear time-varying systems. *IMA Journal of Mathematical Control and Information* **23**, 113–126.

Zhu, Y. (2001). *Multivariable System Identification for Process Control*. Pergamon Press.

Zhu, Yucai, Rohit Patwardhan, Stephen B Wagner and Jun Zhao (2013). Toward a low cost and high performance mpc: The role of system identification. *Computers & Chemical Engineering* **51**, 124–135.

List of Publications

Journal papers

A.A. Bachnas, R. Tóth, A. Mesbah, J. Ludlage (2013). A review on data-driven linear parameter-varying modeling approaches: A high-purity distillation column case study. *Journal of Process Control, vol 24, no. 4, pp. 272-285.*

Conference proceedings

A.A. Bachnas, R. Tóth, S. Weiland (2015). Data driven predictive control based on OBF model structures. *Proc. of the 54th IEEE Conf. on Decision and Control*, Osaka, Japan (Dec.), pp. 3025–3031.

A.A. Bachnas, X. Yan, S. Weiland (2016). Complexity Reduction for Uncertain Systems: A Projection-based Approach. *Proc. of the 55th IEEE Conf. on Decision and Control*, Las Vegas, USA (Dec.), pp. 5769–5774.

A.A. Bachnas, R. Tóth, S. Weiland (2014). Optimal basis poles selection for Orthonormal Basis Functions based model. *23rd ERNSI Workshop in System Identification*, Ostend, Belgium (Sep.).

A.A. Bachnas, R. Tóth, A. Mesbah, J.Ludlage (2013). Perspectives of data-driven LPV modeling of high-purity distillation columns. *Proc. of the 12th European Control Conf*, Zurich, Switzerland (July.), pp. 3776–3783.

List of Symbols

Operators

q	Forward shift
$\frac{d}{dt}$	Differentiation
$\ominus$	element wise substraction
$\langle \bullet, \bullet \rangle$	Inner product
$\|\bullet\|$	Norm
$\bullet^{[i,j]}$	Element of the i-th row and j-th column
$\bullet^{\top}$	Transposition
$\bullet^{-1}$	Inverse
$\bullet^{*}$	Optimum
$\succ,\ (\succeq)$	Positive (semi)-definite
$\succ,\ (\succeq)$	Negative (semi)-definite
Re	Real part
Im	Imaginary part
inf	Infinum
sup	Supremum
min	Minimum
max	Maximum
var	Variance
log	Logaritmic
Co	Polytopes from vertices
arg	Argument of a function
dim	Dimension
diag	Diagonal matrix operator
span	Algebraic span
col	Column composition
$\mathcal{Z}$	Z-transformation

$\Pi_{\mathcal{J}}$	Projection into $\mathcal{J}$
$\perp$	Orthogonal

Dynamical systems, Representations, and related variables

G	LTI system
$\mathcal{F}$	LTV system
$\mathcal{S}$	LPV system
$\mathcal{G}$	Unknown discrete time LTI system
$G_{n_\mathrm{e},n_\mathrm{b}}$	LTI-OBF system with n_e expansion of n_b basis
$G(z)$	Transfer function representation
$\varphi_{n_\mathrm{e},n_\mathrm{b}}(z)$	Input to State transfer function representation
$g(\tau)$	Series Expansion representation
δ	Unit pulse
c_i	Expansion coeff
w_i	Expansion coeff OBF model
$G^{[m,n]}(z)$	m-th output and n-th input of MIMO transfer function $G(z)$
$\mathsf{w}_i^{[m,n]}$	m-th and n-th entry of w_i
$\phi_i(z)$	Orthonormal basis function of $\mathcal{RH}_2(\mathbb{E})$
$\{\phi_i(z)\}_{i=1}^{\infty}$	Complete set of Orthonormal basis function of $\mathcal{RH}_2(\mathbb{E})$
$\{\phi_i(z)\}_{i=1}^{n_\mathrm{b}}$	Finite set of Orthonormal basis function of $\mathcal{RH}_2(\mathbb{E})$
$\psi_i(\tau)$	Orthonormal basis function of $\mathcal{R}\ell_2(\mathbb{N})$
$\{\psi_i(\tau)\}_{i=1}^{\infty}$	Complete set Orthonormal basis function of $\mathcal{R}\ell_2(\mathbb{N})$
Φ_{n_b}	Set of OBFs with n_b elements
$\mathbf{T}$	State Transformation
ξ_k	System pole
$\mathfrak{x}_k$	Real part of re-parameterized system pole
$\mathfrak{y}_k$	Imaginary part of re-parameterized system pole
λ_k	OBFs pole
$\mathfrak{a}_k$	Real part of re-parameterized OBFs pole
$\mathfrak{b}_k$	Imaginary part of re-parameterized OBFs pole
$\bar{\mathsf{a}}$	Set of real valued OBFs pole
a, b	Set of complex conjugate OBFs pole pairs
Ω	Pole region
ρ	Convergence rate of the series expansion
γ	Upperbound of the attained minimum of Convergence rate
$\|\cdot\|_n$	n^{th} vector norm
$\ell_n(\cdot)$	n^{th}-signal norm

π_n	Kolmogorov n-width
$d_{\mathcal{RH}_2(\mathbb{E})}$	Distance on $\mathcal{RH}_2(\mathbb{E})$

Signals, and variables

u	Input signal
y	Output signal
x	State signal
p	Scheduling variable
w	Extended state
v, e	Noise, stochastic process
k	running time / discrete time
k_o	initial time
τ	time selector
$\mathbf{u}$	MPC input sequence
$\mathbf{p}$	Scheduling trajectory
$\mathcal{D}$	Data record

Functions

J	Cost-function of OBF pole selection problem
L	Lagrangian function
f_γ	Probability density function
$\mathbb{I}_{RA}$	Indicator function
W_N	Quadratic identification criterion
V	Lyapunov function
V_N	MPC cost function
V_f	Terminal cost function
V_o	Target penalty function
l	stage cost function

Spaces and fields

$\mathbb{R}$	Set of real numbers
$\mathbb{R}_{[a,b]}$	Real numbers with value $\geq a$ and $\leq b$
$\mathbb{R}_{(a,b)}$	Real numbers with value $> a$ and $< b$
$\mathbb{Z}$	Set of integers
$\mathbb{C}$	Set of complex numbers
$\mathbb{N}$	Set of natural numbers
$\mathbb{D}$	Unit disk

$\mathbb{J}$	Unit circle
$\mathbb{E}$	Exterior of the unit disk
$\mathbb{X}$	State-space
$\mathbb{U}$	Input-space
$\mathbb{Y}$	Output-space
$\mathbb{I}_{n_1}^{n_2}$	Index set $[n_1, \ldots, n_2]$
$\mathbb{P}$	Scheduling domain
$\mathcal{I}$	Set of indices
$\mathcal{H}$	Hilbert space
$\mathcal{H}_2(\mathbb{E})$	Hardyspace
$\ell_2(\mathbb{N})$	Space of square summable sequences
$\mathcal{RH}_2(\mathbb{E})$	Space of all real $\mathcal{H}_{2-}$ functions that are analytic in $\mathbb{E}$
$\mathcal{R}\ell_2(\mathbb{N})$	space of square summable sequences
$\mathcal{U}(n_1, n_2)$	Uniform distribution on interval $[n_1, n_2]$
$\mathcal{N}(n_1, n_2)$	Normal distribution with mean n_1 and variance n_2
$\mathcal{X}_f$	Terminal set
$\mathcal{X}_f^w$	Extended terminal set
$\mathcal{O}_\infty^w$	maximal admissible invariant set

Coefficients, constants, and rates

A, B, C, D	State-space matrices
θ	Parameter vector
θ^*	Asymptotic parameter vector estimate
Θ	Parameter vector space
$\mathbf{Q}_{\hat{\theta}_n}$	Covariance matrix of parameter estimate
ϑ	Parameter vector of LPV expansion coefficient
i	Imaginary unit
α	Confidence level
ϵ	Probabilistic error value / Stopping condition
W_{LS}	LS model weight
W_{RLS}	RLS model weight
r	reference vector
u_s, x_s	input-state steady state value
$u_{\min}$	Lower limit of input
$u_{\max}$	Upper limit of input
ξ	Parameterization variables of steady state

η	Contraction parameter
H_p	Data horizon
H_p	Prediction horizon
H_u	Control horizon
Q	Output/state control matrix
R	Input control matrix
K	Gain matrix
S	LQR matrix
P	Covariance matrix
F	Jacobian matrix
H	Hessian matrix
Q_E, R_E	EKF matrices related to variance of measurement

Dimensions

n_{u}	Input dimension
n_{y}	Output dimension
n_{x}	State dimension
n_{p}	Scheduling dimension
n_{b}	Inner function dimension
n_{e}	Number of basis extension
n_{g}	Inner function dimension multiplied by bases extension
n_{r}	Number of real valued basis poles
n_{c}	Number of complex conjugate basis pole pairs
n_{a}	Order of the denominator polynomial
n_{b}	Order of the nominator polynomial
n_θ	Parameter vector dimension
n_{loc}	Number of local models
n_ψ	Number of used functions in dependency parameterization
n_{w}	Dimension of w_i
N_{av}	Average number of iterations
N_{d}	Data record length
N_{loc}	Number of linearization / local points
n_ξ	Dimension of ξ

List of Abbreviations

APC	Advanced Process Control
BFR	Best Fit Ratio
BIBO	Bounded-Input-Bounded-Output
BJ	Box-Jenkins (model)
CV	Controlled variables
DAE	Differential Algebraic Equation
DCS	Distributed Control System
EKF	Extended Kalman Filter
FIR	Finite Impulse Response
FKcM	Fuzzy Kolmogorov c-Max
GOBF	General Orthonormal Basis Function
HPDC	High Purity Distilation Column
IV	Instrumental Variables
KKT	Karush Kuhn Tucker (optimization)
KnW	Kolmogorov n-Width
LMI	Linear Matrix Inequalities
LPV	Linear Parameter-Varying
LQR	Linear Quadratic Regulator
LS	Least Squares (criterion)
LTI	Linear Time-Invariant
LTV	Linear Time-Varying
MIMO	Multiple-Input Multiple-Output
MISO	Multiple-Input Single-Output
MPC	Model Predictive Control
MSE	Mean Squared Error

MV	Manipulated Variable
NLP	Nonlinear Programming
OBF	Orthonormal Basis Function
OE	Output Error (model)
pdf	Probability Density Function
PE	Persistency of Excitation
PEM	Prediction Error Minimization
PID	Proportional-Integral-Differential (control)
RA	Randomized Algorithm
RBF	Radial Basis Function
RLS	Recursive Least Square
RTO	Real Time Optimization
SISO	Single-Input Single-Output
SIMO	Single-Input Multiple-Output
SNR	Signal to Noise Ratio
SOSP	Sum of Squares Programming
SQP	Sequential Quadratic Programming
SS	State-Space
TCO	Total Cost of Ownership
TM	Takenaka-Malmquist (model)
WLS	Weighted Least Square

Acknowledgments

First of all, I would like to express my sincere gratitude to both Roland Tóth and Siep Weiland for the opportunity to start the Ph.D. track and for their relentless support and guidance during my Ph.D. time. Both of you are the main reason I continue to grow and to stay the course during my Ph.D. time and even after the project was officially finished.

Next, I would like to thank the other committee members Paul Van den Hof, Arnold Heemink, Yucai Zhu, Karel Keesman, and Leon Arians for willingly taking the time to read, find mistakes, and give comments to furthermore improve this thesis.

My grateful thanks are also extended to Diana Heijnerman, Will Hendrix, and to the late Barbara Conelissen-Milner. Without your assistance, I am sure that I would not even complete my Ph.D. journey. In Addition, I would like to thank all of the group members and fellow Ph.D. students in the Control system group. I cherish all the memories with you.

I would also like to thank my parents, Bachnas and Zulhawati. It is really a blessing to be born and raised by the two of you. I wholeheartedly express my deep gratitude for their bottomless support throughout my life. This Thesis is dedicated to them

Finally, I would like to give my warmest love to my wife Anti, and my children Gwen, Garnet, and Gianna. You teach me how to be a father and a better man. Your patience and support helped me to stay strong on this unfinished path of life.

Eindhoven, February 2023
A. A. Bachnas

Samenvatting

De steeds groeiende vraag naar zowel consumenten- als industriële producten verhoogt de chemische stof en petrochemische industrieën om de kwaliteit en de hoeveelheid van hun productie. De bedrijven die de core business hebben in de procesindustrie zijn met elkaar kompetitie om de markt te domineren. Ontwikkeling van de stroom procestechnologieën bieden bedrijven een concurrentievoordeel om hun leidende marktposities. Dit proefschrift onderzoekt nieuwe methoden om de prestaties van Advanced Process Control (APC) door rekening te houden met modelonnauwkeurigheid en variatie in procesdynamiek die de mismatch van het fabrieksmodel veroorzaakt. Het controlemechanisme is gebaseerd op orthonormale basisfuncties (OBF's) als een nieuw voorspellingsmodel.

Het eerste deel van dit proefschrift, Hoofdstuk 2-3, Adressen manieren om optimaal te selecteren basispolen van het OBFs-model uit een eindige set systeempolen. Verder bieden wij een methode om ons voorgestelde algoritme te gebruiken voor een model van een systeem dat wordt verkregen via de systeemidentificatieprocedure. Ten slot, door een simulatie uit te voeren studie bleek dat de voorgestelde methoden beter zijn dan de staat van het kunstbasisselectie-algoritme met behoud van een enigszins computationele belasting van elk algoritme. Dit leidt tot mogelijke directe implementatie in de industriële praktijk.

Het tweede deel van dit proefschrift, Hoofdstuk 4, behandelde het geval waarin het OBF gebaseerd voorspellingsmodel per regelcyclus wordt aangepast om het tijdsafhankelijke gedrag van het systeem van belang. De aanpassing is gebaseerd op een iteratieve identificatieprocedure van de coëfficiënten van het OBF-gebaseerd voorspellingsmodel. Gebruik van systeemidentificatie voor OBF-gebaseerd model een groot voordeel van directe toepasbaarheid van het PEM-identificatieraamwerk en daarmee de consistente schatting van de OBF-modelcoëfficiënten. Daarna is het MPC-schema voor OBF-gebaseerd voorspellingsmodel is opgesteld. De MPC-regeling, de haalbaarheid en stabiliteitsresultaten, worden vervolgens uitgebreid tot het tijdsafhankelijke geval. De voorgestelde MPC wordt eerst getest in een academische casestudy, waar we hebben aangetoond dat de voorgestelde methode de in de tijd variërende dynamiek van een vastgesteld systeem bevestigd en erin slagen om het doel van het volgen van instelpunten te bereiken.

Het derde deel van dit proefschrift, Hoofdstuk 5, behandeld het geval waarin het OBF-analysemodel beschrijft variaties in de dynamiek van het systeem van belang dat kan worden afgeleid door een extern signaal dat de planningsvariabele

wordt genoemd. Er worden twee LPV-identificatiebenaderingen geboden om het LPV-OBF-model te identificatie voordat de MPC in gebruik wordt genomen. De lokale LPV-identificatiebenadering kan worden gezien als een interpolatie van het dynamische gedrag van het systeem, terwijl de globale LPV-identificatiemethode een directe identificatiemethode is op basis van een enkele dataset die vanuit het systeem wordt gemeten. Daarna wordt het MPC-schema LPV-OBF opgesteld. Het MPC-schema maakt gebruik van een aangewezen stationair doel en een extra straftermijn voor trackingdoeleinden. De ruimte van het stationaire paar wordt afgeleid door een vector die wordt gebruikt als argument voor minimalisering van het MPC-probleem. Een soortgelijke instelling helpt ons bij het vaststellen van haalbaarheid en stabiliteitsgaranties van het MPC-schema. De voorgestelde MPC wordt eerst getest in academische casestudy's, waar we laten zien dat de voorgestelde methode de parametervariabele dynamiek van een vastgesteld systeem kan bevestigen en erin slaagt het doel van het volgen van instelpunten te bereiken.

Het laatste deel van dit proefschrift is waar de voorgestelde LTV-OBF MPC en LPV-OBF MPC zijn getest in twee industriële casestudies. Destillatiekolom met hoge zuiverheid case en Dual distillatiekolom case die gemeengoed zijn in de procesindustrie, worden gebruikt voor de demonstratie. Elk van de voorgestelde controles blinkt uit in verschillende toestanden waarin de kennis van de variaties van systeemdynamiek het belangrijkste element wordt dat de twee voorgestelde MPC-schema's onderscheidt.

About the Author

Rian was born on September 25, 1985 in Yogyakarta, Indonesia. After finishing high school in 2003 in Yogyakarta, he went to Bandung for his bachelor's study where his interest in system control started under the umbrella of the Electrical Engineering program at "Institut Teknologi Bandung". With that seed of interest, he pursued a master's degree in System and Control at "TU Delft". This path led him to meet Roland for his Master thesis titled "Linear Parameter Varying Modeling of a High-Purity Distillation column. The experience during his master's and thesis work gave him a stronger foundation and interest in this Field of study.

Rian continued his journey by taking a Ph.D. project under the supervision of Siep and Roland in 2013 at "TU Eindhoven". This Ph.D. was undertaken in the SMART Project which aims at developing a set of breakthrough Advanced Process Control (APC) technologies intended to drastically reduce the total cost of ownership, by means of more streamlined implementation and automatic maintenance.

Rian is a proud father of three beautiful children, Gwen, Garnet, and Gianna. Together with his beloved wife Anti, they like to spend their time together to grow and explore the world.